Modélisation des bilans de gaz à effet de serre des agro-écosystèmes en Europe

Simon Lehuger

THÈSE

pour obtenir le grade de

Docteur

de

l'Institut des Sciences et Industries du Vivant et de l'Environnement

AgroParisTech

Discipline : Agronomie-Environnement

Présentée par :

Simon LEHUGER

MODÉLISATION DES BILANS DE GAZ À EFFET DE SERRE DES AGRO-ÉCOSYSTÈMES EN EUROPE

Modelling the greenhouse gas balance of agro-ecosystems in Europe

---

Soutenue le 4 mai 2009 devant le jury composé de :

Jean-Claude Germon	Directeur de Recherche, INRA, Dijon	Rapporteur
Adrian Leip	Chercheur, JRC, Ispra, Italie	Rapporteur
Claire Chenu	Professeur, AgroParisTech, Paris	Présidente
Bernard Seguin	Directeur de Recherche, INRA, Avignon	Examinateur
Pierre Cellier	Directeur de Recherche, INRA, Grignon	Examinateur
Benoît Gabrielle	Professeur, AgroParisTech, Paris	Directeur de thèse

UMR INRA-AgroParisTech Environnement et Grandes Cultures - F-78 850 THIVERVAL-GRIGNON

Remerciements

Si j'ai réussi à soutenir ma thèse en deux ans et demi, c'est en partie grâce à toi, Benoît, car tu as su me motiver pour croire à ce petit challenge. Je te remercie pour ta confiance, ta disponibilité, tes conseils et ton énergie positive. C'est un véritable plaisir de travailler avec toi et j'espère que nous pourrons continuer à collaborer dans le futur. J'emmène CERES dans mes bagages pour lui faire découvrir de nouvelles conditions pédoclimatiques. S'il s'acclimate, il fera peut-être des petits...

Cette thèse n'aurait pas été possible sans l'aide et surtout la convivialité de l'équipe Biosphère-Atmosphère. Merci particulièrement Patricia et Pierre pour les échanges que nous avons eu sur NitroEurope. Merci Nathalie, Jean-Louis, Michel, Sophie, Benjamin, Brigitte, Céline, Romain, Sébastien pour vos coups de main informatiques, scientifiques et sympathiques. La thèse occasionne des pics fugaces de stress qui deviennent vite ingérables si on ne partage pas quelques moments hilarants entre thésards : Merci Marie-No, Lucas, Alexis, Sylvia. Merci aussi les équipes bibliothèque et secrétariat pour votre assistance.
Merci tout particulier Cécile, Franck et Emmanuelle pour l'ambiance chaleureuse de notre bureau qui fut notre écosystème pendant 3 ans. C'est sûr vous allez me manquer.

During my thesis, I had the chance to travel around Europe, to visit beautiful cities (Garmisch, Aberdeen, Paestum, Gand, Gotebörg, Edimbourg) but above all, to meet people who I would like to warmly thank : Klaus Butterbach-Bahl, Marcel van Oijen, Jagadeesh Yeluripati, Christian Werner, Martin Wattenbach, Daniela Kracher, Pierluigi Calanca and Kairsty Topp.

Je remercie Jean-Claude Germon et Adrian Leip d'avoir accepté de rapporter cette thèse et Claire Chenu, Bernard Seguin et Pierre Cellier d'avoir accepté de faire partie du jury.
Merci à Catherine Hénault, Pierre-Alain Jayet, Nicolas Viovy, David Makowski et Pierre Cellier pour leurs conseils lors des comités de pilotage.
Merci encore à David Makowski pour ses conseils avisés sur le bayésien, à Matiyiendu Lamboni et Hervé Monod pour nos travaux sur l'analyse de sensibilité. Merci à Chris Fléchard et au Cemagref de Rennes pour les analyses de gaz à effet de serre. Merci à Anne Prieur et Frédérique Bouvart pour nos travaux sur les ACV de biocarburants. Merci à Mickael Schulz et Vincent Prieur pour nos collaborations dans le cadre du projet N-TWO-O.

Merci à tous ceux qui sont venus me secouer les puces et m'ont écoutés radoter mes répéts' de soutenance et de concours. Merci aux gars du master Biosphère pour les soirées parisiennes et bonne chance pour vos soutenances de thèse (hihihi !). Merci Pierrick, Alex et Olivier pour les réunions aux sommets et les négociations en cours. Merci Carine, Arnaud, Jérome et Nico pour les weeks-ends bretons et nos expériences de jardinage.
Un grand merci à mes parents, Édith et Michel, et à mes soeurettes, Camille et Gabi, qui m'ont supportés pendant la thèse. Et enfin, un énorme merci Charlotte pour ton soutien, tes encouragements et les week-ends zen loin de Paris.

Résumé

L'agriculture représente 10 à 15 % des émissions anthropiques de gaz à effet de serre (GES), ce qui justifie que ce secteur soit amené à jouer un rôle dans la lutte contre les changements climatiques. Les échanges de GES entre agro-écosystèmes et atmosphère font intervenir trois composés : le protoxyde d'azote (N_2O), le méthane (CH_4) et le dioxyde de carbone (CO_2). Les sols cultivés sont responsables de 60 % des émissions de N_2O, dont le potentiel de réchauffement global équivaut à 300 fois celui du CO_2 à horizon 100 ans. Le protoxyde d'azote est produit dans le sol par les processus microbiologiques de nitrification et de dénitrification, ce qui induit des émissions fugaces qui dépendent fortement des conditions pédoclimatiques locales et des pratiques agronomiques. À l'échelle globale, les flux de CO_2 entre agro-écosystèmes et atmosphère sont pratiquement équilibrés, mais la mise en place de certaines pratiques agronomiques permet d'accroître le stock de C de l'écosystème et de réduire ainsi d'autant le stock atmosphérique.
La prédiction de ces échanges de GES nécessite de prendre en compte les processus sous-jacents au sein du système sol-plante, qui sont fortement régulés par les conditions agro-pédoclimatiques. L'utilisation de modèles biophysiques est actuellement une approche très prometteuse en ce sens, mais encore en émergence. La problématique centrale de ce travail de thèse est l'estimation du pouvoir de réchauffement global des agro-écosystèmes, basée sur une modélisation biophysique des agro-écosystèmes et de leurs échanges de GES avec l'atmosphère.
Le développement du modèle CERES-EGC a permis d'estimer ses paramètres, grâce à une méthode originale de calibration bayésienne, et d'évaluer son erreur de prédiction pour la simulation des flux de N_2O et de CO_2 à l'échelle de la parcelle. Ce modèle, qui intègre le fonctionnement de l'agro-écosystème dans son ensemble et l'effet des pratiques culturales, est désormais en mesure de prédire le bilan de GES des systèmes de cultures, avec une marge d'erreur que nous avons pu quantifier.
L'application du modèle sur des sites expérimentaux aux conditions pédoclimatiques contrastées a permis de quantifier le pouvoir de réchauffement global de systèmes de cultures à l'échelle de rotations, en y incluant les flux de N_2O, de CO_2 et de CH_4. Les émissions indirectes dues à la production des intrants, à leur transport jusqu'à la ferme et aux opérations culturales ont également été intégrées au bilan final selon une approche d'analyse de cycle de vie. Le modèle a ainsi permis de tester différentes stratégies de mitigation du pouvoir de réchauffement des systèmes de cultures, et mis en exergue certaines pratiques à haut potentiel notamment celles qui induisent des retours importants de résidus de cultures au sol.
L'utilisation et le développement du modèle dans une perspective d'extrapolation spatiale permet de produire des inventaires d'émissions de GES par les surfaces agricoles à échelle régionale.

Mots-clés : agro-écosystème, gaz à effet de serre, protoxyde d'azote (N_2O), modélisation, CERES-EGC, calibration bayésienne, approche de cycle de vie.

Abstract

Agriculture accounts for 10-15 % of anthropogenic emissions of greenhouse gases (GHGs) justifying that this sector must play a role in climate mitigation. The exchanges of GHGs between agro-ecosystems and the atmosphere involve three compounds : nitrous oxide (N_2O), methane (CH_4) and carbon dioxide (CO_2). Agricultural soils contribute 60 % of the global anthropogenic emissions of N_2O, which has a global warming potential equivalent to 300 times CO_2 on a 100-year time horizon. Nitrous oxide is produced in soil by the microbial processes of nitrification and denitrification. These complex processes lead to highly variable fluxes in both time and space depending on the local pedoclimatic and management conditions. At the global scale, the CO_2 fluxes between agro-ecosystems and the atmosphere are approximately balanced, but the introduction of specific agronomic practices makes it possible to increase the ecosystem C stock and by the way reducing as much atmospheric CO_2. The prediction of GHG exchanges needs to take into account the underlying processes within the soil-crop system that are tightly controlled by the agro-pedoclimatic conditions. Using biophysical models is currently a very promising approach in this direction, but still emerging. The central issue of this thesis is the prediction of the global warming potential of agro-ecosystems, based on biophysical modelling of agro-ecosystems and their GHG exchanges with the atmosphere.

The parameters of the CERES-EGC model were estimated using an original method of Bayesian calibration. Independant data sets were used to assess the error of model prediction for the simulation of N_2O and CO_2 fluxes at the plot scale. The model, which integrates the comprehensive functioning of agro-ecosystem and the effects of agronomic practices, is now able to predict the GHG balance of cropping systems with an error of prediction that we have quantified.

The model application on experimental sites with contrasting soil and climatic conditions made it possible to quantify the global warming potential of cropping systems for entire crop rotations, including the fluxes of N_2O, CO_2 and CH_4. The indirect GHG emissions associated with input production and the use of farm machinery were also integrated into the final global warming potential indicator using a life cycle approach. The model made it possible to test various strategies for mitigating the global warming potential of cropping systems and to highlight some promising practices, particularly those that induce significant returns of crop residues to the soil.

The use and development of the model in the perspective of spatial extrapolation can produce inventories of GHG emissions from croplands at the regional scale.

Keywords : agro-ecosystem, greenhouse gases, nitrous oxide (N_2O), modelling, CERES-EGC, Bayesian calibration, life cycle approach.

Table des matières

Chapitre 1

Introduction

Le secteur agricole est à la fois une source et un puits de gaz à effet de serre (GES). En Europe, il contribue à 50 % des émissions de protoxyde d'azote (N_2O) et a un potentiel de stockage estimé à quelques millions de tonnes de C par an. Ces échanges de gaz à effet de serre entre l'atmosphère et les agrosystèmes concernent les flux de dioxyde de carbone (CO_2), de N_2O et de méthane (CH_4) et doivent être quantifiés de manière précise à l'échelle de la parcelle agricole. Le bilan net est exprimé en potentiel de réchauffement global (PRG). Il est fortement régulé par le milieu (climat et type de sol) et par les pratiques agricoles. Les modèles de fonctionnement des agro-écosystèmes permettent d'aborder ces interactions à travers la modélisation des cycles de l'eau, du carbone et de l'azote et fournissent des estimations d'émissions de GES. Toutefois, ces modèles nécessitent d'être calibrés et évalués par rapport à des données expérimentales à une échelle locale pour une gamme de conditions pédoclimatiques la plus large possible, avant d'envisager leur application à une échelle régionale ou pour tester des scénarios de mitigation.

Cette partie introductive situe le contexte de la thèse, synthétise l'état de l'art et définit la démarche générale de modélisation mise en œuvre. Elle présente ensuite les deux grands objectifs de ce travail : 1/ modéliser les flux de N_2O et de CO_2 entre les agrosystèmes et l'atmosphère et 2/ d'en déduire des bilans de GES à l'échelle de rotations pour plusieurs sites et systèmes de cultures en Europe. Le modèle permet de proposer des pistes de réduction des émissions de GES par les agrosystèmes et peut être appliqué pour produire des inventaires à l'échelle régionale.

1.1 Contexte de la thèse

1.1.1 Contribution de l'agriculture aux émissions de gaz à effet de serre

L'agriculture contribue de manière importante aux émissions de gaz à effet de serre (GES) d'origine anthropique avec un flux total de 6.1 Gt CO_2-eq yr^{-1}, ce qui représente 10 à 12 % des émissions anthropiques totales. Les émissions directes d'oxyde nitreux (N_2O) par les sols arables et de méthane (CH_4) par la fermentation entérique des ruminants sont les deux principales sources de GES à hauteurs respectives de 2 128 et 1 792 Mt CO_2-eq yr^{-1} (Smith et al., 2007). Les flux de CO_2 entre les sols cultivés et l'atmosphère sont considérés comme pratiquement équilibrés avec un bilan de 40 Mt CO_2-eq yr^{-1}, pour l'année 2005. Ces valeurs ne prennent pas en compte les émissions indirectes qui ont lieu pendant la phase de production des intrants et leur transport jusqu'à la ferme, et la combustion de carburants pendant les opérations culturales. Les émissions de GES associées aux cycles de vie des intrants peuvent représentées jusqu'à 50 % du bilan final (Biswas et al., 2008; Robertson et al., 2000; West et Marland, 2002) et ne doivent donc pas être négligées dans l'évaluation des bilans GES des produits agricoles. De plus, les estimations globales des flux de GES du secteur agricole sont très incertaines car les connaissances scientifiques actuelles ne permettent pas de quantifier de manière fiable les flux de GES à large échelle (voir section 1.2.4 ; Smith et al. (2007)).

Les changements d'usage des sols pour fournir de nouvelles terres arables sont également des sources importantes d'émissions de GES (IPCC, 2000). Les surfaces continentales contiennent deux fois plus de C que le stock atmosphérique, une émission massive de C par les sols peut avoir un impact important sur la concentration atmosphérique en CO_2 et sur le climat (Ciais et al., 2005; Smith, 2008). Les surfaces agricoles sont parmi les écosystèmes terrestres qui stockent le moins de C (Duxbury et al., 1993; IPCC, 2000). Une conversion en terres arables peut donc être une source nette de CO_2. La déforestation concerne surtout les pays en développement, où les terres arables se sont étendues de 6 à 7 Mha par an pendant les 40 dernières années (Smith et al., 2007).

Les émissions de CH_4 et de N_2O ont augmenté globalement de 17 % entre 1990 et 2005. Les projections à 2030 prévoient une augmentation de 35 à 60 % des émissions de N_2O principalement à cause de l'augmentation de l'utilisation des engrais azotés minéraux et organiques d'origine animale et une augmentation de 60 % des émissions de méthane directement proportionnelles à la croissance du cheptel mondial (Galloway et al., 2008; Smith et al., 2007; Vergé et al., 2007).

1.1.2 Les flux d'azote réactif

L'azote réactif (Nr) regroupe toutes les formes d'azote réactives d'un point de vue biologique, radiatif et photochimique. Il peut être sous forme oxydée (NO_x, N_2O, NO_3^-) ou réduite (NH_4^+, NH_3) et seul le diazote (N_2) est considéré comme une forme non-réactive. Les flux d'azote réac-

tif ont un rôle crucial dans l'établissement des bilans de GES des écosystèmes terrestres (Sutton et al., 2007). En effet, les apports d'azote dans les écosystèmes affectent directement le cycle du carbone : la production primaire et la décomposition de la matière organique du sol. De plus, les entrées de Nr peuvent être directement sources d'émissions de N_2O, et d'oxydes d'azote (NO_x) qui sont des précurseurs d'ozone (O_3) qui lui-même participe au réchauffement climatique additionnel (IPCC, 2007).

Avant l'ère pré-industrielle, l'entrée d'azote dans la biosphère était assurée par la fixation biologique du N_2 atmosphérique. Les retours d'azote vers l'atmosphère était assurés par la dénitrification de l'azote réactif (Nr) en N_2. Depuis le début du 20ème siècle, la production anthropique d'azote réactif, pour la fabrication des engrais, est passée d'une production marginale pour devenir actuellement la principale source de fixation de N_2 en Nr, devant les processus de fixation biologique (Galloway et al., 2004). La majorité de l'azote fixé est destinée à la production d'engrais agricoles dont l'utilisation est en pleine croissance en Asie du sud-est mais a tendance à se stabiliser ou à décroître en Europe (Smith et al., 2007). Certes, sans une fourniture d'azote optimale, les cultures ne peuvent pas exprimer leur potentiel de rendement, cependant, selon Galloway et Cowling (2002) pour 100 atomes d'azote fixés et utilisés comme engrais, seulement 14 sont consommés comme aliments végétaux (Fig. 1.1) et 4 pour les aliments carnés. L'azote restant subit alors une série de transferts et de transformations dans les compartiments air, sol, eau, biosphère et engendre des impacts multiples sur les écosystèmes, la qualité de l'air, les changements globaux et la santé humaine. L'agriculture est au centre de cette «cascade de l'azote», et le défi scientifique actuel est de quantifier, prévoir et réduire les émissions et dépôts d'azote réactif (Erisman et al., 2007; Galloway et al., 2008; Sutton et al., 2007). Le projet NitroEurope décrit dans l'encadré 1 se consacre à cette problématique et ce travail de thèse participe et s'intègre à ce projet.

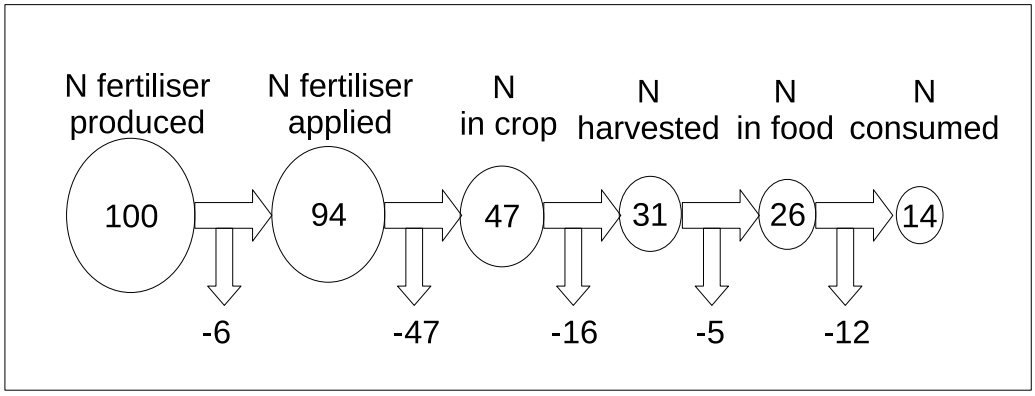

FIG. 1.1 : *Devenir de l'engrais azoté de l'usine de production jusqu'à la consommation d'un produit alimentaire d'origine végétal (pour 100 atomes d'azote ; Galloway et Cowling (2002)).*

Encadré 1 : Le projet européen NitroEurope

Le projet européen **NitroEurope** (2006-2011) a pour objectif principal d'étudier les mécanismes d'émissions de gaz à effet de serre par les écosystèmes terrestres en lien avec les flux d'azote réactif. Dans ce projet, différentes échelles spatiales et temporelles sont étudiées allant de l'échelle de la parcelle jusqu'au continent européen. Les méthodes développées à chacune des échelles reposent principalement sur des mesures expérimentales et la modélisation. Le projet rassemble une soixantaine d'instituts provenant de 25 pays, majoritairement européens, et 160 scientifiques sont fortement impliqués. Le projet est organisé selon les 6 composantes scientifiques présentées dans la figure suivante.

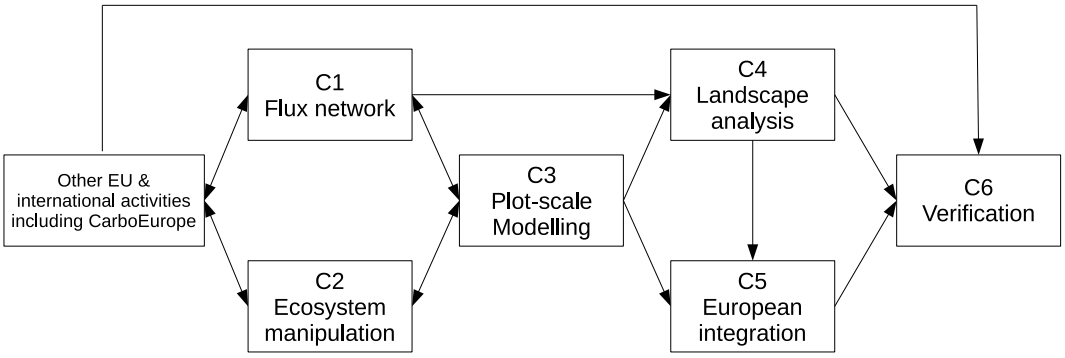

La composante «Flux Network» a pour objectif de mesurer les échanges biosphère-atmosphère à travers un réseau de sites de mesures pour les principaux écosystèmes terrestres européens (forêt, prairie, culture, zone humide et lande). Dédiée à la modélisation à l'échelle de la parcelle, la composante «Plot Scale Modelling» a pour objectifs :

- d'évaluer l'incertitude des modèles d'écosystème,
- de simuler et d'interpréter les flux de GES mesurés dans le réseau de mesures NitroEurope,
- et de tester des scénarios de mitigation sur certains sites en Europe.

Les écosystèmes anthropisés (forêt, prairie, culture) et les écosystèmes naturels (zone humide, lande) sont modélisés avec des modèles dédiés à un écosystème ou des modèles multi-écosystèmes. Ce travail de thèse s'intègre à cette composante.

1.2 État de l'art

Cet état de l'art rassemble une partie de l'état des connaissances sur la problématique des bilans de GES des agro-écosystèmes. Tout d'abord, les processus biologiques d'échanges de GES entre le système sol-plante et l'atmosphère sont détaillés. Ensuite, nous présentons des bilans de GES d'agro-écosystèmes issus de la bibliographie et leurs potentiels de mitigation. Enfin, les différentes méthodes d'estimation des flux de GES des agro-écosystèmes sont décrites[1].

1.2.1 Processus biologiques des échanges de GES

Les flux de CO_2 entre les surfaces agricoles et l'atmosphère mettent en jeu les processus de fixation du C par la photosynthèse et la minéralisation des résidus de cultures et de la matière organique du sol. Les flux de méthane sont le bilan net entre production et consommation. Le N_2O est produit lors des processus de nitrification et de dénitrification dans les sols.

Les entrées de carbone dans la biosphère continentale se font exclusivement par la production primaire nette (PPN). Les plantes chlorophylliennes fixent le CO_2 atmosphérique dans leur tissu par le processus de **photosynthèse**. Rojstaczer et al. (2001) ont estimé qu'environ 40 % de la PPN était utilisée pour les activités humaines. Une grande partie de C retourne au sol sous forme de matière organique ou sous forme de CO_2 dans l'atmosphère après des temps de résidence variables selon les produits (aliments, fibres, construction ; Smith et al. (2008b)). Le bilan entre les entrées de C, fixé par photosynthèse, et la minéralisation reflète l'évolution du stock de C de l'écosystème.

La **minéralisation** est le processus de transformation de la matière organique qui retourne au sol en éléments minéraux sous l'action des micro-organismes hétérotrophes du sol. L'azote organique est transformé en azote ammoniacal par la réaction d'ammonification et le bilan avec l'immobilisation (N consommé par les micro-organismes) reflète la quantité d'azote potentiellement disponible pour les plantes (Fig. 1.2, Balesdent et al. (2005)).

La **nitrification** est le processus d'oxydation de l'ammonium (NH_4^+) ou de l'ammoniac (NH_3) en nitrites (NO_2^-) et en nitrates (NO_3^-) en condition aérobie par des micro-organismes majoritairement autotrophes du genre *Nitrosomas* pour l'oxydation de NH_4^+ en NO_2^- et du genre *Nitrobacter* pour l'oxydation de NO_2^- en NO_3^- (Fig 1.3). La nitrification est principalement contrôlée par la teneur en NH_4^+, la pression partielle en O_2, l'humidité et la température du sol. L'observation d'émissions de N_2O dans des sols bien aérés et dépourvus de NO_3^- montre qu'elles sont corrélées à la concentration en NH_4^+ (Khalil et al., 2004). La production de N_2O a lieu à partir de l'hydroxylamine (NH_2OH) quand la disponibilité en O_2 diminue. Le N_2O ainsi formé est un sous-produit de la réaction de nitrification. Les émissions de N_2O produites sont mineures relativement aux quantités d'azote nitrifiées, mais le cumul des émissions sur une saison

[1]Une partie de l'état de l'art consacré aux méthodes et aux résultats de la bibliographie est incluse directement dans les chapitres de la thèse et n'est pas détaillée en introduction.

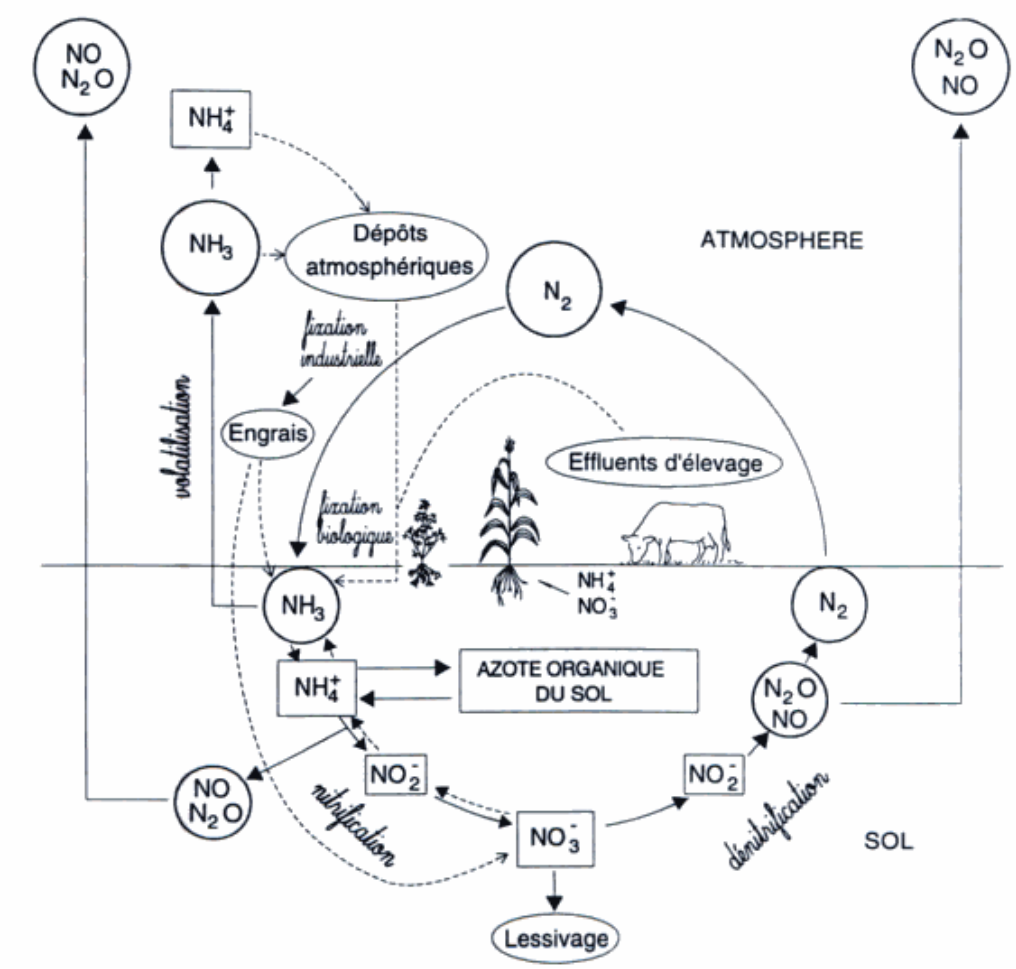

FIG. 1.2 : *Le cycle de l'azote des écosystèmes agricoles (les composés gazeux sont entourés d'un cercle, Cellier et al. (1996)).*

de culture peut représenter au final une fraction importante des émissions totales de N_2O. Des oxydes nitriques (NO_x) sont également produits pendant la transformation de nitrites en nitrates et peuvent représenter de 1 à 4 % de l'ammonium oxydé (Laville et al., 2005). La nitrification dénitrifiante est la succession de l'oxydation de l'ammonium en nitrites, suivie directement par la réduction des nitrites en N_2O et N_2. Cette réaction a lieu en condition d'O_2 limitante. Peu de travaux sont disponibles pour quantifier la part de N_2O émise par cette réaction par les sols agricoles (Wrage et al., 2001).

La **dénitrification** est l'unique processus biologique de retour de l'azote fixé à l'atmosphère sous forme de N_2 (Fig. 1.2). Le nitrate provenant de la nitrification ou directement des applications d'engrais peut être réduit en N_2 (Fig. 1.3). La réaction a lieu en condition anaérobie par des micro-organismes dénitrifiants hétérotrophes qui ont la particularité de pouvoir utiliser le NO_3^- comme accepteur d'électrons lors de la respiration en condition d'O_2 limitante (Hutchinson et Davidson, 1993). Les bactéries des genres *Pseudomonas* et *Bacillus* présentent cette faculté. Les

produits intermédiaires de la réaction de dénitrification, NO et N_2O, sont échangés avec le milieu et peuvent être émis dans l'atmosphère. La dénitrification dépend : i) du degré d'anaérobiose du sol directement relié au niveau de saturation en eau, ii) de la concentration en substrats carbonés et en nitrates, et iii) de la température qui régule les réactions biologiques (Conrad, 1996). Le ratio N_2O sur N_2 varie en fonction des facteurs précédents et les émissions de N_2O peuvent représenter le produit terminal dominant de la réaction. Des conditions de faibles teneurs en N du sol et d'humidité importante peuvent également engendrer une consommation de N_2O atmosphérique. Les facteurs contrôlant cette consommation sont encore assez peu connus et méritent d'être mieux étudiés (Chapuis-Lardy et al., 2007).

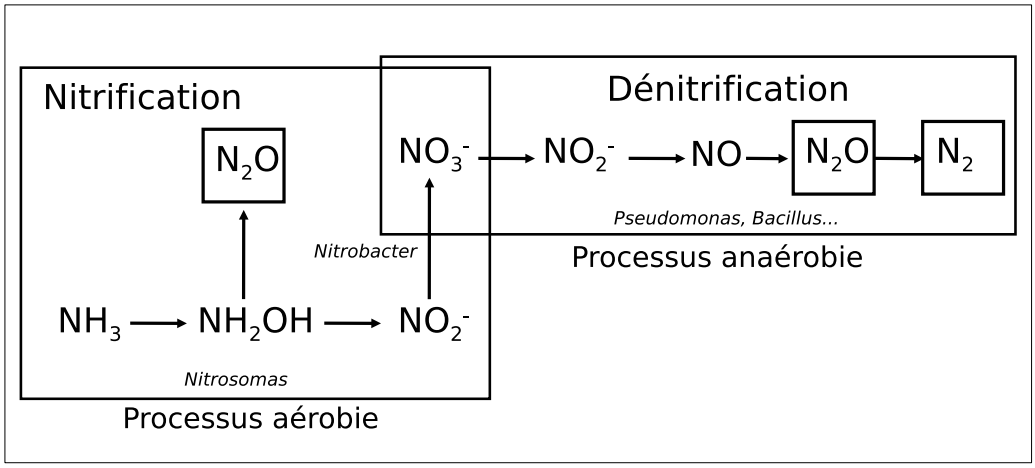

FIG. 1.3 : *Réactions de transformation de l'azote dans le sol par nitrification et dénitrification.*

Le flux net de CH_4 d'un sol agricole est le bilan entre production de CH_4 par **méthanogenèse** et consommation de CH_4 par **méthanotrophie**. La méthanogenèse est un processus microbien de décomposition de la matière organique qui a lieu en condition anaérobie (Knowles, 1993). Les principales sources de méthane des écosystèmes sont les terres immergées, les zones humides et la riziculture inondée. Le méthane est consommé par les horizons de surface des sols en condition aérée et ce puits pourrait représenter 5 à 8 % des sources globales de CH_4 (Mosier et al., 1998; Ojima et al., 1993). En 2006, Keppler et al. rapportèrent que les plantes pouvaient être directement une source importante de méthane (10 à 40 % des sources globales actuelles). Depuis, cette observation a été contestée et Nisbet et al. (2009) ont montré que les plantes sont un média par lequel le méthane peut transiter mais ne peuvent être une source de CH_4 aussi importante.

1.2.2 Bilan de gaz à effet de serre des agro-écosystèmes

Afin de comptabiliser les flux de GES des systèmes de cultures, il est important de prendre en compte toutes les émissions de GES de l'agrosystème (CarboEurope, 2004; Soussana et al., 2007). Les flux de GES sont quantifiés en terme de pouvoir de réchauffement global (PRG), exprimés relativement au forçage radiatif du CO_2 à horizon 20, 100 ou 500 ans (IPCC, 2007). Par

ailleurs, plusieurs travaux suggèrent qu'il est nécessaire de considérer la totalité des émissions directes de GES afin de quantifier le PRG total du système et de prendre en compte les effets antagonistes de certaines pratiques sur les flux. Par exemple, Li et al. (2005a) mettent en garde sur l'effet de pratiques, qui pourraient stocker du C dans le sol, sur les émissions de N_2O. En effet, les auteurs ont montré que les bénéfices du travail du sol réduit en terme de stockage de C pouvaient être annulés par une augmentation des émissions de N_2O. Par ailleurs, il s'avère que les émissions indirectes ont un poids important sur le bilan global (Robertson et al., 2000; Smith et al., 2001). Bernacchi et al. (2005) ont montré que le potentiel de stockage de carbone dans le sol lors de la conversion au non-labour est diminué quasiment d'un tiers lorsqu'on prend en compte les émissions indirectes.

Robertson et al. (2000) ont montré qu'un système conventionnel avec une rotation maïs-soja-blé aux États-Unis possédait un potentiel de réchauffement global de 114 g CO_2-eq m^{-2} dont une moitié provient des émissions de N_2O (52 g CO_2-eq m^{-2}) et l'autre moitié des émissions indirectes (66 g CO_2-eq m^{-2}), le sol étant un puits de méthane de 4 g CO_2-eq m^{-2}. Dans le cas d'un système sans travail du sol, le stockage de C dans le sol permet de diminuer le potentiel de réchauffement à 14 g CO_2-eq m^{-2}, les émissions de N_2O et les émissions indirectes étant pratiquement identiques au système conventionnel. Mosier et al. (2005) et Del Grosso et al. (2005) ont calculé le PRG de systèmes de cultures et leurs estimations donnent des résultats plus élevés en moyenne que ceux de Robertson et al. (2000) (voir Tableau 1.1).

Pour réaliser un bilan complet de gaz à effet de serre d'un agrosystème, les émissions directes de GES biogéniques (CO_2, N_2O et CH_4) et les émissions indirectes dues à la consommation d'intrants et aux pratiques culturales doivent être comptabilisées selon la démarche inspirée de l'analyse de cycle de vie (ACV). L'encadré 2 présente la méthodologie de l'ACV appliquée à la production agricole.

1.2.3 Potentiel de mitigation

Le potentiel de mitigation des GES d'origine agricole se divise en trois grandes catégories basées sur les mécanismes suivants (Smith et al., 2008a) :

- **Réduire les émissions** : Une gestion plus efficace des flux de C et de N permet de réduire de manière substantielle les émissions de GES.
- **Augmenter les prélèvements de CO_2 atmosphérique** : Les techniques culturales qui permettent d'augmenter les entrées de C photosynthétique ou de diminuer la respiration de la matière organique du sol permettent d'accroître le stock de C du sol et donc de diminuer d'autant le stock atmosphérique.
- **Substituer le C fossile** : La biomasse peut être utilisée comme source de bioénergie directement en combustion ou après conversion en biocarburants. Le carbone fixé est renouvelable et le bénéfice net en terme de GES est calculé par rapport à l'évitement des émissions générées par la combustion des carburants fossiles.

Ces trois mécanismes peuvent être mis en pratique à travers la gestion agronomique des cultures, le changement d'usage des sols et la bioénergie. La gestion de la fertilisation basée sur des apports en adéquation avec la demande des plantes permet de réduire les émissions de N_2O. McSwiney et Robertson (2005) ont montré que les émissions de N_2O doublaient dès que les apports d'azote dépassaient les besoins des cultures (pour du maïs, Michigan, États-Unis, Fig.1.4).

Selon Arrouays et al. (2002), les techniques culturales simplifiées pourraient stocker 0.2 t C ha^{-1} an^{-1} et selon Freibauer et al. (2004), le potentiel de stockage de C à l'échelle européenne pourrait être de 2.4 Mt C ha^{-1} an^{-1} à l'horizon 2012. Le bilan net de ces pratiques entre stockage de carbone et émissions de N_2O n'est toujours pas démontré globalement et dépend largement du type de sol, du climat et des pratiques de gestion (Beheydt et al., 2008; Desjardins et al., 2005; Li et al., 2005a; Six et al., 2004). L'implantation de couverts végétaux et de cultures intermédiaires (Freibauer et al., 2004) et la conception de systèmes de cultures à bas niveaux en intrants avec l'intégration de légumineuses (Dick et al., 2008; Rochette et Janzen, 2005; Tonitto et al., 2007), peuvent aussi participer à la réduction des bilans de GES des systèmes de cultures.

Le changement de couverture du sol est la méthode la plus efficace pour réduire les émissions mais elle entraîne inévitablement un changement d'usage. La conversion de surface cultivée en prairie ou en forêt, permet d'augmenter le stock de C du sol et pourrait réduire les émissions de N_2O du fait d'apports azotés réduits (Arrouays et al., 2002). De même, le reboisement de terres cultivées conduit à une accumulation moyenne de 0.5 t C ha^{-1} an^{-1} sur 100 ans selon Arrouays et al. (2002).

1.2.4 Méthodes d'estimation des flux de GES des agro-écosystèmes

Les échanges de gaz à effet de serre entre les écosystèmes cultivés et l'atmosphère dépendent de processus biologiques, dont l'intensité est en relation avec les conditions du milieu et la gestion par l'agriculteur. Des méthodes basées sur les mesures permettent de quantifier les flux de l'échelle de la parcelle agricole à quelques km^2. Une autre voie basée sur des facteurs d'émission (FE) consiste à calculer directement les flux de GES en fonction des activités (IPCC, 2006). Mais l'approche qui semble la plus prometteuse est l'utilisation de modèles mécanistes orientés sur les processus (Butterbach-Bahl et al., 2004; Gabrielle et al., 2006a).

1.2.4.1 Systèmes de mesures

Échanges de CO_2 entre l'atmosphère et le système sol-plante

La mesure de la variation du stock de carbone du système sol-plante peut être envisagée de 2 manières possibles : i) soit en mesurant les flux de CO_2 à l'interface du système sol-plante et de l'atmosphère, en prenant en compte les entrées et les sorties de C aux frontières de la parcelle, ii) soit en mesurant directement l'évolution du stock de C du sol (résidus, litière, matière organique). Nous présenterons ici, seulement les techniques de mesure de flux de CO_2 avec la

Références	Méthode d'estimation des émissions directes de GES	Systèmes de cultures	Net CO_2	Émissions indirectes	N_2O	CH_4	PRG net
Robertson et al. (2000)	Mesures	Cultures annuelles (maïs-soja-blé) (Michigan, USA)	NT=-300 CT=0	NT=200 CT=180 (carburant, engrais, chaux))	NT=153 CT=140	NT=-13 CT=-10	NT=40 CT=310 Luzerne=-50
Del Grosso et al. (2005)	Modèle	Moyenne nationale pour les systèmes de grandes cultures dominants (USA)	NT=-140 CT=-25	NT=175 CT=160 (carburant)	NT=255 CT=300	NT=-1 CT=-5	NT=290 CT=430
Mosier et al. (2005)	Mesures	3 sites, 18 traitements (culture, fertilisation, climat ; Michigan et Colorado, USA)	de -838 à 42	de 31 à 252 (carburant+machine +engrais)	De 31 à 200 40 à 45 % du PRG	De -5 à -9	De 481 à 753
Adviento-Borbe et al. (2007)	Mesures	1 système monoculture de maïs (CC) 1 système maïs-soja (CS) 2 traitements par système : gestion recommandée (R) et intensive (I) (Nebraska, USA)	CC-R=-440 CC-I =-620 CS-R=300 CS-I=-20	CC-R=690 CC-I=920 CS-R=490 CS-I=71	CC-R=320 CC-I=570 CS-R=250 CS-I=340	CC-R=-3 CC-I=-3 CS-R=-2 CS-I=-1	CC-R=540 CC-I=840 CS-R=1020 CS-I=1020
Ram (2000) rapporté par Robertson et Grace (2004)	Mesures	Système tropical riz-blé-haricot (Plaine indo-gangétique, Inde)	NT=311 CT=625	NT=123 CT=169	NT=475 CT=475	NT=1527 CT=1527	NT=2435 CT=2795

TAB. 1.1 : *Comparaison de bilans de GES exprimés en kg CO_2-C eq ha^{-1} an^{-1} pour différentes études (CT : travail du sol conventionnel, NT : sans travail du sol).*

première méthode, la seconde étant plus généralement utilisée pour rendre compte de changement de systèmes ou de pratiques sur le long terme (labour à semis direct, par exemple).
Les flux de CO_2 et de vapeur d'eau sont habituellement mesurés par la technique micrométéorologique des corrélations turbulentes (*eddy covariance*). La méthode est largement répandue à travers le monde, en particulier au sein de réseaux de mesures, comme le réseau international FluxNeT (Baldocchi et al., 2001) ou le réseau européen CarboEurope (Aubinet et al., 2000). La méthode d'*eddy covariance* perturbe très peu l'environnement étudié et permet des mesures de manière continue sur des périodes de plusieurs années à l'échelle de plusieurs hectares. Elle consiste à mesurer la vitesse verticale du vent et la concentration des gaz étudiés au-dessus du couvert, les flux des gaz mesurés (vapeur d'eau, CO_2) étant proportionnels à la covariance entre les fluctuations de la vitesse verticale du vent et la concentration des gaz. Les composantes de vitesse du vent sont mesurées avec un anémomètre sonique et les concentrations des gaz avec un analyseur à infrarouges (Denmead et Raupach, 1993). Les données brutes mesurées nécessitent d'être retraitées afin d'éliminer les données qui ne répondent pas à certains critères. Les données manquantes sont recalculées, selon différentes stratégies de remplissage des vides (*gap filling*, Falge et al. (2001)). Les flux de N_2O et de CH_4 peuvent également être mesurés selon ces méthodes micrométéorologiques pour une évaluation des flux à une échelle spatiale de quelques hectares.

Mesures des flux de GES par la méthode des chambres statiques

La méthode des chambres statiques est couramment utilisée pour mesurer les flux de CO_2, CH_4 et N_2O à la surface du sol, à l'échelle d'une parcelle homogène. Le principe est basé sur un confinement des échanges sol-atmosphère dans une enceinte hermétiquement fermée par un couvercle. L'évolution de la concentration des gaz à l'intérieur de la chambre permet de calculer un flux selon l'équation :

$$F = \frac{V}{A}\frac{\triangle C}{\triangle T}$$

Avec F, le flux de gaz, V le volume d'air de la chambre, A la surface au sol couverte par la chambre et $\frac{\triangle C}{\triangle T}$, l'évolution de la concentration du gaz en fonction du temps. Des prélèvements de gaz à l'intérieur de la chambre permettent de suivre l'évolution de la concentration des gaz. Cette dernière est analysée au laboratoire en chromatographie en phase gazeuse. Un détecteur à ionisation de flamme (FID) mesure la concentration en CH_4 et un détecteur à capture d'électrons (ECD), le N_2O. Le CO_2 est mesuré avec le FID après transformation en méthane grâce à un méthaniseur. Rochette et Eriksen-Hamel (2008) proposent une série de critères à respecter pour mettre en place des mesures avec des chambres statiques. Par exemple, les auteurs conseillent de réaliser au moins quatre prélèvements de gaz pour élaborer la cinétique d'accumulation et de limiter le temps d'accumulation à 40 minutes maximum.
Des systèmes de chambres automatiques, dont la fermeture et l'analyse des gaz sont faites en continu et de manière automatisée sont en développement depuis quelques années (Laville et al., 2009; Pape et al., 2009; Yao et al., 2008). Ces systèmes permettent de mesurer les flux sur de longues périodes avec une résolution infra-journalière. Mais la charge de maintenance est importante car le système nécessite d'être déplacé avant chaque opération culturale.

Encadré 2 : L'Analyse de Cycle de Vie de produits agricoles

L'Analyse de Cycle de Vie (ACV) est une méthode d'évaluation environnementale qui se base sur un inventaire des ressources utilisées et des émissions vers l'environnement inhérentes à la production d'un bien ou d'un service (Guinée et Lindeijer, 2002). L'analyse de cycle de vie repose sur une approche globale du système de production ("du berceau à la tombe"). L'inventaire de l'utilisation des ressources et des émissions vers l'environnement concerne les étapes de production depuis l'extraction des matières premières jusqu'à la mise en déchet du produit. De plus, c'est une méthode multicritère qui renseigne l'ensemble des impacts environnementaux liés à une activité : effet de serre, eutrophisation, écotoxicité... L'application de l'ACV dans le cas des produits agricoles est délicate du fait qu'il faille estimer les émissions vers l'environnement qui ont lieu sur la parcelle agricole : les émissions directes. Traditionnellement, dans les analyses de cycle de vie des produits agricoles, les émissions directes sont estimées soit avec de simples facteurs d'émissions qui relient la quantité d'intrants aux émissions, ou soit par des modèles simples, basés sur des bilans de matière (bilan de métaux lourds, bilan d'azote ; Lehuger et al. (2009a); Nemecek et al. (2003)).

Les analyses de cycle de vie de produits agricoles ont deux objectifs principaux : soit de comparer différents systèmes de production, par exemple, un système biologique vs. un système conventionnel (Thomassen et al., 2008) ; soit d'évaluer les impacts sur l'environnement d'une filière ou d'un produit et de repérer les points sensibles qui peuvent être améliorés (Gabrielle et Gagnaire, 2008; Prieur et al., 2008).
Dans les ACV de produits agricoles transformés (produits carnés ou laitiers, biocarburants), l'étape de production au champ est déterminante sur les impacts finaux du produit. En effet, la contribution de l'étape de culture est majeure pour les impacts de réchauffement climatique, d'eutrophisation et d'acidification.

Le choix de l'unité fonctionnelle est d'une portée importante sur le résultat de ces impacts. Le choix d'une unité fonctionnelle basée sur la surface (*area-based indicator*) privilégie la fonction d'entretien de l'espace (services environnementaux de l'agriculture) et implique des impacts qui ont lieu à une échelle locale. L'impact sera alors exprimé par ha et ne tiendra pas compte de l'efficacité de la production. Au contraire, si l'unité fonctionnelle est basée sur la quantité produite (*product-based indicator*), la fonction de production est mise en valeur, les impacts sont alors exprimés par kg produit (kg de grain, kg de lait, kg de viande... ; Halberg et al. (2005)). Les systèmes de production extensifs sont privilégiés lorsque les impacts sont exprimés par ha. Au contraire, les systèmes plus intensifs sont privilégiés lorsque les impacts sont exprimés par kg produit. Pour les ACV de cultures, la prévision du rendement devient alors de première importance.

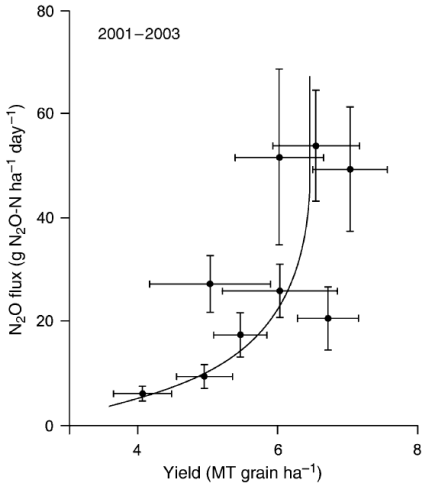

FIG. 1.4 : *Relation entre le rendement en maïs grain et les flux de N_2O pour 9 niveaux de fertilisation azotée (McSwiney et Robertson, 2005).*

Les mesures avec les chambres statiques demandent un niveau de technicité inférieur aux mesures micrométéorologiques mais une charge en main d'œuvre beaucoup plus conséquente. Les chambres manuelles peuvent être utilisées pour tout type de terrain et d'écosystème (forêt, prairie, sol cultivé, zone lacustre...) alors que les mesures micrométéorologiques doivent être implantées sur des surfaces étendues et planes. Les chambres statiques ont tendance à perturber fortement le milieu, elles ne permettent d'explorer qu'une faible proportion de l'espace et ne donnent que des valeurs ponctuelles dans le temps. Par contre, elles sont très pratiques pour comparer différents traitements ou pratiques agronomiques (Cellier et al., 1996; Hénault et al., 2005b).

La Fig. 1.5 illustre les points forts et les points faibles de la méthode des chambres statiques en prenant l'exemple du suivi des flux de N_2O sur trois parcelles. Des mesures de GES ont été réalisées sur le site de Grignon (France) pour trois parcelles (PAN1, PAN2, PAN3) sur lesquelles une rotation maïs-blé-orge-moutarde est décalée de 0, 1 et 2 ans afin d'avoir chaque année les différentes cultures de la rotation en place. Cette expérimentation permet d'étudier, sur plusieurs traitements en parallèle, l'effet des cultures et des pratiques agronomiques sur les émissions de GES pour un climat et un sol constants (voir chap. 4). En revanche, on remarque que la méthode ne donne que des valeurs ponctuelles dans le temps (entre 15 et 20 points par an et par parcelle).

1.2.4.2 Méthode d'estimation par facteur d'émission

Les pays signataires de la Convention des Nations Unies sur le Changement Climatique (*United Nations Framework Convention on Climate Change*, UNFCCC) doivent réaliser leurs inventaires nationaux de GES, en précisant les méthodes de calcul employées. Les méthodes d'inventaires de GES du secteur agricole sont plus complexes que pour les autres secteurs du fait de la grande diversité des sources d'émissions et de la variabilité spatiale des émissions (IPCC,

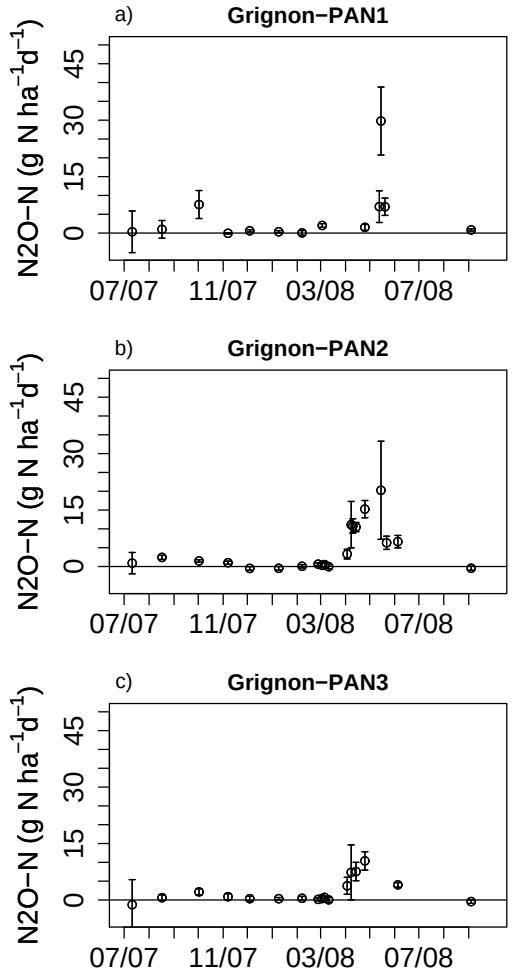

FIG. 1.5 : *Flux de N_2O pour trois parcelles expérimentales suivies sur une année de culture sur le site de Grignon, France (PAN1 : moutarde-maïs, PAN2 : blé, PAN3 : orge).*

2006). Les pays membres doivent utiliser des méthodes de calculs comparables et agréées par la Conférences des Parties (COP, l'institution politique de l'UNFCCC). Les inventaires nationaux sont produits annuellement depuis 1994 et doivent suivre les lignes directrices de l'IPCC (*Intergovernmental Panel on Climate Change*). De nouvelles lignes directrices ont été proposées en 2006. Elles fournissent des méthodes de calcul de complexité croissante : de niveau 1 pour la méthode par défaut (Fig. 1.6), de niveaux 2 ou 3 pour réaliser le calcul des émissions avec des données ou des méthodes spécifiques au pays (Fig. 1.6).

La méthode de niveau 1 consiste en de simples équations et de facteurs d'émissions (décrits dans l'encadré 3 pour le N_2O). La méthode de niveau 2 utilise les mêmes équations que le niveau 1 mais requiert l'utilisation de facteurs d'émissions spécifiques au pays qui prennent en compte le climat local et les types de sol. La méthode de niveau 3 est basée sur l'utilisation de modèles complexes et de systèmes d'information géographique. Le principe est d'estimer les

flux de GES à une échelle spatiale réduite qui puisse prendre en compte les variabilités locales en termes de types de sol, de climat et de pratiques agricoles, puis d'agréger les émissions pour produire les inventaires nationaux. De plus, les pays membres sont encouragés à estimer l'incertitude de leurs inventaires (IPCC, 2006).

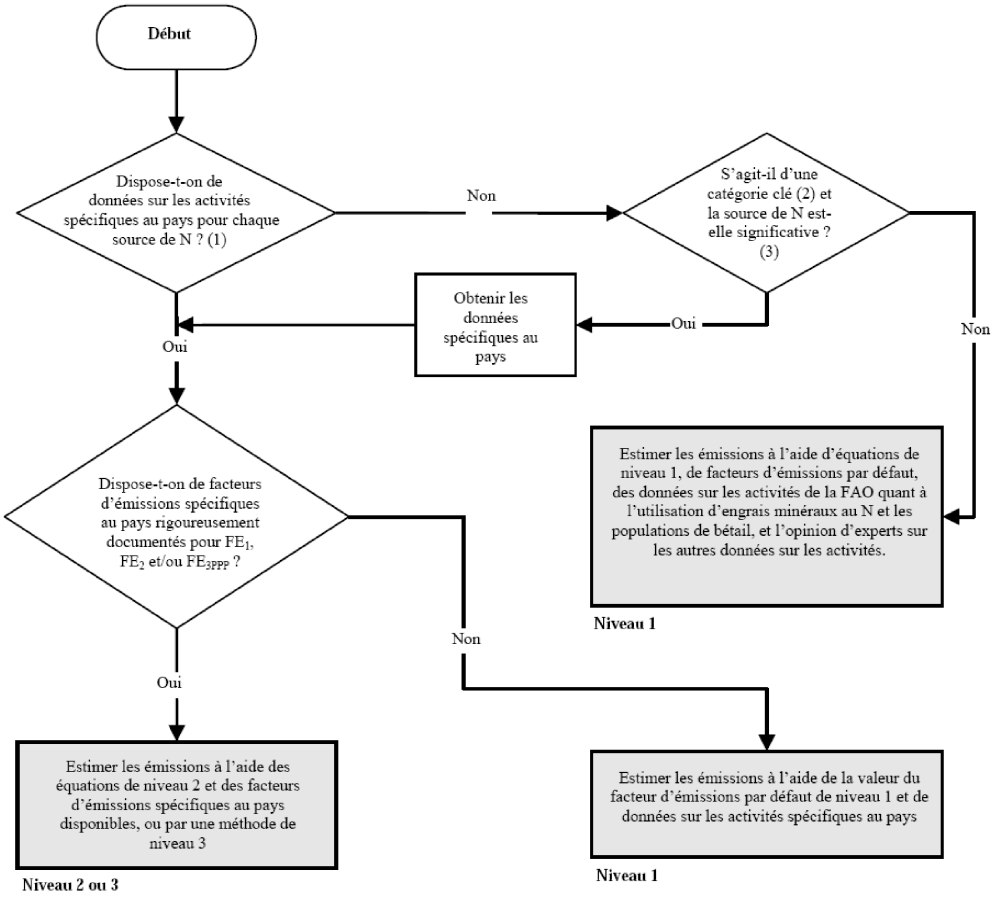

FIG. 1.6 : *Diagramme décisionnel pour le calcul des émissions directes de N_2O des sols cultivés (IPCC, 2006).*

Les lignes directrices de 2006 fournissent une méthodologie pour estimer :

- Les émissions directes de N_2O des sols issues des apports en engrais azotés minéraux ou organiques et du retour d'azote par les résidus de cultures ;
- les émissions indirectes de N_2O produites en aval du champ par les écosystèmes naturels ou les hydrosystèmes à partir de l'azote perdu par voie atmosphérique (volatilisation d'ammoniac, ou émissions de NO_x) puis redéposé sous forme sèche ou humide, ou par voie souterraine (lixiviation de NO_3^-) ;
- les émissions de N_2O induites par les activités d'élevage (émissions pendant le stockage des effluents et par les prairies pâturées) ;

- les flux de CO_2 reflétant les variations de stock de carbone (de la biomasse, de la matière organique du sol et lors de conversion de surface en terres cultivées) ;
- les émissions de méthane dues à la riziculture inondée ;
- les émissions de GES dues au brûlage de biomasse.

La méthodologie IPCC présentée ici est centrée sur le calcul des émissions de N_2O. Le facteur d'émissions (FE_1) de la méthode de niveau 1 est égal à 1 % avec une gamme d'incertitude variant entre 0.3 et 3 %. Ce facteur d'émission a été établi à partir de la compilation des données issues de la bibliographie (Stehfest et Bouwman, 2006). Pour le calcul des émissions indirectes, les quantités d'azote lixiviées ou volatilisées puis redéposées sont multipliées, respectivement, avec des facteurs d'émissions de 0.75 % et 1 %.

La plupart des pays utilisent la méthode de niveau 1 par défaut et seuls quelques-uns ont commencé à mettre en place des méthodologies de niveau 3 (Allemagne, Canada, États-Unis ; Lokupitiya et Paustian (2006)). La méthode de niveau 1 a le mérite d'être simple à mettre en place et les émissions peuvent être directement reliées aux consommations d'engrais minéral et organique. Toutefois, elle est de plus en plus critiquée car sa simplicité induit une grande incertitude due à l'application de valeurs universelles pour les facteurs d'émissions. L'utilisation de valeurs globales peut entraîner des erreurs importantes d'appréciation des émissions de GES dès lors que la région ou le pays considéré est en dehors de la moyenne globale (Biswas et al., 2008). De plus, les processus d'émissions des GES sont contrôlés par les conditions d'humidité du sol, de température, de concentration en azote et par les pratiques agricoles. L'utilisation de données agrégées au niveau national annihile toute variabilité spatiale des échanges de GES aux échelles inférieures. De plus, plusieurs études montrent que les émissions de N_2O ne sont pas directement proportionnelles aux quantités d'azote apportées (voir Fig. 1.7, Barton et al. (2008); Del Grosso et al. (2008); Kaiser et Ruser (2000); McSwiney et Robertson (2005); Roelandt et al. (2005)).

L'utilisation de modèles d'agro-écosystème pour prédire les émissions de N_2O agricoles correspond à la mise en place de la méthodologie IPCC de niveau 3. Par exemple, Li et al. (2001) ont utilisé le modèle DNDC pour calculer l'inventaire national des émissions de N_2O provenant des terres agricoles pour la Chine. Ils ont comparé leurs résultats avec les émissions de N_2O basées sur l'utilisation de facteurs d'émission de l'IPCC. Les émissions directes de N_2O selon cette méthode sont de 0.36 Tg N_2O-N, alors que le modèle DNDC pour l'année 1990 prédit des émissions totales de 0.31 Tg N_2O-N. Avec le modèle, les émissions induites par la fertilisation azotée varient de 0.25 à 4 % de la quantité d'engrais apportée selon la région, avec une moyenne nationale de 0.8 %. Del Grosso et al. (2005) ont utilisé le modèle DAYCENT pour simuler les émissions de N_2O de systèmes de grandes cultures aux États-Unis, qu'ils ont comparées aux estimations calculées par les facteurs d'émission de l'IPCC. Au niveau national, les simulations des émissions de N_2O sont 25 % inférieures aux estimations par les FE. De même, Roelandt et al. (2005) ont montré que l'utilisation de deux modèles empiriques (MCROPS et MGRASS) permettait d'améliorer la prédiction des données observées en comparaison avec celle réalisée avec la méthodologie IPCC. Les modèles ont été ensuite appliqués pour prédire les émissions directes de N_2O des sols agricoles de Belgique pour la période 1990-2050 (Roelandt et al., 2007). A une

échelle plus réduite mais basée sur une résolution spatiale plus fine, le modèle CERES-EGC a permis d'estimer les émissions de N_2O pour la région de la Beauce (France, 59 000 ha) et de les comparer aux estimations de la méthode IPCC (Gabrielle et al., 2006a). Les émissions à l'échelle de ce territoire sont de 2.1 kg N_2O-N ha^{-1} an^{-1} pour le modèle CERES-EGC ce qui correspond à un FE de 0.44 %. La méthode IPCC donne une valeur largement supérieure : 3.1 kg N_2O-N ha^{-1} an^{-1} (avec un FE de 1.25 %).

L'application de modèles biophysiques ou empiriques à des échelles spatiales qui permettent de prendre en compte la variabilité du climat, du type de sol et des pratiques agricoles, puis leur agrégation à échelle régionale ou nationale, montre que la méthode proposée par l'IPCC semble surestimer les émissions directes de N_2O des sols cultivés (Brown et al., 2002; Del Grosso et al., 2005; Gabrielle et al., 2006a; Li et al., 2001; Roelandt et al., 2005). Une vérification des modèles grâce à des réseaux de mesures permettra de tester la qualité des prédictions des modèles et d'estimer leur incertitude.

1.2.4.3 Modélisation biophysique des agro-écosystèmes

La modélisation des cycles de l'eau, de C et N, au sein de l'agro-écosystème permet de simuler les émissions de gaz trace vers l'atmosphère. Plusieurs modèles proposent une modélisation spécifique de l'écosystème agricole et des fonctions de réponses différentes pour simuler les émissions de GES.
Chen et al. (2008) proposent de différencier les approches de modélisation selon l'échelle d'étude : le laboratoire, l'écosystème agricole et l'échelle globale. Les modèles d'agro-écosystème à l'échelle du champ sont les plus utilisés et les deux défis majeurs actuellement sont : i) d'appliquer ces modèles à des échelles spatiales supérieures (paysage, région, globe) et ii) de quantifier le bilan complet des GES des systèmes de cultures (Chen et al., 2008). Les principales différences entre les modules d'émissions de N_2O des modèles d'agro-écosystème concerne la modélisation des processus de nitrification et de dénitrification. Le modèle DNDC (Li et al., 1992) et le modèle ECOSYS (Grant et Pattey, 2003) simulent directement la dynamique microbienne nitrifiante et dénitrifiante et la production de NO et de N_2O dépend directement de la biomasse microbienne. D'autres modèles tels que DAYCENT (Parton et al., 1996), FASSET (Chatskikh et al., 2005) et CERES-EGC (Gabrielle et al., 2006b) ne simulent pas directement l'activité microbienne mais calculent les processus de nitrification et dénitrification avec des fonctions de réponse liées aux variables de l'environnement du sol (humidité, température, substrats, pH). Le tableau 1.8 permet une comparaison des principaux modèles d'écosystème qui simulent les émissions de GES. Nous décrivons ici trois modèles mécanistes d'agro-écosystème : DAYCENT, DNDC et CERES-EGC. DAYCENT et DNDC sont des modèles capables de simuler le fonctionnement de différents écosystèmes (forêt, prairie, culture) alors que le modèle CERES-EGC est dédié aux grandes cultures.

Encadré 3 : Équations de la méthode IPCC pour le calcul des émissions directes de N_2O par les sols cultivés

Le calcul des émissions directes de N_2O par les sols cultivés selon la méthode IPCC (IPCC, 2006) est effectué selon les équations suivantes :

$$N_2O_{directes}{-}N = N_2O{-}N_{N\,entrées} + N_2O{-}N_{SO} + N_2O{-}N_{PPP}$$

avec $N_2O_{directes}$-N : émissions annuelles directes de N_2O-N imputables aux sols gérés, kg N_2O-N an^{-1} ;
N_2O-$N_{N\,entrées}$: émissions annuelles directes de N_2O-N imputables aux apports d'azote N sur les sols gérés, kg N_2O-N an^{-1} ;
N_2O-N_{SO} : émissions annuelles directes de N_2O-N imputables aux sols organiques gérés, kg N_2O-N an^{-1}
N_2O-N_{PPP} : émissions annuelles directes de N_2O-N imputables aux entrées d'urine et de fèces sur les sols pâturés, kg N_2O-N an^{-1}.

Les émissions directes annuelles de N_2O-N imputables aux apports d'azote N sont calculées selon :

$$N_2O{-}N_{N\,entrées} = \left\{ \; [F_{SN} + F_{ON} + F_{RR} + F_{MOS}] \bullet FE_1 \; \right\}$$

avec F_{SN} : quantité annuelle de N d'engrais synthétiques appliquée aux sols, kg N an^{-1} ;
F_{ON} : quantité annuelle d'effluents organiques (composts, boues d'épuration, engrais organiques) appliquée aux sols, kg N an^{-1} ;
F_{RR} : quantité annuelle de N retourné aux sols dans les résidus de récoltes (aériens et souterrains), y compris les cultures fixatrices d'azote, kg N an^{-1} ;
F_{MOS} : quantité annuelle de N minéralisé associé aux pertes de C des sols et de la matière organique des sols en raison de changements d'affectation des terres ou de gestion, kg N an^{-1} ;
FE_1 : facteur d'émissions dues aux entrées de N, kg N_2O–N par kg d'entrées de N. Un facteur d'émissions FE_{1RI} est spécifique à la riziculture inondée.

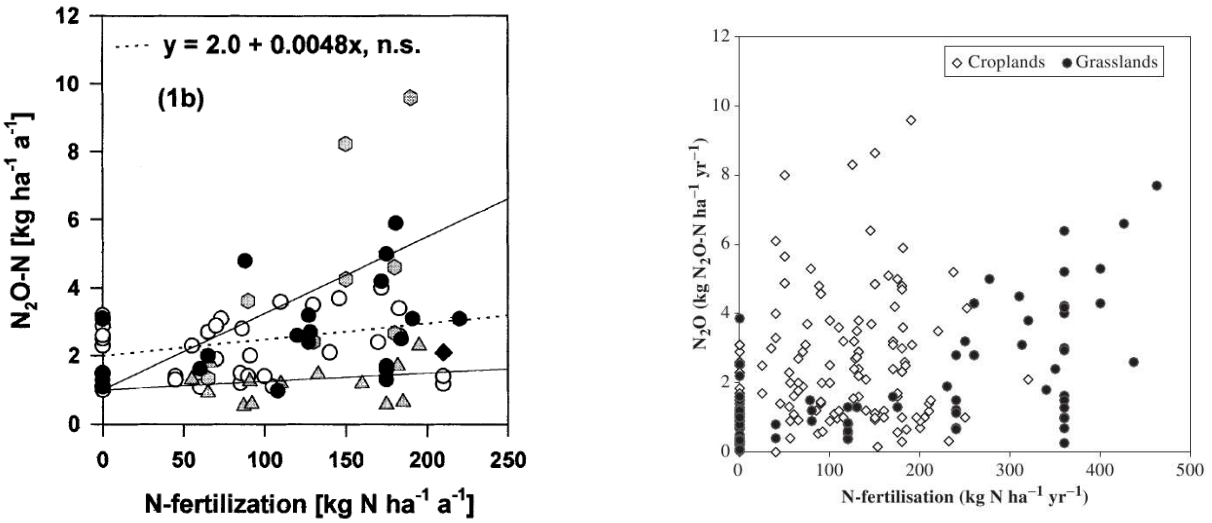

FIG. 1.7 : *Relation entre les apports d'engrais azotés et les émissions de N_2O. Figure de gauche : pour différentes années, différents sites en Allemagne et différentes cultures (représentés par les différents symboles). La ligne en pointillé représente la régression entre les apports de N et les émissions de N_2O, et la ligne continue la relation proposée par l'IPCC (méthodologie 1996, N_2O-N= 1 kg + 1.25 % engrais N ; Kaiser et Ruser (2000)). Figure de droite : émissions annuelles de N_2O en fonction de la quantité d'engrais azoté apportée (Roelandt et al., 2005).*

Présentation des modèles

Le modèle DAYCENT est un modèle d'écosystème à pas de temps journalier adapté du modèle CENTURY (Del Grosso et al., 2000; Parton et al., 2001, 1996). DAYCENT possède un module nommé NGAS qui calcule les émissions de N_2O, NO, N_2. Le modèle simule la croissance des plantes, la décomposition de la matière organique, les flux d'eau, de chaleur et d'azote dans le sol. NGAS calcule les taux de nitrification et de dénitrification selon plusieurs fonctions de réponse liées à la température et au taux de saturation en eau du sol, aux concentrations de NO_3^- et de NH_4^+ et à la respiration du sol. La nitrification est limitée lorsque le contenu en eau du sol est trop faible ou trop élevée. L'humidité optimale correspond à une part de la porosité du sol remplie par l'eau de 55 %. La dénitrification est fonction de la concentration en NO_3^- (accepteur d'e-), de la disponibilité en C labile (donneur d'e-), de l'humidité du sol et des propriétés de texture du sol. La fraction de N_2O résultante de la nitrification est fixée à 2 % des flux d'azote nitrifié. Les émissions de N_2O provenant de la dénitrification augmentent avec le taux de saturation en eau du sol. DAYCENT a été testé avec des données mesurées de GES (Del Grosso et al., 2008) et a été utilisé pour simuler les émissions des sols agricoles à l'échelle des États-Unis (Del Grosso et al., 2005) et à l'échelle du globe (Del Grosso et al., 2009).

Le modèle DNDC (DeNitrification and DeComposition, Li (2000); Li et al. (1992); Zhang et al. (2002)) est un modèle qui simule les cycles biogéochimiques de l'eau, de C et N, à l'échelle de l'écosystème. Il a été développé à la base pour simuler spécifiquement les émissions de N_2O

Model		NGAS-DAYCENT	DNDC	*ecosys*	NLOSS	Expert-N	WNMM	FASSET	CERES-NOE
Time step		Daily	Daily	Seconds–centuries	Daily	Daily	Daily	Daily	Daily
Plant growth		Own	Own and MACRO	Own	CERES	CERES, SUCROS, LEACHM, PLAGEN and SPASS	EPIC, SUCROS, CERES and GRASSGRO	Own	CERES
Water dynamics		Water balance	Water balance	Richards and Green-Ampt equations	Richards equation	Richards equation/water balance	Richards equation/water balance	Water balance	Richards equation
C cycling		8 C pools	8 C pools	6 organic states, 4 organic matter-microbe complexes and 6 biological organization	8 C pools	3–7 C pools	5 C pools	6 C pools	6 C pools
		Gases: CO_2 and CH_4	Gases: CO_2 and CH_4	Gases: CO_2 and CH_4	Gases: CO_2	Gases: CO_2 and CH_4	Gases: CO_2	Gases: CO_2	Gases: CO_2
N cycling		Processes: mineralization, immobilization, ammonia volatilization, nitrification, denitrification and nitrate leaching	Processes: mineralization, immobilization, ammonia volatilization, nitrification, denitrification and nitrate leaching	Processes: mineralization, immobilization, ammonia volatilization, nitrification, denitrification and nitrate leaching	Processes: mineralization, immobilization, ammonia volatilization, nitrification, denitrification and nitrate leaching	Processes: mineralization, immobilization, nitrification, denitrification and nitrate leaching	Processes: mineralization, immobilization, ammonia volatilization, nitrification, denitrification and nitrate leaching	Processes: mineralization, immobilization, ammonia volatilization, nitrification, denitrification and nitrate leaching	Processes: mineralization, immobilization, ammonia volatilization, nitrification, denitrification and nitrate leaching
		Gases: NH_3, NO, N_2O and N_2	Gases: NH_3, NO, N_2O and N_2	Gases: NH_3, N_2O and N_2	Gases: NH_3, N_2O and N_2	Gases: N_2O and N_2	Gases: NH_3, NO (not tested), N_2O and N_2	Gases: NH_3, N_2O and N_2	Gases: NH_3, N_2O and N_2
N_2O emissions	Nitrification	Nitrification: first-order kinetics	Nitrification: nitrifier dynamics	Nitrification: Nitrifier dynamics	Nitrification: nitrifier dynamics	Nitrification: zero or first-order kinetics	Nitrification: first-order kinetics	Nitrification: first-order kinetics	Nitrification: first-order kinetics
		N_2O: fixed proportion (2%)	N_2O: fixed proportion (0.25%)	N_2O: dynamic	N_2O: fixed proportion (0.25%)	N_2O: fixed proportion (0.5%)	N_2O: fixed proportion (0.1–0.5%)	N_2O: fixed proportion (calibrated)	N_2O: fixed proportion (calibrated)
	Denitrification	Denitrification: WFPS threshold driven and first-order kinetics	Denitrification: denitrifier dynamics and "anaerobic balloon" driven	Denitrification: denitrifier dynamics	Denitrification: denitrifier dynamics and "anaerobic balloon" driven	Denitrification: WFPS threshold driven and first-order kinetics	Denitrification: WFPS threshold driven and first-order kinetics	Denitrification: WFPS threshold driven and first-order kinetics	Denitrification: WFPS threshold driven and first-order kinetics
		$N_2O/N_2O/N_2$ ratio division	N_2O: dynamic	N_2O: dynamic	N_2O: dynamic	$N_2O/N_2O/N_2$ ratio division/ first-order kinetics	$N_2O/N_2O/N_2$ ratio division	$N_2O/N_2O/N_2$ ratio division	$N_2O/N_2O/N_2$ ratio division
	Gas diffusion	Soil diffusivity based on soil texture	Diffusion proportion	Dynamic	Dynamic	Dynamic	No	No	No
Source code	Availability	By request	By request	No	By request	No	By request	By request	By request
	Language	C++	C++	FORTRAN	FORTRAN	FORTRAN and Visual Basic	Visual Basic	C++	FORTRAN
Landuse		Crops, pastures and forests	Crops, pastures and forests	Crops, pastures and forests	Crops	Crops	Crops and pastures	Crops and pastures	Crops
Applications		USA, Canada, Australia, New Zealand and Europe	USA, Canada, Australia, New Zealand, Europe, China and India	USA and Canada	Mexico	Germany, UK, USA and Canada	China, Australia, Korea and Mexico	Europe	France

FIG. 1.8 : *Comparaison de la structure et des fonctionnalités de différents modèles d'agro-écosystème (Chen et al., 2008).*

par nitrification et dénitrification, et la décomposition de la matière organique. Il est construit selon deux modules principaux. Le premier consiste en la modélisation du "climat du sol", de la croissance des plantes et de la décomposition des matières organiques qui prédisent les variables de température, d'humidité, de pH, de potentiel redox (Eh) et de concentration des substrats dans le profil du sol. Le second module simule les processus de nitrification, de dénitrification et de fermentation afin de prédire les flux de NO, N_2O, CH_4 et NH_3. Le modèle nécessite comme données d'entrées les données météorologiques journalières qui permettent de simuler à l'échelle horaire, les flux d'eau et de chaleur dans le sol, le profil de potentiel redox et l'absorption d'eau par les racines. Le sous-module de décomposition de la matière organique est basé sur un modèle à 4 compartiments de matière organique analogue au modèle NCSOIL de Molina et al. (1983). La nitrification est contrôlée par la température, l'humidité, le pH et la concentration en NH_4^+ du sol. Le sous-module de dénitrification s'active quand l'humidité du sol augmente ou quand la disponibilité en O_2 diminue, et quand le sol gèle limitant ainsi la diffusion d'O_2. La dénitrification est simulée selon la réaction séquentielle ($NO_3^- \rightarrow NO_2^- \rightarrow NO \rightarrow N_2O \rightarrow N_2$) qui dépend des conditions d'oxydo-réduction, du pH, du carbone dissous disponible et des cinétiques des différentes réactions. Le concept de "ballon anaérobique" (*anaerobic balloon*) a été développé afin de diviser la matrice du sol en zones aérobie et anaérobie. En simulant la diffusion et la consommation d'O_2 dans le sol, le modèle calcule l'accroissement et la diminution du ballon anaérobique. Ainsi seulement les substrats de la zone anaérobie sont utilisés pour la dénitrification. Les deux processus de nitrification et dénitrification peuvent avoir lieu simultanément.
Le modèle DNDC a été largement appliqué à travers le monde dans différentes conditions de sol et de climat pour différents écosystèmes (Babu et al., 2006; Beheydt et al., 2008, 2007; Kurbatova et al., 2008; Pathak et al., 2005; Tonitto et al., 2007). Le modèle est également utilisé pour produire des inventaires de gaz à effet de serre à échelle nationale et continentale (Butterbach-Bahl et al., 2004; Leip et al., 2008; Li et al., 2001).

Le modèle CERES-EGC (Crop Environment REsource Synthesis - Environnement et Grandes Cultures[2]) est basé sur la famille des modèles CERES développés aux États-Unis par Jones et Kiniry (1986). Ces modèles sont développés et diffusés au sein du réseau international DSSAT (Decision Support System for Agrotechnology Transfert[3]) ce qui permet sa validation dans différentes conditions pédoclimatiques et agricoles. Les modèles mécanistes de croissance de culture sont regroupés au sein d'une plate-forme modulaire et partagent le même sous-modèle pour simuler les dynamiques de l'eau, de C et N dans le sol. Le modèle CERES-EGC est conçu de manière similaire bien qu'il ait ses propres modules de transfert d'eau, de chaleur et de solutés dans le sol (Gabrielle et al., 1995), et de décomposition de la matière organique basé sur NCSOIL (Gabrielle et al., 2002a; Molina et al., 1983). Le modèle CERES-EGC simule le développement et la croissance de nombreuses cultures (maïs, blé, orge, colza, sorgho, tournesol, pois, betterave, soja) à un pas de temps journalier. L'originalité du modèle CERES-EGC est sa conception basée sur l'évaluation des impacts environnementaux des cultures. En conséquence, les fonctions de production sont couplées avec des modules d'émissions vers l'environnement

[2]www-egc.grignon.inra.fr/ceres_mais/ceres.html
[3]www.icasa.net/dssat

(Fig. 1.9). Les émissions de N_2O sont calculées avec le module NOE (Nitrous Oxide Emission, Hénault et al. (2005a)). Dans ce module, la dénitrification dépend du potentiel de dénitrification du sol, du ratio $\frac{N_2O}{N_2O+N_2}$, qui sont mesurés in situ selon les méthodologies de Hénault et Germon (2000) et Garrido et al. (2002), et de trois variables de contrôle : la température, l'humidité et la concentration en NO_3^- du sol. La nitrification est calculée de la même manière : le taux potentiel de nitrification (mesuré in situ) est multiplié à des facteurs de température et d'humidité du sol. Les émissions de N_2O résultantes de ces processus sont des fractions constantes des flux d'azote nitrifiés et dénitrifiés. Le module d'émissions de N_2O est détaillé dans le chapitre 2. Le modèle CERES-EGC simule également les émissions de NO (Rolland et al., 2008), les échanges d'ammoniac entre le système sol-plante et l'atmosphère selon le concept de Génermont et Cellier (1997) et les échanges de CO_2 sol-plante-atmosphère (chap. 3).
Les modules de croissance de culture du modèle CERES-EGC ont été largement validés à travers le monde (Gabrielle et al., 2002b; Langensiepen et al., 2008; Rezzoug et al., 2008; Xiong et al., 2007). De plus, le modèle a été appliqué à diverses problématiques de bilans environnementaux des activités agricoles aux échelles parcellaires et régionales (Gabrielle et al., 2005; Gabrielle et Gagnaire, 2008; Gabrielle et al., 2006b).

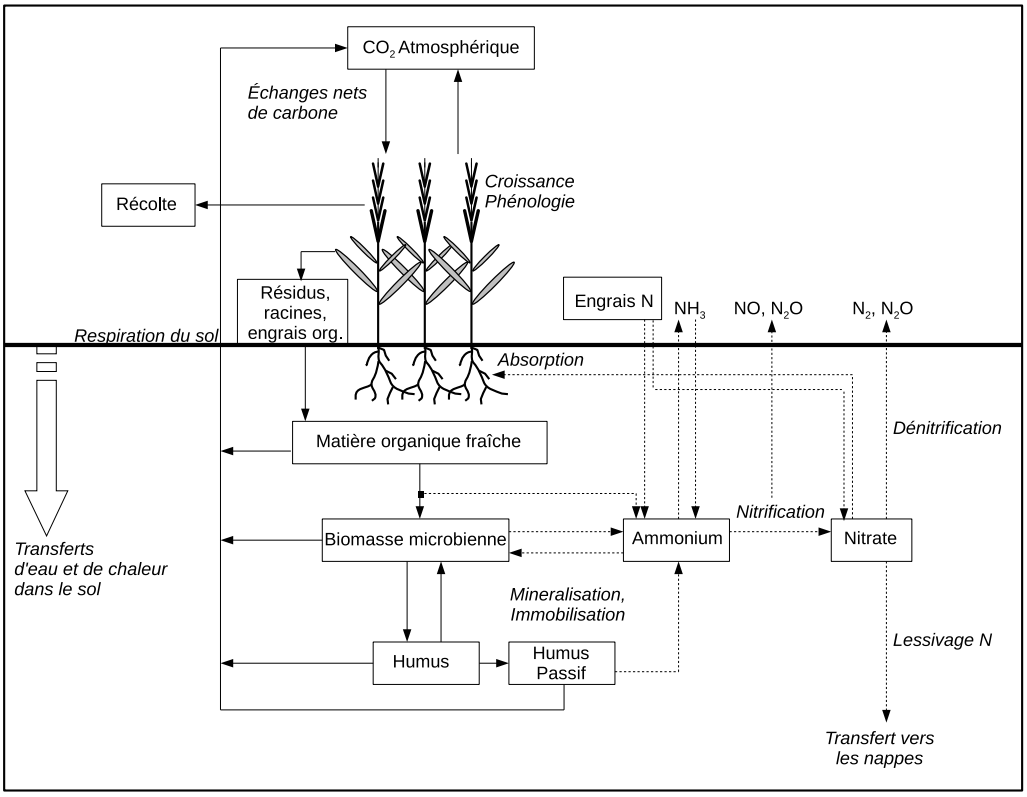

FIG. 1.9 : *Représentation schématique générale du modèle CERES-EGC.*

Comparaison des modèles

Une multitude d'autres modèles existent pour simuler les émissions de GES des écosystèmes agricoles qui ont chacun été développé selon une approche et des objectifs spécifiques. Les modèles mécanistes dynamiques permettent d'analyser la variabilité des émissions de GES en lien avec la variabilité journalière, saisonnière et inter-annuelle du climat, les types de sol et la gestion des pratiques agronomiques. Il existe actuellement peu de comparaisons des modèles basées sur la qualité de prédiction des émissions de N_2O en relation avec des données observées (Frolking et al., 1998; Gabrielle et al., 2006b; Li et al., 2005b).

Frolking et al. (1998) ont comparé les performances des modèles DAYCENT, DNDC, Expert-N et NASA-CASA avec des mesures de N_2O provenant de 5 sites de culture et de prairie différenciés selon le climat, les pratiques agricoles et le niveau d'émissions observées. Les simulations ont été réalisées sur deux années consécutives et comparées avec les données observées. Tous les modèles prédisent des dynamiques de N dans le sol comparables mais les flux de gaz trace sont assez différents entre les modèles. Les modèles DAYCENT et Expert-N prédisent des émissions les plus proches des observations alors que DNDC et NASA-CASA sont moins performants. De plus, aucun des modèles n'a pu simuler les brefs pics d'émission consécutifs aux épisodes de gel observés sur un site de culture en Allemagne. Cette comparaison de modèles ne permet pas d'identifier un modèle plus performant mais préconise de porter les efforts de développement sur la modélisation des contenus en eau dans le sol et de sa relation avec les émissions de N_2O. Depuis cette étude, les modèles DAYCENT et DNDC ont largement évolué et Chen et al. (2008) recommandent de réaliser une nouvelle comparaison de ces modèles.

Li et al. (2005b) ont couplé le modèle WNMM (*Water and Nitrogen Management Model*) avec 3 modules d'émissions de N_2O (comprenant les processus de nitrification et dénitrification) provenant de DNDC, DAYCENT et le propre module de WNMM. Les processus de transfert d'eau, de chaleur et de solutés dans le sol, de décomposition de la matière organique et de croissance des plantes étaient simulés avec les équations propres à WNMM. La comparaison a été réalisée avec des observations de N_2O provenant de 3 sites expérimentaux. Au final, les auteurs concluent que la performance des modèles est comparable au regard des simulations des dynamiques de NO_3^- et NH_4^+ dans les 20 premiers cm de sol, mais que l'approche simplifiée utilisée dans WNMM est plus performante que DNDC et DAYCENT pour simuler les émissions de N_2O.

De la même manière que Li et al. (2005b), Gabrielle et al. (2006b) ont couplé les modules d'émissions de N_2O, NOE et NGAS, en incluant la nitrification et la dénitrification propres à chaque module, au modèle sol-plante CERES. La performance de CERES-NOE et CERES-NGAS a été testée avec trois jeux de données collectés dans la Beauce (France). CERES-NGAS a tendance à surestimer les émissions de N_2O dans les trois sites du fait d'une réponse excessive des émissions de N_2O au contenu en eau du sol. CERES-NOE parvient à simuler les niveaux moyens d'émissions pour les trois sites mais échoue à simuler les pics d'émissions qui suivent les apports d'engrais N. La meilleure performance de CERES-NOE tient en partie à l'inférence de paramètres locaux mesurés in situ.

La comparaison des modèles ne permet pas de faire ressortir le modèle idéal, qui serait multi-écosystèmes, multi-échelles, multi-polluants et qui permettrait de répondre à divers objectifs. Le défi actuel est plutôt d'améliorer les modèles existants selon une démarche de progrès qui permet d'inclure de nouveaux processus, et de les tester et les calibrer avec des observations provenant de conditions agro-pédoclimatiques variées. Les objectifs de l'approche par modélisation sont de pouvoir quantifier les flux de GES là où les mesures ne sont pas envisageables de manière exhaustive, de prendre en compte les conditions locales du milieu et de gestion des pratiques agricoles là où les méthodes par facteurs d'émissions échouent, et enfin de pouvoir appliquer les modèles avec une incertitude mimimum pour tout nouveau site d'étude ou dans l'optique d'une extrapolation spatiale.

1.3 Objectif et démarche de modélisation

Les échanges de gaz à effet de serre (azotés et carbonés) entre les écosystèmes cultivés et l'atmosphère dépendent étroitement de processus liés à l'activité microbiologique des sols (nitrification, dénitrification, minéralisation) et aux processus physiologiques de croissance des cultures. Ces processus sont eux-mêmes régulés par les conditions climatiques, le type de sol et sa structure, la culture en place et sa gestion par l'agriculteur. Pour quantifier les échanges nets de GES, l'utilisation de modèles mécanistes simulant les processus biophysiques sous-jacents est actuellement l'approche qui semble la plus prometteuse. De plus, modéliser les processus avec une approche intégrée permet de prédire les modifications du système en réponse à des forçages anthropiques, d'intégrer les flux dans le temps, d'extrapoler les modèles dans l'espace et de tester des scénarios de pratiques culturales visant à réduire ces émissions. L'objectif central de ce travail est de **modéliser les émissions de N_2O et les échanges nets de CO_2 à l'échelle de la parcelle pour prédire le pouvoir de réchauffement global (PRG) des systèmes de cultures**.

Le développement des modèles mécanistes -dans le cas de ce travail, des modèles biophysiques dynamiques- nécessite de suivre différentes étapes de progression qui sont décrites dans la partie suivante. Ce travail de thèse se situe dans cette démarche et a pour objectif de l'appliquer au modèle CERES-EGC.

1.3.1 Boucle de progrès des modèles

La (re)formulation des modèles, leur calibration et leur évaluation sont des étapes primordiales pour permettre leur application. L'utilisation des données observées joue un rôle central dans la calibration et l'évaluation des modèles. Williams et al. (2009) définit le concept de "fusion modèle-données" (*model-data fusion, MDF*) comme une série de procédures qui combine les données avec le modèle, tout en quantifiant l'incertitude respective des deux parties. Notre démarche se rapproche de celle-ci en suivant les étapes décrites en Fig. 1.10.

La boucle de progrès a comme intérêt d'intégrer les nouvelles connaissances sur les processus élémentaires. Elle a pour effet le développement d'un système complexe qui intègre différentes

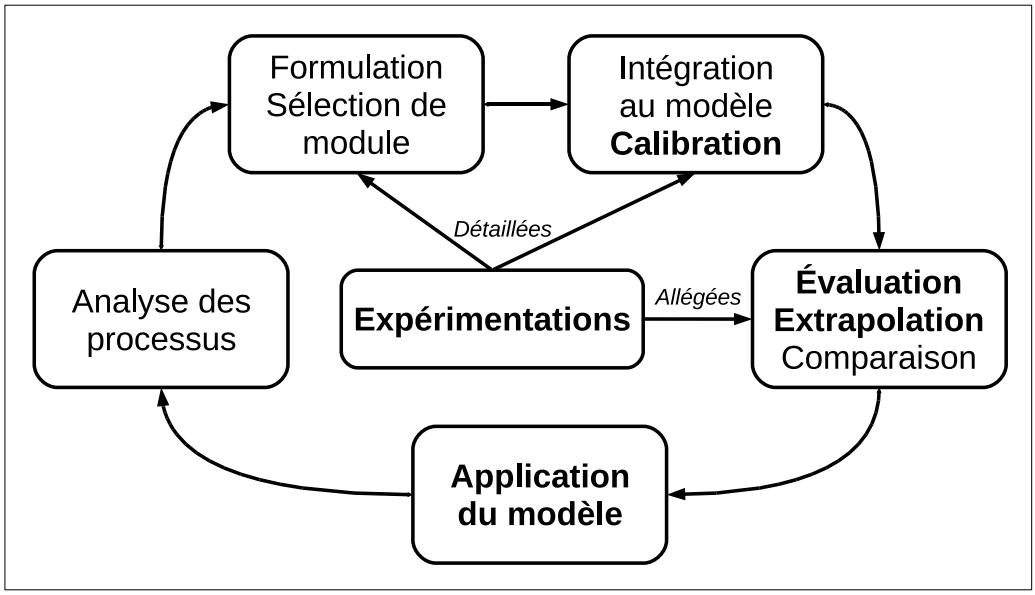

FIG. 1.10 : *Schéma de développement et d'application des modèles d'agro-écosystème (adapté de Williams et al. (2009) et Gabrielle (2006a)).*

composantes (eau, sol, plante, microflore du sol) et différents niveaux d'organisation. Le caractère heuristique de la boucle de progrès permet d'améliorer la compréhension du fonctionnement des écosystèmes. La boucle a également un intérêt opérationnel, elle peut commencer par une définition d'un objectif de développement en relation avec son application future. Pour cela, les équations relatives aux processus étudiés sont sélectionnées et formulées, avant d'être intégrées au code existant sous forme d'un module qui doit rester compréhensible séparément du reste du modèle.

La **calibration** est une étape majeure. En effet, les modèles décrits ci-dessus ont l'inconvénient d'impliquer un nombre très important de paramètres pour simuler les nombreux processus en jeu. Chaque paramètre contient une part d'incertitude qui lui est propre et souvent mal connue, ce qui rend les sorties des modèles très incertaines. La mise au point de méthodes de calibration des paramètres couplées avec une quantification de l'incertitude des paramètres et des sorties du modèle est un défi majeur (Sutton et al., 2007). Les principales méthodes de calibration des modèles sont décrites dans l'encadré 4.
Comme il semble illusoire de pouvoir estimer simultanément un nombre important de paramètres ($>$20), une étape de sélection d'un sous-ensemble de paramètres en amont de l'étape de calibration est nécessaire (Harmon et Challenor, 1997; Makowski et al., 2006). Les méthodes d'analyse de sensibilité globale permettent d'estimer les paramètres qui ont le plus d'influence sur les variables de sorties et donc de déterminer les paramètres à estimer avec les données. Les paramètres qui ont le moins d'influence conservent leurs valeurs nominales (Monod et al., 2006).

Encadré 4 : Méthodes de calibration des paramètres

L'objectif de l'étape de calibration (ou d'estimation) des paramètres est de déterminer une valeur approchée des paramètres du modèle à partir de données observées. Deux grandes familles de méthodes d'estimation se différencient selon une approche fréquentiste ou une approche bayésienne.
La description des méthodes ci dessous provient de Makowski et Jeuffroy (2002a) et Makowski et al. (2006). Les approches fréquentistes utilisent des méthodes d'estimation qui permettent d'approcher une valeur fixe du vecteur de paramètres en utilisant un échantillon de données. Elles utilisent des fonctions appelées estimateurs qui permettent de relier les valeurs estimées des paramètres aux données observées.
La méthode des moindres carrés ordinaires est appliquée quand un seul de type de mesure est utilisé pour calculer l'estimateur du vecteur des paramètres. Celui-ci minimise la somme des carrés des écarts entre les observations et les prédictions. Cette méthode est mise en application pour des modèles non-linéaires avec des algorithmes itératifs de type Gauss-Newton. Le principal défaut de ces méthodes locales est que le résultat est très dépendant de la valeur de départ du vecteur de paramètres et que l'algorithme peut converger vers un minimum local. Des algorithmes itératifs d'optimisation globale permettent de s'assurer d'une convergence vers le minimum global (eg, l'algorithme du «recuit simulé»). La méthode des moindres carrés pondérés permet d'estimer les paramètres quand plusieurs types de mesures sont disponibles. L'estimateur des moindres carrés pondérés minimise la somme des carrés des écarts pondérés par les variances sur les mesures obtenues par les répétitions. Dans les cas où il n'y a pas ou peu de répétitions, on peut définir un modèle de variance et utiliser la méthode du maximum de vraisemblance pour estimer les paramètres.

L'utilisation de la connaissance a priori sur les paramètres peut être mise à profit avec les **méthodes bayésiennes**, dont la première étape est la définition de la distribution a priori et la deuxième étape est le calcul de la distribution a posteriori.
La distribution a priori peut être définie comme une loi uniforme dont les bornes définissent une gamme de variation des paramètres et reflète le niveau d'incertitude des valeurs de paramètres avant de les confronter avec les données observées. L'étape suivante consiste à estimer une nouvelle distribution des paramètres à partir des données expérimentales en utilisant le théorème de Bayes. La distribution des paramètres obtenue est alors appelée **distribution a posteriori** et reflète à la fois les données de la littérature et les données expérimentales. Différentes valeurs des paramètres, par exemple l'espérance ou le mode de la distribution a posteriori, peuvent alors être utilisés dans le modèle. De plus, la distribution a posteriori permet de générer la distribution de probabilité des sorties du modèle et ainsi de quantifier l'incertitude du modèle. L'application des méthodes bayésiennes aux modèles non-linéaires requiert l'utilisation d'algorithmes de type Markov Chain Monte Carlo (MCMC), comme l'algorithme de Metropolis-Hastings décrit en détail dans le chapitre 2.

L'évaluation des modèles est réalisée en aval de la calibration. Les prédictions sont confrontées aux mesures observées indépendantes et des indicateurs statistiques permettent de juger de la performance du modèle (Makowski et Jeuffroy, 2002b; Wallach, 2006). Les données pour l'évaluation doivent être indépendantes des données utilisées pour construire ou calibrer les modèles. L'évaluation permet de juger de la qualité de prédiction du modèle et quantifie l'erreur de prédiction (Wallach, 2006). Un choix doit donc être effectué quant à l'utilisation des données pour la calibration ou l'évaluation. Par ailleurs, le **test multi-sites** du modèle, grâce à un réseau multi-local de mesures, permet de s'assurer de sa robustesse à couvrir diverses conditions agro-pédoclimatiques. Cette étape est indispensable avant d'envisager une extrapolation spatiale du modèle. Une étape supplémentaire pour l'évaluation concerne la comparaison des modèles sur la base de jeux de données identiques. Nous avons vu dans la section 1.2.4.3 qu'elle a été assez peu appliquée pour les modèles d'écosystème mais est envisagée en perspective de cette thèse.

La mise en place d'**expérimentations** détaillées ou allégées permet d'appliquer les étapes de calibration et d'évaluation. Les données nécessaires pour la calibration des modèles ont besoin d'être détaillées, d'être mises en place sur plusieurs années avec une fine résolution temporelle et avec une incertitude quantifiée. Les observations doivent comprendre à la fois les données de flux mais aussi les variables qui régulent les processus. Par exemple, le suivi de l'humidité du sol, de sa concentration en azote et de la production de biomasse sont des données indispensables qui permettent de s'assurer de la pertinence globale du système simulé. Les mesures intensives de flux de GES peuvent être assurées en continu par la méthode des chambres automatiques ou par les méthodes micrométéorologiques. Les données pour le test multi-sites sont plus allégées et les points de mesure peuvent être ponctuels dans le temps. La mise en place de chambres manuelles convient à ce type de suivi.

L'étape d'**application du modèle** permet d'extrapoler les flux dans le temps, pour produire des bilans, ou dans l'espace, pour produire des inventaires. Cette étape ne peut être envisagée à condition que les étapes de calibration et d'évaluation aient été réalisées. Le passage de l'étape de la formulation ou d'intégration directement à l'étape d'application n'est pas concevable sans un minimum de vérifications de la performance avec des données expérimentales.

La confrontation du modèle avec des données expérimentales et son application permet d'identifier les processus manquants qui nécessitent d'être examiné. Par exemple, les processus d'échanges de CH_4, de consommation de N_2O par le sol, et les émissions de N_2O consécutives aux épisodes de gel-dégel ont été identifiés comme manquants ou inadaptés dans les modèles d'agro-écosystème (Frolking et al., 1998). Ils devront être caractérisés par des mesures au laboratoire et au champ puis intégrés au modèle. Le retour à l'étape d'analyse des processus ou d'intégration peut également être envisagé à la suite de l'étape de calibration ou d'évaluation. Si un paramètre considéré comme universel se révèle varier d'un site à un autre ou varier dans le temps, il est probable que certains mécanismes sont manquants dans le modèle et qu'il faut de nouveau analyser les processus. De même, si l'étape d'évaluation montre que la qualité de

prédiction du modèle est faible, la comparaison de modules puis leur intégration dans le modèle peuvent être requises.

1.3.2 Sélection du modèle et application de la boucle de progrès

Sélection du modèle CERES-EGC

Pour ce travail de thèse, nous avons choisi d'utiliser le modèle CERES-EGC. La comparaison des modèles d'agro-écosystème capables de simuler les émissions de N_2O n'a pas permis d'identifier un modèle mécaniste plus performant (voir partie 1.2.4.3). De plus, l'incertitude des modèles et leur qualité de prédiction n'ont pas été quantifiées et une comparaison selon ces caractéristiques n'est pas possible (Chen et al., 2008). Par ailleurs, les modèles multi-écosystèmes, tels que DAYCENT et DNDC, ne sont pas spécifiquement développés pour simuler les systèmes de cultures et leur productivité. En revanche, le modèle CERES-EGC est développé à l'unité Environnement et Grandes Cultures depuis une quinzaine d'années avec comme objectif central de réaliser le bilan environnemental des systèmes de cultures. De plus, les modèles de culture CERES sont développés depuis les années 80 et ont démontré leur capacité à simuler la croissance des cultures à travers le monde (voir partie 1.2.4.3). Par ailleurs, le modèle CERES-EGC inclut des modules d'émissions de gaz traces, dont les émissions de N_2O, et il peut simuler le cycle du carbone de l'écosystème cultivé dans son ensemble. Enfin, CERES-EGC a été sélectionné comme un des modèles centraux (*core mode*) du projet NitroEurope et son investissement dans ce projet doit permettre d'améliorer l'évaluation des bilans de GES des cultures en Europe.

Ce travail de thèse a pour objectif de modéliser les bilans de GES des agro-écosystèmes. Pour cela, nous avons appliqué la boucle de progression des modèles à CERES-EGC et, plus particulièrement, nous nous sommes consacrés aux étapes de **calibration**, d'**évaluation**, de **test multi-sites** et d'**application** (indiquées en gras dans la Fig. 1.10 et décrites dans la partie 1.3.1). Ces étapes sont cruciales pour répondre à notre objectif et compte tenu de l'état de l'art, nous avons montré que les modèles nécessitent d'être calibrés selon des méthodes adaptées telle que la calibration bayésienne. Par ailleurs, l'évaluation doit être bien distincte de la phase de calibration et les jeux de données utilisés pour ces étapes doivent être indépendants. Enfin, le test multi-sites permet d'évaluer la robustesse du modèle à simuler tout nouveau site et est une étape préalable pour l'extrapolation spatiale.

Sélection des paramètres et calibration

Lamboni et al. (2009) ont mis au point une méthode de **sélection des paramètres** basée sur une analyse de sensibilité globale multivariée pour les modèles dynamiques décrite en détail en annexe B. Nous avons appliqué cette méthode au modèle CERES-EGC afin d'identifier les paramètres à estimer par calibration bayésienne. De plus, nous avons montré que l'écart quadratique moyen (MSEP) entre les valeurs prédites par le modèle et les observations diminue dès lors qu'on estime les paramètres les plus sensibles (voir annexe B ; Lamboni et al. (2009)). Cette méthode a été appliquée pour sélectionner les six paramètres les plus sensibles du module d'émissions de N_2O de CERES-EGC avant de les estimer par calibration bayésienne (voir chap. 4).

La méthode de calibration bayésienne développée dans ce projet est décrite en détail dans le chapitre 2. Nous rappelons ici, brièvement, les raisons de ce choix.
Dans le cas des modèles biophysiques, tel que CERES-EGC, les paramètres que nous étudions ont une signification biologique ou physique. Il est donc possible d'obtenir des informations a priori sur les valeurs de ces paramètres par une étude des travaux antérieurs publiés dans la littérature. Par exemple, les paramètres de potentiel de dénitrification des sols ou l'efficience de conversion du rayonnement en biomasse (RUE) sont des paramètres largement décrits dans la littérature (voir chapitres 2 et 3), ce qui permet de leur attribuer une distribution de probabilités a priori. Il semble donc important d'utiliser cette connaissance a priori pour estimer les paramètres et seules les méthodes bayésiennes permettent cette prise en compte. Par ailleurs, la calibration bayésienne permet de quantifier l'incertitude des sorties du modèle et la méthode peut être appliquée efficacement même avec très peu de données. Enfin, la calibration bayésienne est une méthode qui permet de mettre à jour continuellement la distribution a posteriori dès qu'un nouveau jeu de données est disponible.
Un des objectifs principaux du projet NitroEurope est de diminuer l'incertitude des modèles d'écosystème selon une approche bayésienne (Van Oijen et al., 2005). Ce travail de thèse s'inscrit dans cette démarche et a participé au développement du protocole technique et de programmation informatique du projet NitroEurope (Lehuger et al., 2008).

Évaluation

Le modèle CERES-EGC calibré a été évalué sur sa performance à simuler les flux de CO_2 (chap. 3) et les émissions de N_2O (chap. 4) avec des jeux de données mesurées indépendants . Des représentations graphiques des prédictions du modèle vs. les valeurs observées permettent d'évaluer en un coup d'œil si les mesures prédites correspondent aux valeurs observées (chap. 3). Une autre représentation graphique consiste à comparer les données mesurées et prédites en fonction du temps (chaps. 2, 3, 4). Enfin, nous avons évalué le modèle en calculant des indicateurs de performance comme l'erreur quadratique moyenne de prédiction : MSEP, *mean squared error of prediction*, et le RMSEP, *root mean squared error of prediction* (chaps. 3, 4). L'évaluation nous a permis de quantifier l'erreur de prédiction, de juger de la confiance que l'on peut accorder aux résultats et d'envisager des améliorations pour faire progresser le modèle.

Expérimentations

Le site d'étude de Grignon (78, France), suivi pendant ce travail de thèse, se compose d'une parcelle principale avec une rotation maïs-blé-orge-moutarde sur laquelle est assurée un suivi intensif des émissions de N_2O avec des chambres automatiques et manuelles et des flux de CO_2 avec la méthode d'*eddy covariance*. Trois parcelles annexes supplémentaires, pour lesquelles, la rotation de la parcelle principale est décalée de 0, 1 et 2 ans afin d'avoir toutes les cultures chaque année, sont suivies de manière plus allégée avec la méthode des chambres manuelles. Les mesures aux champs effectuées pendant ce travail de thèse ont été consacrées spécifiquement aux mesures de GES avec la technique des chambres manuelles sur les quatre parcelles de Grignon et au suivi des concentrations en N et d'humidité du sol.
Par ailleurs, l'investissement de l'unité EGC dans les réseaux de mesures européens NitroEurope

et CarboEurope ont permis de partager les données entre expérimentateurs et modélisateurs et de pouvoir utiliser les données provenant de différents sites européens. L'utilisation de données antérieures permet aussi de multiplier le nombre de jeux de données.

Applications

L'étape d'application de CERES-EGC a permis de réaliser des bilans de GES des agro-écosystèmes en prenant en compte de manière intégrée les différents flux à l'interface sol-plante-atmosphère (chap. 4). Le modèle permet également d'estimer des facteurs d'émissions de N_2O et des bilans de C à l'échelle de rotations de cultures (chaps. 2, 3). Par ailleurs, l'application du modèle permet de comparer différents scénarios de mitigation en vue d'une réduction des émissions des systèmes de cultures (chap. 4). Enfin, la calibration et l'évaluation multi-sites permettent d'envisager l'extrapolation spatiale du modèle afin de produire des inventaires spatialisés des émissions de N_2O (chap. 5 et annexe A).

1.4 Organisation du mémoire

Le modèle CERES-EGC est approprié pour répondre à l'objectif général de modélisation des bilans de GES des agro-écosystèmes, cependant, il nécessite d'être développé pour la prédiction des flux de N_2O et de CO_2 à l'échelle de la parcelle, selon la boucle de progression décrite ci-dessus.
La démarche générale mise en œuvre pendant cette thèse peut être résumée selon les trois sous-objectifs suivants qui correspondent aux chapitres 2, 3 et 4 de ce mémoire et qui sont représentés schématiquement en Fig. 1.11 :

1. **Améliorer la prédiction des émissions de N_2O**
   Le module d'émissions de N_2O de CERES-EGC est calibré par calibration bayésienne grâce à une base de données multi-sites de mesures d'émissions de N_2O. La méthodologie de calibration bayésienne avec l'application de chaînes de Markov Monte Carlo selon l'algorithme de Metropolis-Hastings a été appliquée et développée pour les modèles d'agro-écosystème. Une base de données constituée de jeux de données indépendants représentatifs du nord de la France a permis de comparer une procédure de calibration site-par-site ou multi-sites et de déterminer un jeu de paramètres universel dont les valeurs sont le meilleur compromis pour une extrapolation spatiale.
2. **Prédire les échanges nets de CO_2**
   Le modèle CERES-EGC est calibré pour simuler les échanges nets de CO_2 entre le système sol-plante et l'atmosphère pour différentes conditions pédoclimatiques à l'échelle de rotations de cultures. La qualité de prédiction du modèle est évaluée avec deux jeux de données indépendants de mesures des échanges nets de l'écosystème. L'application du modèle permet de quantifier les bilans nets de C à l'échelle de rotations de cultures pour trois sites en Europe.

3. **Estimer le pouvoir de réchauffement global d'agro-écosystèmes**
   Le modèle CERES-EGC est calibré sur un nouveau jeu de données d'émissions de N_2O journalières et en continu provenant du site expérimental de Grignon (Fr.). Sa qualité de prédiction pour simuler les émissions de N_2O journalières est évaluée sur trois parcelles annexes à Grignon et sur un site expérimental en Allemagne. Le modèle est ensuite appliqué pour quantifier les émissions directes de N_2O et de CO_2, et une estimation des flux de CH_4 basée sur des mesures permet de réaliser le bilan des flux de GES qui ont lieu au champ. Les émissions indirectes provenant de la production des intrants, de leur transport jusqu'à la ferme et des opérations culturales sont également prises en compte selon une approche d'analyse de cycle de vie. Enfin, le pouvoir de réchauffement global des rotations de cultures est quantifié en combinant les différents flux. De plus, plusieurs scénarios de mitigation sont testés afin de proposer des pistes de réduction.

Les trois chapitres sont présentés sous forme d'articles. Le premier article a été accepté pour publication dans une revue à comité de lecture, le deuxième est soumis et le troisième est prêt à être soumis pour publication.
La dernière partie du mémoire présente la synthèse des principaux résultats et les perspectives envisagées qui portent principalement sur **l'extrapolation spatiale** des modèles d'agro-écosystème à une échelle régionale.

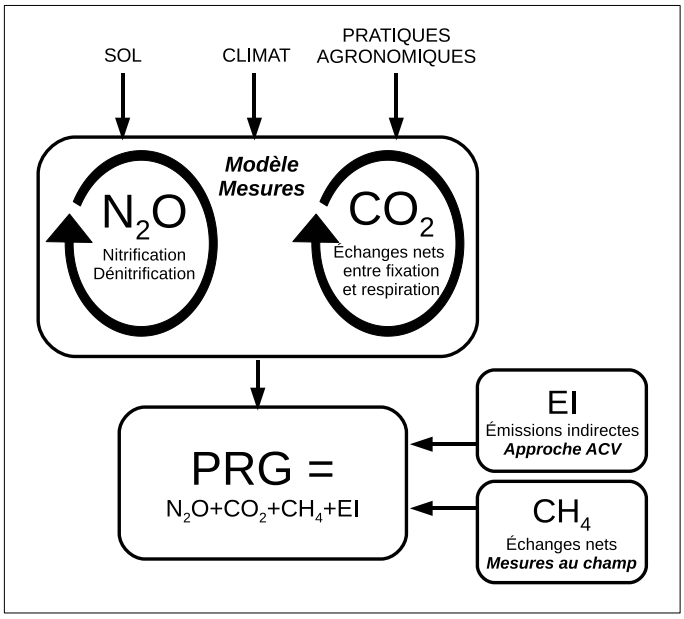

FIG. 1.11 : *Démarche générale de la thèse dont l'objectif central est de prédire le pouvoir de réchauffement global (PRG) des agro-écosystèmes en modélisant les flux de N_2O et de CO_2 et en appliquant la boucle de progrès au modèle CERES-EGC. Sont ajoutés les émissions indirectes (EI) estimées selon une approche d'analyse de cycle de vie (ACV) et les flux nets de CH_4.*

Chapitre 2

Calibration bayésienne d'un module d'émissions de protoxyde d'azote d'un modèle d'agro-écosystème

Ce chapitre est consacré à la calibration bayésienne du module d'émissions de N_2O du modèle d'agro-écosystème CERES-EGC. Il est présenté sous la forme d'un article qui a été accepté en 2009 pour publication dans la revue *Agriculture, Ecosystems and Environment*. Il s'intitule : "Bayesian calibration of the nitrous oxide emission module of an agroecosystem model" et les co-auteurs sont : B. Gabrielle[a], M. van Oijen[b], D. Makowski[c], J.-C. Germon[d], T. Morvan[e] et C. Hénault[d].
Les émissions de N_2O, en réponse aux apports d'engrais azotés, sont un terme clé dans le bilan des échanges de gaz à effet de serre des agro-écosystèmes. Comme présenté en introduction, les modèles simulant ces émissions nécessitent d'être développés et, dans un premier temps, il convient d'estimer les paramètres du modèle avec des données. La première étape de ce travail consiste donc à développer une méthode de calibration bayésienne pour estimer les paramètres du module d'émissions de N_2O de CERES-EGC. Ce module simule les processus de nitrification et dénitrification et les émissions de N_2O résultantes. Il inclut 11 paramètres globaux considérés comme invariants dans le temps et dans l'espace qui sont estimés par une calibration bayésienne. Celle-ci est mise en œuvre grâce à une base de données d'émissions de N_2O collectées sur 7 sites expérimentaux en France. Il en résulte que le modèle est fortement amélioré et que l'incertitude des sorties est réduite. Enfin, une méthode basée sur la calibration "multi-sites" permet d'estimer les valeurs universelles des paramètres qui serviront à extrapoler le modèle dans l'espace.

a : UMR 1091 INRA-AgroParisTech Environnement et Grandes Cultures, Thiverval-Grignon, France.
b : Centre for Ecology and Hydrology-Edinburgh, Bush Estate, Penicuik, UK.
c : UMR 211 INRA-AgroParisTech Agronomie, Thiverval-Grignon, France.
d : UMR 1229 Microbiologie du sol et de l'environnement, Dijon, France.
e : UMR 1069 INRA-Agrocampus Sol Agro et hydrosystème Spatialisation, Rennes, France.

Abstract

Nitrous oxide (N_2O) is the main biogenic greenhouse gas contributing to the global warming potential (GWP) of agro-ecosystems. Evaluating the impact of agriculture on climate therefore requires a capacity to predict N_2O emissions in relation to environmental conditions and crop management. Biophysical models simulating the dynamics of carbon and nitrogen in agro-ecosystems have a unique potential to explore these relationships, but are fraught with high uncertainties in their parameters due to their variations over time and space. Here, we used a Bayesian approach to calibrate the parameters of the N_2O submodel of the agro-ecosystem model CERES-EGC. The submodel simulates N_2O emissions from the nitrification and denitrification processes, which are modelled as the product of a potential rate with three dimensionless factors related to soil water content, nitrogen content and temperature. These equations involve a total set of 15 parameters, four of which are site-specific and should be measured on site, while the other 11 are considered global, i.e. invariant over time and space. We first gathered prior information on the model parameters based on literature review, and assigned them uniform probability distributions. A Bayesian method based on the Metropolis-Hastings algorithm was subsequently developed to update the parameter distributions against a database of seven different field-sites in France. Three parallel Markov chains were run to ensure a convergence of the algorithm. This site-specific calibration significantly reduced the spread in parameter distribution, and the uncertainty in the N_2O simulations. The model's root mean square error (RMSE) was also abated by 73% across the field sites compared to the prior parameterization. The Bayesian calibration was subsequently applied simultaneously to all data sets, to obtain better global estimates for the parameters initially deemed universal. This made it possible to reduce the RMSE by 33% on average, compared to the uncalibrated model. These global parameter values may be used to obtain more realistic estimates of N_2O emissions from arable soils at regional or continental scales.

Keywords

Bayesian calibration ; Parameter uncertainty ; CERES-EGC, Nitrous oxide ; Markov Chain Monte Carlo ; Greenhouse gases

2.1 Introduction

Soils are the main source of nitrous oxide (N_2O) in the atmosphere, via the microbial processes of nitrification and denitrification. Because of its heavy reliance on synthetic N-fertilisers, agriculture has enhanced these two processes, as a result of which agro-ecosystems contribute 55-65% of the global anthropogenic emissions of N_2O. Compared to other ecosystem types or economic sectors, they are thus responsible for the major part of the atmospheric build-up of N_2O (Smith et al., 2007). Compared to other greenhouse gases (GHG) such as CO_2, N_2O fluxes are of small magnitude and highly variable in space and time, being tightly linked to the local climatic sequence and soil properties.
Predicting N_2O emissions from agro-ecosystems thus requires taking into account complex processes and interactions which originate from both environmental conditions and agricultural practises (Duxbury and Bouldin, 1982; Grant and Pattey, 2003; Pattey et al., 2007). This poses a serious challenge to the estimation of the source strength of arable soils, which is currently mostly based on available statistics on fertilizer ignoring these environmental factors (IPCC, 2006; Lokupitiya and Paustian, 2006). On the other hand, process-based agro-ecosystem models may in principle capture these effects, and have thereby a unique potential to predict N_2O emissions from arable soils at the plot-scale as well as at regional and continental scales (Butterbach-Bahl et al., 2004; Del Grosso et al., 2006; Gabrielle et al., 2006a; Li et al., 2001). Examples of biophysical N_2O-models include DAYCENT (Parton et al., 2001), DNDC (Li, 2000), FASSET (Chatskikh et al., 2005) and CERES-EGC (Gabrielle et al., 2006b). However, a major limitation to the wide-spread use of these models lies in the fact that their predictions are highly dependent on parameter settings, and carry a large uncertainty due to uncertainties in parameter values, driving variables and model structure (Gabrielle et al., 2006a).

Although model parameterisation and uncertainty analysis are widely developed in the literature on agro-ecosystem models, they are rarely considered simultaneously (Makowski et al., 2006; Monod et al., 2006). Bayesian calibration makes it possible to combine the two types of analysis by providing estimates of parameters values under the form of probability density functions (pdfs), which may be also propagated to model outputs as pdfs (Gallagher and Doherty, 2007). Probability density functions are initially the expression of current imprecise knowledge about model parameter values, this prior probability is then updated with the measured observations into posterior probability distribution by means of Bayes' theorem (Makowski et al., 2006).

In ecological and environmental sciences, Bayesian calibration has been applied to a wide range of models (Hong et al., 2005; Larssen et al., 2006; Ricciuto et al., 2008), and this field is developing actively, mainly using Markov Chain Monte Carlo (MCMC) methods to estimate the posterior pdf for the model parameters. The Bayesian methodology described by Van Oijen et al. (2005) was applied to dynamic process-based forest models with the objective of calibrating model parameters with various types of observed data from forested experimental sites (Klemedtsson et al., 2007; Svensson et al., 2008). In these examples, Metropolis-Hastings MCMC-algorithm was used to generate samples from the posterior parameter distributions. Although there is an increasing body of literature on the application of Bayesian approaches to environ-

mental sciences, the latter have not been applied to process-based model of soil N_2O emission models, to the best of our knowledge.

The overall purpose of this paper was thus to calibrate the parameters of the N_2O emission module of the CERES-EGC agro-ecosystem model and to quantify uncertainty of model simulations by developing a suitable Bayesian calibration method. Data sets of measured N_2O emission rates were collected from seven field-sites in Northern France, which represent major soil types, crops and management practices of the area. The Bayesian procedure was first applied separately to each experimental site, and secondly to the ensemble of the sites. This made it possible to explore the spatial variability of model parameters, and to test whether they could be considered as universal and with which uncertainty range.

2.2 Material and Methods

We carried out Bayesian calibration using the Metropolis-Hastings algorithm, to estimate the joint probability distribution for the parameters of the N_2O emission module of the CERES-EGC model. The equations of this module involve 15 parameters, of which 11 were considered as global (i.e. invariant over time and space) by the model's author, the remaining 4 being site-specific (Hénault et al., 2005a). While the latter were laboratory-measured in all experimental sites and set to the resulting values throughout, the subset of 11 global parameters was estimated by our Bayesian procedure. We collated a database of N_2O flux measurements including 7 different field-sites in France, and various N fertilizer forms and rates in 2 of the sites. Bayesian calibration was applied either to each site or treatment individually, or directly to the ensemble of the data sets.

2.2.1 The CERES-EGC model

2.2.1.1 A process-based agro-ecosystem model

CERES-EGC was adapted from the CERES suite of soil-crop models (Jones and Kiniry, 1986), with a focus on the simulation of environmental outputs such as nitrate leaching, emissions of N_2O and nitrogen oxides (Gabrielle et al., 2006a). CERES-EGC runs on a daily time step, and requires daily rain, mean air temperature and Penman potential evapo-transpiration as forcing variables. The CERES models are available for a large number of crop species, which share the same soil components (Jones and Kiniry, 1986).
CERES-EGC comprises sub-models for the major processes governing the cycles of water, carbon and nitrogen in soil-crop systems. A physical sub-model simulates the transfer of heat, water and nitrate down the soil profile, as well as soil evaporation, plant water uptake and transpiration in relation to climatic demand. Water infiltrates down the soil profile following a tipping-bucket approach, and may be redistributed upwards after evapo-transpiration has dried some soil layers. In both of these equations, the generalised Darcy's law has subsequently been introduced in order to better simulate water dynamics in fine-textured soils (Gabrielle et al., 1995).

A biological sub-model simulates the growth and phenology of the crops. Crop net photosynthesis is a linear function of intercepted radiation according to the Monteith approach, with interception depending on leaf are index based on Beer's law of diffusion in turbid media. Photosynthates are partitioned on a daily basis to currently growing organs (roots, leaves, stems, fruits) according to crop development stage. The latter is driven by the accumulation of growing degree days, as well as cold temperature and day-length for crops sensitive to vernalisation and photoperiod. Lastly, crop N uptake is computed through a supply/demand scheme, with soil supply depending on soil nitrate and ammonium concentrations and root length density.
A micro-biological sub-model simulates the turnover of organic matter in the plough layer. Decomposition, mineralisation and N-immobilisation are modelled with three pools of organic matter (OM) : the labil OM, the microbial biomass and the humads. Kinetic rate constants define the C and N flows between the different pools. Direct field emissions of CO_2, N_2O, NO and NH_3 into the atmosphere are simulated with different trace gas modules.

2.2.1.2 The nitrous oxide emission module

This module simulates the production of N_2O in soils through both the nitrification and the denitrification pathways, and was adapted from the semi-empirical model NOE (Hénault et al., 2005a). The denitrification component is derived from the NEMIS model (Hénault and Germon, 2000) that calculates the actual denitrification rate (Da, kg N ha^{-1} d^{-1}) as the product of a potential rate at 20 °C (PDR, kg N ha^{-1} d^{-1}) with three unitless factors related to water-filled pore space (F_W), nitrate content (F_N) and temperature (F_T) in the topsoil, as follows :

$$Da = PDR\ F_N\ F_W\ F_T \tag{2.1}$$

In a similar fashion, the daily nitrification rate (Ni, kg N ha^{-1} d^{-1}) is modelled as the product of a maximum nitrification rate at 20 °C (MNR, kg N ha^{-1} d^{-1}) with three unitless factors related to water-filled pore space (N_W), ammonium concentration (N_N) and temperature (N_T) and expressed as follows :

$$Ni = MNR\ N_N\ N_W\ N_T \tag{2.2}$$

Nitrous oxide emissions resulting from the two processes are soil-specific proportions of total denitrification and nitrification pathways, and are calculated according to :

$$N_2O = r\ Da + c\ Ni \tag{2.3}$$

where r is the fraction of denitrified N and c is the fraction of nitrified N that both evolve as N_2O. The N_2O sub-model of CERES-EGC involves a total set of 15 parameters of which four of them are site-specific and must be measured on site, while the other 11 are considered global, i.e. invariant over time and space. The local (site-specific) parameters are the potential denitrification rate (PDR), the maximum nitrification rate (MNR) and the fractions of nitrified (c) and denitrified (r) N that are evolved as N_2O. They were measured in the laboratory for all sites using a protocol that proved representative of field conditions in a wide range of situations (Dambreville et al., 2008; Gabrielle et al., 2006b; Hénault et al., 2005a; Hénault and Germon, 2000). The 11 global parameters are the constants of the N_2O module equations which are considered invariant over

time and space. They were estimated by Hénault and Germon (2000) for the denitrification pathway and by Garrido et al. (2002) and Laville et al. (2005) for nitrification. The equations of the response functions with the associated parameters are described in Appendix A (Eqs. 2.7-2.12).

Prior information was gathered on all parameters on a literature review. For lack of information on the form of the pdf of these parameters, the latter were assigned uniform distributions within their likely range derived from literature data (Table 2.1). Parameters were supposed to be entirely independent (i.e. non-correlated). This type of hypotheses, which are likely to be violated in ecosystem models, is not a significant issue in the application of Bayesian calibration. For example, Naud et al. (2007) tested different levels of correlation of prior distributions and concluded that correlation was not a very important factor. In addition, Hong et al. (2005) reported that the assumption of a priori independence does not imply independence a posteriori, and the calibration may still provide a posterior estimate of correlations across parameters.

2.2.2 The database of nitrous oxide measurements

The N_2O measurements were carried out on seven experimental sites located in Northern France. The experiments were conducted on major arable crop types and soils types representative of this part of France. For some sites, different treatments were conducted with various N-fertiliser amounts supplied to the crop, giving a total of 11 site/treatment combinations (Table 2.2).
Nitrous oxide emissions were monitored by the static chamber method with eight replicates for all sites (Hénault et al., 2005a), except at Grignon where measurements were monitored with three automatic chambers during 31 successive days from 13 May 2005 to 12 June 2005 (Lehuger et al., 2007). The variance in the measurements was estimated as the variance across the different replicate chambers in the field. Soil nitrogen and moisture contents were monitored in the soil profile for each site with different sampling frequencies (see references of Table 2.2 for details). The resulting samples were analysed for moisture content and inorganic N using colorimetric samples in the laboratory. Soil temperature was continuously monitored using thermocouples in most of the sites, except for the sites of Champnoël and Le Rheu. The input data required to run the model were also collected in each site : the weather data were taken from a local meteorological station, and detailed information on soil properties and crop management were compiled to generate CERES-EGC input files using a standard parameterization procedure (Gabrielle et al., 2006b). Uncertainty on these input data was not considered here since CERES-EGC had already been tested in most of the sites (Gabrielle et al., 2006b). Besides, it likely had little impact on the N_2O simulations since we checked that the model gave correct predictions of the major N_2O drivers (topsoil environmental conditions and nitrate content).

2.2.3 Bayesian calibration

2.2.3.1 Markov Chain Monte Carlo

Bayesian methods are used to estimate model parameters by combining two sources of information : prior information about parameter values and observations on output variables. The prior information is based on expert knowledge, literature review or by measuring parameters directly in the field or laboratory. In our case, the observations on output variables are field measurements of the different fluxes between soil-crop-atmosphere compartments. Bayes' theorem makes it possible to combine the two sources of information in order to calibrate the model parameters. The first step is to assign a probability distribution to the parameters, representing our prior uncertainty about their values. In our case, we specified lower and upper bounds of the parameters' uncertainty, defining the prior parameter distributions as uniform. The aim of Bayesian calibration is to reduce this uncertainty by using the measured data, thereby producing the posterior distribution for the parameters. This is achieved by multiplying the prior with the likelihood function, which is the probability of the data given the parameters. The likelihood function is determined by the probability distribution of errors in observations. We assumed errors to be independent and normally distributed with mean zero following Van Oijen et al. (2005) and in the same fashion as Svensson et al. (2008) and Klemedtsson et al. (2007). Because probability densities may be very small numbers, rounding errors needed to be avoided and all calculations were carried out using logarithms. The logarithm of the data likelihood is thus set up, for each data set Y_i, as follows :

$$logL_i = \sum_{j=1}^{K} \left(-0.5 \left(\frac{y_j - f(\omega_i; \theta_i)}{\sigma_j} \right)^2 - 0.5log(2\pi) - log(\sigma_j) \right) \tag{2.4}$$

where y_j is the mean N_2O flux measured on sampling date j in the data set Y_i and σ_j the standard deviation across the replicates on that date, ω_i is the vector of model input data for the same date, $f(\omega_i; \theta_i)$ is the model simulation of y_j with the parameter vector θ_i, and K is the total number of observation dates in the data sets.

To generate a representative sample of parameter vectors from the posterior distribution, we used a Markov Chain Monte Carlo (MCMC) method : the Metropolis-Hastings algorithm (Metropolis et al., 1953) (see Appendix B for details). We formed Markov chains of length 10^4-10^5 using a multivariate Gaussian pdf to generate candidate parameter vectors. The variance matrix of this Gaussian was tuned so that the Markov chains would explore parameter space efficiently. We followed the procedure of Van Oijen et al. (2005) and defined the variances equal to the square of 1 to 5 % of the prior parameter range (θ_{min}-θ_{max}) and zero covariances. Subsequently, the variances were tuned so that the fraction of candidates accepted during the random walk was between 20 to 30%. Ten percent of the total number of iterations at the beginning of the chain were discarded as unrepresentative "burn-in" of the chains (Van Oijen et al., 2005).

For each calibration, three parallel Markov chains were started from three different starting points (θ_0) : the default parameter value and their lower and upper bounds (θ_{min} and θ_{max}).

Parameter vector $\theta = [\theta_1 ... \theta_{11}]$					Prior probability distribution			Posterior probability distribution		
θ_i	Symbol	Description	Unit	Default value	θ_{min}(i)	θ_{max}(i)	References	Mean	SD	Correlated $\{\theta_i\}$
θ_1	Tr_{WFPS}	WFPS threshold for denitrification	%	0.62	0.40	0.80	Gabrielle (2006b); Hénault et al. (2005a) Hénault and Germon (2000); Johnsson et al. (2004)	0.689	0.007	{2,6}
θ_2	Km_{denit}	Half-saturation constant (denit)	mg N kg^{-1} soil	22.00	5.00	120.00	Ding et al. (2007); Gabrielle (2006b) Del Grosso et al. (2000); Parton et al. (2001) Bateman and Baggs (2005); Parton et al. (1996) Johnsson et al. (2004)	66.94	22.47	{1,6}
θ_3	TTr_{denit}	Temperature threshold	°C	11.00	10.00	15.00	Gabrielle (2006b); Johnsson et al. (2004) Renault et al. (1994)	10.27	0.17	
θ_4	$Q10_{denit,1}$	Q10 factor for low temperature	Unitless	89.00	60.00	120.00	Maag and Vinther (1999); Stanford et al. (1975)	89.46	18.28	{5}
θ_5	$Q10_{denit,2}$	Q10 factor for high temperature	Unitless	2.10	1.00	4.80	Gabrielle (2006b); Stanford et al. (1975)	2.62	1.17	{4,10}
θ_6	POW_{denit}	Exponent of power function	Unitless	1.74	0.00	2.00	Smith et al. (1998); Stanford et al. (1975) Johnsson et al. (2004); Maag and Vinther (1999) Maag and Vinther (1996); Skopp et al. (1990)	1.53	0.23	{1, 2}
θ_7	OPT_{WFPS}	Optimum WFPS for nitrification	%	0.60	0.35	0.75	Jambert et al. (1997); Laville et al. (2005)	0.59	0.12	
θ_8	MIN_{WFPS}	Minimum WFPS for nitrification	%	0.10	0.05	0.15	Jambert et al. (1997); Linn and Doran (1984) Ding et al. (2007); Skopp et al. (1990) Bateman and Baggs (2005); Parton et al. (2001)	0.095	0.02	
θ_9	MAX_{WFPS}	Maximum WFPS for nitrification	%	0.80	0.80	1.00	Linn and Doran (1984); Parton et al. (2001) Bateman and Baggs (2005)	0.88	0.05	
θ_{10}	Km_{nit}	Half-saturation constant (nit)	mg N kg^{-1} soil	10.00	1.00	50.00	Jambert et al. (1997); Linn and Doran (1984) Pihlatie et al. (2004)	25.69	14.17	{5}
θ_{11}	$Q10_{nit}$	Q10 factor for nitrification	Unitless	2.10	1.90	13.00	Laville et al. (2005); Maag and Vinther (1996) Dobbie and Smith (2001); Smith (1997)	7.36	3.04	

TAB. 2.1 : *Description of the 11 parameters of the N_2O emissions module. The prior probability distribution is defined as multivariate uniform between bounds θ_{min} and θ_{max} which were extracted from a literature review. The posterior parameter distributions are based on the multi-dataset procedure, and are characterised by the mean value of the posterior, their standard deviation (SD). Correlations with other parameters are reported if their absolute value exceeds 0.4 (underlined parameters express a negative correlation).*

Site	Treatment	Year	Soil texture class	Crop type	N fertiliser (kg N ha^{-1})	Number of observations	Source
Rafidin	N0	1994-1995	Rendzina	Rapeseed	0	7	Gosse et al. (1999)
	N1	1994-1995	Rendzina	Rapeseed	155	8	Gosse et al. (1999)
	N2	1994-1995	Rendzina	Rapeseed	262	9	Gosse et al. (1999)
Villamblain		1998-1999	Loamy Clay	Winter Wheat	230	15	Hénault et al. (2005a)
Arrou		1998-1999	Loamy Clay	Winter Wheat	180	18	Hénault et al. (2005a)
La Saussaye		1998-1999	Clay Loams	Winter Wheat	200	14	Hénault et al. (2005a)
Champnoël	CT	2002-2003	Silt Loam	Maize	0	15	Dambreville et al. (2008)
	AN	2002-2003	Silt Loam	Maize	110	23	Dambreville et al. (2008)
Le Rheu	CT	2004-2005	Silt Loam	Maize	18	24	Dambreville et al. (2008)
	AN	2004-2005	Silt Loam	Maize	180	22	Dambreville et al. (2008)
Grignon		2005	Silt Loam	Maize	140	31	Lehuger et al. (2007)

TAB. 2.2 : *Main characteristics of the N_2O emissions data base used in the model calibration. At Rafidin, the treatments N0, N1 and N2 correspond to various N-fertilizer applications and at Le Rheu and Champnoël, the treatments AN correspond to ammonium nitrate application and CT to the control plot.*

Convergence was checked with the diagnostic proposed by Gelman and Rubin (1992), which is based on the comparison of within-chain and between-chain variances, and is similar to a classical analysis of variance. Convergence is reached when variance between chains no longer exceeds the variance within each individual chain. The chains of parameter values resulting from the random walk of the Metropolis-Hastings algorithm are auto-correlated because each iteration depends on the previous one. We therefore thinned the chains in two steps : the auto-correlation was first computed for increasing lags and then the posterior chain was extracted by keeping the iterations defined by the thinning interval. We defined this as the number of iterations between consecutive samples in a chain for which the auto-correlation was less than 60%. The chains filtered in this way were considered to be a representative sample from the posterior pdf, and from this sample were calculated the mean vector, the variance matrix and the 90% confident interval for each parameter.
The generation and analysis of the Markov chains were carried out with the statistical package R (R Development Core Team, 2008) and in particular its *coda* package (Plummer et al., 2006). The CERES-EGC model was encapsulated within R as a library, generated from the original Fortran code.

2.2.3.2 Procedure for the nitrous oxide emission module

The calibration procedure had two main objectives : (i) to calibrate the parameters for each dataset Y_i, to explore the variations of global parameters across experimental sites and treatments, and (ii) to obtain better estimates for the global parameters (initially deemed universal in the model). The first objective was pursued by calibrating the parameters for each data set separately, which is referred to later on as the *dataset-by-dataset procedure*. In a second step, the global parameters were calibrated by running our procedure with the 11 data sets simultaneously

(*multi-dataset procedure*), i.e. by calculating the posterior distribution as :

$$p(\theta|Y_1, ..., Y_{11}) \propto p(Y_1, ..., Y_{11}|\theta)\, p(\theta) \tag{2.5}$$

where Y_i is the data of the i^{th} site and the $\propto$ symbol means 'proportional to'. In this case, the log-likelihood is calculated as the sum of the log-likelihoods of all the data sets (for a given parameter set in the MCMC chain).

2.2.4 Evaluation of model predictions

The performance of the calibration procedures was assessed by calculating the root mean square error (RMSE). RMSE was defined, for each data set Y_i, as follows (Smith et al., 1996) :

$$RMSE = \sqrt{\frac{\sum_{j=1}^{K}(y_j - f(\omega_i; \theta_i))^2}{K}} \tag{2.6}$$

In both following cases, simulations f($\omega_i; \theta_i$) were carried out using either the posterior expectancy of parameters ($\overline{\theta}$) or the maximum a posteriori (MAP) estimate of θ (θ_{MAP}). θ_{MAP} is the single best value of the parameter vector in each MCMC chain, at which the posterior probability distribution is maximal (Van Oijen et al., 2005). In the case of prior parameter pdfs, the simulations were defined as the prior expectancy of the model predictions in which parameters were randomly drawn from the prior pdfs. For the posterior parameters pdfs, the simulations were the posterior expectancy of predictions. RMSE was computed after calibration resulting from the dataset-by-dataset or multi-dataset procedure.

2.3 Results

2.3.1 Simulation of soil state variables

Soil temperature, soil water content and nitrate and ammonium contents were simulated by the model and confronted against the measurements. Table 2.3 summarizes the mean deviation (MD), which is the mean difference between measurement and simulation, and RMSEs computed with the different topsoil state variables used as input variables of the N_2O emission module. Soil temperature and water content were well predicted by the model with RMSE ranging from 1.2 to 3.0 ° C for the soil temperature and from 3 to 6 % (v/v) for the soil water content across the 11 sites and treatments. The model's RMSE over the 11 sites and treatments ranged between 3.7 to 27.9 kg N ha^{-1} for the prediction of nitrate content and to 0.7 to 25.3 kg N ha^{-1} for the ammonium content. Dynamics of surface nitrate and ammonium contents were mainly driven by the fertiliser applications and mineralization of crop residues. Ammonium was rapidly nitrified across all the sites but the model failed to reproduce the background topsoil ammonium stock. Nitrate content was relatively well simulated except for 3 treatments for which N plant uptake was under-estimated (La Saussaye, Champnoël AN and Le Rheu AN).

2.3.2 Posterior parameter distributions

Figure 2.1 shows boxplots of the posterior parameter distributions after calibration with the dataset-by-dataset and the multi-dataset procedures. Such representation makes it possible to visualize differences between parameter pdfs across datasets, while the shape of the boxplot reveals the dispersion and symmetry of the marginal distributions.Our Bayesian procedure generally generated uni-modal distributions, and convergence test corroborated that the MCMC chains converged. Figure 2.2 presents the 50 and 97.5% quantiles of the Gelman-Rubin shrink factor for the 11 parameters calibrated with the data set of La Saussaye, and shows that it approached 1 for all parameters, evidencing the convergence of the calibration.

Figure 2.1 shows that the posterior distributions became narrower compared to the uniform prior distributions, which is undoubtedly due to the efficiency of our calibration procedure. The posterior pdfs converged to normal or log normal distributions, as already observed by Svensson et al. (2008) in the Bayesian calibration of a process-based forest model. Thus, the choice of an uniform distribution for the prior pdfs had little influence, as the information contained in the experimental data gradually became dominant in the calibration process (Van Oijen et al., 2005). For example, the posterior distributions of parameter θ_1 (the WFPS threshold triggering denitrification) had a narrow range for all datasets, suggesting that the calibration had drastically reduced its uncertainty. On the contrary, parameters θ_8 and θ_9 (corresponding to the minimum and maximum WFPS for nitrification activity, respectively) remained spread across their prior range of variation, and centered around their prior median. This means that the calibration did not significantly reduce their uncertainty. Conversely, some posterior distributions were flattened on one of the prior bounds, implying that their optimal values was outside the prescribed range. This was particular true for parameters θ_{10} (the half-saturation constant of nitrification response to ammonium) and θ_{11} (the Q10 factor for nitrification) for the data sets of Champnoël AN, La Saussaye and Grignon. We should therefore reconsider the prior ranges for these parameters.

The rightmost boxplot in each of the 11 graphs in Figure 2.1 depicts the distribution obtained with the multi-dataset procedure. The shape of this boxplot and its median value appeared to be more constrained by certain datasets than others, which may be explained by the fact that data sets with a comparatively larger number of observations of higher precision had substantially more weight in the log-likelihood function. For example, the boxplots of the multi-dataset calibration exhibited high similarity with those of the La Saussaye site for parameters θ_1, θ_3 and θ_6. Some data sets were collected in the same sites, i.e. under identical climate patterns and soil types but with differentiated crop management (the Rafidin, Le Rheu and Champnoël datasets). Since the parameters of the N_2O module are mostly related to soil properties, it was expected that the calibration should produce similar distributions for these three sites. To a certain extent, this was the case for the parameters θ_2, θ_3 and θ_6, giving support to the idea that these parameters are mostly soil-dependent, and are little influenced by crop management. Conversely, the strong variation of posterior pdfs across sites challenges the original idea in model development that these parameters may be considered constant. The purpose of the multi-dataset procedure sought to investigate this option, by seeking the best-fit parameter pdfs in relation to the ensemble of

Site	Treatment	Soil temperature				Soil water content				Nitrate content				Ammonium content			
		N	Mean	MD	RMSE	N	Mean	MD	RMSE	N	Mean	MD	RMSE	N	Mean	MD	RMSE
				(°C)				(v/v)			(kg NO_3-N ha^{-1})				(kg NH_4-N ha^{-1})		
Rafidin	N0	294	8.7	-1.2	3.0	20	0.253	-0.027	0.043	21	10.8	5.5	9.9	21	3.7	3.5	4.1
	N1	294	8.7	-1.2	3.0	20	0.244	-0.035	0.051	21	12.9	8.0	11.8	21	5.6	5.0	6.8
	N2	294	8.7	-1.2	3.0	20	0.240	-0.039	0.050	21	23.5	17.0	22.6	21	6.2	5.6	8.0
Villamblain		250	8.4	0.1	1.3	7	0.344	0.024	0.027	7	17.6	8.7	11.0	7	6.5	4.8	6.0
Arrou		250	8.4	0.2	1.2	7	0.343	0.053	0.056	7	18.1	11.8	14.9	7	9.1	9.0	10.6
La Saussaye		250	8.4	-1.2	2.4	7	0.307	0.030	0.038	7	15.3	-15.9	27.9	7	5.9	5.8	8.8
Champnoël	CT	no data	no data	no data	no data	14	0.239	-0.009	0.049	2	28.8	3.4	3.7	2	0.9	0.7	0.7
	AN	no data	no data	no data	no data	14	0.239	-0.006	0.027	11	22.4	-20.8	29.5	11	13.4	8.0	14.6
Le Rheu	CT	no data	no data	no data	no data	13	0.212	0.004	0.028	9	17.8	-1.4	15.4	9	4.6	4.3	4.6
	AN	no data	no data	no data	no data	13	0.212	0.004	0.028	10	54.3	-16.6	27.8	10	4.5	-7.8	25.3
Grignon		364	11.7	-0.4	2.4	13	0.249	0.002	0.028	11	71.4	-1.7	14.2	11	12.3	6.8	13.6

TAB. 2.3 : *Sample size (N), mean of measured in situ soil variables (Mean), mean deviation (MD) and root mean square errors (RMSE) computed with the predicted and measured soil variables : soil temperature, soil water content and topsoil nitrate and ammonium contents for the 11 data sets.*

the experimental situations collated in our database. It could be expected to lead to parameter pdfs with a wider spread (and thus higher uncertainty) than in the dataset-by-dataset calibration, owing to the wide ranges covered by the dataset-specific pdfs. While this was true of some parameters (e.g., θ_4, θ_5, and θ_7), it was the opposite for others (most notably θ_1 and θ_3).

Figure 2.3 depicts the ranges of response functions of the N_2O emission module resulting from the various calibrations, and evidences ample differences across datasets. The responses of nitrification to soil ammonium content (N_N, Fig. 2.3.a) were highly variable, reflecting the range taken by their shape parameter θ_{10}. The response of nitrification to soil WFPS (N_W, Fig. 2.3.b) shows that the minimum WFPS for nitrification activity (θ_8) were centred on a unique value, while the optimum WFPS (θ_7) was lower in the calibration with two data sets. The calibrated maximum WFPSs for nitrification (θ_9) were centred on 90%. The shapes of the response function N_T (Fig. 2.3.c) were similar for two sites (La Saussaye and Grignon), but strikingly different for the other sites. The calibrated responses of denitrification to nitrate content (F_N, Fig. 2.3.d) were highly variable such as the response of nitrification to ammonium content. The shapes of the response of denitrification to WFPS (F_W) varied widely, as a consequence of the large variations of parameters θ_1 (the WFPS threshold triggering denitrification) and θ_6 (the exponent of the power-law). Hénault and Germon (2000) and Heinen (2006) showed that denitrification was highly sensitive to θ_1, and that this parameter was dependent on soil type. The response of denitrification to soil temperature (F_T) had a similar shape across the various parameterizations, for temperatures lower than 25 °C which corresponds to the range encountered in the field experiments. This leads to the conclusion that the function calibrated with the multi-dataset procedure could be considered universal.

Bayesian calibration also quantifies correlations between parameters in the posterior. Most parameters were cross-correlated, with coefficients higher than 0.4 for 6 of them (Table 2.1) suggesting that our uncertainty about their values is linked and implies that some parameters should be treated in clusters, as suggested by Svensson et al. (2008). Parameters θ_1 and θ_2 are positively correlated, and are both negatively correlated with θ_6.

2.3.3 Model prediction uncertainty

The simulations of N_2O emissions generated with the posterior MCMC parameter chains provided statistical distributions of model outputs resulting from parameter uncertainty, which is a straight benefit of Bayesian approaches. Figure 2.4 shows the mean of simulated daily N_2O emissions for all datasets (Fig. 2.4.a to 2.4.k). Some discrepancies between measurements and simulations remained, due to uncertainty on both sides. Measurement points with high standard deviations had less weight in the log likelihood function, and thus in the posterior probability, compared to lower fluxes with lower variability. For example, the two N_2O spikes measured in Villamblain in springtime (Fig. 2.4.a) had a large experimental error, but did not appear to constrain the calibration as much as the more frequent lower N_2O fluxes with much lower standard deviations. The same remark applies to Arrou (Fig. 2.4.b). For the dataset of Champnoël AN (Fig. 2.4.e), a high spike of N_2O was observed in autumn that the model failed to predict,

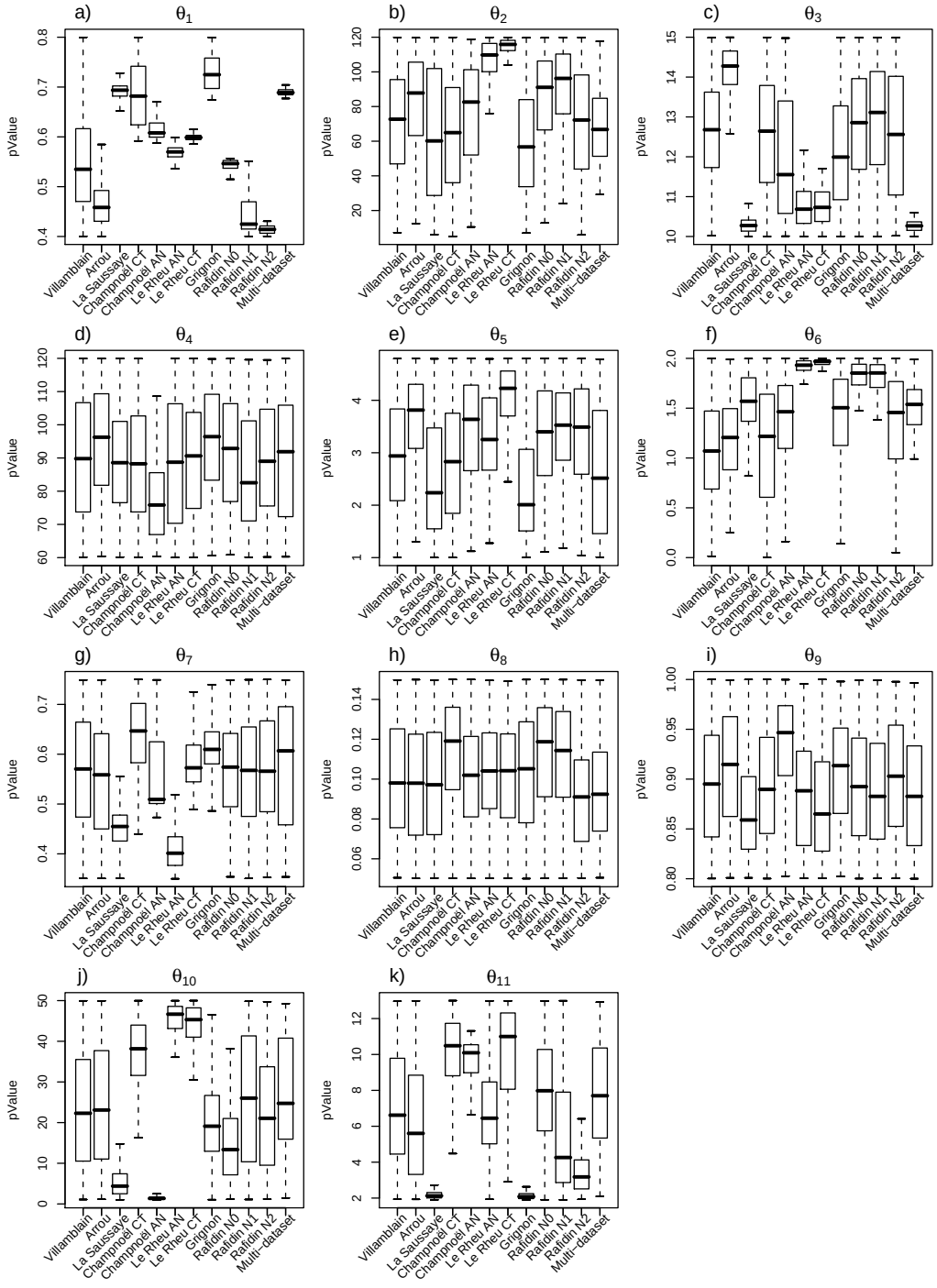

FIG. 2.1 : *Posterior distributions of the 11 calibrated parameters (θ_1 to θ_{11}) represented as boxplots over the prior range of variation (corresponding to the range of the y-axis). The boxplots are computed from calibration dataset-by-dataset and with the "multi-dataset" procedure. The boxplots depict the median (solid line), the 2nd and 3rd quartiles (bars), the 1st and 4ht quartiles (dotted line), and the extreme values (excluding outliers).*

whereas it otherwise successfully simulated fluxes under 10 g N_2O-N ha^{-1} d^{-1}.
For the Grignon site (Fig. 2.4.h), the observation points were concentrated on 31 successive days (from 13 May 2005 to 12 June 2005), and started a peak flux. With its default parameter set, the model simulated that peak along with two others in the following weeks that were not observed in the field (results not shown, see Lehuger et al. (2007)), in response to significant rains. The Bayesian calibration managed to circumvent the simulation of these two unobserved peak fluxes by raising the WFPS threshold for denitrification (θ_1) from 62% (default value) to 73%, which is the highest value in all the calibrations (Fig. 2.1.a). As a result of this change in the response to rainfall and soil water content, no N_2O-peaks were simulated throughout the year in Grignon (Fig. 2.4.h). For the dataset of Rafidin N0 (Fig. 2.4.i), observations also were concentrated on two short periods, but with fewer observations points than at Grignon. The calibration highly constrained the model during the measurement period, but appeared less constraining on the N_2O-fluxes outside this period.

Table 2.4 summarises the statistics of the annual N_2O emissions predicted by CERES-EGC for the different datasets. The mean annual fluxes ranged between 88 and 3672 g N_2O-N ha^{-1} y^{-1}, with a large confidence interval especially for the datasets with higher emission rates. An overall conversion factor of fertilizer inputs to N_2O-N was calculated as the ratio of the annual flux to the N fertiliser dose. This is different from an "emission factor", which takes background emissions of N_2O into account. Here, we also calculated this factor as the difference between the annual N_2O-N emissions of fertilised and unfertilised crops (g N_2O-N ha^{-1} y^{-1}) to the N-fertiliser dose. The emission factors ranged from 0.05 and 1.12% across experimental sites, with a mean value of 0.26%. This value is four times lower than the default value recommended by the IPCC tier 1 methodology (IPCC, 2006).

Site	Treatment	Year	N_2O Fluxes (g N ha^{-1} y^{-1})	0.05 quantile (g N ha^{-1} y^{-1})	0.95 quantile (g N ha^{-1} y^{-1})	IPCC (g N ha^{-1} y^{-1})	Conversion factor (%)	Emission factor (%)
Rafidin	N0	1994-1995	689	578	741	0	-	-
	N1	1994-1995	584	473	824	1550	0.4 (0.3-0.5)	0.07 (0.00-0.22)
	N2	1994-1995	819	629	1183	2620	0.3 (0.2-0.5)	0.10 (0.03-0.24)
Villamblain		1998-1999	1465	454	2989	2300	0.6 (0.2-1.3)	0.36 (0.00-1.02)
Arrou		1998-1999	3672	1676	5874	1800	2.0 (0.9-3.3)	0.26 (0.00-1.49)
La Saussaye		1998-1999	3215	572	6035	2000	1.6 (0.3-3.0)	1.12 (0.00-2.53)
Champnoël	CT	2002-2003	218	49	746	0	-	-
	AN	2002-2003	336	106	855	1100	0.3 (0.1-0.8)	0.06 (0.00-0.53)
Le Rheu	CT	2004-2005	88	66	115	180	0.5 (0.4-0.6)	-
	AN	2004-2005	183	146	220	1800	0.10 (0.08-0.12)	0.05 (0.03-0.08)
Grignon		2005-2006	150	143	163	1400	0.11 (0.10-0.12)	0.05 (0.04-0.05)

TAB. 2.4 : *Annual N_2O fluxes (g N_2O-N $ha^{-1}y^{-1}$) calculated as the sum of mean, 0.05 and 0.95 quantiles of daily simulations with the calibrated parameter sets. Annual estimates from IPCC methodology (corresponding to the emissions due to fertiliser application), conversion factor (%) and emission factor (%) are also reported (see text for definition), along with their 90% confidence band.*

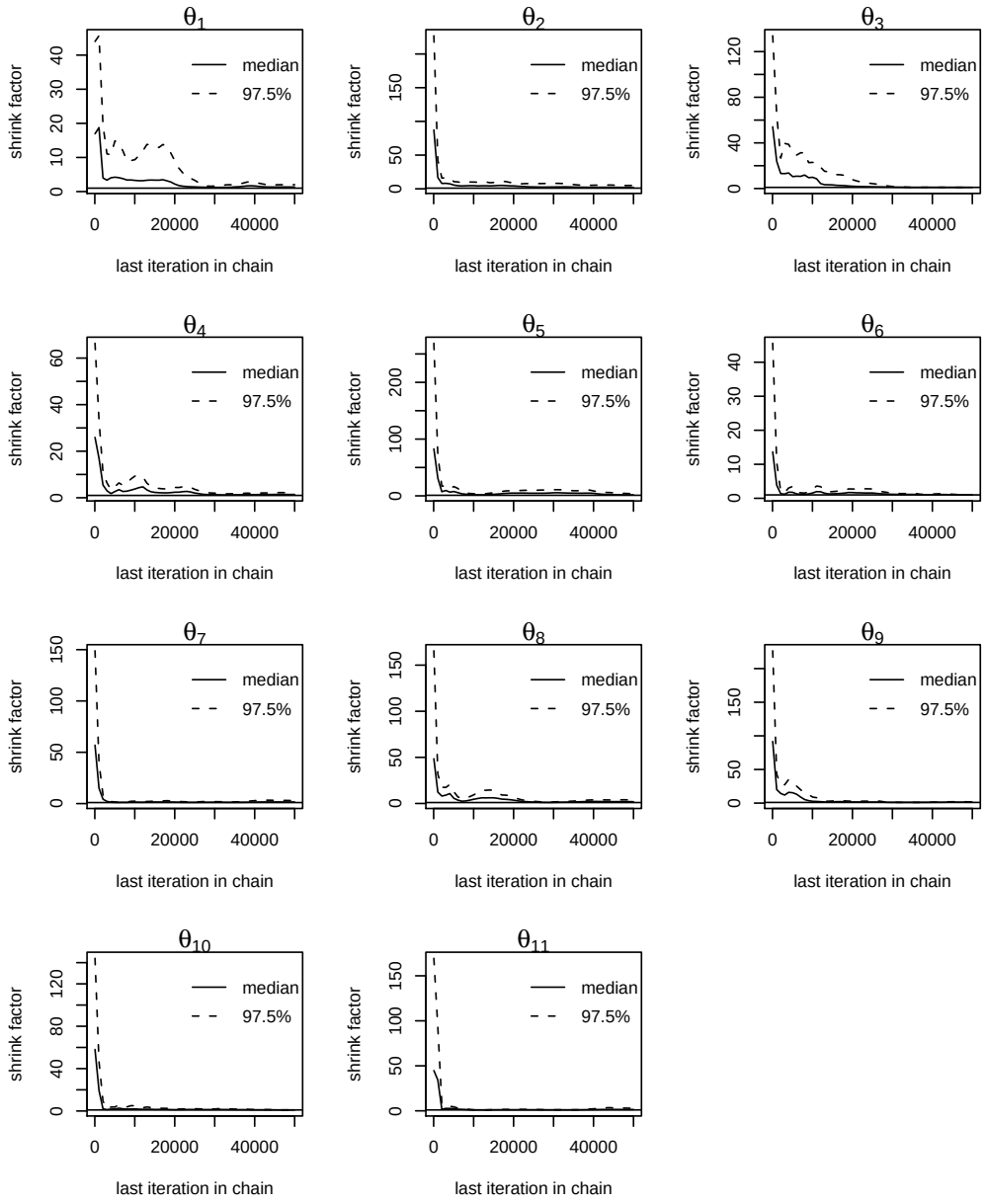

FIG. 2.2 : *Evolution of the Gelman and Rubin's shrink factor for the calibration of the site La Saussaye.*

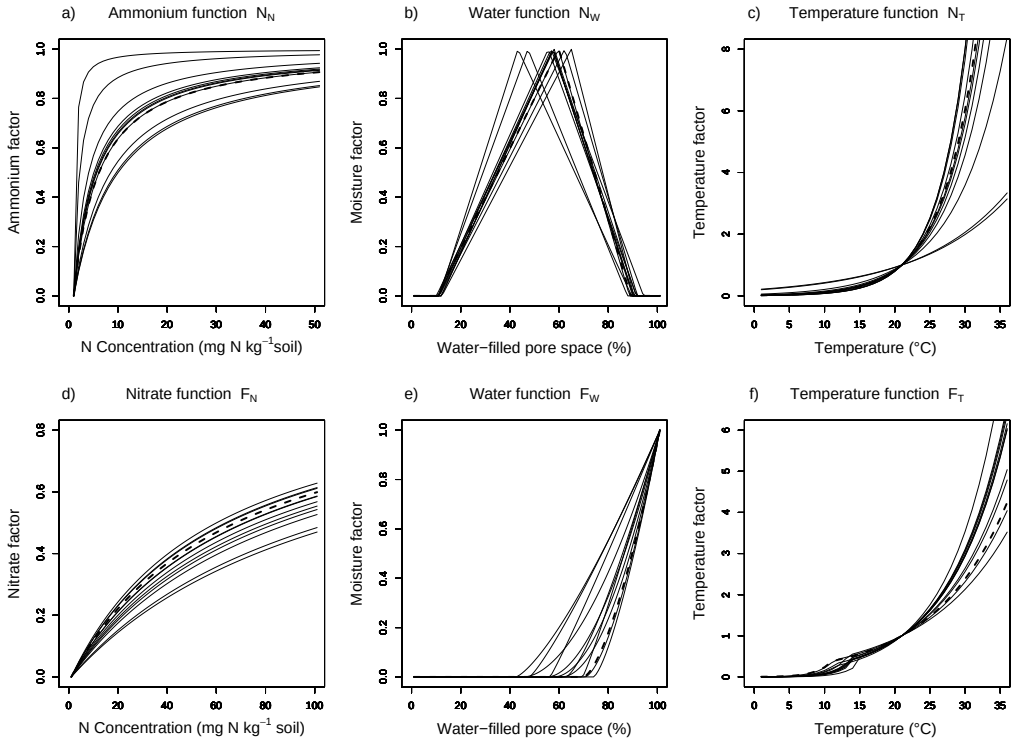

FIG. 2.3 : *Response functions of the N_2O emission module traced with different parameters sets : mean of the posterior for each dataset-by-dataset calibration (line), and mean of the posterior for the multi-dataset calibration (dashed line).*

2.3.4 Calibration efficiency and model prediction error

Table 2.5 summarises the RMSEs obtained with the various parameters sets, and made it possible to compare the efficiency of model calibration whether in the dataset-by-dataset or in the multi-dataset mode. In the dataset-by-dataset procedure, the RMSEs computed with the posterior expectancy of predictions were lower than those computed with the prior expectancy of predictions for all datasets except one (Arrou), with a 73% reduction on average and a maximum of 98% in La Saussaye. In 8 of the remaining 9 datasets, calibration lead to a reduction of 79% to 96% in the model's RMSE. On average across all datasets, the RMSE dropped from 39 down to 6 g N_2O-N ha^{-1} d^{-1} after calibration. There were no differences in the RMSEs calculated either with simulations based on the posterior mean of parameters ($\overline{\theta}$) or with posterior mean of predictions. Thus, the mean of our sample from the posterior could be directly used for the sites of our database or for sites with similar soil types. The use of the parameter set with maximum posterior probability (θ_{MAP}), i.e. when likelihood was maximum and given that we used a uniform prior, logically improved the RMSE compared to the use of the posterior mean of parameters ($\overline{\theta}$). As could be expected, the multi-dataset calibration was less efficient than the dataset-by-dataset one, enabling a decrease of only 33% of the RMSE computed with posterior expectancy of predictions compared to the prior expectancy of predictions. This would lead us

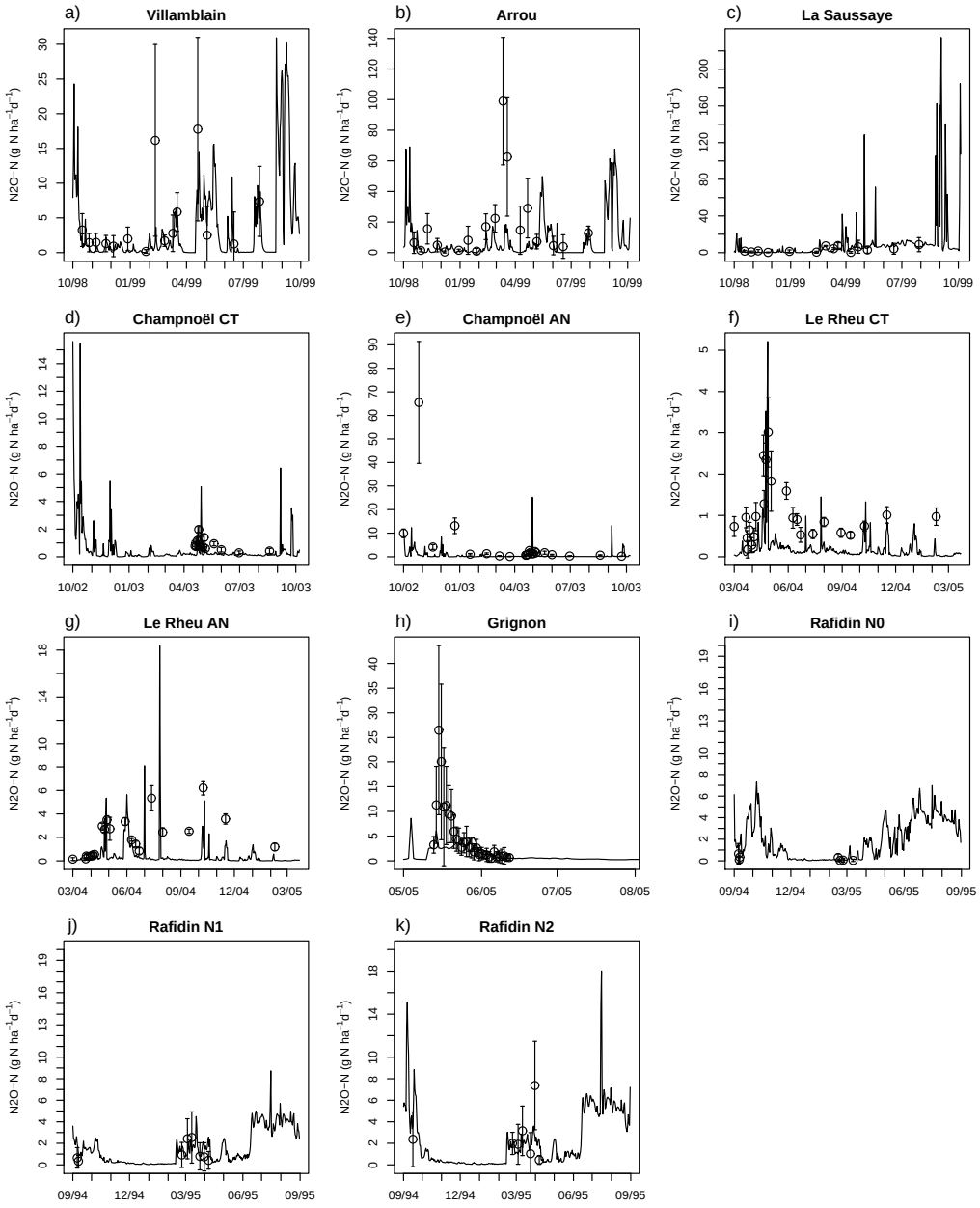

FIG. 2.4 : *Simulated (lines) and observed (symbols) N_2O emissions for the different sites and treatments. The simulated line is the posterior expectancy of predictions from dataset-by-dataset calibrations.*

Site	Treatment	RMSE (in g N_2O-N ha^{-1} d^{-1}) computed with :				
		Prior expectancy of predictions	Posterior expectancy of predictions	Posterior expectancy of parameters	Maximum a posteriori parameter vector	Posterior expectancy of predictions with the multi-dataset procedure
Rafidin	N0	4.6	0.7	0.3	0.3	4.6
	N1	7.5	1.2	1.4	1.2	12.8
	N2	10.5	2.1	3.0	2.8	20.4
Villamblain		5.2	4.8	4.9	4.9	5.5
Arrou		25.4	27.1	25.3	23.8	29.2
La Saussaye		93.0	2.0	2.3	2.4	2.3
Champnoël	CT	21.5	1.4	0.9	0.9	0.9
	AN	65.58	13.8	14.0	13.8	14.0
Le Rheu	CT	149.5	6.1	6.0	6.0	6.0
	AN	30.4	2.0	2.2	2.2	2.4
Grignon		16.9	1.0	1.2	1.3	1.1

TAB. 2.5 : *Root mean square errors (RMSE, in g N_2O-N ha^{-1} d^{-1}) based on : the prior expectancy of predictions, the posterior expectancy of predictions, the posterior expectancy of parameters, the maximum a posteriori parameter vector and the posterior expectancy of predictions from the multi-dataset procedure.*

to believe that the parameter set summarised in Table 2.1 could be a good compromise when the model will be applied for a new site.

In addition, Table 2.5 shows that the calibration did not really improve the simulations for two datasets : Villamblain and Arrou. For both datasets, the data were not informative enough to significantly improve parameter estimation. In the case of Arrou, the discrepancies may also be explained by the poor ability of CERES-EGC to simulate water-logging effects, as observed in this experiment. The N_2O module and in particular its denitrification part (Eqs. 2.1, 2.7, 2.8, 2.9 - Appendix A) were already shown unable of correctly rendering the dynamics of denitrification or N_2O emissions for soils with high degrees of water saturation. Still, RMSE values quantify the mismatch between simulations and the mean of the measurements without taking measurement uncertainty into account, or diagnosing whether problem lies with the simulations or the data. As a consequence, RMSE values should be interpreted with caution. More in-depth model evaluation would require comparing the behaviour of multiple models.

2.4 Discussion

2.4.1 Suitability and benefits of Bayesian calibration

Our main goal was to demonstrate the potential of a Bayesian-type calibration procedure to improve the parameterization of a N_2O-emission model, quantify parameter uncertainty and reduce uncertainties of model outputs.

In recent years, Bayesian calibration was successfully applied to process-based ecosystem models, such as forest biomass growth models (Klemedtsson et al., 2007; Svensson et al., 2008; Van Oijen et al., 2005). Among the various possible Bayesian methods, MCMC is in principle particularly well adapted to such models (and in particular CERES-EGC) because they can handle a high number of parameters simultaneously (Makowski et al., 2002). Their efficiency

is also not hampered by a poor knowlegde of the prior distributions, as is often the case with this type of models, and may be judged from the large variation range of the parameters we calibrated here. Method of expert elicitation have been recently developed and could be used in the future in order to refine prior distributions of model parameters. In short, elicitation is the process of translating expert knowledge about uncertain quantities into a probability distribution (Oakley and O'Hagan, 2007). However, no attempts had been made yet to calibrate processes so uncertain and irregular in time and space as N_2O emissions. This raised a number of issues in the adaptation of the MCMC algorithm. In particular, the chains were strongly auto-correlated, which required a substantial number of iterations (10^4 to 10^5), and drastic thinning. Also, the convergence had to be tested by running three parallel chains and using a variance-based diagnostic. An accurate simulation of the soil environmental drivers (temperature, moisture and mineral N contents) was a pre-requisite for the prediction of N_2O fluxes. Tests against field data showed that this condition was overall met, as noted in a previous test of CERES-EGC in a subset of the sites used here (Gabrielle et al., 2006b). In some instances, some discrepancies in the simulation of topsoil water content (Arrou) or nitrate content (La Saussaye, Champnoël AN and Le Rheu AN) which affected the prediction of N_2O fluxes. However, these errors point to structural deficiencies of the model (for instance in the simulation of soil water dynamics in the water-logged soil of Arrou), and did not interfere with the calibration. This was evidenced by the fact that inclusion of measured drivers improved model performance only marginally and in a few sites. This option was thus disregarded.

Our procedure significantly reduced parameter uncertainty for the datasets, and the uncertainty in simulated N_2O rates as a result. We have also established a database of N_2O emissions for Northern France and in the future, it will be interesting to use this one to parameterise other models or to compare the performance of different N_2O emissions process-based module integrated in CERES-EGC. Another direction could also be to use other kind of output data to parameterise specific module, for example the use of NO emission measurements for calibration of the nitrification sub-module (Eqs. 2.2, 2.10, 2.11, 2.12) of CERES-EGC (Rolland et al., 2008). The procedure we successfully implemented here may be readily used for other components of CERES-EGC, such as soil C turnover or crop photosynthesis and growth.

The calibration significantly reduced the model's RMSE compared with the prior parameter values, on average by 73% with the data-by-dataset procedure and by 33% with the multi-dataset procedure. Still, the calibration did not result in a perfect match between model simulations and observations of the daily N_2O fluxes. Measured data with high uncertainty were in particular less well predicted because they presented a high spatial variability and consequently were less constraining in the calculation of the likelihood function. This may also be seen as an advantage since these extreme data points with large variance did not artificially influence the parameter values compared to lower-range values with better accuracy. Heinen (2006) also showed with a different calibration method that the optimised denitrification sub-module did not result in perfect fit at the daily compared to the seasonal scale.

Lastly, the dataset-by-dataset calibration points to ways of optimising calibration efficiency : when using manual chambers, N_2O measurements should be carried out at least once a month throughout the year, with a higher frequency during the peak fluxes subsequent to N-fertiliser and crop residues inputs and when soil conditions are favourable to denitrification , e.g. when soil moisture, soil temperature and mineralization rate are high.

2.4.2 Spatial variability of model parameters

We sought to calibrate model parameters either on a dataset-by-dataset basis in order to minimise model error or simultaneously on all datasets to find parameter values that would be universally applicable, following the premise behind the original development of the N_2O model. Such values would be extremely useful to apply the model to new soil conditions and to spatially extrapolate it. However, it was suggested that simple process-based models such as the one we used here needs to be parameterised on a site-specific basis (Heinen, 2006). The latter authors concluded to the impossibility of defining a set of response functions for denitrification (Eqs 2.2, 2.7, 2.8, 2.9 - appendix A) that would equally apply to sandy, loamy and peat soil types. Our dataset-by-dataset calibration gave further evidence to that statement for the N_2O module of CERES-EGC, judging from the large variations in parameter pdfs across sites. However, our multi-dataset procedure also demonstrated that it is still possible to find global estimates for those parameters that encompass a wide range of experimental conditions, at the cost of a higher RMSE than with optimal, site-specific parameter sets. The parameter pdfs we obtained in the multi-dataset calibration shows which parameter values would be plausible, and may thus be used to improve the accuracy of N_2O simulations in new sites.

Models are often developed with the purpose of providing predictions over a large domain (in space and time). However, ensuring that their parameterisation is accurate is a pre-requisite to such application. When attempting at simulating N_2O fluxes in a new site where no measured data are available, the results of our calibration points to the following strategy to meet this requirement. First, the user should check if calibrated parameter sets already exist for similar soil types, based on soil taxonomy or physico-chemical characteristics. If not, the parameter values derived from the multi-dataset calibration may be used. They may also serve as default values for the spatial extrapolation of the model at the regional scale. In the future, new data sets may be assimilated in the calibration to reduce the uncertainty of global parameters and to increase the application domain of the model. Alternatively, it is clearly advisable to favour the collection of N_2O emissions data for the new sites, which lead to a much better performance of the model.

One last obstacle to the extrapolation of CERES-EGC lies in the 4 site-specific parameters, which are supposed to be measured in the laboratory. We chose to exclude them from the calibration in accordance with the original model design. However, including them would be interesting to simulate a situation where such experimental determination is not possible, and to see to what extent it influences the outcome of the calibration. It is likely to result in different parameter values since, for instance, the potential denitrification rate (a local parameter) was shown to significantly correlate with three global parameters related to denitrification (Gabrielle, 2006b).

However, testing such a scenario appeared beyond the scope of this paper since it implied too strong a deviation from the model hypotheses.

2.4.3 Prediction of nitrous oxide fluxes from agro-ecosystems

CERES-EGC and its specific N_2O module have already been used in a range of soil conditions (Dambreville et al., 2008; Heinen, 2006; Hénault et al., 2005a), and model uncertainty had only been quantified using simple Monte Carlo techniques for a subset of 5 parameters (Gabrielle et al., 2006a). The effect of parameter uncertainty was seldom analysed with ecosystem models simulating N_2O emissions, although (or perhaps also because) N_2O measurements are fraught with a daunting spatial and temporal variability (Duxbury and Bouldin, 1982). Our Bayesian calibration resulted in a probabilistic simulation of the time course of N_2O emissions taking such variability and uncertainty into account, through their consequences on parameters' distributions. The calibrated model could predict daily N_2O fluxes rather well, except for the highest peaks with high experimental error which it failed to predict in some cases.

In addition, the procedure makes it possible to quantify model output uncertainty in the calculation of annual N_2O budget and emission factors (EFs). The model predicted annual N_2O fluxes were ranging from 88 to 3672 g N_2O-N $ha^{-1}y^{-1}$ over the various sites, and EFs ranging from 0.05 to 1.12%. On the basis of these results, alongside those of Gabrielle et al. (2006a), it appears that the 1% default EF value of the IPCC Tier 1 methodology is not suitable for the sites we studied because it would considerably overestimate the annual emissions (Table 2.4). In Belgium, Beheydt et al. (2007) used the DNDC model to calculate EFs corresponding to various scenarios involving high N input levels and N surpluses, and obtained an average value of 6.49%, which is 25 times higher than ours, compared to an estimate of 3.16% using the N_2O measurements. Their observed emission range was an order of magnitude higher than that of our database. Assimilate such extreme data with our procedure would be helpful to enlarge the prediction range of CERES-EGC, and to check its ability to predict annual emissions higher than 10 kg N_2O-N ha^{-1} y^{-1}.

Our results also suggested that annual N_2O emissions were not strictly proportional to fertiliser N rate, which is in agreement with the results of Barton et al. (2008). The latter showed that, in a semi-arid climate, in spite of the application of N fertiliser the annual N_2O emissions were not significantly increased in comparison with background emissions. They concluded that the emissions of N_2O from arable soils could not be directly derived from the application of N fertiliser, and that other factors (e.g., soil properties) should be taken into account.

Bayesian calibration provided valuable insight into the uncertainty of the simulated N_2O fluxes, making it possible to take risk into account in a range of model applications : estimation of the global warming potential (GWP) of agro-ecosystems, assessment of cropping systems' environmental balance, or decision support in agriculture. It would also be interesting to compare the ability of various agro-ecosystem models to predict N_2O emissions on the same data sets, in a similar fashion as Frolking et al. (1998) and Li et al. (2005b). Furthermore, Bayesian

Model Comparison (Kass and Raftery, 1995; Van Oijen et al., 2005) could be applied to examine multiple models and to quantify their relative likelihood, i.e. by determining which model is most probable in view of the data and prior information. Finally, the outputs of several models could be combined to improve the accuracy of the prediction, as was suggested with atmospheric models (Fisher et al., 2002).

2.5 Conclusion and future work

Bayesian calibration was successfully applied to the CERES-EGC agro-ecosystem model to improve the parameterization of its N_2O emission module, thanks to a careful analysis and diagnostic of the MCMC chains of parameters generated by the Metropolis-Hastings algorithm. The parameters were calibrated either (i) against separately data sets or (ii) by using all the data sets simultaneously, to satisfy our objectives which were, respectively, to improve model simulations at the field scale and to find universal values of parameters in order to spatially extrapolate the model. In addition, Bayesian calibration provided a means of quantifying uncertainties in both parameters and model outputs. Furthermore, it appears reasonable to assume that when the model should be applied at a larger scale than the plot-scale, the parameter values resulted from the multi-dataset procedure could then be used for soil types which will have never been parameterised. In fact, the posterior parameter distributions encompass all our current observations and give us the possibility of quantifying their uncertainty.

A remaining obstacle to the extrapolation of the N_2O module lies in the 4 local parameters that should be measured or estimated on site (Hénault et al., 2005a), and that were accordingly not calibrated here. Identifying the key soil or landscape characteristics that control these parameters appears as a pre-requisite to the large-scale use of CERES-EGC.

Based on our results, we recommended a strategy to deal with model extrapolation and parameters' variability. Nevertheless, another option to tackle spatial variability would consist in using other types of prior information (e.g. on soil properties) to infer the parameters of the N_2O module. In future work, it would be beneficial to identify such "hyperparameters" which may explain spatial variability (Clark, 2005), and to develop a hierarchical Bayesian approach to derive their pdfs.

Acknowledgements

This work was part of the NitroEurope Integrated Project (EU's Sixth Framework Programme for Research and Technological Development) which investigates the nitrogen cycle and its influence on the European greenhouse gas balance. We wish to thank Matieyiendu Lamboni and Hervé Monod (INRA Jouy-en-Josas) for useful advice and discussions. Special thanks to Christophe Dambreville for making available the data from the Champnoël and Le Rheu sites.

Appendix A. Equations of the nitrous oxide emission module

The response functions are unitless and read :

$$F_N = \frac{\left[NO_3^-\right]}{Km_{denit} + \left[NO_3^-\right]} \tag{2.7}$$

where F_N is the denitrification response factor to [NO_3^-] the soil nitrate content (mg N kg^{-1} soil), and Km_{denit} the half-saturation constant (mg N kg^{-1} soil).

$$\begin{gathered} F_W = 0,\ WFPS < Tr_{WFPS} \\ F_W = \left[\frac{WFPS - Tr_{WFPS}}{1 - Tr_{WFPS}}\right]^{POW},\ WFPS \geq Tr_{WFPS} \end{gathered} \tag{2.8}$$

where F_W is the denitrification response factor to soil WFPS, Tr_{WFPS} is a threshold value below which no denitrification occurs and POW is the exponent of the power law.

$$\begin{gathered} F_T = exp\left[\frac{(T - TTr_{denit})\, ln\left(Q10_{denit,1}\right) - 9ln\left(Q10_{denit,2}\right)}{10}\right],\ T < TTr_{denit} \\ F_T = exp\left[\frac{(T-20)ln(Q10_{denit,2})}{10}\right],\ T \geq TTr_{denit} \end{gathered} \tag{2.9}$$

where F_T is the denitrification response function to soil temperature (T, °C), in the form of two sequential Q10 functions below and above a threshold temperature (TTr_{denit}). The two Q_10 values ($Q10_{denit,1}$ and $Q10_{denit,2}$) correspond to the relative increase in denitrification activity for every 10 °C increase in T.

$$N_N = \frac{\left[NH_4^+\right]}{Km_{nit} * Hp + \left[NH_4^+\right]} \tag{2.10}$$

where N_N is the nitrification response factor to [NH_4^+], the soil ammonium content (mg N kg^{-1} soil). The half-saturation constant Km_{nit} (mg N kg^{-1} soil) is calculated at each soil water content (Hp, w/w).

$$\begin{gathered} N_W = \frac{WFPS - MIN_{WFPS}}{OPT_{WFPS} - MIN_{WFPS}},\ MIN_{WFPS} < WFPS \leq OPT_{WFPS} \\ N_W = \frac{MAX_{WFPS} - WFPS}{MAX_{WFPS} - OPT_{WFPS}},\ OPT_{WFPS} \leq WFPS < MAX_{WFPS} \\ else\ N_W = 0 \end{gathered} \tag{2.11}$$

where N_W is the nitrification response function to soil water content. Nitrification is assumed to increase linearly from a minimum WFPS (MIN_{WFPS}) up to an optimal value (OPT_{WFPS}) and

then to linearly decrease down to a maximum WFPS (MAX_{WFPS}) (Rolland et al., 2008).

$$N_T = exp\left[\frac{(T-20)ln(Q10_{nit})}{10}\right] \tag{2.12}$$

where N_T is the response factor to soil temperature (T, °C) and $Q10_{nit}$ is the Q10 factor for this reaction.

Appendix B. The Metropolis-Hastings algorithm

The Metropolis-Hastings algorithm consists of three steps :

Step 1. Randomly generate a new "candidate" parameter vector

$$\theta^* = \theta_{i-1} + \delta \tag{2.13}$$

where δ is a random vector generated using a multivariate normal distribution ;

Step 2. Calculate the ratio of the posterior probability of the candidate vector over the posterior probability of the current candidate :

$$\alpha = \frac{p(\theta^*|Y)}{p(\theta_{i-1}|Y)} = \frac{p(Y|\theta^*)p(\theta^*)}{p(Y|\theta_{i-1})p(\theta_{i-1})} \tag{2.14}$$

In our case, since calculations are made using logarithms, we compute the log of α as the difference between the log of the posterior probability of the candidate vector minus the log of the posterior probability of the current vector.

Step 3. Accept θ^* if $\alpha \geq u$ where u is an uniform random variable from an uniform distribution on the interval (0,1), else reject and $\theta_i = \theta_{i-1}$.

The new point θ^* is always accepted if its posterior value is no lower than the posterior value of θ_{i-1}. Once the chain has attained the N iterations, the chain must have converged to the target distribution which is the posterior parameter distribution.

Chapitre 3

Prédiction des échanges nets de carbone de rotations de cultures en Europe avec un modèle d'agro-écosystème

Ce chapitre traite de la prédiction des échanges nets de carbone entre les agro-écosystèmes et l'atmosphère. Il est sous la forme d'un article soumis à la revue *Agriculture, Ecosystems and Environment* et s'intitule : "Predicting the net carbon exchanges of crop rotations in Europe with an agro-ecosystem model". Les co-auteurs sont : B. Gabrielle[a], P. Cellier[a], B. Loubet[a], R. Roche[a], P. Béziat[b], E. Ceschia[b] et M. Wattenbach[c].

Certaines pratiques agronomiques permettent de stocker du carbone dans le sol et ainsi compenser les émissions de N_2O. Ce terme du bilan a donc un impact important sur le pouvoir de réchauffement global des agro-écosystèmes et nécessite d'être estimé avec précision. La production nette de l'écosystème cultivé est fortement conditionnée par les pratiques culturales qui entraînent des fixations de C intenses pendant la saison de culture. Après calibration bayésienne des paramètres impliqués dans la modélisation du cycle du C de l'écosystème, le modèle CERES-EGC est appliqué pour produire des bilans de C à l'échelle de rotations de cultures pour deux sites expérimentaux. La qualité de prédiction du modèle est ensuite évaluée avec deux autres jeux de données indépendants. Le modèle simule les échanges nets de C depuis l'échelle journalière jusqu'à la rotation entière. Le bilan entre la production nette de l'écosystème, le C exporté par la récolte et les entrées de C par les engrais organiques, permet de quantifier la production nette du biome. Celle-ci reflète la variation du stock de C de l'écosystème. L'apport d'engrais organique, la fixation de C par les cultures intermédiaires ou les repousses de cultures ont un effet bénéfique significatif sur le bilan final.

a : UMR 1091 INRA-AgroParisTech Environnement et Grandes Cultures, Thiverval-Grignon, France

b : CESBIO, Toulouse, France

c : University of Aberdeen, Aberdeen, UK.

Abstract

Carbon fluxes between croplands and atmosphere are highly conditioned by farmer practices that involved intense atmospheric CO_2 uptake during crop growing season compared to other terrestrial ecosystems. Modelling and measuring land-atmosphere carbon exchanges from arable lands are important tasks to predict the influence of vegetation dynamics on climate change and its retroactive effects on crop productivity. We tested the agro-ecosystem model CERES-EGC against gap-filled daily net CO_2 exchanges over crop rotations monitored in three arable sites in Europe. The model parameters were estimated using Bayesian calibration and the model prediction accuracy was assessed with two supplementary independent data sets. As a result, the calibrated model allows us to compute the net ecosystem production (NEP) and net biome production (NBP) for entire crop rotations. The Bayesian calibration method results in an improvement of goodness of fit compared to initial parameter-based simulations. The calibrated model was accurate to estimate the NEP from daily time scale to aggregated NEP for entire crop rotation. The carbon returns from application of organic manure and the carbon uptake from catch crops and crop volunteers generated an important C sink effect on the NBP. Adding the nitrous oxide and methane fluxes from soils to the CO_2balance will allow us to compute the global warming potential of agro-ecosystems.

Keywords

Carbon dioxide ; Agro-ecosystem model ; CERES-EGC ; Bayesian calibration ; Independent validation ; Greenhouse gases ; Carbon balance ; Net Biome Production

3.1 Introduction

Agriculture contributes about 10-12% of the global anthropogenic emissions of greenhouse gases (GHGs), a share expected to rise due to an increase in land use and management intensity of agriculture worldwide (Smith et al., 2007). The direct GHG emissions of agro-ecosystems comprise nitrous oxide (2.8 Gt CO2-eq yr^{-1}), methane (3.3 Gt CO2-eq yr^{-1}), their exchanges of CO_2 being considered approximately balanced with a net emission of 0.04 Gt CO2-eq yr^{-1} to the atmosphere (Smith et al., 2007).
The net fixation of CO_2 by crops and soil respiration are the two main processes by which adapted management practices may increase the potential of C sequestration in soils (Johnson et al., 2007). The balance of these two terms corresponds to the net ecosystem production (NEP) of carbon, which is a measure of the C source or sink strength of ecosystems respective to the atmospheric compartment.

Experimental monitoring of net ecosystem exchanges (NEE) have been increasingly carried out using eddy-covariance (EC) techniques, and for all types of managed ecosystems : grasslands (Ammann et al., 2007; Veenendaal et al., 2007), forests (Kurbatova et al., 2008; Pilegaard et al., 2001), and croplands (Anthoni et al., 2004; Moureaux et al., 2006). Their values varied across ecosystem types but also within each class due to pedoclimatic differences and management practices.
In Russia, Kurbatova et al. (2008) reported annual net ecosystem production (NEP=-NEE) of -2000 kg C ha^{-1} yr^{-1} (denoting a C source) and 1440 kg C ha^{-1} yr^{-1} (C sink) for a wet and dry spruce forest, respectively, during the same time period.
In the Netherlands, the NEP of two grasslands on peat soils were measured at 57 kg C ha^{-1} yr^{-1} when they were managed extensively, and at -1339 kg C ha^{-1} yr^{-1} for an intensive management (Veenendaal et al., 2007). Soussana et al. (2007) reported an averaged NEP for nine grassland sites in Europe of 2400 ± 700 kg C ha^{-1} yr^{-1}, correspond to strong C sinks.
In Nebraska, Verma et al. (2005) measured NEP for irrigated and rainfed maize crops which were 3800 and 5200 kg C ha^{-1} yr^{-1}, respectively. Croplands are usually characterized by episodes of high C uptake during the crops growing season, directly related to farmers' management practices. A large part of the fixed C is removed from the field after harvest, and the residues are returned to the soil and processed by soil microbial biomass.

Accounting the absolute carbon balance of croplands requires to take into consideration the export and import of organic C within the agricultural field. This balance, called the net biome production (NBP), presents large range of variations between crop species, management intensity and temporal variations at interannual scale. For example, Grant et al. (2007) reported that a maize-soybean rotation in Nebraska (USA) was a net C source because of the failure of positive maize NBP to offset negative soybean NBP in the next year.
Anthoni et al. (2004) estimated the effect of manure application on NBP, and pointed out that manure largely offsets the C loss in the year of application. They also noticed that C input in the previous years significantly contributed to the next year C exchanges. Turner et al. (2007) mentioned the strong influence of climate on the interannual variations of the C budget over a large

domain (Oregon state, USA). Accordingly, it appears that croplands may be sources or sinks of C and that entire crop rotations should be considered to compute the C balance.

Because the C balance of croplands is heavily manipulated by farmers, and regulated by environmental conditions, biophysical models that simulate the turnover of C in agro-ecosystems appear a promising approach to estimate them (Huang et al., 2009). Grant et al. (2007) considered that process-based ecosystem models are the best method to predict net ecosystem production for known or hypothesized management practices or climate and where NEP measurements are incomplete or non available. Complexity, provenance and applications explained the main differences between the modelling approaches of C exchanges from crops. Carbon models were developed either from agronomic sciences (*Agro-C*, Huang et al. (2009)), biogeochemical sciences (*Ecosys*, Grant et al. (2007) ; *DNDC*, Zhang et al. (2002)), or for land surface models for use in larger-scale atmospheric models (*ORCHIDEE-STICS*, Gervois et al. (2008) ; *ChinaAgrosys*, Wang et al. (2007)).

Eddy-covariance measurements have widely been used for development and testing of the latter category of models, generally known as soil-vegetation-atmosphere transfer (SVAT) models, which couple C to energy and water balances on an hourly (or less) time step. There is a wide body of work on forests (Dufrêne et al., 2005; Klemedtsson et al., 2007; Kurbatova et al., 2008; Svensson et al., 2008) or cropland (de Noblet-Ducoudré et al., 2004; Wang et al., 2007), but limited to maximum one year time span.
Crop models integrate longer timeframes (growing season or crop rotation), and may include more regulators (eg, N cycling) and drivers (crop management). They have been widely used to simulate the growth and development of arable crops, and tested against field data such as crop dry matter or leaf area index (Zhang et al., 2002), but have rarely been compared to data of daily net C exchanges. Adiku et al. (2006) were surprised that such measurements had not been amply used before their study for the development and validation of crop gas exchange and growth models. They developed a model for simulating the net carbon exchanges of spring barley and compared its predictions with observations of gross primary production over one cropping season. Since their pioneering study, EC measurements are actively used for SVAT model development and validation but their use is still limited for crop model development.
In a large number of crop models, crop mass accumulation is estimated with the relationship between plant dry matter and interception of solar radiation. Daily biomass production is usually calculated as the product of the daily cumulative radiation intercepted with the radiation use efficiency (RUE, g DM MJ^{-1}). Radiation use efficiency is determined by measuring crop growth commonly based on measurements of above-ground biomass without estimating root compartment (Sinclair and Muchow, 1999). Gabrielle et al. (2002a) noticed that low C mineralization fluxes in soil simulated by soil-crop models may be attributed to a strong under-estimation of the turnover of below-ground plant biomass. The authors advised that much more dry matter should be partitioned to the roots and that RUE should be accordingly increased. Here we assume that calibration of RUE parameters of crop growth sub-models against net C exchanges would allow us to take into account the whole plant C fixation integrating the root growth and rhizodeposition.

Our general objective was to test the capacity of the soil-crop model CERES-EGC to predict daily NEP over crop rotations, using experimental data from arable sites in Europe (part of the CarboEurope measurement network). We first calibrated the model parameters against field data using Bayesian techniques, and subsequently assessed the model prediction error using two supplementary independent data sets. Finally, we calculated the carbon balances of the crop rotations involved in the various field sites.

3.2 Material and Methods

We used four different data sets from intensively monitored cropping systems to test the ability of the biophysical CERES-EGC model to simulate CO_2 exchanges at the field scale. The experimental sites are located in Grignon (Fr.), Auradé (Fr.) and Gebesee (Germ.), and involved different pedoclimatic conditions, crop types and management. At the three sites, net carbon fluxes were measured using the eddy covariance technique following the methodology of the CarboEurope integrated project. The model was parameterized using a Bayesian calibration method based on the Metropolis-Hastings algorithm against two data sets of daily NEP measurements collected over crop rotations. We also tested the prediction accuracy of calibrated model with two other independent data sets and finally, we applied the model to compute carbon balances for crop rotations.

3.2.1 The CERES-EGC model

3.2.1.1 A process-based agro-ecosystem model

CERES-EGC was adapted from the CERES suite of soil-crop models (Jones and Kiniry, 1986), with a focus on the simulation of environmental outputs such as nitrate leaching, emissions of N_2O and nitrogen oxides (Gabrielle et al., 2006a). CERES-EGC runs on a daily time step, and requires daily rain, mean air temperature and Penman potential evapo-transpiration as forcing variables. The CERES models are available for a large number of crop species, which share the same soil components (Jones and Kiniry, 1986).

CERES-EGC comprises sub-models for the major processes governing the cycles of water, carbon and nitrogen in soil-crop systems. A physical sub-model simulates the transfer of heat, water and nitrate down the soil profile, as well as soil evaporation, plant water uptake and transpiration in relation to climatic demand. Water infiltrates down the soil profile following a tipping-bucket approach, and may be redistributed upwards after evapo-transpiration has dried some soil layers. In both of these equations, the generalised Darcy's law has subsequently been introduced in order to better simulate water dynamics in fine-textured soils (Gabrielle et al., 1995).

A biological sub-model simulates the growth and phenology of the crops. Crop net photosynthesis is a linear function of intercepted radiation according to the Monteith approach, with interception depending on leaf area index based on Beer's law of diffusion in turbid media. Ra-

diation use efficiency (RUE) is defined for each crop as the dry biomass produced per unit of radiation intercepted by the crop. Photosynthates are partitioned on a daily basis to currently growing organs (roots, leaves, stems, fruits) according to crop development stage. The latter is driven by the accumulation of growing degree days, as well as cold temperature and day-length for crops sensitive to vernalisation and photoperiod. Lastly, crop N uptake is computed through a supply/demand scheme, with soil supply depending on soil nitrate and ammonium concentrations and root length density.

A micro-biological sub-model simulates the turnover of organic matter in the plough layer. Decomposition, mineralisation and N-immobilisation are modelled with three pools of organic matter (OM) : the labil OM, the microbial biomass and the humads. Kinetic rate constants define the C and N flows between the different pools. Direct field emissions of CO_2, N_2O, NO and NH_3 into the atmosphere are simulated with different trace gas modules.

3.2.1.2 Modelling of net carbon exchange

Carbon dioxide exchanges between soil-plant system and the atmosphere are modelled via the net photosynthesis and soil organic carbon (SOC) mineralization processes. Net primary production (NPP) is simulated by the crop growth modules of the different crop species (wheat, maize, barley, rapeseed and sunflower), while soil heterotrophic respiration (Rs) is deduced from the SOC mineralization rates calculated by the microbiological sub-model such as represented in Fig. 3.1. The net ecosystem production (NEP), which is calculated as NPP minus Rs, may be computed on a daily basis and directly tested against the net ecosystem exchanges measured by eddy covariance. The confrontation between the daily rates of simulated and measured NEP provides a good opportunity to calibrate the parameters related to CO_2 flux modelling and to test the simulation of C dynamics by the ecosystem model. In all sites, a complete rotation was ran before the measurement period to stabilize the soil C and N pools and dampen the effects of initial conditions.
The net biome production was calculated by aggregating daily NEP estimated by simulation or observation over cropping cycles, plus organic manure imports, minus C exported by harvested biomass.

3.2.2 Field sites

Net ecosystem exchange measurements were carried out with eddy covariance technique at three experimental sites located in Europe : Grignon (northern France, 48.9 N, 1.95 E), Auradé (southern France, 43.5 N, 1.1 E) and Gebesee (Germany, 51.1 N, 10.9 E). The site characteristics and crop rotations are detailed in Table 3.1.
The Grignon site is located about 40 km W of Paris, France. The soil was a silt loam with 18.9% clay and 71.3% silt in the topsoil and in the top 15 cm, organic carbon content was 20 g kg^{-1}, the pH (water) was 7.6 and the bulk density 1.3 g cm^{-3}. In Grignon, two field-sites experiments (*NitroEurope*, NEU-Grignon and *BioPollAtm*, BPA-Grignon) were conducted on adjacent plots with the same soil characteristics. The crop rotation of the NEU-Grignon experiment included

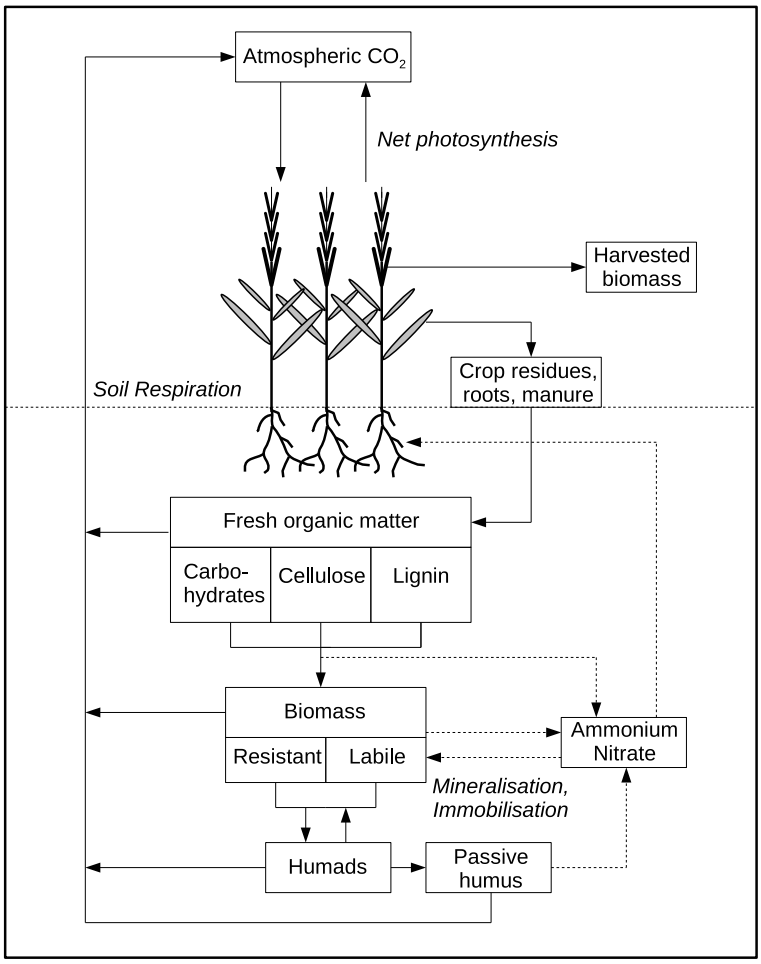

FIG. 3.1 : *Schematic of C fluxes (solid arrows) and N flows (dashed arrows) within the CERES-EGC model.*

maize, winter wheat, winter barley and mustard which was planted to serve as a catch crop to reduce nitrate leaching during winter. Dairy cow slurry was applied between the harvest of barley and the planting of mustard on 31 August 2004, and before the maize sowing on 16 April 2008. For the BPA-Grignon experiment, NEE measurements were carried during the maize growing season in 2002.

Auradé is located about 30 km W of Toulouse, France. The soil was a clay loam with 30.2% clay and 48.4% silt in the top 15 cm, organic carbon was 10 g kg^{-1}, the pH (water) was 6.9 and the bulk density 1.4 g cm^{-3}. The Auradé site involved a winter wheat-sunflower-winter wheat-rapeseed rotation since at least 2000.

The Gebesee experimental site is located about 20 km NW of Erfurt in Germany. The soil was a Chernozerm (silty clay loam) with 35.8% clay and 60.3% silt in the top 20 cm, organic carbon was 23 g kg^{-1}, the pH (water) was 6.7 and the bulk density 1.3 g cm^{-3}. The crop sequence from 2003 to 2007 was rapeseed-winter barley-sugar beet-winter wheat. Two applications of organic

fertilizers were carried out in 2007, one application of cattle slurry (18 m^3 ha^{-1}) on the wheat crop in 11 Apr. and 35 t ha^{-1} of farmyard manure in 4 Sept.

Site	Experiment	Year	Soil texture class	Sequence of crops	Number of daily NEP measurements
Grignon	NEU	2004-2008	Silt Loam	M-WW-WB-m	1627
Grignon	BPA	2002	Silt Loam	M	115
Auradé		2005-2007	Clay Loam	R-WW-SF	926
Gebesee		2007	Silty Clay Loam	WW	310

TAB. 3.1 : *Selected characteristics of the various sites and experiments (M : Maize ; WW : winter wheat ; WB : winter barley ; m : mustard ; R : rapeseed ; SF : sunflower).*

3.2.3 Carbon dioxide fluxes and biomass measurements

In all sites, the measurements of CO_2 fluxes at the field scale were carried out following the methodology the CarboEurope integrated project (IP ; Aubinet et al. (2000)). Water vapour and CO_2 fluxes were measured at a 2 to 3 m height above the crop canopy using the eddy covariance technique. Wind speed was monitored with three-dimensional sonic anemometers (Grignon model : R3-50, Gill Solent, Lymington, UK ; Auradé model : Campbell Csat3, Campbell Scientific Inc, Logan, UT, USA), and CO_2 concentration with infrared gas analysers (model Li-7500 in Grignon and Auradé and model Li-7000 in Gebesee ; Li-Cor Inc., Lincoln, NE, USA). Daily NEP of carbon dioxide (g C m^{-2} d^{-1}) and evapotranspiration rate (mm m^{-2} d^{-1}) were calculated by integrating the 30-minute fluxes obtained with the micrometeorological measurements over 24 h periods. The data sets were processed following the standardised methodology described in Papale et al. (2006). Carbon dioxide fluxes were corrected for CO_2 storage below EC measurement height, low turbulence conditions were filtered using a friction velocity threshold criterion. The eddy covariance technique and subsequent data processing produce gaps in the half-hourly C flux data, making it necessary to fill the missing values before integration at the daily time scale. The gap-filling methodology of CarboEurope-IP was applied to the experimental data sets (Falge et al., 2001).

Above-ground plant dry matter (DM) was measured every two weeks during crop growth, over the full crop sequences of the Auradé, NEU-Grignon and BPA-Grignon experiments. Daily weather data were recorded with automatic meteorological station, including maximum and minimum daily air temperatures (°C), rainfall (mm d^{-1}), solar radiation (MJ m^{-2} d^{-1}) and wind speed (m s^{-1}) at each site.

3.2.4 Parameter calibration

The parameters were estimated using the Bayesian calibration method described in Lehuger et al. (2009b). Table 3.2 lists the parameters involved in the calibration as well as their prior

probability density functions (pdf). Briefly, Bayesian methods are used to estimate model parameters by combining two sources of information : prior information about parameter values and observations of model output variables. In our case, the observations consisted of the NEP measurements. Bayes' theorem makes it possible to combine the two sources of information in order to calibrate the model parameters.
The first step is to assign a probability distribution to the parameters, representing our prior uncertainty about their values. We specified lower and upper bounds of the parameters' uncertainty, and defined the prior pdfs as uniform (Table 3.2). The aim of Bayesian calibration is to reduce this uncertainty by using measured data, thereby producing the posterior distribution for the parameters. This is achieved by multiplying the prior with the likelihood function, which is the probability of the data given the parameters. Because probability densities may be very small numbers, rounding errors needed to be avoided and all calculations were carried out using logarithms. The logarithm of the data likelihood was thus calculated for each data set D_i as follows :

$$logL_i = \sum_{j=1}^{K} \left(-0.5 \left(\frac{y_j - f(\omega_k; \theta_l)}{\sigma_j} \right)^2 - 0.5log(2\pi) - log(\sigma_j) \right) \tag{3.1}$$

where y_j is the NEP measured on sampling date j in the data set D_i, and σ_j the standard deviation, ω_k is the vector of model input data for the same date, $f(\omega_k; \theta_l)$ is the model simulation of y_j with the parameter vector θ_l, and K is the total number of observation dates in the data sets. Two additional parameters were involved in the calibration, corresponding to a site-specific experimental error of NEE measurements. Parameters *psys1* for systematic error of measurement in NEU-Grignon and *psys2* for Auradé were introduced in the log-likelihood function as multiplicative factors of D_i. We defined their prior pdfs as uniform over the [0.5-2] range.

To generate a representative sample of parameter vectors from the posterior distribution, we used a Markov Chain Monte Carlo (MCMC) method : the Metropolis-Hastings algorithm (Metropolis et al., 1953). We formed Markov chains of length 10^4-10^5 using a multivariate Gaussian pdf to generate candidate parameter vectors. The variance matrix of this Gaussian was adjusted to ensure an efficient exploration of the parameter space by the Markov chains. We first set the marginal variances to the square of 1% of the prior parameter ranges, and the covariances to zero (Van Oijen et al., 2005). In addition, the acceptance rate was artificially adjusted by increasing the measurement uncertainty in order to smooth the likelihood surface and make the calibration easier. Due to the large amount of observed data involved, the likelihood surface presented sharp peaks and the probability for the model to hit a 'target area' for a successful calibration was too small otherwise. Ten percent of the total number of iterations at the beginning of the chain were discarded as unrepresentative 'burn-in' segments of the chains (Van Oijen et al., 2005). The rest of the chains were considered as a representative sample from the posterior pdf, and were used to calculate the mean vector, the variance matrix and the 90% confidence interval for each parameter. Bayesian calibration was successively applied to the Auradé experiment and the NEU-Grignon treatment.

Parameter vector $\theta = [\theta_1 ... \theta_{16}]$					Prior probability distribution			Posterior probability distribution			
θ_i	Symbol	Description	Unit	Default value	θ_{min}(i)	θ_{max}(i)	References	Mean NEU-Grignon	SD NEU-Grignon	Mean Auradé	SD Auradé
θ_1	ruemaize	Radiation use efficiency of maize	g DM MJ^{-1}	4.5	1.0	5.5	Choudhury (2001); Sinclair and Muchow (1999) Andrade et al. (1993); Lindquist et al. (2005)	3.0	0.1	NA	NA
θ_2	ruewheat	Radiation use efficiency of winter wheat[a]	g DM MJ^{-1}	7.5	2.5	8.0	Choudhury (2000); Hui et al. (2001); Sinclair and Muchow (1999)	6.3	0.2	5.4	0.6
θ_3	ruerap1	Radiation use efficiency of rapeseed for vegetative phase	g DM MJ^{-1}	2.7	0.8	4.0	Gabrielle et al. (1998a); Justes et al. (2000)	1.83	0.04	4.75	1.48
θ_4	ruerap2	Radiation use efficiency of rapeseed for reproductive phase	g DM MJ^{-1}	2.7	0.8	3.2	Gabrielle et al. (1998a)	2.81	0.17	1.85	0.17
θ_5	sflo1	Radiation use efficiency of sunflower for vegetative phase	g DM MJ^{-1}	1.4	0.7	3.0	Sinclair and Muchow (1999); Villalobos et al. (1996) Albrizio and Steduto (2005)	NA	NA	0.72	0.03
θ_6	sflo2	Radiation use efficiency of sunflower for reproductive phase	g DM MJ^{-1}	1.3	0.9	1.5	Sinclair and Muchow (1999); Villalobos et al. (1996)	NA	NA	1.62	0.61
θ_7	prop1	Partitioning coefficient of total C into microbial biomass pool	%	0.015	0.010	0.030	Gabrielle et al. (2004); Molina et al. (1983) Corbeels et al. (1999); Molina et al. (1997); Nicolardot and Molina (1994) Nicolardot et al. (1994)	0.024	0.006	0.014	0.003
θ_8	prop2	Partitioning coefficient of total C into humads pool	%	0.12	0.10	0.35	Corbeels et al. (1999); Molina et al. (1997) Gabrielle et al. (2002a); Nicolardot and Molina (1994)	0.142	0.040	0.209	0.060
θ_9	coef1	Partitioning coefficient of residue C into residue carbohydrate pool	%	0.20	0.15	0.23	Henriksen and Breland (1999)	0.204	0.015	0.210	0.014
θ_{10}	coef2	Partitioning coefficient of residue C into residue cellulose pool	%	0.70	0.65	0.73	Henriksen and Breland (1999)	0.69	0.03	0.70	0.01
θ_{11}	cf1	Decomposition rate of labile microbial biomass pool	d^{-1}	0.332	0.25	0.50	Godwin and Jone (1991); Henriksen and Breland (1999) Lengnick and Fox (1994); Nicolardot and Molina (1994)	0.29	0.03	0.35	0.06
θ_{12}	cf2	Decomposition rate of resistant microbial biomass pool	d^{-1}	0.0404	0.0250	0.0600	Henriksen and Breland (1999); Nicolardot and Molina (1994) Dou and Fox (1995); Lengnick and Fox (1994)	0.0362	0.0062	0.0416	0.0083
θ_{13}	cf3	Decomposition rate of humads pool	d^{-1}	0.003	0.002	0.007	Molina et al. (1997); Nicolardot and Molina (1994) Dou and Fox (1995); Gabrielle et al. (2002a)	0.004	0.002	0.003	0.001
θ_{14}	cfres1	Decomposition rate of residue carbohydrate pool	d^{-1}	0.20	0.15	0.80	Corbeels et al. (1999); Henriksen and Breland (1999) Godwin and Jone (1991)	0.29	0.11	0.61	0.13
θ_{15}	cfres2	Decomposition rate of residue cellulose pool	d^{-1}	0.050	0.013	0.055	Corbeels et al. (1999); Henriksen and Breland (1999) Godwin and Jone (1991); Hadas et al. (1993)	0.045	0.006	0.022	0.010
θ_{16}	cfres3	Decomposition rate of residue lignin pool	d^{-1}	0.0090	0.0095	0.015	Corbeels et al. (1999); Dou and Fox (1995)	0.0099	0.0008	0.0120	0.0017

[a]For wheat, net photosynthesis rate is fonction of ruewheat$\times$PAR$^{0.6}$

TAB. 3.2 : *Description of the 16 model parameters involved in the Bayesian calibration. The prior probability distribution is a multivariate uniform distribution between bounds θ_{min} and θ_{max}, as extracted from the above-cited literature references. The posterior parameter distributions are characterised by the mean value of the posteriors and their standard deviation (SD).*

3.2.5 Goodness of fit

The goodness of fit between simulations and observations was assessed by calculating the root mean square error (RMSE). The RMSE was used to judge the performance of the parameter calibration as well as the model prediction error for the two independent data sets. It was calculated for each data set D_i as follows (Wallach, 2006) :

$$RMSE = \sqrt{\frac{1}{K}\sum_{j=1}^{K}(y_j - f(\omega_k;\theta_l))^2} \tag{3.2}$$

where y_j is the observed NEP on day j of data set D_i, and f($\omega_k;\theta_l$) is the corresponding model predictions with input variables ω_k and parameters θ_l. Simulations were carried out using either the posterior expectancy of parameters ($\overline{\theta_l}$) or the maximum a posteriori (MAP) estimate of θ ($\theta_{MAP,l}$). θ_{MAP} is the single best value of the parameter vector in MCMC chain, which maximizes the posterior probability density (Van Oijen et al., 2005). The posterior expectancy of predictions were obtained from the posterior parameters pdfs. The root mean square errors were computed for the experiments used in the parameter calibration (NEU-Grignon and Auradé) and in the subsequent model testing against independent data sets (BPA-Grignon and Gebesee). In the latter case, the RMSE corresponded to the root mean squared error of prediction (RMSEP(θ)), since the data were involved neither in parameter estimation nor model development (Wallach, 2006). RMSEP is a measure of the model's accuracy in the prediction of NEP.

3.3 Results

3.3.1 Model calibration

Table 3.2 recapitulates the mean and standard deviations of the posterior parameter distributions obtained after calibration against the NEU-Grignon and Auradé data sets. The posterior radiation use efficiencies (RUEs) of maize and wheat were lower than their default values for both sites, by 30% for maize, and 15% to 30% for wheat. Thus, the uncalibrated wheat and maize crop components of CERES-EGC tended to over-estimate crop biomass. Conversely, the calibrated RUEs of rapeseed and sunflower were lower or higher than their initial values, depending on development phase and experimental site.

The posterior parameter values of SOC mineralization parameters were generally close to their default values excepted for the parameters *prop1*, *prop2*, *cfres1* and *cfres2*. The decomposition rate of residue carbohydrate pool (*cfres1*) was substantially increased for calibration against Auradé data set (0.61 vs. 0.20 d^{-1}) and slightly for calibration against NEU-Grignon data set (0.29 vs. 0.20 d^{-1}). The coefficients partitioning endogenous soil organic C into the microbial biomass (*prop1*) and humads (*prop2*) pools were also higher than their default values, respectively 60% for *prop1* in NEU-Grignon and 75% for *prop2* in Auradé. The parameters *psys1* and *psys2* were calibrated within the BC at the same time as the model parameters and their mean posterior values were 1.38 (± 0.26) and 0.87 (± 0.20) for NEU-Grignon and Auradé respectively. This result

Site	Output variables	Unit	RMSE computed with :			
			Initial parameter values	Posterior expectancy of parameters	Maximum a posteriori parameter vector	Posterior expectancy of predictions
NEU-Grignon	Daily NEP	g CO_2-C m^{-2} d^{-1}	2.22	1.90	1.90	1.89
	Cumulative sum of NEP	g CO_2-C m^{-2}	415.85	137.65	92.57	127.11
	Above-ground biomass	t DM ha^{-1}	1.87	1.82	1.99	1.83
Auradé	Daily NEP	g CO_2-C m^{-2} d^{-1}	2.68	1.88	1.80	1.88
	Cumulative sum of NEP	g CO_2-C m^{-2}	217.83	68.68	83.36	70.03
	Above-ground biomass	t DM ha^{-1}	1.84	1.24	2.93	1.24

TAB. 3.3 : *Root mean square errors (RMSEs) of daily NEP, cumulative sum of NEP and above-ground biomass based on the initial (prior) parameters values, the posterior expectancy of parameters, the maximum a posteriori parameter vector and the posterior expectancy of predictions.*

means that the measurements in NEU-Grignon would be under-estimated whereas they would be over-estimated in Auradé.

Table 3.3 summarizes the RMSEs for daily and cumulative NEP, and above-ground plant biomass obtained with the various parameter sets (prior and posterior). The calibration led to a 15% to 30% reduction of the RMSE relative to the uncalibrated parameter set. There were small differences between the RMSEs computed with posterior expectancy of parameters and posterior expectancy of predictions. The simulations computed with the parameter set with maximum posterior probability, i.e. when likelihood is maximal, involved RMSE values for daily NEP lower than RMSEs computed with posterior expectancy of parameters. But this parameter set may involve higher RMSE values for cumulative sum of NEP and ABG biomass, compared to RMSEs computed with posterior expectancy of prediction and posterior expectancy of parameters.

3.3.2 Dynamics of net carbon exchanges

Figure 3.2 (a and d) compares the simulations of daily NEP after calibration and the observations for the crop rotations of the NEU-Grignon and Auradé experiments. There was good agreement between the two series at the time scale of a growing season (from sowing to harvest), and also for the time intervals in between two crops. The growing seasons of spring crops (maize and sunflower) were shorter than those of winter crops (rapeseed, wheat, barley), but simulations of daily C uptake reached higher values for maize and sunflower. The net carbon exchanges reached a peak value of 15 g C m^{-2} d^{-1} for the maize crop in Grignon, while they did not exceed 10 g C m^{-2} d^{-1} with winter crops. The net fixation of C was directly related to global solar radiation, which led to irregular patterns of net photosynthesis. Crop residues, senescent roots and the application of organic manure fed the fresh organic matter pool of soil and were slowly decomposed after incorporation in soil. Soil respiration mainly occurred in autumn and winter following the incorporation of crop residues in soil, with daily rates ranging between -5 and 0 g C m^{-2} d^{-1}.

In Grignon, after the harvest of barley crops in years 2004 and 2007, mustard was planted as a catch crop. Its growth was well simulated in 2008, whereas in 2004, the simulated time span of crop growth and net C fixation was shorter than observed. As a result, the total C fixa-

tion by the mustard was under-estimated in 2004 by the model, as was that of the maize crop in 2008 (Fig. 3.2.c). In Auradé, no catch crop was sown after the harvests of rapeseed in 2005 and wheat in 2006, but volunteers of previous crops grew up and entailed a net C uptake. This effect was modelled by resowing the same crop after harvest and stopping its growth upon tillage. Net ecosystem production was remarkably well predicted during the rapeseed and wheat growing seasons, but it was over-estimated over the sunflower crop. This was due to the model under-estimation of soil respiration rates in the months preceding the sowing of sunflower.

Figures 3.2.b and 3.2.e show the regressions between observed and modelled daily NEP at NEU-Grignon and Auradé. The coefficients of determination were fairly good, with an R^2 of 0.76 and 0.59 in Grignon and Auradé, respectively. There was also little systematic error in the predictions : the slope of the regressions was equal to unity (Grignon) or close to this value (0.82) in Auradé, and the intercepts were negligible (0.25 and 0.00 g C m^{-2} d^{-1} in Grignon and Auradé, respectively). When cumulated over the measurement period, net C fluxes were correctly predicted by the model for the NEU-Grignon and Auradé experiments (Fig. 3.2.c and 3.2.e), which proves its capacity to integrate the various C fluxes and turnover rates within the agro-ecosystem.

The simulations of above-ground biomass of crops were also well within the experimental measurement errors (Fig. 3.3.a and 3.3.c), for the various crop species, with the exception of the 2008 maize upon harvest in Grignon, whose dry matter was under-predicted. The regression analysis evidenced a good match between observed and simulated data (after calibration). For the NEU-Grignon experiment, we obtained an R^2 of 0.95, an intercept of -0.75 t DM ha^{-1} and a slope of 1.2, and for Auradé, an R^2 of 0.94, an intercept of 0.35 t DM ha^{-1} and a slope of 1.12. Six different crop species, involving 6 crop-specific sub-models, were involved in the rotations but did not hamper a good match to the field-measurements.

3.3.3 Model prediction assessment

The experiments of Gebesee and BPA-Grignon were used to assess the model prediction accuracy by computing the RMSEP, after calibration against the data from the NEU-Grignon trial (Table 3.4). The field experiments used in model testing represented different climate and soil conditions compared to the calibration sites, with similar crop management. The RMSEP for daily NEP was lower for the wheat in Gebesee than for the maize in BPA-Grignon, amounting to 1.55 and 3.78 g C m^{-2} d^{-1}, respectively. Conversely, the RMSEP for cumulative NEP was 3 times lower for BPA-Grignon than for Gebesee, being respectively of 31.61 and 90.95 g C m^{-2}. The RMSEP of above-ground (ABG) biomass was computed only for BPA-Grignon due to a lack of biomass measurements in Gebesee. Figures 3.4.a and 3.4.d depicts the dynamics of daily NEP for Gebesee and BPA-Grignon. At Gebesee, the model accurately captured the dynamics of net C fixation by the crop and the post-harvest soil respiration. In the BPA-Grignon trial, the measurement period was focused on the maize growing season, and the spike of net C fixation measured in July was not captured by the model.

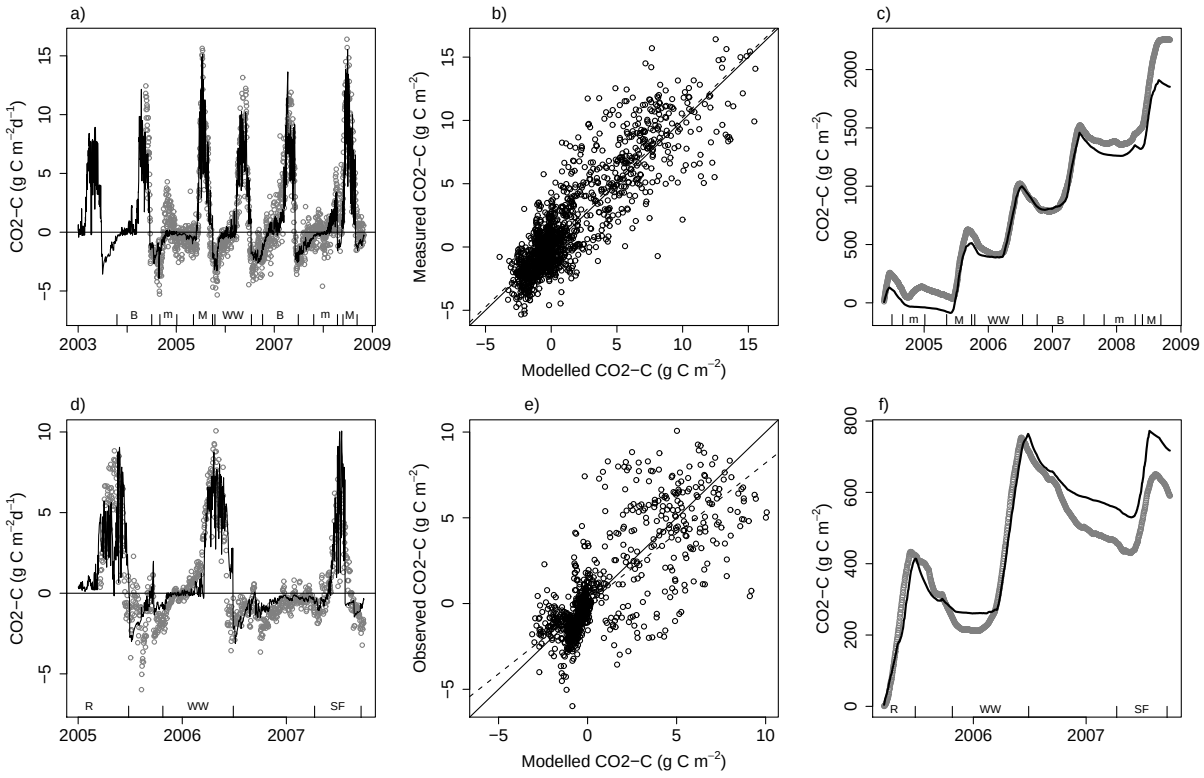

FIG. 3.2 : *Time course of simulated (black line) and observed (grey symbols) of net ecosystem production (NEP), on a daily time scale (a,d) or cumulated for each growing season (c,f), and scatter plot of simulated versus measured NEP (b,e). The top graphs pertain to the Grignon-NEU experiment (a,b,c), the bottom one to the Auradé experiment (d,e,f). Simulation lines correspond to the posterior expectancies of simulations, and the crop cycles are represented with the following letters : B : barley, m : mustard, M : maize, WW : winter wheat, R : rapeseed and SF : sunflower.*

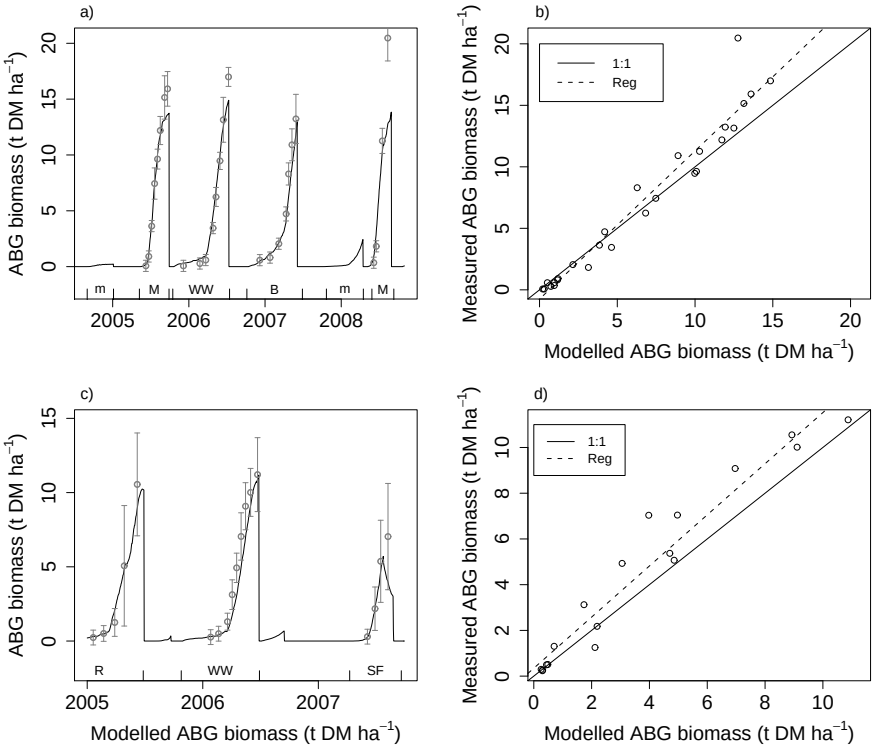

FIG. 3.3 : *Simulations (black line) and observations (grey points) of above-ground (ABG) crop biomass (a,c) and simulated versus measured ABG biomass (b,d) for the crop sequence of Grignon site (a,b) and Auradé site (c,d). Simulation lines correspond to the posterior expectancies of simulations, and the crop cycles are represented with the following letters : B : barley, m : mustard, M : maize, WW : winter wheat, R : rapeseed and SF : sunflower.*

The radiation use efficiency of maize calibrated with the NEU-Grignon dataset appeared suboptimal for the BPA-Grignon experiment. The regressions between observed and simulated daily NEP were overall satisfactory, with an R^2 of 0.49 and 0.79 in Grignon and Gebesee, respectively, while the slopes ranged from 0.77 to 0.88, and the intercepts ranged from -0.37 to 0.79 g C m^{-2} d^{-1} (Figs 3.4.b and 3.4.e). The relatively low R^2 for the Grignon-BPA experiment stems from the model failing to mimic the peak C fixation fluxes in July, probably because it over-estimated the effect of water stress on photosynthesis. The model overestimated the cumulative sum of NEP in Gebesee whereas it slightly underestimated this variable in BPA-Grignon (Figs 3.4.c and 3.4.f).

Figure 3.5 depicts the time course of ABG dry matter for the maize crop of the BPA-Grignon experiment. Simulations were computed either with the posterior expectancy of parameters derived from the calibration of NEU-Grignon or with the initial (uncalibrated) parameter values. Surprisingly, the latter resulted in a more accurate simulation of crop biomass accumulation than the calibrated parameters. On the basis of these results, it appears that the calibration impro-

Site	RMSEP of :		
	Daily NEP g CO_2-C m^{-2} d^{-1}	Cumulative sum of NEP g CO_2-C m^{-2}	Above-ground biomass t DM ha^{-1}
Gebesee	1.55	90.95	no data
BPA-Grignon	3.78	31.61	3.65

TAB. 3.4 : *Root mean square errors of prediction (RMSEP) based on the posterior expectancy of parameters for daily NEP, cumulative sum of NEP over crop rotation and above-ground biomass.*

ved the simulation of NEP but without improving the prediction of biomass accumulation. As a result, the RMSEP for ABG biomass with calibrated model was quite high (Table 3.4).

3.3.4 Carbon balance of crop rotations

Figure3.6 shows the time course of carbon balance in all sites, as broken down across crops during the time period extending from their sowing to the sowing of the following crop. In the NEU-Grignon experiment, NPP was higher for the 2006 winter wheat and 2007 barley than for the 2005 and 2008 maize crops. On the other hand, soil respiration after winter wheat and barley were higher than for maize crops due to a longer period of net soil respiration from harvest to sowing. As a result, NEP was higher for maize than for winter cereals, averaging 4770 and 4090 kg C ha^{-1}, respectively. The mustard sown in 2004 was a net source of CO_2, i.e its net photosynthesis was lower than the net soil respiration. This pattern was reversed with the mustard sown in 2008, which was overall a net sink of CO_2. In both cases, the introduction of a catch crop between winter cereals and the following spring crop increases ecosystem uptake of C at the rotation scale.

In Auradé, seasonal net photosynthesis, soil respiration and net ecosystem production were similar for the 2005 winter rapeseed crop and the 2006 winter wheat (Fig. 3.6.b), resulting in a NEP (equivalent to a net C-uptake by the ecosystem) of 2800 kg C ha^{-1}. The net photosynthesis of sunflower was underestimated by the model, resulting in a NEP lower than for winter crops (1600 kg C ha^{-1}). In Gebesee, the net photosynthesis of winter wheat reached 6230 kg C ha^{-1}, soil respiration totalled -4000 kg C ha^{-1} and net ecosystem production 2230 kg C ha^{-1} (Fig. 3.6.c). In this site, soil organic carbon was higher than in the other sites, generating higher soil respiration rates. In the BPA-Grignon experiment, the net ecosystem production of maize totalled 6490 kg C ha^{-1} over the growing season, corresponding to the balance between net photosynthesis (7740 kg C ha^{-1}) and soil respiration (-1250 kg C ha^{-1} - Fig. 3.6.c).

Table 3.5 recapitulates the modelled and observed carbon inputs and exports for the 4 experiments, by crop. As in the previous section, the C budget for each crop started upon sowing and ended upon sowing of the following crop, except for Auradé, Gebesee and BPA-Grignon where the starting date was the first day of measurement. In the NEU-Grignon experiment, the model predicted the 3-yr rotation to be a net sink of 215 kg C ha^{-1} whereas the observations indicated

a net source of C (-1520 kg C ha^{-1} over the three years). This discrepancy was due to the under-estimation of C fixation by the 2005 maize crop and of the amount of straw removed after winter wheat in 2006. In this site, the straw of winter wheat and barley was harvested, whereas in the other sites it was incorporated into the soil. The experimental determination of straw removal rate may also have led to an over-estimation of this term, since losses probably occurred upon harvest. The simulated year-round NEP for the year 2005 at NEU-Grignon (encompassing the maize cropping cycle) was 4350 kg C ha^{-1} yr^{-1} (vs. 3120 kg C ha^{-1} yr^{-1} observed) and was 5200 kg C ha^{-1} yr^{-1} for the year 2002 at BPA-Grignon.

In Gebesee, cattle slurry and farmyard manure were applied in 2007 during the winter wheat growing season, making this crop cycle a large C sink. The simulated year-round NEP for 2007 (encompassing a part of the wheat cropping cycle) was 2400 kg C ha^{-1} yr^{-1}, which is much lower than the total of 1133 kg C ha^{-1} measured from 1 Jan. 2007 to 5 Oct. 2007 (the end of measurement period). The modelled NEP was slightly higher than the value of 1930 kg C ha^{-1} yr^{-1} reported by Anthoni et al. (2004) and based on measurements for the same site in 2001 for winter wheat. In addition, Anthoni et al. (2004) reported that when they removed C exported by the harvest to the NEP, the site became a net source of CO_2 (of -970 kg C ha^{-1} yr^{-1}), whereas we modelled for the year 2007 a NBP of 4765 kg C ha^{-1} yr^{-1} when we removed harvested biomass to the NEP.

In Auradé, we overestimated the C sink of the rotation 2005-2007 as compared with the observations, 2270 vs. 500 kg C ha^{-1} over 2.5 years which is due to a 30% underestimation of rapeseed grain yield in 2005 and an overestimation of NEP for rapeseed and winter wheat by 10 and 35% respectively as compared with observations. In the BPA-Grignon experiment, the model underestimated harvested biomass by 40% which induced a large bias in NBP : 25 vs. 2575 kg C ha^{-1} over 117 days.

Site	Crop	Time period		Net ecosystem production (kg C ha^{-1})		Harvested biomass (kg DM ha^{-1})		Manure (kg C ha^{-1})	Net biome production (kg C ha^{-1})	
		Start	End	Modelled	Observed	Modelled	Observed		Modelled	Observed
NEU-Grignon	Mustard	2004-09-01	2005-05-08	-822	-456			988	166	532
	Maize	2005-05-09	2005-10-15	5515	5139	-13510	-15470		111	-1049
	Winter wheat	2005-10-16	2006-10-05	3510	2621	-7597 (-5859)	-7500 (-8430)		-1872	-3751
	Barley	2006-10-06	2007-10-21	4485	5377	-8630 (-3632)	-8200 (-3640)		-419	641
	Mustard	2007-10-22	2008-04-26	632	875			1763	2395	2638
	Maize	2008-04-27	2008-10-14	6627	8005	-13730	-20470		1135	-183
	Rotation	2005-05-09	2008-04-26	14143	14012				215	-1521
Auradé	Rapeseed	2005-03-18	2005-10-24	2745	2504	-3768	-5300		1237	384
	Winter wheat	2005-10-25	2007-04-09	2816	2088	-6378	-6000		265	-312
	Sunflower	2007-04-10	2007-09-29	1611	1311	-2116	-2200		765	431
	Rotation	2005-03-18	2007-09-29	7172	5903				2267	503
Gebesee	Winter wheat	2007-01-01	2007-10-05	2622	1134	-7165	-4700	4460	4216	3714
BPA-Grignon	Maize	2002-06-15	2002-10-07	6476	6643	-16130	-23040		24	-2573

TAB. 3.5 : *Carbon budgets of the crop sequences of NEU-Grignon, Auradé, Gebesee and BPA-Grignon. The C balance is broken down into net ecosystem production, harvested biomass, manure inputs.*

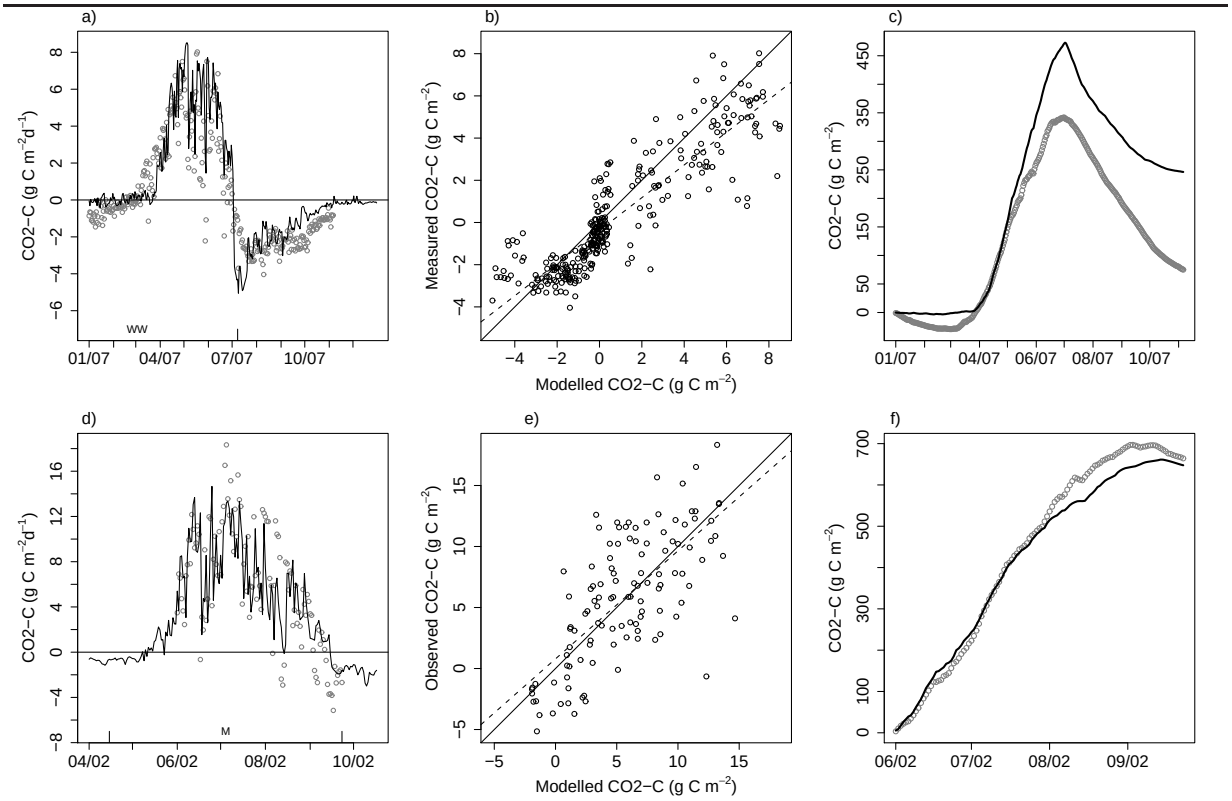

FIG. 3.4 : *Simulations (black line) and observations (grey points) of daily net ecosystem production (NEP), simulated versus measured NEP and simulations (black line) and observations (grey points) of cumulative sum of NEP for the wheat crop cycle of Gebesee site (a,b,c) and the maize crop cycle of Grignon-BPA experiment (d,e,f).*

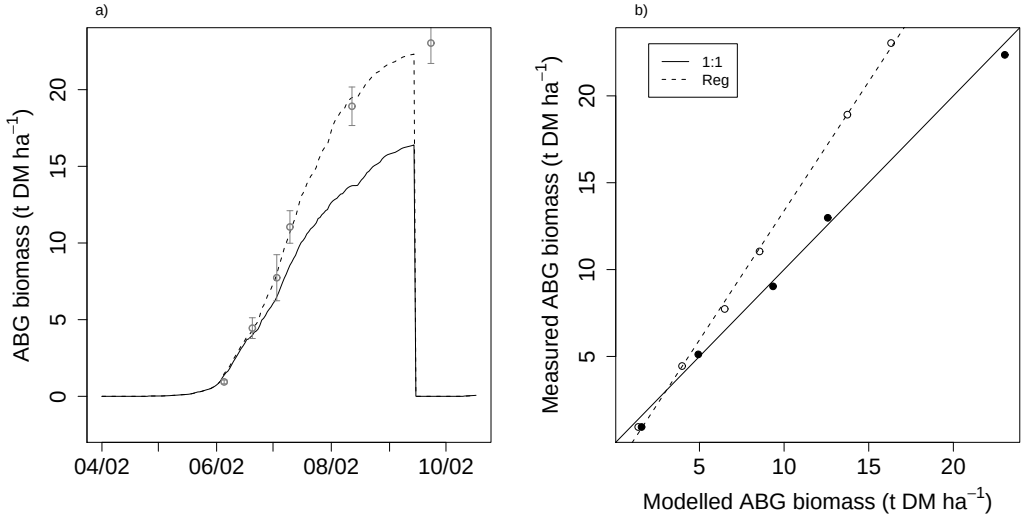

FIG. 3.5 : *Simulations with calibrated parameter values (solid line) and initial parameter values (dashed line) and observations (grey points) of above-ground (ABG) crop biomass (a). Simulated versus measured ABG biomass for simulations with calibrated parameters (empty points) and initial parameter values (full points) for the maize crop cycle of BPA-Grignon site (b, the measurement of 7 Oct. 2002 was removed of the data set). Simulated lines with calibrated parameters are the posterior expectancies of simulations.*

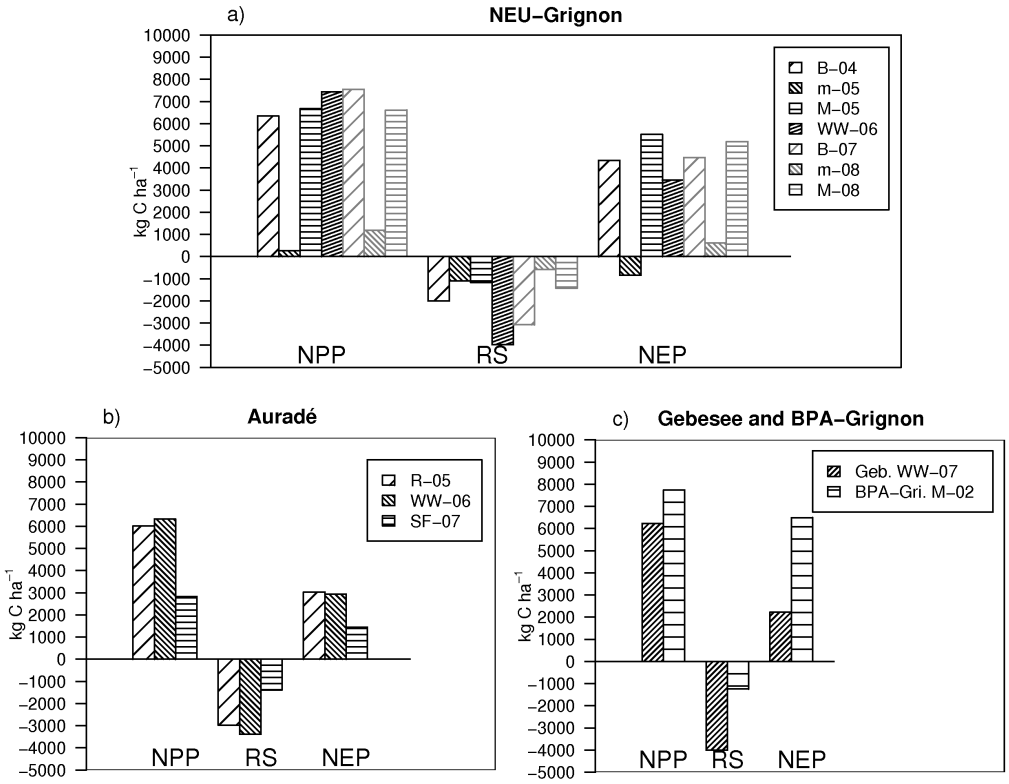

FIG. 3.6 : *Carbon balances of the crop sequences at Grignon, Auradé and Gebesee based on simulations with the calibrated model. Net ecosystem production (NEP) is broken down into net primary production (NPP) and heterotrophic soil respiration (Rs).*

3.4 Discussion

3.4.1 Model calibration and prediction error

Our goal was to parameterise the agro-ecosystem model CERES-EGC in order to estimate the daily NEP over crop rotations, assuming that the calibration against daily NEP data would simultaneously improve the predictions of net ecosystem production, crop growth and carbon balance at rotation scale.

In order for the calibration algorithm to converge, we had to artificially increase the measurement uncertainty to smooth the likelihood surface. The large number of daily observations in our sample (several hundreds of data points) led to a sharply peaked likelihood which is difficult to reach and explore by traditional Metropolis-Hastings algorithm. Processing the data in weekly or monthly means would help in reducing the amount of information and thus it would improve the calibration process. Using an adaptive MCMC sampling algorithm, such as developed by Haario et al. (2001), could also help in adapting the proposal distribution and in optimising MCMC algorithm. Bayesian calibration was applied on daily NEP data, making the assumption that whether daily values were well simulated, thus the cumulative sum would also be well estimated. This as-

sumption could be questioned and we should compare a calibration against NEP data cumulated for cropping cycles with daily NEP. The processing of data and time length of summary statistics (daily, weekly..) would then depend on the goal to which the model is applied for.
The Bayesian calibration on the NEU-Grignon and Auradé experiments resulted in a slight reduction of RMSE compared to the initial parameterization. There was also a close correlation between observed and modelled NEP on daily or seasonal basis, evidencing a good capacity of the model to predict NEP at both scales. The coefficients of determination (R^2) we obtained ranged from 0.59 to 0.76, and compare well to literature. Huang et al. (2009) reported an R^2 of 0.43 when simulating two years of NEP data over an arable field in China with an agro-ecosystem model. Wang et al. (2005) parameterised an ecosystem model against NEP measurements over a wheat-maize sequence in China, and obtained R^2 between 0.74 and 0.76, in the range we obtained in the NEU-Grignon experiment.
After calibration, we estimated the model prediction error (RMSEP) using independent data sets from two experiments with similar crop management but different soil or climate conditions (BPA-Grignon and Gebesee). The RMSEP ranged between 1.5 and 3.8 g C m^{-2} d^{-1}, indicating a good capacity of CERES-EGC to capture NEP at daily and seasonal scales, and were 4 to 7 times lower than the value of 11.3 g C m^{-2} d^{-1} reported by Huang et al. (2009). However, the crop growth at BPA-Grignon was not well simulated because the RUE parameter for maize, calibrated against NEU-Grignon dataset, was not accurate for the maize crop of the BPA-Grignon field site experiment.

3.4.2 Using a crop model to simulate the net carbon exchanges

We originally assumed that calibration of RUE parameters of crop growth sub-models against net C exchanges would allow us to take into account the whole plant C fixation by integrating the root growth and the RUEs would have been increased. As a result, the RUEs of maize and wheat were substantially reduced after calibration, in comparison with their initial values. An underlying explanation of such results could be that the calibration directly applied on C balance between net C fixation and heterotrophic respiration do not make possible to well calibrate simultaneously both processes. Calibrating each process separately with their specific measured data may help in better estimating the RUEs and soil respiration. The main limitation being that it is difficult to measure separately the C fluxes from soil and plants compartments, especially for roots.
While the modelled estimates of NEP were in agreement with observations, those for grain yield and straw removal were lower than observed, which had a large effect on the final C balances. However, the observations of straw removal in the NEU-Grignon experiment were relatively uncertain since they were based on destructive sampling of plants prior to harvest, and did not take harvest losses or cutting height into account. The differences in the modelled and measured C balances should therefore be mitigated, considering the potentially large experimental error on the removal terms.
Grant et al. (2007) showed that the *Ecosys* model well captured the ABG biomass dynamic for maize and soybean crops and that the model predicted with high accuracy the grain removal for the two crops of the rotation. The CERES-EGC predicted above-ground biomass and grain yield

in the same range of accuracy but it remains an uncertainty with the estimation of straw removal. At the crop rotation scale, the simulated NEP of the year encompassing maize cropping season in Grignon are in accordance with literature data for temperate climates. Verma et al. (2005) measured NEP values for irrigated and rainfed maize crops ranging from 3800 to 5200 kg C ha^{-1} yr^{-1}. Wang et al. (2005) simulated with a biogeochemical model a NEP of 3340 kg C ha^{-1} yr^{-1} for wheat and 3850 kg C ha^{-1} yr^{-1} for maize, while Moureaux et al. (2006) measured a higher value of 6100 kg C ha^{-1} yr^{-1} for a spring crop, sugar beet in Belgium.
Lastly, Huang et al. (2009) measured a NEP over 608 days for a winter wheat-maize-winter wheat rotation in Yucheng (China ; semi-humid and monsoon climate), and obtained a mean NEP of 7200 kg C ha^{-1}, with no time interval between two successive crops. Their modelled estimate was very similar, at 7810 kg C ha^{-1}. We estimated for a similar crop sequence of maize-winter wheat-winter barley (893 days) in Grignon an observed NEP of 13137 kg C ha^{-1} and simulated NEP of 13510 kg C ha^{-1}. The difference between both studies is due to difference between the estimation of NPP. In fact, Wang et al. (2005) modelled the NPP for the same site in China equal to 3340 for wheat growing season and 3850 kg C ha^{-1} for maize growing season, whereas we estimated NPP of 6680 kg C ha^{-1} for maize in 2005 and 7435 kg C ha^{-1} for winter wheat in 2006.
Net biome production is very sensitive to the estimation of biomass removal from the field and organic manure inputs. Our model predicted the rotations of NEU-Grignon and Auradé to be net C sinks, whereas Grant et al. (2007) simulated rainfed or irrigated maize-soybean rotations as being net sources of C, emitting between 400 and 800 kg C ha^{-1} yr^{-1} into the atmosphere. They compared their estimation of NBP by simulating the variation of soil C stock over 100-year simulation periods. In this way, they estimated a soil organic C loss of 300 kg C ha^{-1} yr^{-1} for rainfed system and an increase of 600 kg C ha^{-1} yr^{-1} for irrigated system. The carbon returns from application of organic fertilizers generates also an important effect on NBP reducing it by 50 to 115% in case of the rotation of NEU-Grignon. Carbon uptake from catch crops and volunteers also appear as non negligible input of C in the crop system.
Our agro-ecosystem model simulates water, C and N cycling and GHG fluxes as well as the drivers controlling plant and microbial processes. Simulating net carbon exchanges and crop productivity for various crop species requires to combine a large number of processes. In particular special attention should be focused on simulating accurate crop phenology (date of harvest), water and N stress on crop growth, sharing between biomass exported out of the field and residue return to soil.

3.5 Conclusion and future work

We applied a Bayesian method to calibrate the CERES-EGC model against two data sets of NEP from contrasted pedoclimatic conditions and crop sequences (NEU-Grignon and Auradé). The calibrated model allows us to predict the net carbon exchanges between soil-crop and atmosphere from daily to rotation time-scale. We computed the error of model prediction by comparing simulations and observations of NEP from two other independent data sets (BPA-Grignon and Gebesee). The model correctly predicted NEP in both sites, but under-estimated crop biomass in

one of them. The originality of our approach is that we can compute the different terms of the C balance for entire crop rotations and then assign equally the C source and sink between the crops of the rotation. The model estimates the crop productivity that is exported out of the field for being used in food, feed or bioenergy supply chains. The C balance at the field gate could then be introduced into life cycle assessment of agricultural products such as recommended by Rabl et al. (2007) who advised to count C-uptake and emissions at each stage of the life cycle instead of counting a zero C balance between C fixation and emission.

Anthoni et al. (2004) reported that up-scaling C fluxes from croplands from plot to regional scale was the most complicated task to establish C budget of a selected region due to wide variations in crop species, rotations, residue and fertilizer management and soil C stocks. The use of process-based models such as CERES-EGC would help in estimating the regional net carbon fluxes. The calibration developed in Lehuger et al. (2009b) for N_2O makes it possible to apply plot-scale models at regional level by providing robust estimates for generic (ie non site-specific) parameters over this domain. Such a strategy could also be used for CO_2 using the calibration method we used here on a wider range of data sets to find parameter values that would be universally applicable. The calibrated model could then be used to simulate a wide range of environmental conditions, and coupled with GIS databases to generate high-resolution regional maps of net CO_2 fluxes with daily time resolution. Estimating C fluxes from forests, grasslands and other ecosystems (shrublands, wetlands...) would also be integrated for budgeting biospheric C fluxes at regional or landscape scale (Turner et al., 2007). Regional validation of model simulations with landscape or regional measurements, such as carried out by Soegaard et al. (2003), would combine the different sources and sinks of carbon. Regional strategies of C-abatement would then be tested using the model at this spatial scale.

Acknowledgements

This work was part of the CarboEurope and NitroEurope Integrated Projects (EU's Sixth Framework Programme for Research and Technological Development), which both investigate the European terrestrial greenhouse gas balance. We express special thanks to A. Freibauer and W. Kutsch (Max Plank Institute, Jena) for making available the data from Gebesee.

Chapitre 4

Prédiction et mitigation du pouvoir de réchauffement global des agro-écosystèmes

Ce chapitre concerne l'estimation du pouvoir de réchauffement global (PRG) des agro-écosystèmes. Il fera prochainement l'objet d'une soumission à la revue *Agricultural and Forest Meteorology*. Il s'intitule : "Predicting and mitigating the global warming potential of agro-ecosystems" et les co-auteurs sont : B. Gabrielle[a], P. Laville[a], M. Lamboni[b], P. Cellier[a] et B. Loubet[a].

Le modèle a été calibré pour simuler les émissions de N_2O et les flux de CO_2 des systèmes de cultures. À présent, sur la base de nouvelles simulations et de données observées, nous pouvons calculer le pouvoir de réchauffement global des agro-écosystèmes. Le modèle est de nouveau calibré avec des mesures de N_2O journalières obtenues avec la technique des chambres automatiques sur le site expérimental de Grignon. Puis, il est évalué avec deux jeux de données indépendants afin d'estimer son erreur de prédiction. Ensuite, le modèle est appliqué pour calculer les bilans de CO_2 et de N_2O des rotations de cultures sur 30 années climatiques passées afin d'analyser la variabilité des bilans de GES due au climat. Nous déterminons alors le PRG des systèmes de cultures en y incluant les mesures de méthane au champ et les émissions indirectes estimées selon une approche d'analyse de cycle de vie. Enfin, nous testons des stratégies agronomiques afin d'identifier des options pour réduire le PRG des agro-écosystèmes.

a : UMR 1091 INRA-AgroParisTech Environnement et Grandes Cultures, Thiverval-Grignon, France

b : Institut National de la Recherche Agronomique, UR 341 INRA Mathématiques et Informatique Appliquées, 78352 Jouy-en-Josas, France

Abstract

Nitrous oxide, carbon dioxide and methane are the main biogenic greenhouse gases (GHG) contributing to the global warming potential (GWP) of agro-ecosystems. Evaluating the impact of agriculture on climate thus requires a capacity to predict the net exchanges of these gases in an systemic approach, as related to environmental conditions and crop management. Here, we used experimental data sets from intensively-monitored cropping systems in Western Europe to calibrate and evaluate the ability of the biophysical crop model CERES-EGC to simulate GHG exchanges at the plot-scale. The experiments involved major crop types (maize-what-barley-rapeseed) on loam and rendzina soils. The model was subsequently extrapolated to predict CO_2 and N_2O fluxes over entire crop rotations. Indirect emissions (IE) arising from the production of agricultural inputs and from use of farm machinery were also added to the final GWP. One experimental site (involving a wheat-maize-barley rotation on a loamy soil) was a net source of GHG with a GWP of 670 kg CO_2-C eq ha^{-1} yr^{-1}, of which half were due to IE and half to direct N_2O emissions. The other site (involving a rapeseed-wheat-barley rotation on a rendzina) was a net sink of GHG for -650 kg CO_2-C eq ha^{-1} yr^{-1}, mainly due to a higher predicted C sequestration potential and C return from crops. Some mitigation options were tested to design productive agro-ecosystems with low global warming impact.

Keywords

Global warming potential ; Agro-ecosystem model ; CERES-EGC ; Bayesian calibration ; Greenhouse gases ; Nitrous oxide

4.1 Introduction

While the security of food supply to an increasing population has turned into a pressing issue worldwide, the growing environmental footprint of agriculture due to land use change and management intensification is posing an unprecedented challenge. Assessing the contribution of agriculture to climate change is one of the key questions that environmental scientists have to address in order to identify possible measures to reduce the burden of agriculture on global warming (Galloway et al., 2008; Sutton et al., 2007). Agriculture significantly contribute to anthropogenic greenhouse gas (GHG) emissions with a global flux of 6.1 Gt CO_2-eq yr^{-1} which represent 10-12% of the total GHG anthropogenic emissions (Smith et al., 2007). In the case of arable crops, these emissions include the exchanges of GHG in the cultivated field but exclude the upstream (indirect) emissions.

The direct emissions of GHG by agro-ecosystems are made up of three terms : emissions of nitrous oxide, net carbon fluxes between soil-plant system and the atmosphere, and methane exchanges. Nitrous oxide (N_2O) is produced by soil micro-organisms via the processes of nitrification and denitrification (Hutchinson and Davidson, 1993). Arable soils are responsible for 60% of the global anthropogenic emissions of N_2O (Smith et al., 2007), and their source strength primarily depends on the fertilizer N inputs necessary for crop production. Other environmental factors regulate these emissions : soil temperature, soil moisture, soil NO_3^- and NH_4^+ concentrations, and the availability of organic C substrate to micro-organisms (Conrad, 1996). The effect of these factors results in a large spatial and temporal variability of N_2O emissions (Jungkunst et al., 2006; Kaiser and Ruser, 2000).

The second term in the GHG balance, the net C exchanges, is taken as the variations of ecosystem C stock. These variations reflect the balance between C inputs to the agro-ecosystems, via crop residue return, root deposition and organic amendments, and outputs via harvested biomass and soil organic matter mineralization. This term may be assessed either from long term C stock evolution or, at the rotation scale, by computing the C balance between net carbon exchanges between the soil-plant system and the atmosphere, minus the harvested biomass removed out of the field plus the import of organic C from manure application (Ammann et al., 2007; Grant et al., 2007). Lastly, non-flooded cropland are usually considered as a weak methane-sink that mitigates the global warming potential (GWP) of cropping systems by 1% to 3% (Mosier et al., 2005; Robertson et al., 2000).
Indirect emissions of GHG arising from the production of agricultural inputs (fertilizers, pesticides and lime), fuel combustion and use of machinery on the farm may contribute as much as half of the total GHG budget of agricultural crops (Adviento-Borbe et al., 2007; Mosier et al., 2005; Robertson et al., 2000). Thus, this term provides good leverage to mitigate their impact on global warming (West and Marland, 2002).

The global GHG balance may be expressed as the global warming potential (GWP) of an agro-ecosystem considered, in CO_2 equivalents, using the GWPs of all the trace gases with radiative forcing (IPCC, 2007). Various agricultural practices impact the GHG balance of agro-

ecosystems. Some of them may first enhance the carbon sink-strength of soils : conversion to no-tillage practices, the introduction of catch crops, and the incorporation of crop residues into the topsoil were shown to lead to possible C sequestration into the organic carbon pool of the agricultural soils (Arrouays et al., 2002; Smith et al., 2001). The evaluation of candidate agricultural practices to reduce the GWP of agro-ecosystems should encompass indirect and direct emissions of all GHG, to avoid trade-off effects. For instance, because the C and N biogeochemical cycles are interconnected, CH_4 and N_2O emissions may offset the beneficial C storage associated with practices targeting at C sequestration (Desjardins et al., 2005; Li et al., 2005a; Six et al., 2004).

The different crops occurring within a given rotation are inter-related in terms of nutrients' turn-over, and soil organic and mineral status. In addition, the nutrients derived from fertilizers or biological fixation may be recycled or stored into the pools of the SOM, and may be re-emitted into air or water in subsequent years (Anthoni et al., 2004; Del Grosso et al., 2005). That is the reason why it is not relevant to calculate the GWP of a single crop, but rather of a complete sequence of crops. The GWP of this rotation may subsequently be re-allocated to a particular crop based on its frequency of occurrence in the rotation, or similar rules.

In the literature, the GWP of agro-ecosystems is either calculated to assess the effect of the conversion to a new management practice (e.g., no-till, catch crops, farmyard manure application, or land use change ; (Bhatia et al., 2005; Mosier et al., 2005; Robertson et al., 2000), or for inclusion into the life cycle assessment of a crop-derived product. These include biofuels, animal feed, or human food (Adler et al., 2007; Gabrielle and Gagnaire, 2008; Kim and Dale, 2005). Direct GHG emissions may be either estimated from direct field measurements (Adviento-Borbe et al., 2007; Bhatia et al., 2005; Mosier et al., 2005; Robertson et al., 2000), or by using biogeochemical models simulating GHG emissions (Adler et al., 2007; Del Grosso et al., 2005; Desjardins et al., 2005; Pathak et al., 2005). Most agro-ecosystems have a positive net GWP (meaning they enhance global warming), but this trend is mainly controlled by the C storage potential of the soil.

In the US Midwest, Robertson et al. (2000) measured the GWP of an annual crop rotation (maize-soybean-wheat) as 40 and 310 kg CO_2-C eq ha^{-1} yr^{-1} for no-till and conventional tillage systems, respectively. In Colorado, for rainfed crops under no-till practices, Mosier et al. (2005) measured a topsoil C-storage of about 300 kg CO_2-C eq ha^{-1} yr^{-1} in perennial, rainfed crops under no-till, which offset the other terms in the GHG balance and resulted in a negative net GWP of -85 kg CO_2-C eq ha^{-1} yr^{-1}.
Adviento-Borbe et al. (2007) quantified GWPs in four high-yielding maize systems in Nebraska (USA) for continuous maize system and maize-soybean rotations, with recommended and intensive management for both systems. The authors reported that the N_2O fluxes were similar in the different treatments despite the large differences in crop management and N fertilizer applications. As a result, all the systems were net sources of GHGs with GWPs between 540 and 1020 kg CO_2-C eq ha^{-1} yr^{-1}. Grace et al. (1993) reported GWPs of tropical rice-wheat-cowpea systems in India. In these systems, the net GWP was an order of magnitude higher than GWP from temperate region and ranged between 2400-3200 kg CO_2-C eq ha^{-1} yr^{-1} for no-till and

conventional treatments. Three factors explained the difference between temperate and tropical systems : the high soil C loss, the CH_4 emissions from rice cultivation and higher N_2O fluxes (Robertson et Grace, 2004).

The various terms of the net GWP should be predicted with similar accuracy. Indirect emissions may be easily calculated thanks to databases of life cycle inventories (Nemecek et al., 2003; West and Marland, 2002), but direct field emissions of N_2O and C storage in soil are extremely dependant of pedoclimatic conditions and agricultural management practices. To take into account these sources of variability, and to devise mitigation strategies, the processes occurring in the soil-crop-atmosphere system should be modelled simultaneously, together with the effect of agricultural practices. In the past, modelling approaches were developed in parallel either by agronomists seeking to predict crop growth and yields in relation to their management (Boote et al., 1996), or by ecologists focusing on biogeochemical cycles and in particular mineralization, nitrification and denitrification in soils (eg, Li et al. (1992)). With the increasing interest for the prediction of trace gas emissions from arable soils (or pollutants in general), both approaches should be linked together in a more systemic perspective (Gijsman et al., 2002; Zhang et al., 2002). The CERES-EGC model was designed following this philosophy to estimate site-and-management specific environmental balance, or regionalised inventories of trace gas emissions (Gabrielle et al., 2006a).
The objectives of this work were : i/ to test and calibrate the CERES-EGC crop model with experimental data from cropping systems representative of northern Europe, ii/ to apply the model to assess the GWP of the cropping systems, including direct and indirect emissions of GHG and iii/ to assess the sensitivity of GWPs to different agricultural practices to purpose options for mitigation.

4.2 Material and Methods

4.2.1 Experimental data

4.2.1.1 Field sites

The field experiments were carried out at three locations in northern Europe, at Rafidin (northern France, 48.5 N, 2.15 E) in the Champagne region in 1994-1995 (Gosse et al., 1999), at Grignon near the city of Paris (northern France, 48.9 N, 1.95 E) in 2004-2008 and at Gebesee (20 km NW of Erfurt in Germany, 51.1 N, 10.9 E) in 2006-2007.
In Rafidin, the soil was a grey rendzina overlying a subsoil of mixed compact and cryoturbed chalk. The topsoil (0-30 cm) has a clay loam texture, with (31% clay and 28% sand, an organic matter content of 19.5 g kg^{-1}, a pH (water) of 8.3, and a bulk density of 1.23 g cm^{-3}. In Grignon, the soil was a silt loam with 18.9% clay and 71.3% silt in the topsoil. In the top 15 cm, organic carbon content was 20.0 g kg^{-1}, the pH (water) was 7.6 and the bulk density 1.30 g cm^{-3}. In Gebesee, the soil was a Chernozerm (silty clay loam) with 35.8% clay and 60.3% silt in the top 20 cm, organic carbon was 23.0 g kg^{-1}, the pH (water) was 6.7 and the bulk density 1.3 g cm^{-3}.
The Table 4.1 recapitulates the crop sequences of the experimental sites and the main cropping

operations. The Rafidin site involved a rapeseed - winter wheat - winter barley rotation, and the measurements essentially took place during the rapeseed growing cycle, from its sowing on 9 Sept., 1994 to its harvest on 11 July, 1995. Three fertilizer N treatments (N0=0 kg N ha^{-1}, N1=135 kg N ha^{-1} and N2=270 kg N ha^{-1}) were established on 30×30 m blocks arranged in a split-plot design with three replicates. For this site, the rotations we simulated were only different regarding the fertilizer N inputs on the rapeseed crop. The other crops in the rotation (wheat and barley) were managed identically in the N0, N1 and N2 rotations.
At the Grignon site, two experiments were monitored in parallel on two fields : a principal field (Grignon-PP, 19 ha), on which a maize - winter wheat - winter barley - mustard rotation was monitored since 2004 and 3 adjacent plots (Grignon-PAN1, -PAN2, -PAN3, 2500 m^{-2} each) on another field on which the same rotation was applied since 2006, with 0, 1 and 2 years time-lag interval in order to have all the crops each year. The adjacent plots were monitored since 2006. In the rotation, a mustard was planted following the harvest of barley the year before to serve as a catch crop to reduce nitrate leaching. On the principal field, dairy cow slurry was applied between the harvest of barley and the planting of mustard on 31 August 2004, and before the maize sowing on 16 April 2008.
In Gebesee, the crop sequence from 2003 to 2007 was rapeseed - winter barley - sugar beet - winter wheat. Two applications of organic fertilizers were carried out in 2007, one application of cattle slurry (18 m^3 ha^{-1}) on the wheat crop in 11 Apr. and 35 t ha^{-1} of farmyard manure in 4 Sept after harvest.

4.2.1.2 Soil and crop measurements

Soil mineral nitrogen content (NO_3^- and NH_4^+) and moisture content were monitored in the following layers : 0-15 cm, 15-30 cm, 30-60 cm and 60-90 cm at Grignon, 0-30 cm, 30-60 cm, 60-90 cm, and 90-120 cm at Rafidin, and 0-10 cm and 10-20 cm at Gebesee. Soil samples were taken in triplicates with an automatic (Rafidin) or manual (Grignon and Gebesee) auger every 1 to 4 weeks, and analysed for moisture content and mineral N. The latter involved an extraction of soil samples with 1 M KCl and colorimetric analysis of the supernatant. In the three sites, soil moisture and temperature were also continuously recorded using TDR (Time Domain Reflectrometry, Campbell Scientific, Logan, Utah, USA) and thermocouples. Soil bulk density was measured once in each site, using steel rings. For both experiments of Grignon and Rafidin, plants were collected every 2 to 4 weeks, and separated into leaves, stems, ears or pods, and roots. Leaf area index was measured with an optical leaf area meter or analysis of leaf scans. The plant samples were dried for 48 h at 80° C and weighted, and analysed for C, N, P and K content by flash combustion.

4.2.1.3 Trace gas fluxes and micrometeorological measurements

At the three sites, daily climatic data were recorded with an automatic meteorological station, including maximum and minimum daily air temperatures (° C), rainfall (mm day^{-1}, solar radiation (MJ m^{-2} day^{-1}) and wind speed (m s^{-1}).
At Grignon and Gebesee, the measurements of CO_2 fluxes at the field scale were carried out

in the framework of the CarboEurope integrated project (European Commission Framework VI research programme ; Aubinet et al. (2000)). Water vapour and CO_2 fluxes were measured using the eddy covariance method above the crop canopy. Wind speed was monitored with a three-dimensional sonic anemometers, and CO_2 concentration with infrared gas analysers (model Li-7500 in Grignon and model Li-7000 in Gebesee ; Li-Cor Inc., Lincoln, NE, USA) located on a mast at two meters above the canopy. Daily net ecosystem carbon dioxide exchange (g C m^{-2} day^{-1}), and its daily evapotranspiration (mm m^{-2} day^{-1}) were calculated by integrating the 30-minute fluxes determined by the micrometeorological measurements over each day. The eddy covariance technique usually produces gaps in the half-hourly C flux data, making it necessary to fill the missing values before integration at the daily time scale. The gap-filling methodology of CarboEurope-IP was applied to the experimental data sets (Falge et al., 2001).

At Rafidin, there were no micrometeorological measurements of CO_2 exchanges. Nitrous oxide emissions were monitored by the static chamber method using circular chambers (0.2 m^{-2}), with 8 replicates. On each sampling date, the chambers were closed with an airtight lid, and the head space was sampled 4 times over a period of 2 hours. The gas samples were analysed in the laboratory by gas chromatography. The measurements were done every 1-3 weeks between September, 1994 and April, 1995 (Gosse et al., 1999).

For the Grignon-PP experiment, N_2O emissions were measured with 3 to 6 automatic chambers (55 L, 0.5 m^{-2}). The chambers were sequentially closed during 15 min and the complete cycle for the six chambers was then fixed to 1h30. The N_2O concentrations were measured using an infrared gas analyser (N_2O Analyser 46C, Thermo Scientific Inc., Waltham, MA, USA) which was connected on line with the chambers. Air was pumped from the chamber to the gas analyser and injected again after the analysis to the chambers. Nitrous oxide fluxes were calculated from the slope of the gas accumulation rate. The electric jacks used to open and close the chambers and the solenoid valves were controlled by a Campbell data logger (CR23X, Logan, Campbell Scientific, Utah, USA) that recorded the N_2O concentration every 10 seconds. Nitrous oxide emissions were monitored for 442 days from January 1, 2007, to August 31, 2008. During this period, the mean value of the emissions was 8.7 g N_2O-N ha^{-1} d^{-1}. Eight manual chambers were also disposed in the field in order to measure N_2O, CO_2 and CH_4 fluxes on a monthly frequency or following the fertiliser application. A more intensive monitoring of the GHG emissions was carried out following the slurry application in spring 2008.
For the three Grignon-PAN plots, the three GHGs (N_2O, CO_2 and CH_4) were measured with 5 static circular chambers (0.2 m^{-2}) per plot. The chambers were closed over a period of 30 minutes and 4 gas samples were collected with a syringe at 0, 10, 20 and 30 minutes after closure. Gas samples were analysed by gas chromatography fitted with an electron capture detector for N_2O analysis and with a flame ionisation detector and a methaniser for CO_2 and CH_4 analysis.

In Gebesee, GHG measurements were carried out with manual chambers ($100 \times 100 \times 30$ cm - when crop is higher than 30cm height was expanded to 60cm) from Feb. 2006 to Dec. 2007, weekly during growing season and every two weeks otherwise. The chambers were closed for one hour and sampling was carried out every 20 minutes during closure. From Feb. to Dec.

Site	Crop	Sowing date	N Fertilizer	
			Date	Amount (kg N ha^{-1})
GRIGNON-PP	Wheat	16/10/2002	26/02/2003	52
			27/03/2003	60
	Barley	17/10/2003	18/02/2004	59
			19/03/2004	59
			02/04/2004	39
	Mustard	02/09/2004	31/08/2004	Slurry (90)
	Maize	09/05/2005	09/05/2005	140
	Wheat	16/10/2005	15/03/2006	55
			14/04/2006	55
	Barley	06/10/2006	22/02/2007	55
			22/03/2007	55
	Mustard	22/09/2007	17/04/2008	Slurry (80)
	Maize	28/04/2008	05/05/2008	60
RAFIDIN	Rapeseed N0	09/04/1994		
	Rapeseed N1	09/04/1994	20/02/1995	80
			15/03/1995	75
	Rapeseed N2	09/04/1994	12/09/1994	49
			20/02/1995	80
			15/03/1995	75
			29/03/1995	38
	Wheat	27/10/1995	10/02/1996	60
			10/03/1996	95
			10/05/1996	65
	Barley	27/10/1995	10/02/1997	90
			10/03/1997	80
GRIGNON-PAN1	Wheat	27/10/2005	06/03/2006	50
			07/04/2006	110
	Barley	06/10/2006	04/03/2007	50
			26/03/2007	70
	Mustard	31/08/2007		
	Maize	07/05/2008	08/05/2008	140
GRIGNON-PAN2	Barley	05/10/2005	06/03/2006	50
			07/04/2006	50
	Mustard	30/09/2006		
	Maize	26/04/2007	02/05/2007	150
	Wheat	24/10/2007	14/02/2008	50
			03/04/2008	120
			15/05/2008	40
GRIGNON-PAN3	Mustard	02/09/2005		
	Maize	26/04/2006	04/05/2006	160
	Wheat	10/10/2006	05/03/2007	50
			26/03/2007	70
	Barley	08/10/2007	15/02/2008	50
			05/04/2008	90
GEBESEE	Sugar beet	20/10/2006	10/04/2006	30
	Wheat	27/10/2006	27/03/2007	80
			11/04/2007	Slurry (20)
			03/05/2007	85
			03/09/2007	FYM (200)

TAB. 4.1 : *Experimental treatments and N input rates at the Grignon, Rafidin and Gebesee sites.*

2007, two automatic chambers ($95 \times 25 \times 125$ cm) were installed in the same plot. Gas samples were automatically collected every 20 minutes during one hour of closure and each chamber was closed 6 times in a day. In both cases, gas samples were analysed with gas chromatography such as described above.
At the dates of mineral or organic fertiliser application, the chambers were closed during the spreading operation and then, the amount corresponding to the chamber surface was applied by hand within the chambers.

4.2.2 The indirect GHG emissions

The GHG emissions (CO_2, N_2O and CH_4) associated with input production and use of farm machinery were calculated from the Ecoinvent life cycle inventory database (Nemecek et al., 2003). The inventory of elementary management operations comprises soil tillage, fertilisation, sowing, plant protection, harvest and transport, and may be translated in terms of GHG emissions thanks to emission factors. Similarly, the production of agricultural inputs (fertilizers, pesticides, seeds and agricultural machinery) induces GHG emissions that arise mainly from fossil fuel combustion, and were included in the indirect emissions.

4.2.3 Global warming potentials of crop rotations

For arable fields, the carbon balance is calculated as the net biome production (NBP) equal to :

$$NBP = NEP - Exported\,biomass + Imported\,biomass \tag{4.1}$$

The NEP is the net ecosystem production and corresponds to the net C exchanges between soil-plant system and the atmosphere, above the canopy. The exported biomass is the harvest and the imported biomass may be application of manure or compost. The carbon dioxide exchanges for a crop growing cycle were assumed to start from their sowing to the sowing of the following crop. The sign convention used to express NBP as positive quantity with net carbon fixation, were inverted in the calculation of the GWP. The values of NBP were obtained by averaging the NBP simulated over 12 maize-wheat-barley-mustard rotations on a 36-yr series of historical weather data (1972-2008) in Grignon-PP, with constant crop management. The same simulation was done for the three treatments of Rafidin over 9 rapeseed-wheat-barley rotations on a 28-yr series of weather data. The 30-yr simulation allowed us to explore the climatic variability and its effect on the net primary production and soil respiration.
The global warming potential of crop sequences was computed by adding NBP, N_2O emissions, CH_4 exchanges and the indirect emissions using global warming potential of the GHGs at the 100-year time horizon (CO_2=1, CH_4=25 and N_2O=298, IPCC (2007)).

4.2.4 The CERES-EGC model

CERES-EGC was adapted from the CERES suite of soil-crop models (Jones and Kiniry, 1986), with a focus on the simulation of environmental outputs such nitrate leaching, emissions

of N_2O ammonia, and nitric oxide (Gabrielle et al., 2006a). It can therefore be used as an agronomic tool to improve the management of major arable crops, based on crop productivity and environmental criteria. The model simulates the cycles of water, carbon and nitrogen within agroecosystems (Gabrielle et al., 2006a, 1995).
Direct field emissions of CO_2, N_2O, NO and NH_3 into the atmosphere are simulated with different trace gas modules. Here, we focus on gas fluxes with global warming potential, i.e. CO_2 and N_2O.
Carbon dioxide exchanges between soil-plant system and the atmosphere are modelled via the net photosynthesis and SOC mineralization processes. Net primary production (NPP) is simulated by the crop growth module while heterotrophic respiration (Rs) is deduced from the SOC mineralization rates calculated by the microbiological sub-model. The net ecosystem production (NEP), which is calculated as NPP minus Rs, may be computed on a daily basis and directly tested against the net ecosystem exchanges measured by eddy covariance.
CERES-EGC uses the semi-empirical model NOE (Hénault et al., 2005a) for simulating the N_2O production in the soil through both the nitrification and the denitrification pathways. Denitrification component is derived from the NEMIS model (Hénault and Germon, 2000) that calculates the denitrification as the product of a potential rate with three unitless factors related to soil water content, nitrate content and temperature. Nitrification is modelled as a Michaëlis-Menten reaction with NH_4^+ as substrate that additionally is controlled by response functions of the soil water content and temperature. Nitrous oxide emissions resulting from the two processes are soil-specific proportions of total denitrification and nitrification pathways.
CERES-EGC runs on a daily time step and requires input data for agricultural management practices, climatic variables (mean air temperature, daily rain and Penman potential evapotranspiration), and soil properties.

4.2.5 Parameter selection and model calibration

Dynamic biophysical models include a large number of parameters whose values are uncertain and it is often impossible to estimate all these parameters accurately and simultaneously. A common practice consists in selecting a subset of parameters by global sensitivity analysis, then estimating the selected parameters against experimental data and setting the others to nominal values (Makowski et al., 2006). In our case, a multivariate global sensitivity analysis, developed by Lamboni et al. (2009), allowed us to select the 6 most sensitive parameters of the N_2O emission module of CERES-EGC. The most influent parameters were then estimated with a Bayesian calibration approach. Table 4.2 recapitulates the parameters involved in the calibration. The calibration was applied with the N_2O emission measurements of the experimental site of Grignon-PP and the calibrated parameters were then used to simulate the fields of Grignon-PAN and Gebesee experiments. The parameters values used for the Rafidin site originated from a previous calibration (Lehuger et al., 2009b).

Van Oijen et al. (2005) and Lehuger et al. (2009b) described in details the Bayesian method that was used in this work. Briefly, the aim of Bayesian calibration is to reduce the prior parameter uncertainty by using measured data, thereby producing the posterior distribution for the

parameters. In our case, we specified lower and upper bounds of the parameters' uncertainty, defining the prior parameter distributions as uniform (Table 4.2). Posterior pdf is then computed by multiplying the prior with the likelihood function, which is the probability of the data given the parameters. Because probability densities may be very small numbers, rounding errors needed to be avoided and all calculations were carried out using logarithms. The logarithm of the data likelihood is thus set up, for each data set Y_i, as follows :

$$logL_i = \sum_{j=1}^{K} \left(-0.5 \left(\frac{y_j - f(\omega_i; \theta_i)}{\sigma_j} \right)^2 - 0.5log(2\pi) - log(\sigma_j) \right) \tag{4.2}$$

where y_j is the mean N_2O flux measured on sampling date j in the data set Y_i and σ_j the standard deviation across the replicates on that date, ω_i is the vector of model input data for the same date, $f(\omega_i; \theta_i)$ is the model simulation of y_j with the parameter vector θ_i, and K is the total number of observation dates in the data sets. To generate a representative sample of parameter vectors from the posterior distribution, we used a Markov Chain Monte Carlo (MCMC) method : the Metropolis-Hastings algorithm (Metropolis et al., 1953). For each calibration, three parallel Markov chains were started from three different starting points in the parameter space (θ_0). Convergence was checked with the diagnostic proposed by Gelman and Rubin (1992). The chains were considered to be a representative sample from the posterior pdf, and from this sample were calculated the mean vector, the variance matrix and the 90% confident interval for each parameter.

Parameter vector $\theta = [\theta_1 ... \theta_6]$					Prior probability distribution		Posterior probability distribution		
θ_i	Symbol	Description	Unit	Default value	θ_{min}(i)	θ_{max}(i)	Mean	SD	Correlated $\{\theta_i\}$
θ_1	r	Ratio of N_2O to total denitrification	%	0.20	0.09	0.90	0.36	0.09	{2,4,5,6}
θ_2	PDR	Potential denitrification rate	kg N ha^{-1} d^{-1}	6.0	0.1	20.0	0.33	0.61	{2,1,5,6}
θ_3	Tr_{WFPS}	WFPS threshold for denitrification	%	0.62	0.40	0.80	0.61	0.05	{2,4,5}
θ_4	POW_{denit}	Exponent of power function	Unitless	1.74	0.00	2.00	0.46	0.21	{1, 3}
θ_5	Km_{denit}	Half-saturation constant (denit)	mg N kg^{-1} soil	22.00	5.00	120.00	24.69	17.53	{1,2,3,6}
θ_6	TTr_{denit}	Temperature threshold	°C	11.00	10.00	15.00	10.05	0.17	{1,2,5}

TAB. 4.2 : *Description of the 6 selected parameters of the N_2O emissions module. The prior probability distribution is defined as multivariate uniform between bounds θ_{min} and θ_{max}. The posterior parameter distributions are based on the calibration with the Grignon-PP data set, and are characterised by the mean value of the posterior, their standard deviation (SD). Correlations with other parameters are reported if their absolute value exceeds 0.4 (underlined parameters express a negative correlation).*

4.2.6 Model evaluation

Two statistical indicators were used to evaluate the performance of the model to fit with the observed data. Mean deviation (MD) was defined as :

$$MD = \frac{1}{K}\sum_{j=1}^{K}(y_j - f(\omega_k;\theta_l)) \tag{4.3}$$

and the root-mean squared error (RMSE) as :

$$RMSE = \sqrt{\frac{1}{K}\sum_{j=1}^{K}(y_j - f(\omega_k;\theta_l))^2} \tag{4.4}$$

where y_j is the time series of the observed data on day j of data set D_i, and f($\omega_k;\theta_l$) is the corresponding model predictions with input variables ω_k and parameters θ_l.
The RMSE was computed for the experiments used in the calibration (Grignon-PP and Rafidin) and in the subsequent model testing against the independent data sets of Grignon-PANs, and Gebesee. In both last cases, the RMSE corresponds to the root mean square error of prediction (RMSEP(θ)), since the data were involved neither in parameter estimation nor model development (Wallach, 2006). The RMSEP was computed for the predictions of N_2O emissions.

4.2.7 Scenarios of mitigation

Five scenarios of mitigation were tested in order to assess the effect of agricultural practices on the GWP, and to explore the potential of GHG abatement for crop systems. The scenarios were tested on the Grignon-PP rotation simulated on a 30 year time period. The first scenario (“Straw”) was designed to asses the effect of non removing straw out of the field. The scenario (“Catch crop”) was designed to assess the effect of catch crop in the rotation by comparing rotations with and without catch crop, which was mustard between a winter crop and a spring crop in our case. We also tested the effect of N fertilisation on the GWP by simulating rotations with 50% less N fertiliser application (scenario “N-”) or with with 50% more (scenario “N+”). The last scenario (“Organic”) was run to evaluate the effect of C and N input from slurry application every three years on the GWP of the rotation.

4.3 Results

4.3.1 Model testing

4.3.1.1 Crop growth

At Grignon, the crop growth was well simulated for the various crop species of the rotation, as reported in Fig. 4.1. The time course of total above ground biomass was correctly captured

by the model with the exception of the 2008 maize upon harvest whose dry matter was under-estimated. The maize silage yields were under-estimated in 2005 and 2008 with bias (observed - simulated yields) of 1960 and 6740 kg DM ha^{-1}, respectively, due to too high water stress simulated. Grain yields of barley and winter wheat were correctly predicted and the bias between simulations and observations were -100 and -430 kg DM ha^{-1}

At the Rafidin site, CERES-EGC provided good simulations of rapeseed growth for the N1 and N2 treatments (Fig. 4.2). The simulated patterns of biomass, LAI and N content variations matched the observations over the entire growing cycle. Final grain yields were correctly estimated, with a simulated value of 3.8 t DM ha^{-1} and an observed one of 4.1 t DM ha^{-1} for N1, and an exact match at 4.9 t DM ha^{-1} for N2. For the N0 treatment (unfertilized), the model overestimated LAI by a factor of 2 throughout the growing season, but total above ground biomass was underestimated by about 25% when compared to the data (not shown). For this treatment, the simulated N stress was too high at the end of the crop's growing cycle to allow sufficient grain filling, and the final grain yield was under-estimated as a result.

4.3.1.2 Net carbon exchanges

The carbon dioxide exchanges measured with micrometeorological systems were used to calibrate the CERES-EGC model against net ecosystems exchange measurements and to evaluate the model prediction accuracy with independent data (Lehuger et al., 2009b). The measurements from Grignon-PP were used for the parameter estimation and those of Gebesee for evaluation of the model prediction accuracy. For both sites, NEP was well simulated at daily and seasonal scales (Fig. 4.1 and Fig. 4.3). The RMSE computed for the Grignon-PP experiment was 1.90 g C $m^{-2}d^{-1}$ (n=1627) and the RMSEP of Gebesee 1.5 g C $m^{-2}d^{-1}$ (n=310).

4.3.1.3 Soil drivers of nitrous oxide emissions

Figure 4.4 provides a test for the simulation of the key drivers of N_2O emissions at the Grignon-PP site. Soil moisture, temperature and inorganic N content control N_2O emissions by their influence on the nitrification and denitrification processes. At Grignon, for the period of measurement (2006-2008), their dynamics were well simulated (Fig. 4.4.a, 4.4.b, 4.4.c). Table 4.3 recapitulates the mean deviations (MD) and RMSEs computed with the different soil drivers used as input variables of the N_2O emission module. Soil temperature and soil water content were well predicted by the model with RMSE close to 3°C for the soil temperature and from 4 to 8% (v/v) for the soil water content across the field-site experiments. The model's RMSE over the 8 experiments ranged between 9.9 and 57.0 kg N ha^{-1} for the simulation of nitrate content and to 4.1 to 28.6 kg N ha^{-1} for the ammonium content. The model did not captured the N dynamic in the Grignon-PAN2 field site due to a lack of correlation between N content and N fertiliser applications in this plot.

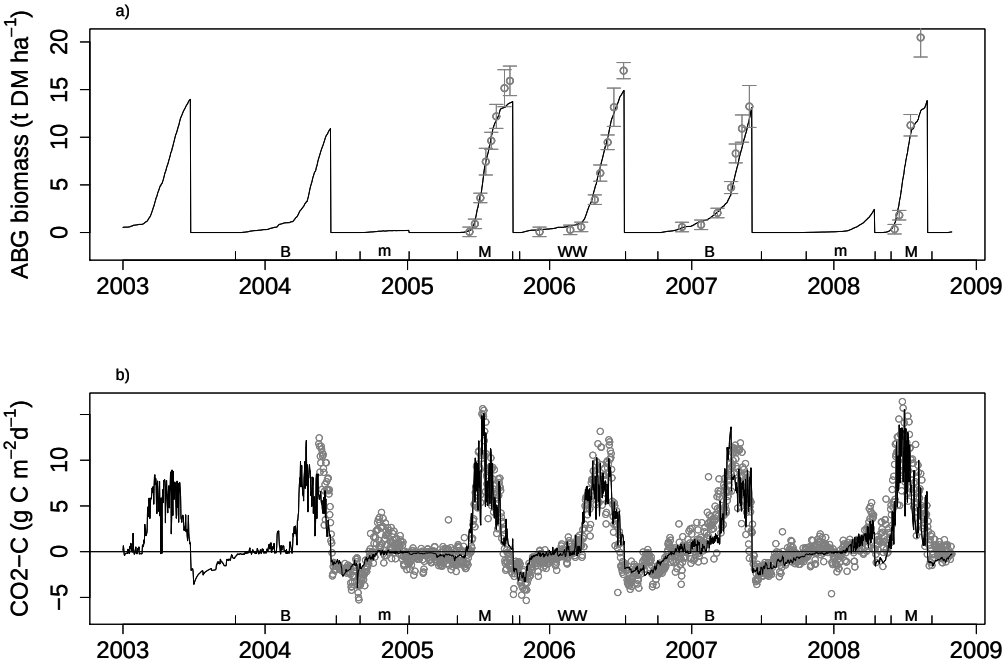

FIG. 4.1 : *Simulations (black line) and observations (grey points) of above-ground (ABG) crop biomass (a) and times course of simulated (black line) and observed (grey symbols) of net ecosystem production (NEP) on a daily time scale (b), at the Grignon-PP experimental field.*

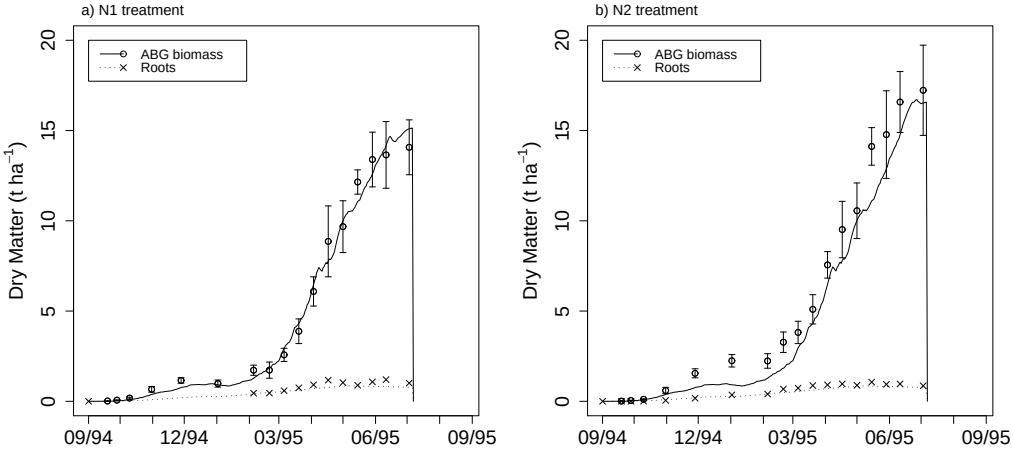

FIG. 4.2 : *Simulated (lines) and measured (symbols ± sd) data for (a) above ground (ABG) dry matter and roots for N1 treatment, (b) above ground (ABG) dry matter and roots for N2 treatment, in 1995 at Rafidin (France).*

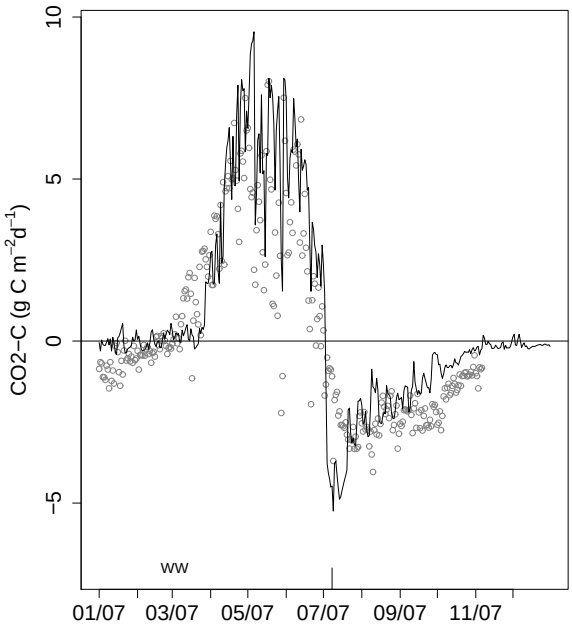

FIG. 4.3 : *Simulated (black line) and observed (grey points) of daily net ecosystem production (NEP) for the wheat crop cycle of Gebesee.*

Site	Treatment	Soil temperature				Soil water content				Nitrate content				Ammonium content			
		N	Mean	MD	RMSE	N	Mean	MD	RMSE	N	Mean	MD	RMSE	N	Mean	MD	RMSE
			(°C)				(v/v)				(kg NO_3-N ha^{-1})				(kg NH_4-N ha^{-1})		
GRIGNON	PP	637	10.9	-1.1	3.0	492	0.318	0.016	0.033	24	49.4	23.2	40.7	24	10.6	7.2	11.0
	PAN1	-	-	-	-	14	0.238	-0.039	0.064	13	36.7	-2.3	21.6	13	10.1	6.8	12.5
	PAN2	-	-	-	-	17	0.238	-0.045	0.064	16	71.9	31.2	57.0	16	17.8	14.2	23.5
	PAN3	-	-	-	-	15	0.255	-0.029	0.042	14	26.5	-3.8	22.7	14	6.1	3.4	4.9
GEBESEE		729	10.7	-0.2	3.3	649	0.260	-0.065	0.080	78	18.1	-1.1	24.5	78	7.7	4.4	28.6
RAFIDIN	N0	294	8.7	-1.2	3.0	20	0.253	-0.027	0.043	21	10.8	5.5	9.9	21	3.7	3.5	4.1
	N1	294	8.7	-1.2	3.0	20	0.244	-0.035	0.051	21	12.9	8.0	11.8	21	5.6	5.0	6.8
	N2	294	8.7	-1.2	3.0	20	0.240	-0.039	0.050	21	23.5	17.0	22.6	21	6.2	5.6	8.0

TAB. 4.3 : *Sample size (N), mean of measured in situ soil variables (Mean), mean deviation (MD) and root mean square errors (RMSE) computed with the predicted and measured soil variables : soil temperature, soil water content and topsoil nitrate and ammonium contents for the 8 data sets.*

4.3.2 Nitrous oxide emissions

The three parallel chains ran for the Bayesian calibration against Grignon-PP site, converged well for all the parameters after 50 000 iterations. The Table 4.2 summarizes the posterior expectancy of parameters and their standard deviation. Correlations with other parameters are also reported in Table 4.2. The posterior ratio of N_2O to total denitrification was higher than is default value, while the posterior potential denitrification rate was highly reduced in comparison with its default values, 0.33 vs. 6.00 kg N ha^{-1} d^{-1} respectively. The posterior value of WFPS threshold

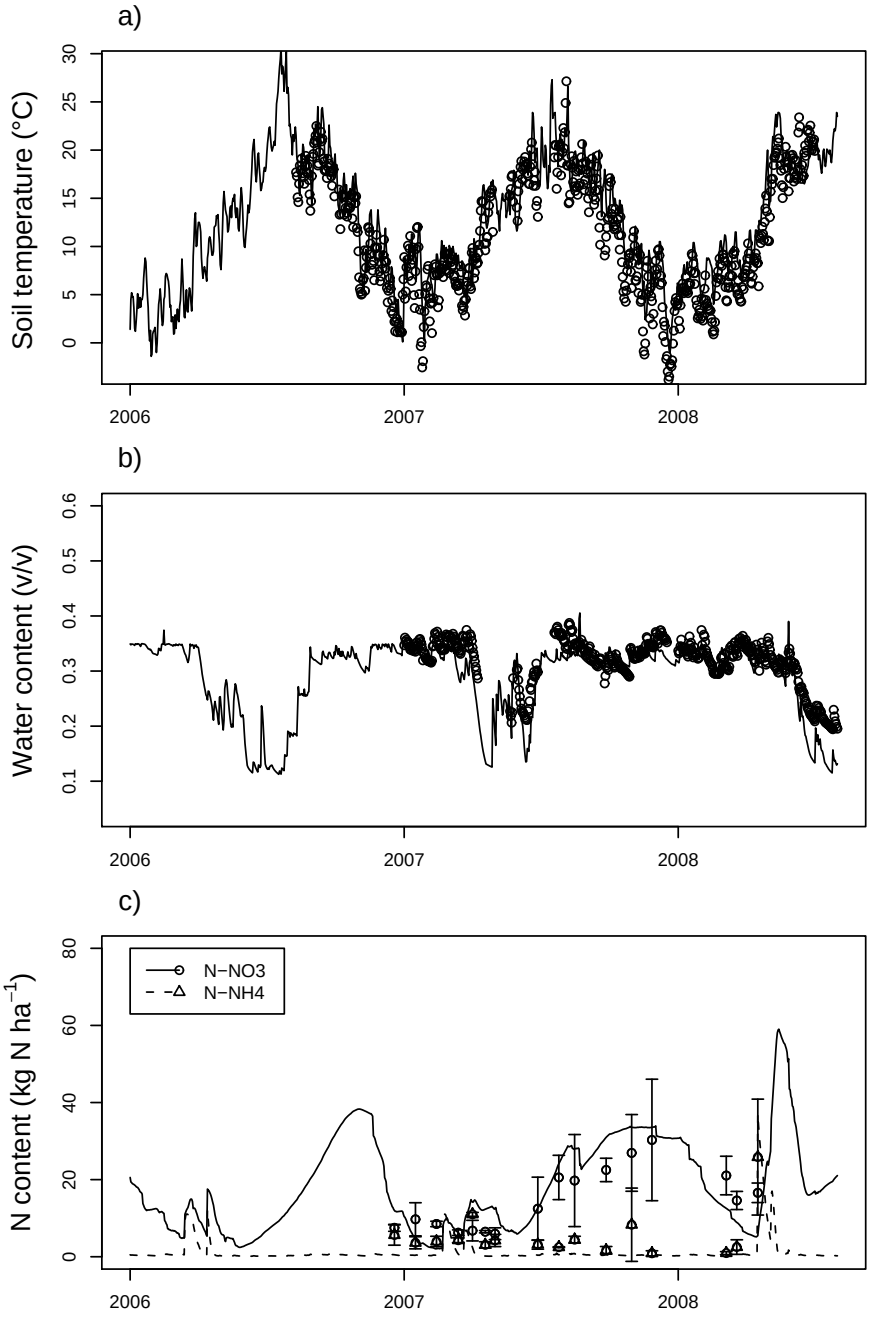

FIG. 4.4 : *Simulated (line) and observed (symbols $\pm sd$) of daily soil temperature (a), soil water content (b) and nitrogen content in the 0-15 cm topsoil layer (c), for the experimental field site of Grignon-PP.*

for denitrification, the half-saturation constant for denitrification and the temperature threshold were similar of their default values.

The Fig. 4.5 compares the simulations of daily N_2O emissions after calibration and the observations of the Grignon-PP experiment. There was good agreement between simulated and observed data during the mineralization of crop residues of the barley at the end of 2007 and beginning of 2008. The first peak flux in March 2007, corresponding to the first N fertiliser application, was not captured by the model due to WFPS simulated above 61% - the threshold that triggers denitrification in the model. The high peak fluxes that occurred in spring 2008 consecutive to the slurry and N-fertiliser applications for maize were correctly predicted. The N_2O emissions observed during the time period consecutive to theses peaks were low and the model simulated emissions close to zero. The RMSE obtained with the posterior expectancy of parameters was reduced by 30% in comparison with the default parameter values (Table 4.4).
The Fig. 4.6 shows the dynamic of N_2O emissions for the three treatments of the Rafidin sites. At this site, N_2O emissions were very low even for the high-N input treatment (N2). In fact, for this treatment, the highest emission rate measured was 7.4 g N_2O-N ha^{-1} d^{-1}. In this site, the rates of N_2O emissions from denitrification were close to zero. Hénault et al. (2005a) estimated that 98% of the N_2O emissions originated from the nitrification process at the same Rafidin site. The predicted rates of N_2O emissions were satisfactory, with RMSEs of 0.3, 1.4 and 3.0 g N_2O-N ha^{-1} d^{-1} after calibration for the N0, N1 and N2 treatments respectively (Table 4.4).

The calibrated model was used to simulate the experiments of Grignon-PAN1,-PAN2 and -PAN3 and of Gebesee. By this way, we assessed the model prediction accuracy by computing the RMSEP, reported in Table 4.4. The predictions computed with the calibrated parameter set were improved in comparison with the predictions with default parameters values, by 6.3% in average for the Grignon-PAN1, -PAN2, -PAN3 treatments and by 39% for Gebesee experiment.
The Fig. 4.7 depicts the N_2O emissions over one year for the three treatments PAN1, PAN2 and PAN3 of the Grignon site and shows that the model correctly predicts the N_2O emission peaks consecutive to the N-fertiliser application that occurred in spring 2008, and also the period of low emissions.
The Fig. 4.8 shows the time course of N_2O emissions at Gebesee. The low emissions and most of the N_2O peaks were well simulated by the model. However, the model can not predict the N_2O deposition and N_2O emissions due to freeze-thaw cycles in winter.

4.3.3 Simulation of crop rotations

In the previous section, we tested and calibrated the CERES-EGC model against datasets from 8 field site experiments involving different sets of crop types, pedoclimatic conditions, and agricultural practices. The present section deals with the extrapolation of the model to calculate the GWP of complete cropping systems, including net C exchanges, direct emissions of N_2O and CH_4 fluxes in the field. The last term of the GHG balance, namely the indirect emissions, was also added.

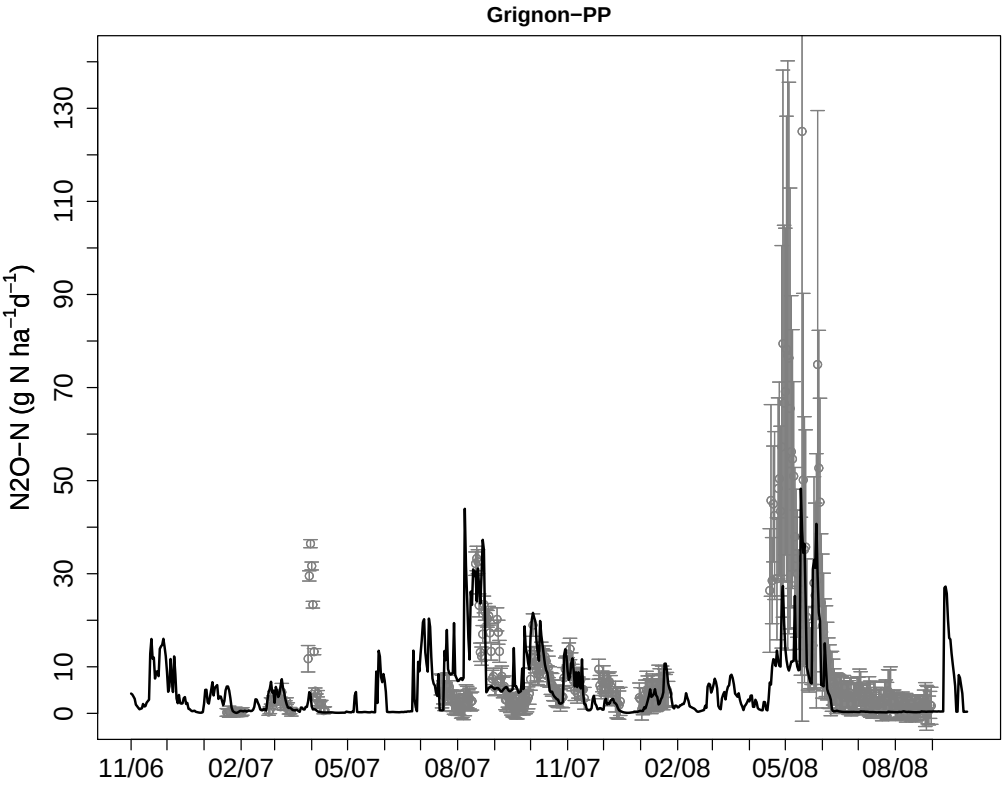

FIG. 4.5 : *Simulated (black line) and observed (symbols $\pm sd$) of daily nitrous oxide emissions for the Grignon-PP experimental site.*

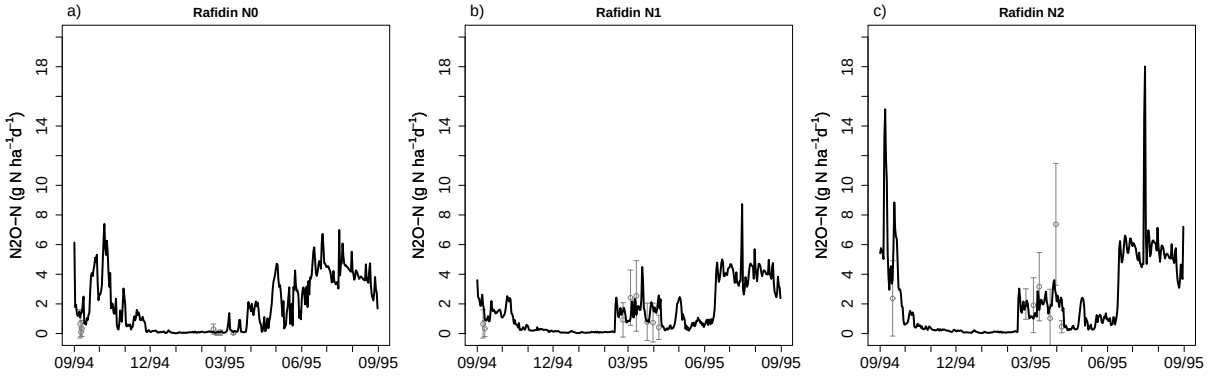

FIG. 4.6 : *Simulated (line) and observed (symbols $\pm sd$) of daily nitrous oxide emissions for the N0 (a), N1 (b) and N2 treatment (c) of the Rafidin experimental site.*

Site	Treatment	RMSE or RMSEP (in italics) computed with :	
		Initial parameter values	Posterior expectancy of parameters
Grignon-PP		20.2	14.2
Rafidin	N0	4.6	0.3
	N1	10.4	1.4
	N2	15.9	3.0
Grignon-PAN1		10.4	*9.6*
Grignon-PAN2		7.4	*7.0*
Grignon-PAN3		7.6	*7.3*
Gebesee		7.6	*4.6*

TAB. 4.4 : *Root mean square errors (RMSEs) of daily nitrous oxide emissions, based on the initial parameters values and the posterior expectancy of parameters. The posterior expectancy of parameters was computed from the the Bayesian calibration of the nitrous oxide module of CERES-EGC against the N_2O measurements of the Rafidin site and of the Grignon-PP experimental site. For the Grignon-PAN1, -PAN2, -PAN3 and the Gebesee sites, the RMSEP was computed with the posterior expectancy of parameters based on the Bayesian calibration against the N_2O measurements of the Grignon-PP site.*

4.3.3.1 Net biome production

Fig. 4.9 displays the breakdown of the NBP for the Grignon-PP rotation. The net ecosystem production was highest with the maize crop, amounting to 5830 $\pm$ 690 kg C ha^{-1}, whereas the NEP of the wheat was 5300$\pm$750 and those of barley close to 4800$\pm$630 kg C ha^{-1}. For the mustard, the soil respiration term was greater than net photosynthesis, and NEP was -440 kg C ha^{-1}. In Rafidin, the NEP of rapeseed was 1300$\pm$1420, 4260$\pm$995 and 4640$\pm$1170 kg C ha^{-1} for the N0, N1 and N2 treatments, respectively, the NEP of wheat was between 4870 and 5190 and the NEP of barley between 3150 and 3440 kg C ha^{-1}. Inter-annual variability was quite large for the net primary production, showing a strong dependence of the climate on crop growth.
Over long-term simulation period with the maize-wheat-barley-mustard rotation in Grignon-PP, we estimated a stable C stock with 10 kg C ha^{-1} yr^{-1} sequestered on average. In Rafidin, we estimated large C accumulation of 525, 1153 and 1269 kg C ha^{-1} yr^{-1} for the N0, N1 and N2 treatments, resp., due to a minor part of the fixed C which was exported out of the field. In Grignon, the straw of wheat and barley was removed for use as litter for animal production, whereas in Rafidin the straw was left on the soil surface at harvest, and subsequently incorporated into the topsoil layer. As a consequence, the C inputs from crop residues were much higher in Rafidin than in Grignon, averaging 4250 kg C ha^{-1} yr^{-1} for the N1 rotation and 4290 kg C ha^{-1} yr^{-1} for the N2 rotation. With these levels of C inputs to the soil, the CERES-EGC model predicted a high C sequestration for the rotations of Rafidin suggesting that the Rafidin soil was a potentially large sink for atmospheric CO_2.
For the other experimental fields of Grignon, the NBPs were 85 for the PAN1 treatment, -256 for the PAN2 treatment and -32 kg C ha^{-1} yr^{-1} for the PAN3 treatment.

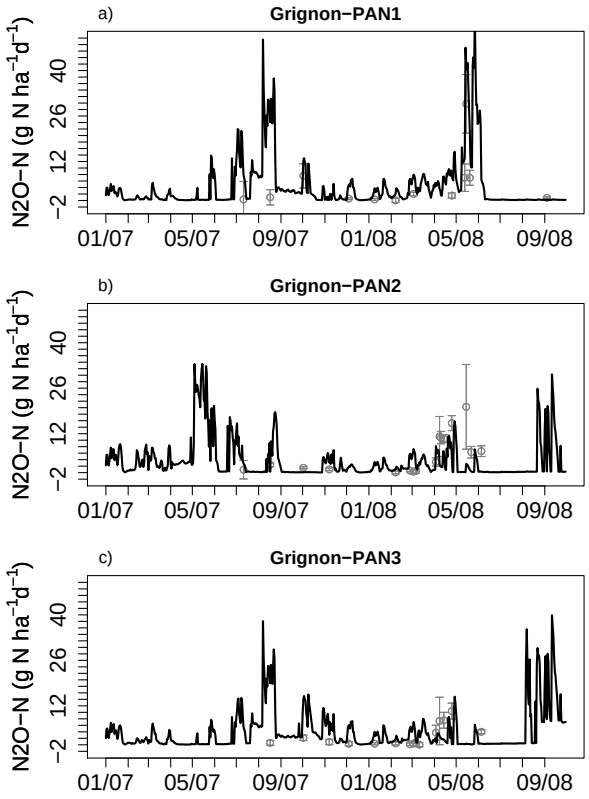

FIG. 4.7 : *Simulated (line) and observed (symbols $\pm sd$) of daily nitrous oxide emissions for the Grignon-PAN1 (a), -PAN2 (b) and -PAN3 (c) experiments.*

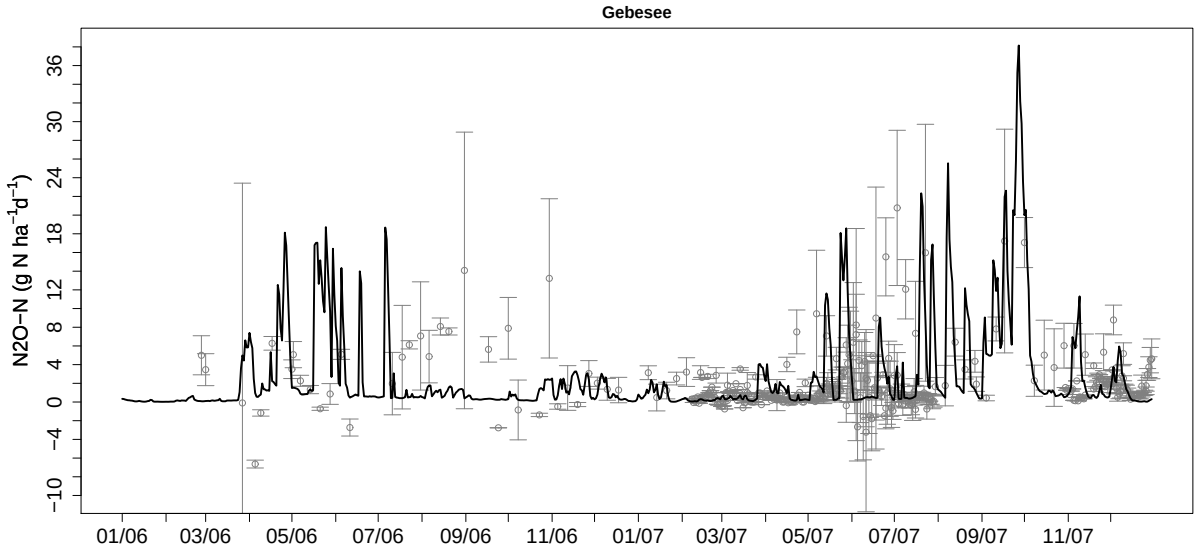

FIG. 4.8 : *Simulated (line) and observed (symbols $\pm sd$) of daily nitrous oxide emissions for the Gebesee experimental field sites.*

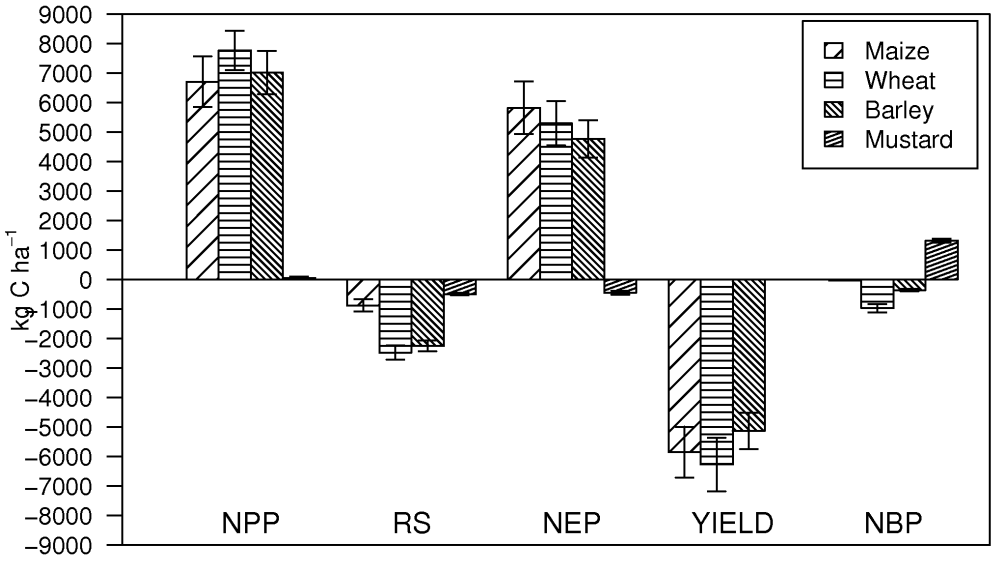

FIG. 4.9 : *Breakdown of net biome production (NBP) into net primary production (NPP), soil respiration (Rs), net ecosystem production (NEP), grain or silage yields plus straw removal (YIELD) for the four crops of the rotation (maize, wheat, barley, mustard) at the Grignon-PP experimental site.*

4.3.3.2 Indirect emissions

The GHG cost of agricultural inputs contributes a large part of the GWP of agro-ecosystems. For the Grignon-PP cropping system, the mean indirect emissions were 350 kg CO_2-C eq ha^{-1} yr^{-1}, for the Rafidin system, the mean IE were 320, 410 and 460 kg CO_2-C eq ha^{-1} yr^{-1} for the N0, N1 and N2 treatments, respectively. For the Grignon-PAN treatments, the mean IE were 420, 480 and 410 kg CO_2-C eq ha^{-1} yr^{-1} for PAN1, PAN2, PAN3 treatments. The IE were 590 kg CO_2-C eq ha^{-1} yr^{-1} for the wheat crop cycle of Gebesee, a higher value compared to the other site due to more frequent cropping operations. N fertilizer production is the top contributor to the IE by a wide margin, with a 55-75% share (Fig. 4.10). Cropping operations came next, with a 30-40% in the total IE term, mainly due to from fossil-fuel combustion by farm machinery. The transport of inputs from the production plant to the farm was the lowest contributor to the GWP with less than 1% of IE.

4.3.4 Global Warming Potential

The 30-yr simulation period enabled us to explore the effect of climate variability on biomass production and N_2O emissions. At Grignon-PP, N_2O emissions averaged 316$\pm$ 82 kg CO_2-C eq ha^{-1} yr^{-1} (CV=26%) over maize-wheat-barley-mustard rotation, and we estimated a GWP of 670$\pm$150 kg CO_2-C eq ha^{-1} yr^{-1} (Table 4.5) for this system. Methane measurements from manual chambers allowed us to estimate its contribution to the final GWP. The soil of Grignon

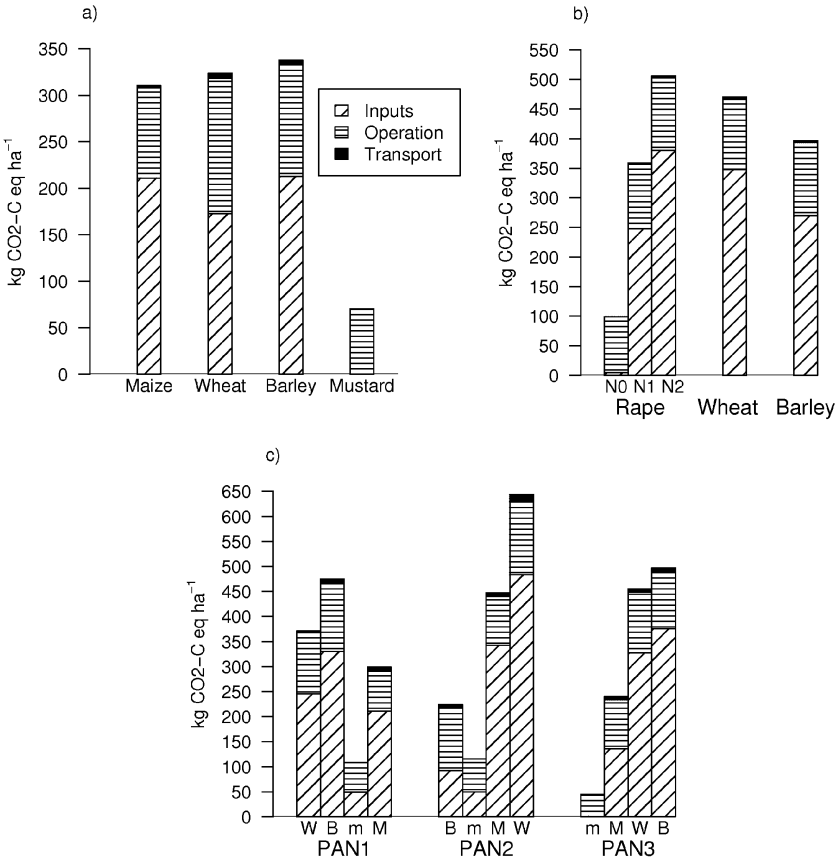

FIG. 4.10 : *Greenhouse gas cost of agricultural inputs and cropping operations for crop production (indirect emissions) for the Grignon-PP (a), Rafidin (b) and Grignon-PANs (c) cropping systems. The emissions are broken down into the input production, agricultural operations and transport steps.*

was a weak methane sink that mitigated the GWP of the rotation by 2%. However, the slurry application during mustard cropping cycle induced a large methane emission of 660 g CH_4-C d^{-1} the day of application.
At Rafidin, we estimated three times lower N_2O emissions than in Grignon-PP ($<$140 kg CO_2-C eq ha^{-1} yr^{-1}), and a large C storage potential resulting from the high level of residue return. The more than offset the emissions of N_2O and the indirect emissions, so that the GWP were -90$\pm$150, -621$\pm$135 and -673$\pm$139 kg CO_2-C eq ha^{-1} yr^{-1} for the N0, N1 and N2 systems, respectively (Table 4.5). The Rafidin crop rotation is an intensive system with a high level of inputs and indirect emissions of GHG, but it is compensated for by the resulting high potential of biomass production and SOC storage. Overall, the Rafidin system emerges a potentially strong sink of GHG.
The Table 4.6 summarizes the GWP for the PAN1, PAN2, PAN3 treatments of Grignon and that of the wheat crop cycle of Gebesee. For each field site, only one crop sequence was simulated. The Grignon-PANs experiments had the same crop sequences as Grignon-PP but without slurry application and maize was harvested for grain and not for silage as it was the case in Grignon-PP. The PAN1, PAN2 and PAN3 treatments were net sources of GHGs with 509, 913 and 547 kg CO_2-C eq ha^{-1} yr^{-1}, resp. The net GWP was higher in the PAN2 treatment due to an additional N fertiliser application on wheat in comparison with the two other treatments. In Gebesee, the wheat crop was a high sink of GHGs due to high C input from manure and slurry applications during its cropping cycle.

4.3.5 Mitigation strategies

Figure 4.11 compares the GWP of five scenarios with differentiated management crop practices. The initial scenario was the cropping system of Grignon-PP described in section 4.2.7 and the sensitivity of its GWP was assessed by changing management of crop residues, catch crop in the rotation, N mineral fertiliser amount and CN inputs from organic fertiliser application. The scenario SW with straw not removed out of the field presents the lowest GWP due to a high negative CO_2 balance. Despite of a substantial increase of soil respiration (+50% compared to the initial scenario), the return of C from crop residues makes the soil C stock increased by 265 kg C ha^{-1} yr^{-1} that offsets the other GHG emissions and makes the GWP 35% less emitter of GHGs than the initial scenario (434 kg CO_2-C ha^{-1} yr^{-1}).
The effect of catch crop was assessed by running simulations without sowing mustard between barley and maize. The effect on the GWP was minor (+6% compared to the initial scenario) due to a very low C fixation simulated in the initial scenario and the C input from slurry application that made mustard a strong C sink was displaced on the barley crop.
The N fertilisation affects the GWP due to its effects on fixation, N_2O emissions and indirect emissions. Increasing the amount of mineral N fertilisers by 50% involved a GWP 22% higher than that of the initial scenario for which the N fertilisation was balanced in relation to N crop demand. N_2O emissions were increased by 17%, indirect emissions by 27% and net primary production only by 1% meaning that optimal yield was already reached with fertilisation of initial scenario. On the contrary, decreasing the N fertiliser by 50% led to a 27% decrease of GWP compared to initial scenario.

	Time period		CO_2	N_2O	CH_4	Agricultural inputs	Net GWP
	Start	End	kg CO_2-C eq ha^{-1}				
GRIGNON-PP							
Maize	9 May n	15 Oct. n	27(4)	179(45)	-2	310	514(55)
Wheat	16 Oct. n	5 Oct. n+1	969(139)	235(66)	-5	324	1522(204)
Barley	6 Oct. n+1	21 Oct. n+2	356(45)	400 (94)	-5	338	1087(138)
Mustard	22 Oct. n+2	8 May n+3	-1322(68)	136(41)	3	70	-1112(55)
Rotation	9 May n	8 May n+3	29(255)	949(247)	-9	1042	2011(453)
RAFIDIN							
Rapeseed N0	10 Sept. n	26 Oct. n+1	187(144)	101(18)	-	99	387(162)
Wheat	27 Oct n+1	26 Oct n+2	-1701(473)	128(41)	-	471	-1102(246)
Barley	27 Oct n+2	9 Sept. n+3	-61(12)	108(43)	-	397	444(43)
Rotation N0	10 Sept. n	9 Sept. n+3	-1575(629)	338(101)	-	967	-270(451)
Rapeseed N1	10 Sept. n	26 Oct. n+1	-1850(348)	121(27)	-	359	-1370(220)
Wheat	27 Oct n+1	26 Oct n+2	-1355(361)	135(44)	-	471	-750(155)
Barley	27 Oct n+2	9 Sept. n+3	-255(47)	117(44)	-	397	258(31)
Rotation N1	10 Sept. n	9 Sept. n+3	-3460(756)	372(114)	-	1226	-1862(406)
Rapeseed N2	10 Sept. n	26 Oct. n+1	-2158(429)	159(28)	-	506	-1493(241)
Wheat	27 Oct n+1	26 Oct n+2	-1339(354)	136(45)	-	471	-732(150)
Barley	27 Oct n+2	9 Sept. n+3	-309(58)	119(44)	-	397	206(25)
Rotation N2	10 Sept. n	9 Sept. n+3	-3806(841)	414(116)	-	1374	-2019(417)

TAB. 4.5 : *Predictions of net global warming potential (GWP) from simulations of net biome production (CO_2=-NBP) and N_2O emissions, estimation of methane fluxes from chamber measurements and indirect GHG costs of agricultural inputs. Simulations were averaged over 36 and 28 years for Grignon-PP and Rafidin cropping systems, resp.*

We assessed in the last scenario, the effect of slurry application on the GWP. Organic fertiliser application represent large C and N inputs in the crop system and its elimination of the rotation resulted in a three-times higher GWP in comparison with initial scenario. Slurry brought in the crop system 1760 kg C ha^{-1} yr^{-1} which represented half of the C removed by straw removal.

4.4 Discussion

4.4.1 Relevance of modelling to estimate GHG balances

The first objective of this work was to test and calibrate the CERES-EGC model against experimental data of CO_2, N_2O, soil variables and crop biomass, from 3 temperate sites located in Western Europe. The model well captured the time course of total above-ground biomass for the crops of the rotations (maize, wheat, barley, rapeseed). The net carbon exchanges between the soil-plant system and the atmosphere were in agreement with the measurements from daily time scale to cropping cycle season and rotations. For the 8 experimental sites and treatments, the soils drivers for N_2O emissions were correctly reproduced and, accordingly, N_2O emissions

	Time period		CO_2	N_2O	CH_4	Agricultural inputs	Net GWP
	Start	End	kg CO_2-C eq ha^{-1}				
GRIGNON-PAN1							
Wheat	27/10/05	05/10/06	1587	117	-6	371	2070
Barley	06/10/06	30/08/07	-209	208	-5	475	469
Mustard	31/08/07	06/05/08	579	101	-4	109	784
Maize	07/05/08	26/10/08	-2211	119	-3	299	-1796
Rotation	27/10/05	26/10/08	-254	545	-18	1253	1526
GRIGNON-PAN2							
Barley	05/10/05	29/09/06	548	154	-13	224	913
Mustard	30/09/06	25/04/07	537	164	-8	115	808
Maize	26/04/07	23/10/07	-2310	140	-7	448	-1729
Wheat	24/10/07	04/10/08	1994	123	-13	643	2747
Rotation	05/10/05	04/10/08	769	580	-40	1430	2739
GRIGNON-PAN3							
Mustard	02/09/05	25/04/06	372	71	-3	45	485
Maize	26/04/06	09/10/06	-2592	80	-2	241	-2274
Wheat	10/10/06	07/10/07	2023	221	-4	455	2695
Barley	08/10/07	01/09/08	101	139	-4	497	734
Rotation	02/09/05	01/09/08	-97	511	-12	1238	1640
GEBESEE							
Wheat	27/10/06	05/10/07	-3773	158	-4	589	-3030

TAB. 4.6 : *Predictions of net global warming potential (GWP) from simulations of net biome production (CO_2=-NBP) and N_2O emissions, estimation of methane fluxes from chamber measurements and indirect GHG costs of agricultural inputs, for the one-year wheat crop cycle of Gebesee and the three treatments PAN1, PAN2 and PAN3 of Grignon.*

were in agreement with the observations in all sites with RMSEs or RMSEPs ranging from 0.3 to 14.2 g N_2O-N ha^{-1} d^{-1}. Bayesian calibration applied on the six most influent parameters of the nitrous oxide emission module of CERES-EGC allowed us to reduce error of prediction by 6-40% compared to default parameters-based simulations against 4 independent data sets of N_2O measurements.

Other studies with similar modelling approaches mention that the discrepancies between modelled and observed N_2O data were in the same range of errors as our simulations. For example, Del Grosso et al. (2005) showed that the DAYCENT model gave daily prediction of N_2O emissions with a quite high discrepancy (RRMSE=64%, n=21) for major crops in the USA. Del Grosso et al. (2008) also reported that DAYCENT largely overestimated N_2O emissions in irrigated system due to an over responsive effect of soil NO_3^- on N_2O. In the same way, Babu et al. (2006) indicate that the DNDC model predicted daily N_2O fluxes with a large lack of fit (RMSE=529.6 g N_2O-

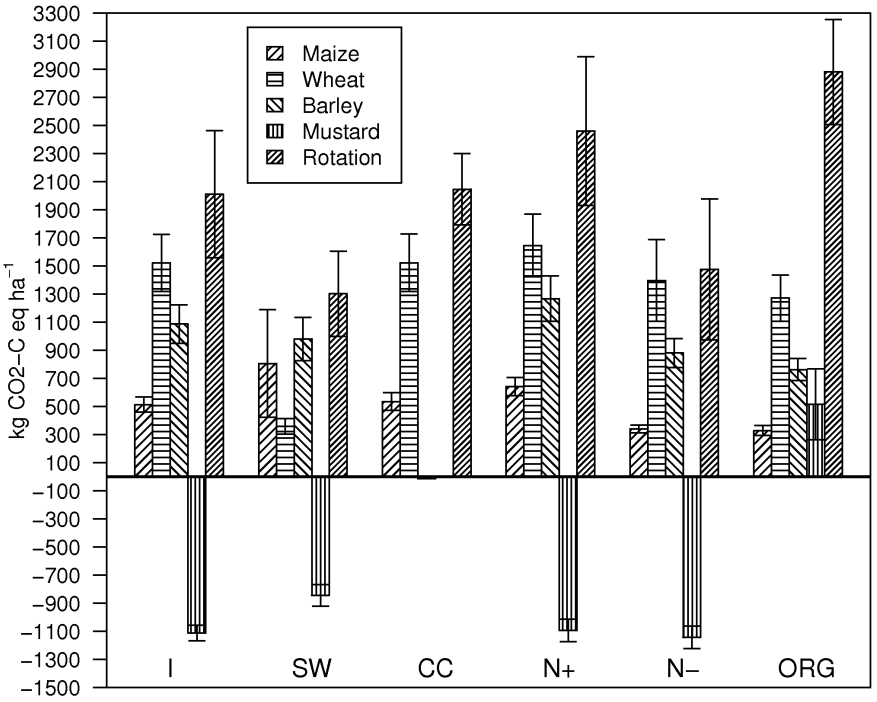

FIG. 4.11 : *Comparison of net global warming potentials of five scenarios averaged over 36-years for the Grignon-PP experiment (I : initial scenario, SW : straw left on soil, CC : without catch crop, N+ : 50% more N fertiliser, N- : 50% less N fertiliser, ORG : without organic fertiliser).*

N ha^{-1} d^{-1}, n=134) for rice-based production systems in India with high level of N_2O emissions (observed daily mean=49.4 g N_2O-N ha^{-1} d^{-1}). Frolking et al. (1998) and Li et al. (2005b) compared different models or sub-models for their capacity to simulate N_2O emissions from cropland. In most cases, the models were not able to capture the daily N_2O flux patterns because of time lag between observed and modelled peaks and over- or underestimation of the measured N_2O spikes.

Regarding the C balance, we assumed that the net biome production reflected the SOC changes. The balance between C inputs and C losses of the Grignon-PP field-site was nearly balanced, while Rafidin had a high potential of C sequestration resulting from a high C fixation by crops and a large fraction of inputs as crop residues. As a consequence, C storage was estimated between 500 and 1300 kg C ha^{-1} yr^{-1} for the various treatments of Rafidin. This is in agreement with the relatively low SOC mineralization rate of rendzina soils ($<$0.5% of SOC yr^{-1}), such as that of Rafidin, due to physical protection process by the formation of calcite formation on the organic fractions (Trinsoutrot et al., 2000). The high level of biomass production made possible by ample fertilizer inputs, together with this low SOC mineralization rate induced a large net fixation of atmospheric CO_2. Adviento-Borbe et al. (2007) measured the SOC changes over a 5-yr period in continuous maize system with recommended and intensive fertilisation treatments

(+70-100% more N fertiliser applied than in the recommended treatment) in Nebraska (USA). They reported that C sequestration rates ranging from 440 to 620 kg C ha^{-1} yr^{-1} for recommended and intensive treatments, resp., mainly due to high C residue returns from maize crops. The latters ranged between 5500 and 6500 kg C ha^{-1} yr^{-1} in both cropping systems. In Rafidin, C storage for the intensive rotation was almost twice greater than those of the intensive treatment reported by Adviento-Borbe et al. (2007) whereas the crop residues were slightly lower.
The C dynamics predicted by the model were evaluated at the daily time scale against micrometeorological measurements of CO_2 exchanges for entire crop rotations, but it will be necessary to supplement this test by further verifying the ability of CERES-EGC to simulate the rate of soil C changes in the long term. With this test, we could also compare the methods of estimation of C term by computing either NBP or long-term simulations for assessing change of soil C stock.

4.4.2 Model application for predicting global warming potential

Applying the model to predict the GWPs of crop rotations was the second objective of this work. Climate variability on the different terms of the GHG balance was taken into consideration by computing the direct emissions over $\sim$30-yr time series as the succession of $\sim$10 rotations. As a result, the GWPs of Rafidin and Grignon-PP were markedly different : the rapeseed-wheat-barley rotation on a rendzina was a net sink of GHG with a GWP of -620 to -670 kg C ha^{-1} yr^{-1} for balanced and intensive treatments, while the wheat-maize-barley-mustard rotation on a loamy soil in Grignon was a net source of GHG, with a GWP of 670 kg C ha^{-1} yr^{-1}.
Few other references of GWP of crop rotations, in particular in Europe were available for comparison with our results. The GWP of Grignon is twice higher than that of 310 kg CO_2-C eq ha^{-1} yr^{-1}, measured by Robertson et al. (2000) for a conventional maize-soybean-wheat system in the US Midwest United States. The latter authors found no measurable soil C sequestration with conventional tillage, and our estimation was also close to zero (-10 kg CO_2-C eq ha^{-1} yr^{-1}). However, their rotation included a legume crop (soybean) that required less N fertilizer amount than cereal or oilseed crops as into our rotation. In addition, the system boundaries they set for the indirect emissions were narrower than ours. They only accounted for the CO_2 emissions occurring during the production of agricultural inputs, and not the other GHGs, although these may account for half of the total IE of GHG. Consequently, we estimated a twice higher IE term. In both cases, N_2O emissions contributed 50% of the GWP but we estimated a N_2O term twice higher than their estimate from measurements, 316 vs. 142 kg CO_2-C eq ha^{-1} yr^{-1}, respectively. Our estimations of indirect emissions are much more closer of those of Adviento-Borbe et al. (2007) who estimated indirect emissions that ranged between 290 and 660 kg CO_2-C eq ha^{-1} yr^{-1} for continuous maize and soybean-maize cropping systems (without accounting GHG contribution of irrigation and grain drying).

4.4.3 Efficiency of mitigation options

The last objective of this work was to assess the sensitivity of GWPs to different agricultural practices in order to test mitigation options. The most efficient strategy we identified was to return crop residues to the soil, ie the wheat and barley straw. The worst one was to remove

the organic fertiliser application which was a substantial input of C for the entire rotation. Although high CH_4 emissions were recorded immediately after application, they were stopped by soil incorporation a few hours later and the soil was a net sink of CH_4 during the rest of the year. The methane has little impact on the GHG balance but the incorporation of organic fertilisers immeditely after spreading appears as good option to reduce CH_4 emissions from organic fertilizer applications. In the same way, Jones et al. (2005) measured GHG fluxes from a managed grassland and reported that application of cattle slurry resulted in an immediate CH_4 peak flux of 2850 g CH_4-C ha^{-1} d^{-1}, during 2-3 days. However, CH_4 fluxes were insignificant compared to N_2O emissions in terme of GWP (1500 times lower).

Reducing N fertiliser rates lowers N_2O and indirect emissions of GHG, but also C fixation by plants. As a result, the fresh organic matter supply in soil from crop residues is diminished. For the Rafidin site, the most intensive system (N2) had the lowest GWP due to its large capacity to store C fixed by crops. On the other hand, adding a third N fertiliser split application on the wheat crop in the rotation of the Grignon-PAN2 treatment resulted in a greater GWP due to higher indirect and N_2O emissions compared to the benefits in term of C fixation. This supplementary application was mostly aimed at increasing protein content and not plant biomass.

Assessing the effects of new mitigation strategies requires an integrated systems approach in order to encompass the indirect effects of mitigation strategies and counter-intuitive or unintentional flux changes (Robertson et Grace, 2004). Implementation of mitigation strategies that combines the options of i) enhancing soil carbon sequestration, ii) reducing N_2O emissions and iii) minimizing synthetic fertilizer use would be highly efficient in term of systemic reduction of GWP.

For example, Del Grosso et al. (2009) showed with the DAYCENT model that the most efficient strategy to reduce GHG fluxes, at the global scale, was to adopt no-till cultivation combined with nitrification inhibitors. However, no-till cultivation led to greater emissions in some wet regions of the world where soil moisture was conserved by no-till effect which enhanced denitrification and N_2O emissions which offseted the overall benefits of C storage.

Although the CERES-EGC model allowed us to quantify GWP of cropping systems and to test some mitigation strategies, it faced with a number of limitations, it lacks a capacity to i) well reproduce the effect of tillage practices on the soil C change, ii) reflect the nitrification inhibitor effects on N_2O emissions and iii) simulate methanogenesis and methanotrophy processes in soil and the resulting CH_4 fluxes. Further developments should focus on these points to improve the accuracy of GWP quantification and the assessment of mitigation options and new mitigation technologies.

4.5 Conclusion

The assessment of the direct emissions at the field scale is paramount in an accurate estimation of GHG balances for agricultural systems. Biophysical modelling of the soil-crop-atmosphere system provides a unique capacity to address this issue while taking into account the complex interactions between C and N cycling, as influenced by anthropogenic actions. Here, we tested and calibrated the CERES-EGC model to simulate the GHG fluxes of the agro-ecosystem,

and showed it achieved satisfactory predictions of N_2O and CO_2 fluxes for different cropping systems representing distinct pedoclimatic conditions and agricultural practices.
The C dynamics predicted by the model were validated at the daily time scale against micrometeorological measurements of CO_2 exchanges in two of the three sites, but it will be necessary to supplement this test by further verifying the ability of CERES-EGC to simulate the rate of changes in the long term.
The modeling approach was used to devise different strategies to mitigate the GWP of cropping systems. Various scenarios involving some modifications of crop management (eg, fertilisation, rotation, crop residue management) were tested for this purpose. Other environmental impacts may be output by the model and included in the analysis, in particular the emissions into air or water of NH_3, NO_3^-, or NO. Thus, the overall environmental balance of the agricultural systems may be approached, making it possible to design agricultural systems with high environmental performance.

Acknowledgements

This work was part of the CarboEurope and NitroEurope Integrated Projects (EU's Sixth Framework Programme for Research and Technological Development), which both investigate the European terrestrial greenhouse gas balance. We express special thanks to Christophe Fléchard for its assistance in the analysis of gas sampling.

Chapitre 5

Conclusion et perspectives

La problématique centrale de ce travail de thèse était d'estimer le pouvoir de réchauffement global des agro-écosystèmes. Pour y répondre, nous avons mis au point une méthodologie générale basée sur la modélisation biophysique. Elle permet de prendre en compte la régulation des flux et des processus sous-jacents par les conditions pédoclimatiques locales et les pratiques agronomiques.
La boucle de progrès de modélisation, décrite en introduction, a été appliquée au modèle CERES-EGC. Elle a permis de calibrer ses paramètres et d'évaluer son erreur de prédiction dans la simulation des flux de N_2O et de CO_2 à l'échelle de la parcelle. Ce modèle, qui intègre le fonctionnement de l'agro-écosystème dans son ensemble, est désormais en mesure de quantifier le bilan de GES des systèmes de cultures, avec une marge d'erreur que nous avons estimée.

Les perspectives de ce travail portent sur l'intégration de nouveaux processus dans le modèle, sa valorisation dans des modèles multi-écosystèmes, l'extrapolation spatiale à l'échelle du paysage et de la région, et le développement d'un couplage écosystème-atmosphère.

5.1 Bilan du travail de thèse

La problématique centrale de ce travail de thèse était d'estimer le pouvoir de réchauffement global (PRG) des agro-écosystèmes. Pour y répondre, nous avons mis au point une méthodologie générale basée sur la modélisation biophysique. La boucle de progrès de modélisation, décrite en introduction, a été appliquée au modèle CERES-EGC et a permis de calibrer ses paramètres et d'évaluer son erreur de prédiction à simuler les flux de N_2O et de CO_2 à l'échelle de la parcelle. Ces flux dépendent de processus liés à l'activité microbiologique des sols et à la croissance des cultures qui sont eux-mêmes régulés par les conditions pédoclimatiques locales et les pratiques agronomiques. Le modèle CERES-EGC intègre le fonctionnement de l'agro-écosystème dans son ensemble et est désormais en mesure de quantifier le bilan de GES des systèmes de cultures.

Amélioration du modèle CERES-EGC

Ce travail de thèse a permis de développer une méthode de calibration des paramètres basée sur une approche bayésienne. Cette approche est peu utilisée pour les modèles d'écosystèmes complexes et nous avons démontré son intérêt pour estimer les paramètres et pour quantifier l'incertitude des sorties.
La calibration bayésienne du module d'émissions de N_2O de CERES-EGC a été réalisée grâce à une base de données de mesures d'émissions de N_2O provenant de 7 sites expérimentaux en France. Elle a été appliquée successivement sur les différents jeux de données afin d'estimer la valeur a posteriori des paramètres et a permis d'améliorer en moyenne de 75 % l'ajustement aux données. La méthode a été utilisée pour estimer les paramètres impliqués dans la modélisation des échanges nets de CO_2 avec des jeux de données provenant de 2 sites expérimentaux aux conditions pédoclimatiques contrastées (Grignon et Auradé). Comme pour le N_2O, la calibration a fortement amélioré la performance du modèle par rapport à l'utilisation des valeurs initiales de paramètres. Le modèle est capable d'estimer les flux de CO_2, depuis l'échelle journalière jusqu'à la rotation entière.

L'erreur de prédiction du modèle a été évaluée avec des jeux de données indépendants de ceux impliqués dans la calibration. Nous avons alors pu juger de sa performance à simuler les flux de N_2O et de CO_2. Les erreurs de prédictions sont comparables, voire inférieures, à celles des modèles DNDC et DAYCENT qui sont largement utilisés à l'heure actuelle pour simuler les échanges de GES.

Mise au point d'une méthode pour l'extrapolation spatiale

Les modèles d'écosystème sont développés pour fournir des prédictions sur un large domaine de temps et d'espace pour lesquels peu d'observations sont disponibles. L'application du modèle à un nouveau site ou à une échelle spatiale plus large a donc nécessité la mise au point d'une stratégie de calibration qui puisse permettre d'estimer les valeurs "universelles" des paramètres. Nous avons proposé une telle méthode basée sur la calibration bayésienne en utilisant simultanément les jeux de données mesurées disponibles dans la procédure dite "multi-sites". Celle-ci

permet d'améliorer en moyenne de 30 % l'ajustement aux données. Certes, cette méthode donne des résultats moins bons qu'une calibration spécifique au site, mais elle permet de rendre le modèle opérationnel pour la spatialisation des émissions et le calcul du PRG pour tout nouveau site. La procédure "multi-sites" fonctionne en routine : dès qu'un nouveau jeu de données d'observation est acquis, il peut être assimilé par la procédure de calibration et participer à l'amélioration du modèle.

Utilisation du modèle pour des applications variées

L'application du modèle permet d'intégrer les flux de gaz à effet de serre dans le temps, pour réaliser des bilans, ou dans l'espace, pour produire des inventaires. Grâce à son amélioration et à l'évaluation de son erreur de prédiction, le modèle est opérationnel pour calculer le bilan de GES des systèmes de cultures et des facteurs d'émissions. Il est aussi en mesure de produire des cadastres de flux de GES à l'échelle régionale. Les bilans de C ou de GES permettront d'affiner les analyses de cycle de vie (ACV) des produits agricoles en prenant en compte les conditions locales du milieu et les pratiques agronomiques. La variation géographique des flux de GES implique que la méthodologie de l'ACV basée sur l'utilisation de facteurs d'émissions universels soit revisitée.

Dans ce travail de thèse, le modèle a permis de quantifier les bilans annuels de N_2O et les facteurs d'émissions pour 7 sites expérimentaux. Les bilans de N_2O pour les sites étudiés présentent des facteurs de conversion qui sont inférieurs au 1 % préconisé par la méthode de niveau 1 de l'IPCC. Les flux annuels de N_2O ont été estimés entre 90 et 3 700 g N_2O-N ha^{-1} an^{-1} et les facteurs d'émissions entre 0.05 et 1.15 % de l'engrais apporté. Il apparaît que la valeur de 1 % surestime les émissions qui, de surcroît, ne sont pas strictement proportionnelles aux quantités d'engrais apportées.

Les bilans de CO_2 ont été quantifiés pour 3 sites expérimentaux en Europe à l'échelle de cycles et de rotations de cultures. L'application du modèle a permis d'évaluer le pouvoir de réchauffement global de systèmes de cultures en y incluant les émissions de N_2O et les bilans de C simulés sur 30 ans. Les flux de méthane mesurés et les émissions indirectes dues à la production des intrants et aux opérations culturales ont également été intégrés au calcul du PRG. Nous avons estimé que la rotation de Grignon (maïs-blé-orge-moutarde) était une source de GES à hauteur de 670 kg CO_2-C ha^{-1} an^{-1} alors que la rotation du site du Rafidin (colza-blé-orge) était un puits net de GES d'environ 650 kg CO_2-C ha^{-1} an^{-1}. Les importants retours de résidus de cultures dans le cas du Rafidin induisent un potentiel de stockage de C qui compense largement les émissions.
La recherche de stratégies de mitigation du PRG des systèmes de cultures a été initiée dans le chapitre 4. Elle nécessite d'être poursuivie afin d'y inclure les autres émissions et pertes vers l'environnement (NO, NH_3, NO_3^-) pour s'assurer de l'absence de transferts de pollutions et d'améliorer le bilan environnemental dans son ensemble.

Le modèle CERES-EGC a également été appliqué pour estimer des inventaires spatialisés d'émissions de N_2O des écosystèmes cultivés, à résolution journalière et à l'échelle de la région Île-de-France (annexe A). Les premières simulations pour la période 2000-2001 montrent une sensibilité importante des émissions de N_2O à la distribution spatiale des types de sols et aux données météo. Les inventaires de CERES-EGC seront couplés au modèle de transport atmosphérique CHIMERE (développé à l'IPSL[1] et utilisé au LSCE[2]). Les concentrations de N_2O prédites seront comparées avec les mesures atmosphériques réalisées au LSCE.

5.2 Perspectives

Les modèles d'agro-écosystème à échelle parcellaire devront continuer à être améliorés afin d'y incorporer les processus manquants (épisodes de gel-dégel, échanges de méthane, diffusion des gaz dans le sol...), avec un objectif d'intégration des nouvelles connaissances. L'obtention de données observées au sein de l'UMR EGC ou via des réseaux de mesures permettra d'élargir le domaine d'application des modèles pour des conditions pédoclimatiques variées et d'améliorer la modélisation des processus et des fonctions de réponse.

Par ailleurs, **l'inter-comparaison des modèles** permettra d'identifier les points faibles et les points forts de chacun. Une méthode de comparaison bayésienne des modèles d'écosystème est développée dans le projet NitroEurope et sera mise en œuvre, à court-terme, pour les modèles d'agro-écosystème. Le modèle CERES-EGC participe à cette comparaison et sera confronté aux modèles DAYCENT et DNDC. La calibration est une étape préalable à l'inter-comparaison et devra être basée sur une méthode similaire pour tous les modèles et appliquée avec des jeux de données identiques.
Une utilisation concomitante de plusieurs modèles pourra également fournir une estimation plus précise des prédictions (Fisher et al., 2002).

Le développement de **modèles modulaires multi-écosystèmes**, à l'image de la plate-forme MOBILE (*Modular biosphere simulation environment*, développée par l'IMK-IFU, Garmisch, All.), ou comme le modèle de végétation ORCHIDEE (développé au LSCE, Krinner et al. (2005)), est une perspective intéressante pour simuler les flux de GES des différents écosystèmes (forêt, prairie, culture). Ces plates-formes pourront valoriser le développement de modèles dédiés aux écosystèmes cultivés, comme CERES-EGC, ce qui leur permettra d'améliorer la modélisation des émissions agricoles et la représentation des pratiques agronomiques.

L'intégration de modèles d'agro-écosystème dans **des modèles à échelle du paysage** (quelques km^2), comme NitroScape, est une perspective intéressante de ce travail. À cette échelle plus fine, il faudra considérer les transferts et la redistribution de l'azote via l'air et l'eau ainsi que le raisonnement des pratiques à l'échelle de la ferme. Dans cette optique, il conviendra de se concentrer sur de nouvelles espèces azotés (NH_3, NO_x) et aux processus de dépôts. Des bilans de GES plus

[1] Institut Pierre Simon Laplace
[2] Laboratoire des Sciences du Climat et de l'Environnement,CEA-CNRS, Saclay, Fr.

complets pourront alors être déterminés en prenant mieux en compte la “cascade de l’azote” et les émissions indirectes qui ont lieu en aval de la parcelle cultivée.

Appliquer les modèles d’écosystème à **une échelle régionale** (10^2-10^6 km^2) permet de fournir des inventaires spatialisés de flux de GES plus précis que ceux issus de calculs par facteurs d’émissions. **L’approche “bottom-up”** décrite en annexe A devra continuer à être développée. Pour cela, la compilation d’informations géoréférencées pour les données d’entrées des modèles est une tâche importante qui nécessite d’être poursuivie.

Un **couplage des modèles d’agro-écosystème avec des modèles atmosphériques** de chimie-transport ou de circulation générale permettra de modéliser le devenir des émissions de N_2O et des autres polluants azotés dans l’atmosphère. Ainsi, nous pourrons estimer l’impact des émissions agricoles sur la qualité de l’air et les concentrations en gaz à effet de serre à l’échelle régionale, voire sur le climat à l’échelle globale. Les échanges sol-végétation-atmosphère et les relations entre les sources et puits de polluants impliqueront d’intégrer dans les modèles d’agro-écosystème des schémas de transferts sol-végétation-atmosphère (*SVAT*) spécifiques aux polluants étudiés. La confrontation des simulations couplées écosystème-atmosphère à l’échelle régionale avec des mesures atmosphériques intégratrices réalisées sur des tours à flux permettra d’évaluer la robustesse de la méthode de modélisation. Cette évaluation garantira le réalisme des simulations des émissions biogéniques pour une extrapolation à des échelles supérieures (continentale voire globale).

Les estimations spatialisées des sources de GES permettent de localiser des zones d’émissions critiques (“hot-spots”) liées aux caractéristiques physiques du milieu, au bassin de production et aux pratiques de gestion agronomique. Cette différenciation spatiale des émissions permettra de focaliser les efforts pour une réduction efficace des impacts. Les effets de filières émergentes comme la bioénergie, de politiques agri-environnementales, ou encore de scénarios de développement de systèmes alimentaires ou énergétiques durables, pourront être évalués du point de vue environnemental à l’échelle d’un territoire. L’évaluation simultanée du pouvoir de réchauffement global des agro-écosystèmes, de la qualité de l’air et des impacts d’eutrophisation et d’acidification, contribuera à élaborer des systèmes durables.

Bibliographie

Adiku, S. G. K., Reichstein, M., Lohila, A., Dinh, N. Q., Aurela, M., Laurila, T., Lueers, J., and Tenhunen, J. D., 2006. PIXGRO : A model for simulating the ecosystem CO2 exchange and growth of spring barley. Ecol. Model. 190, 260–276.

Adler, P. R., Del Grosso, S. J., and Parton, W. J., 2007. Life-cycle assessment of net greenhouse-gas flux for bioenergy cropping systems. Ecological Applications 17, 675–691.

Adviento-Borbe, M. A. A., Haddix, M. L., Binder, D. L., Walters, D. T., and Dobermann, A., 2007. Soil greenhouse gas fluxes and global warming potential in four high-yielding maize systems. Global Change Biology 13, 1972–1988.

Airparif, 2005. Analyse de l'inventaire et du cadastre des émissions des principaux gaz à effet de serre en Île-de-France.

Albrizio, R. and Steduto, P., 2005. Resource use efficiency of field-grown sunflower, sorghum, wheat and chick-pea I. Radiation use efficiency. Agr. Forest Meteorol. 130, 254–268.

Ammann, C., Fléchard, C. R., Leifeld, J., Neftel, A., and Fuhrer, J., 2007. The carbon budget of newly established temperate grassland depends on management intensity. Agr. Ecosys. Environ. 121, 5–20.

Andrade, F. H., Uhart, S. A., and Cirilo, A., 1993. Temperature Affects Radiation Use Efficiency in Maize. Field Crop. Res. 32, 17–25.

Anthoni, P. M., Knohl, A., Rebmann, C., Freibauer, A., Mund, M., Ziegler, W., Kolle, O., and Schulze, E. D., 2004. Forest and agricultural land-use-dependent CO2 exchange in thuringia, germany. Glob. Change Biolo. 10, 2005–2019.

Arrouays, D., Balesdent, J., Germon, J. C., Jayet, P. A., Soussana, J. F., and Stengel, P., 2002. Stocker du carbone dans les sols agricoles de France ?. Expertise scientifique collective. INRA, Paris.

Aubinet, M., Grelle, A., Ibrom, A., Rannik, U., Moncrieff, J., Foken, T., Kowalski, A. S., Martin, P. H., Berbigier, P., Bernhofer, C., Clement, R., Elbers, J., Granier, A., Grunwald, T., Morgenstern, K., Pilegaard, K., Rebmann, C., Snijders, W., Valentini, R., and Vesala, T., 2000. Estimates of the annual net carbon and water exchange of forests : The EUROFLUX methodology. Adv. Ecol. Res. 30, 113–175.

Babu, Y. J., Li, C., Frolking, S., Nayak, D. R., and Adhya, T. K., 2006. Field validation of DNDC model for methane and nitrous oxide emissions from rice-based production systems of India. Nutrient Cycling in Agroecosystems 74, 157–174.

Baldocchi, D., Falge, E., Gu, L. H., Olson, R., Hollinger, D., Running, S., Anthoni, P., Bernhofer, C., Davis, K., Evans, R., Fuentes, J., Goldstein, A., Katul, G., Law, B., Lee, X. H., Malhi, Y., Meyers, T., Munger, W., Oechel, W., U, K. T. P., Pilegaard, K., Schmid, H. P., Valentini, R., Verma, S., Vesala, T., Wilson, K., and Wofsy, S., 2001. FLUXNET : A new tool to study the temporal and spatial variability of ecosystem-scale carbon dioxide, water vapor, and energy flux densities. Bulletin of the American Meteorological Society 82, 2415–2434.

Balesdent, J., Arrouays, D., Chenu, C., and Feller, C., 2005. Stockage et recyclage du carbone. In Girard, M. C., Walter, C., Remy, S. C., Berthelin, J., and Morel, J. L., editors, Sols et Environnement chapter 10, pages 238–261. Dunod.

Barton, L., Kiese, R., Gatter, D., Butterbach-Bahl, K., Buck, R., Hinz, C., and Murphy, D. V., 2008. Nitrous oxide emissions from a cropped soil in a semi-arid climate. Global Change Biology 14, 177–192.

Bateman, E. J. and Baggs, E. M., 2005. Contributions of nitrification and denitrification to N_2O emissions from soils at different water-filled pore space. Biology and Fertility of Soils 41, 379–388.

Beheydt, D., Boeckx, P., Ahmed, H. P., and Van Cleemput, O., 2008. N_2O emission from conventional and minimum-tilled soils. Biology and Fertility of Soils 44, 863–873.

Beheydt, D., Boeckx, P., Sleutel, S., Li, C. S., and Van Cleemput, O., 2007. Validation of DNDC for 22 long-term N2O field emission measurements. Atmospheric Environment 41, 6196–6211.

Bernacchi, C. J., Hollinger, S. E., and Meyers, T., 2005. The conversion of the corn/soybean ecosystem to no-till agriculture may result in a carbon sink. Global Change Biology 11, 1867–1872.

Bhatia, A., Pathak, H., Jain, N., Singh, P. K., and Singh, A. K., 2005. Global warming potential of manure amended soils under rice-wheat system in the Indo-Gangetic plains. Atmospheric Environment 39, 6976–6984.

Biswas, W., Barton, L., and Carter, D., 2008. Global warming potential of wheat production in Western Australia : a life cycle assessment. Water and Environment Journal 22, 206–216.

Boote, K. J., Jones, J. W., and Pickering, N. B., 1996. Potential uses and limitations of crop models. Agronomy Journal 88, 704–716.

Brown, L., Syed, B., Jarvis, S. C., Sneath, R. W., Phillips, V. R., Goulding, K. W. T., and Li, C., 2002. Development and application of a mechanistic model to estimate emission of nitrous oxide from UK agriculture. Atmospheric Environment 36, 917–928.

Butterbach-Bahl, K., Kesik, M., Miehle, P., Papen, H., and Li, C., 2004. Quantifying the regional source strength of n-trace gases across agricultural and forest ecosystems with process based models. Plant and Soil 260, 311–329.

CarboEurope, 2004. Greenhouse Gas Emissions from European Croplands. European Commission. Report 4, Specific Study 3. Clermont-Ferrand, France.

Cellier, P., Germon, J. C., Hénault, C., and Génermont, S., 1996. Les émissions d'ammoniac (NH3) et d'oxydes d'azote (NOx et N2O) par les sols cultivés. In Lemaire, G. and Nicolardot, B., editors, Maîtrise de l'azote dans les agrosystèmes chapter 1. INRA, Paris.

Chapuis-Lardy, L., Wrage, N., Metay, A., Chotte, J. L., and Bernoux, M., 2007. Soils, a sink for N2O ? A review. Global Change Biology 13, 1–17.

Chatskikh, D., Olesen, J., Berntsen, J., Regina, K., and Yamulki, S., 2005. Simulation of effects of soils, climate and management on N2O emission from grasslands. Biogeochemistry 76, 395–419.

Chen, D. L., Li, Y., Grace, P., and Mosier, A. R., 2008. N2O emissions from agricultural lands : a synthesis of simulation approaches. Plant and Soil 309, 169–189.

Choudhury, B. J., 2000. A sensitivity analysis of the radiation use efficiency for gross photosynthesis and net carbon accumulation by wheat. Agr. Forest Meteorol. 101, 217–234.

Choudhury, B. J., 2001. Modeling radiation- and carbon-use efficiencies of maize, sorghum, and rice. Agr. Forest Meteorol. 106, 317–330.

Ciais, P., Reichstein, M., Viovy, N., Granier, A., Ogee, J., Allard, V., Aubinet, M., Buchmann, N., Bernhofer, C., Carrara, A., Chevallier, F., De Noblet, N., Friend, A. D., Friedlingstein, P., Grunwald, T., Heinesch, B., Keronen, P., Knohl, A., Krinner, G., Loustau, D., Manca, G., Matteucci, G., Miglietta, F., Ourcival, J. M., Papale, D., Pilegaard, K., Rambal, S., Seufert, G., Soussana, J. F., Sanz, M. J., Schulze, E. D., Vesala, T., and Valentini, R., 2005. Europe-wide reduction in primary productivity caused by the heat and drought in 2003. Nature 437, 529–533.

Clark, J. S., 2005. Why environmental scientists are becoming bayesians. Ecology Letters 8, 2–14.

Conrad, R., 1996. Soil microorganisms as controllers of atmospheric trace gases (H2, CO, CH4, OCS, N2O, and NO). Microbiol. Rev. 60, 609–640.

Corbeels, M., Hofman, G., and Van Cleemput, O., 1999. Simulation of net N immobilisation and mineralisation in substrate-amended soils by the NCSOIL computer model. Biol. Fert. Soils 28, 422–430.

Dambreville, C., Morvan, T., and Germon, J. C., 2008. N_2O emission in maize-crops fertilized with pig slurry, matured pig manure or ammonium nitrate in Brittany. Agriculture Ecosystems & Environment 123, 201–210.

de Noblet-Ducoudré, N., Gervois, S., Ciais, P., Viovy, N., Brisson, N., Seguin, B., and Perrier, A., 2004. Coupling the soil-vegetation-atmosphere-transfer scheme ORCHIDEE to the agronomy model STICS to study the influence of croplands on the european carbon and water budgets. Agronomie 24, 397–407.

Del Grosso, S. J., Halvorson, A., and Parton, W., 2008. Testing DAYCENT model simulations of corn yields and nitrous oxide emissions in irrigated tillage systems in Colorado. Journal of Environmental Quality 37, 1383–1389.

Del Grosso, S. J., Mosier, A. R., Parton, W. J., and Ojima, D. S., 2005. DAYCENT model analysis of past and contemporary soil N2O and net greenhouse gas flux for major crops in the USA. Soil & Tillage Research 83, 9–24.

Del Grosso, S. J., Ojima, D. S., Parton, W. J., Stehfest, E., Heistemann, M., DeAngelo, B., and Rose, S., 2009. Global scale DAYCENT model analysis of greenhouse gas emissions and mitigation strategies for cropped soils. Global and Planetary Change In Press, Corrected Proof.

Del Grosso, S. J., Parton, W. J., Mosier, A. R., Ojima, D. S., Kulmala, A. E., and Phongpan, S., 2000. General model for N2O and N2 gas emissions from soils due to dentrification. Global Biogeochemical Cycles 14, 1045–1060.

Del Grosso, S. J., Parton, W. J., Mosier, A. R., Walsh, M. K., Ojima, D. S., and Thornton, P. E., 2006. DAYCENT national-scale simulations of nitrous oxide emissions from cropped soils in the united states. Journal of Environmental Quality 35, 1451–1460.

Denmead, O. T. and Raupach, M. R., 1993. Methods for Measuring Atmospheric Gas Transport in Agricultural and Forest Systems. In Rolston, D., Duxbury, J., Harper, L., and Mosier, A., editors, Agricultural Ecosystem Effects on trace Gases and Global Climate Change chapter 2. ASA Special publication 55.

Desjardins, R. L., Smith, W., Grant, B., Campbell, C., and Riznek, R., 2005. Management strategies to sequester carbon in agricultural soils and to mitigate greenhouse gas emissions. Climatic Change 70, 283–297.

Dick, J., Kaya, B., Soutoura, M., Skiba, U., Smith, R., Niang, A., and Tabo, R., 2008. The contribution of agricultural practices to nitrous oxide emissions in semi-arid Mali. Soil Use and Management 24, 292–301.

Ding, W. X., Cai, Y., Cai, Z. C., Yagi, K., and Zheng, X. H., 2007. Nitrous oxide emissions from an intensively cultivated maize-wheat rotation soil in the North China Plain. Science of the Total Environment 373, 501–511.

Dobbie, K. E. and Smith, K. A., 2001. The effects of temperature, water-filled pore space and land use on N_2O emissions from an imperfectly drained gleysol. European Journal of Soil Science 52, 667–673.

Dou, Z. and Fox, R. H., 1995. Using NCSWAP to simulate seasonal nitrogen dynamics in soil and corn. Plant Soil 177, 235–247.

Dufrêne, E., Davi, H., Francois, C., le Maire, G., Le Dantec, V., and Granier, A., 2005. Modelling carbon and water cycles in a beech forest Part I : Model description and uncertainty analysis on modelled NEE. Ecol. Model. 185, 407–436.

Duxbury, J. M. and Bouldin, D. R., 1982. Emission of nitrous oxide from soils. Nature 298, 462–464.

Duxbury, J. M., Harper, L. A., and Mosier, A. R., 1993. Contributions of Agroecosystems to Global Climate Change. In Rolston, D., Duxbury, J., Harper, L., and Mosier, A., editors, Agricultural Ecosystem Effects on trace Gases and Global Climate Change chapter 1. ASA Special publication 55.

Erisman, J. W., Bleeker, A., Galloway, J., and Sutton, M. S., 2007. Reduced nitrogen in ecology and the environment. Environmental Pollution 150, 140–149.

Falge, E., Baldocchi, D., Olson, R., Anthoni, P., Aubinet, M., Bernhofer, C., Burba, G., Ceulemans, R., Clement, R., Dolman, H., Granier, A., Gross, P., Grunwald, T., Hollinger, D., Jensen, N. O., Katul, G., Keronen, P., Kowalski, A., Lai, C. T., Law, B. E., Meyers, T., Moncrieff, H., Moors, E., Munger, J. W., Pilegaard, K., Rannik, U., Rebmann, C., Suyker, A., Tenhunen, J., Tu, K., Verma, S., Vesala, T., Wilson, K., and Wofsy, S., 2001. Gap filling strategies for defensible annual sums of net ecosystem exchange. Agricultural and Forest Meteorology 107, 43–69.

Fisher, B. E. A., Ireland, M. P., Boyland, D. T., and Critten, S. P., 2002. Why use one model ? An approach for encompassing model uncertainty and improving best practice. Environmental Modelling and Assessment 7, 291–299.

Freibauer, A., Rounsevell, M. D. A., Smith, P., and Verhagen, J., 2004. Carbon sequestration in the agricultural soils of Europe. Geoderma 122, 1–23.

Frolking, S. E., Mosier, A. R., Ojima, D. S., Li, C., Parton, W. J., Potter, C. S., Priesack, E., Stenger, R., Haberbosch, C., Dorsch, P., Flessa, H., and Smith, K. A., 1998. Comparison of N_2O emissions from soils at three temperate agricultural sites : simulations of year-round measurements by four models. Nutrient Cycling in Agroecosystems 52, 77–105.

Gabrielle, B., 2006a. L'évaluation environnementale des agrosystèmes : une approche intégrée pour gérer les risques agri-environnementaux. Habilitation à diriger des recherches, Université Pierre et Marie Curie, Paris.

Gabrielle, B., 2006b. Sensitivity and uncertainty analysis of a static denitrification model. In Wallach, D., Makowski, D., and Jones, J. W., editors, Working with dynamic crop models : evaluating, analyzing, parameterizing and using them chapter 14. Elsevier.

Gabrielle, B., Da-Silveira, J., Houot, S., and Francou, C., 2004. Simulating urban waste compost effects on carbon and nitrogen dynamics using a biochemical index. Journal of Environmental Quality 33, 2333–2342.

Gabrielle, B., Da-Silveira, J., Houot, S., and Michelin, J., 2005. Field-scale modelling of carbon and nitrogen dynamics in soils amended with urban waste composts. Agriculture Ecosystems & Environment 110, 289–299.

Gabrielle, B., Denoroy, P., Gosse, G., Justes, E., and Andersen, M. N., 1998a. Development and evaluation of a CERES-type model for winter oilseed rape. Field Crop. Res. 57, 95–111.

Gabrielle, B., Denoroy, P., Gosse, G., Justes, E., and Andersen, M. N., 1998b. A model of leaf area development and senescence for winter oilseed rape. Field Crops Research 57, 209–222.

Gabrielle, B. and Gagnaire, N., 2008. Life-cycle assessment of straw use in bio-ethanol production : A case study based on biophysical modelling. Biomass & Bioenergy 32, 431–441.

Gabrielle, B., Laville, P., Duval, O., Nicoullaud, B., Germon, J. C., and Hénault, C., 2006a. Process-based modeling of nitrous oxide emissions from wheat-cropped soils at the subregional scale. Global Biogeochemical Cycles 20.

Gabrielle, B., Laville, P., Hénault, C., Nicoullaud, B., and Germon, J. C., 2006b. Simulation of nitrous oxide emissions from wheat-cropped soils using CERES. Nutrient Cycling in Agroecosystems 74, 133–146.

Gabrielle, B., Mary, B., Roche, R., Smith, P., and Gosse, G., 2002a. Simulation of carbon and nitrogen dynamics in arable soils : a comparison of approaches. Eur. J. Agron. 18, 107–120.

Gabrielle, B., Menasseri, S., and Houot, S., 1995. Analysis and Field-evaluation of the CERES Models Water-balance Component. Soil Sci. Soc. Am. J. 59, 1403–1412.

Gabrielle, B., Roche, R., Angas, P., Cantero-Martinez, C., Cosentino, L., Mantineo, M., Langensiepen, M., Hénault, C., Laville, P., Nicoullaud, B., and Gosse, G., 2002b. A priori parameterisation of the CERES soil-crop models and tests against several European data sets. Agronomie 22, 119–132.

Gallagher, M. and Doherty, J., 2007. Parameter estimation and uncertainty analysis for a watershed model. Environmental Modelling & Software 22, 1000–1020.

Galloway, J. N. and Cowling, E. B., 2002. Reactive nitrogen and the world : 200 years of change. Ambio 31, 64–71.

Galloway, J. N., Dentener, F. J., Capone, D. G., Boyer, E. W., Howarth, R. W., Seitzinger, S. P., Asner, G. P., Cleveland, C. C., Green, P. A., Holland, E. A., Karl, D. M., Michaels, A. F., Porter, J. H., Townsend, A. R., and Vorosmarty, C. J., 2004. Nitrogen cycles : past, present, and future. Biogeochemistry 70, 153–226.

Galloway, J. N., Townsend, A. R., Erisman, J. W., Bekunda, M., Cai, Z. C., Freney, J. R., Martinelli, L. A., Seitzinger, S. P., and Sutton, M. A., 2008. Transformation of the nitrogen cycle : Recent trends, questions, and potential solutions. Science 320, 889–892.

Garrido, F., Hénault, C., Gaillard, H., Perez, S., and Germon, J. C., 2002. N2O and NO emissions by agricultural soils with low hydraulic potentials. Soil Biology & Biochemistry 34, 559–575.

Gelman, A. and Rubin, D. B., 1992. Inference from iterative simulation using multiple sequences. Statistical Science 7, 457–472.

Gervois, S., Ciais, P., de Noblet-Ducoudré, N., Brisson, N., Vuichard, N., and Viovy, N., 2008. Carbon and water balance of European croplands throughout the 20th century. Global Biogeochem. Cycles 22.

Gijsman, A. J., Hoogenboom, G., Parton, W. J., and Kerridge, P. C., 2002. Modifying DSSAT crop models for low-input agricultural systems using a soil organic matter-residue module from CENTURY. Agronomy Journal 94, 462–474.

Godwin, D. C. and Jone, A. J., 1991. Nitrogen Dynamics in Soil-Plant Systems. In Hanks, J. andRitchie, J. T., editor, Modelin Plant and Soil Systems chapter 13. Agronomy Monograph n°31.

Gosse, G., Cellier, P., Denoroy, P., Gabrielle, B., Laville, P., Leviel, B., Justes, E., Nicolardot, B., Mary, B., Recous, S., Germon, J. C., Hénault, C., and Leech, P. K., 1999. Water, carbon and nitrogen cycling in a rendzina soil cropped with winter oilseed rape : the Chalons Oilseed Rape Database. Agronomie 19, 119–124.

Grace, P. R., Jain, M. C., Harrington, L. W., and Robertson, G. P., 1993. Long-term sustainability of the tropical and subtropical rice and wheat system : An environmental perspective. In Ladha, J. K., Hill, J. E., Duxbury, J. M., Gupta, R. K., and Buresh, R. J., editors, Improving the Productivity and Sustainability of Rice-Wheat System : Issues and Impacts pages 27–43. ASA Special publication 65.

Grant, R. F., Arkebauer, T. J., Dobermann, A., Hubbard, K. G., Schimelfenig, T. T., Suyker, A. E., Verma, S. B., and Walters, D. T., 2007. Net Biome Productivity of Irrigated and Rainfed Maize Soybean Rotations : Modeling vs. Measurements. Agron. J. 99, 1404–1423.

Grant, R. F. and Pattey, E., 2003. Modelling variability in N2O emissions from fertilized agricultural fields. Soil Biology & Biochemistry 35, 225–243.

Guinée, J. B. and Lindeijer, E., 2002. Handbook on life cycle assessment : operational guide to the ISO standards. Kluwer.

Génermont, S. and Cellier, P., 1997. A mechanistic model for estimating ammonia volatilization from slurry applied to bare soil. Agricultural and Forest Meteorology 88, 145–167.

Haario, H., Saksman, E., and Tamminen, J., 2001. An adaptive Metropolis algorithm. Bernoulli 7, 223–242.

Hadas, A., Feigenbaum, S., Sofer, M., Molina, J. A. E., and Clapp, C. E., 1993. Decomposition of nitrogen-15-labeled wheat and cellulose in soil - modeling tracer dynamics. Soil Sci. Soc. Am. J. 57, 996–1001.

Halberg, N., van der, H. M. G., Basset-Mens, C., Dalgaard, R., and de Boer, I. J. M., 2005. Environmental assessment tools for the evaluation and improvement of european livestock production systems. Livestock Production Science 96, 33–50.

Harmon, R. and Challenor, P., 1997. A Markov chain Monte Carlo method for estimation and assimilation into models. Ecological Modelling 101, 41–59.

Heinen, M., 2006. Application of a widely used denitrification model to Dutch data sets. Geoderma 133, 464–473.

Henriksen, T. M. and Breland, T. A., 1999. Nitrogen availability effects on carbon mineralization, fungal and bacterial growth, and enzyme activities during decomposition of wheat straw in soil. Soil Biol. Biochem. 31, 1121–1134.

Hong, B. G., Strawderman, R. L., Swaney, D. P., and Weinstein, D. A., 2005. Bayesian estimation of input parameters of a nitrogen cycle model applied to a forested reference watershed, Hubbard Brook Watershed Six. Water Resources Research 41.

Huang, Y., Yu, Y. Q., Zhang, W., Sun, W. J., Liu, S. L., Jiang, J., Wu, J. S., Yu, W., Wang, Y., and Yang, Z. F., 2009. Agro-C : A biogeophysical model for simulating the carbon budget of agroecosystems. Agr. Forest Meteorol. 149, 106–129.

Hui, D. F., Luo, Y. Q., Cheng, W. X., Coleman, J. S., Johnson, D. W., and Sims, D. A., 2001. Canopy radiation- and water-use efficiencies as affected by elevated [CO2]. Glob. Change Biol. 7, 75–91.

Hutchinson, G. L. and Davidson, E. A., 1993. Processes for Production and Consumption of Gaseous Nitrogen Oxides in Soil. In Rolston, D., Duxbury, J., Harper, L., and Mosier, A., editors, Agricultural Ecosystem Effects on trace Gases and Global Climate Change chapter 5. ASA Special publication 55.

Hénault, C., Bizouard, F., Laville, P., Gabrielle, B., Nicoullaud, B., Germon, J. C., and Cellier, P., 2005a. Predicting in situ soil N2O emission using NOE algorithm and soil database. Global Change Biology 11, 115–127.

Hénault, C. and Germon, J. C., 2000. NEMIS, a predictive model of denitrification on the field scale. European Journal of Soil Science 51, 257–270.

Hénault, C., Roger, P., Laville, P., Gabrielle, B., and Cellier, P., 2005b. Les émissions par les sols de gaz à effet de serre CH4 et N2O. In Girard, M. C., Walter, C., Remy, S. C., Berthelin, J., and Morel, J. L., editors, Sols et Environnement chapter 14, pages 326–344. Dunod.

IPCC, 2000. Land use, land-use change, and forestry : a special report of the Intergovernmental Panel on Climate Change. Cambridge University Press, Cambridge.

IPCC, 2006. 2006 IPCC Guidelines for National Greenhouse Gas Inventories, Prepared by the National Greenhouse Gas Inventories Programme, Eggleston H.S., Buendia L., Miwa K., Ngara T. and Tanabe K. (eds). Published : IGES, Japan.

IPCC, 2007. Climate Change 2007 - The Physical Science Basis : Working Group I Contribution to the Fourth Assessment Report of the IPCC (Climate Change 2007). Cambridge University Press.

Jambert, C., Serca, D., and Delmas, R., 1997. Quantification of N-losses as NH_3, NO, N_2O and N_2 from fertilized maize fields in Southwestern France. Nutrient Cycling in Agroecosystems 48, 91–104.

Johnson, J. M. F., Franzluebbers, A. J., Weyers, S. L., and Reicosky, D. C., 2007. Agricultural opportunities to mitigate greenhouse gas emissions. Environ. Pollut. 150, 107–124.

Johnsson, H., Klemedtsson, L., Nilsson, A., Bo, H., and Svensson, B., 2004. Simulation of field scale denitrification losses from soils under grass ley and barley. Plant and Soil 138, 287–302.

Jones, C. A. and Kiniry, J. R., 1986. CERES-N Maize : a simulation model of maize growth and development. Texas A&M University Press, College Statio, Temple, TX.

Jones, S. K., Rees, R. M., Skiba, U. M., and Ball, B. C., 2005. Greenhouse gas emissions from a managed grassland. Global and Planetary Change 47, 201–211.

Jungkunst, H. F., Freibauer, A., Neufeldt, H., and Bareth, G., 2006. Nitrous oxide emissions from agricultural land use in Germany - a synthesis of available annual field data. Journal of Plant Nutrition and Soil Science-zeitschrift Fur Pflanzenernahrung Und Bodenkunde 169, 341–351.

Justes, E., Denoroy, P., Gabrielle, B., and Gosse, G., 2000. Effect of crop nitrogen status and temperature on the radiation use efficiency of winter oilseed rape. Eur. J. Agron. 13, 165–177.

Kaiser, E. A. and Ruser, R., 2000. Nitrous oxide emissions from arable soils in Germany - An evaluation of six long-term field experiments. Journal of Plant Nutrition and Soil Science-zeitschrift Fur Pflanzenernahrung Und Bodenkunde 163, 249–259.

Kass, R. E. and Raftery, A. E., 1995. Bayes factors. Journal of the American Statistical Association 90, 773–795.

Keppler, F., Hamilton, J. T. G., Brass, M., and Rockmann, T., 2006. Methane emissions from terrestrial plants under aerobic conditions. Nature 439, 187–191.

Khalil, K., Mary, B., and Renault, P., 2004. Nitrous oxide production by nitrification and denitrification in soil aggregates as affected by O_2 concentration. Soil Biology & Biochemistry 36, 687–699.

Kim, S. and Dale, B. E., 2005. Environmental aspects of ethanol derived from no-tilled corn grain : nonrenewable energy consumption and greenhouse gas emissions. Biomass & Bioenergy 28, 475–489.

Klemedtsson, L., Jansson, P.-E., Gustafsson, D., Karlberg, L., Weslien, P., von Arnold, K., Ernfors, M., Langvall, O., and Lindroth, A., 2007. Bayesian calibration method used to elucidate carbon turnover in forest on drained organic soil. Biogeochemistry.

Knowles, R., 1993. Methane : Processes of Production and Consumption. In Rolston, D., Duxbury, J., Harper, L., and Mosier, A., editors, Agricultural Ecosystem Effects on trace Gases and Global Climate Change chapter 10. ASA Special publication 55.

Krinner, G., Viovy, N., de Noblet-Ducoudré, N., Ogee, J., Polcher, J., Friedlingstein, P., Ciais, P., Sitch, S., and Prentice, I. C., 2005. A dynamic global vegetation model for studies of the coupled atmosphere-biosphere system. Global Biogeochemical Cycles 19.

Kurbatova, J., Li, C., Varlagin, A., Xiao, X., and Vygodskaya, N., 2008. Modeling carbon dynamics in two adjacent spruce forests with different soil conditions in Russia. Biogeosciences 5, 969–980.

Lamboni, M., Makowski, D., Lehuger, S., Gabrielle, B., and Monod, H., 2009. Multivariate global sensitivity analysis for dynamic crop model. Soumis à Field Crop Research.

Langensiepen, M., Hanus, H., Schoop, P., and Grasle, W., 2008. Validating CERES-wheat under North-German environmental conditions. Agricultural Systems 97, 34–47.

Larssen, T., Huseby, R. B., Cosby, B. J., Host, G., Hogasen, T., and Aldrin, M., 2006. Forecasting acidification effects using a Bayesian calibration and uncertainty propagation approach. Environmental Science & Technology 40, 7841–7847.

Laville, P., Hénault, C., Gabrielle, B., and Serca, D., 2005. Measurement and modelling of NO fluxes on maize and wheat crops during their growing seasons : effect of crop management. Nutrient Cycling in Agroecosystems 72, 159–171.

Laville, P., Lehuger, S., Fanucci, O., Génermont, S., Loubet, B., and Cellier, P., 2009. Continuous monitoring of nitric and nitrous oxide emissions over a barley-maize rotation with automatic chambers. NitroEurope IP 4th Annual Meeting, 26th-28th January 2009, Gothenburg, Sweden, (Poster).

Lehuger, S., Gabrielle, B., and Gagnaire, N., 2009a. Environmental impact of the substitution of imported soybean meal with locally-produced rapeseed meal in dairy cow feed. Journal of Cleaner Production 17, 616 – 624.

Lehuger, S., Gabrielle, B., Larmanou, E., Laville, P., Cellier, P., and Loubet, B., 2007. Predicting the global warming potential of agro-ecosystems. Biogeosciences Discussions 4, 1059–1092.

Lehuger, S., Gabrielle, B., and van Oijen, M., 2008. Bayesian calibration of CERES-EGC - BC in practice using the R software. Technical report for NitroEurope-IP.

Lehuger, S., Gabrielle, B., Van Oijen, M., Makowski, D., Germon, J. C., Morvan, T., and Hénault, C., 2009b. Bayesian calibration of the nitrous oxide emission module of an agro-ecosystem model. agriculture, ecosystem and environment. Agr. Ecosys. Environ. In Press.

Leip, A., Marchi, G., Koeble, R., Kempen, M., Britz, W., and Li, C., 2008. Linking an economic model for European agriculture with a mechanistic model to estimate nitrogen and carbon losses from arable soils in Europe. Biogeosciences 5, 73–94.

Lengnick, L. L. and Fox, R. H., 1994. Simulation by Ncswap of Seasonal Nitrogen Dynamics in Corn .2. Corn Growth and Yield. Agron. J. 86, 176–182.

Li, C., Zhuang, Y., Cao, M., Crill, P., Dai, Z., Frolking, S., Moore III, B., Salas, W., Song, W., and Wang, X., 2001. Comparing a process-based agro-ecosystem model to the IPCC methodology for developing a national inventory of N_2O emissions from arable lands in China. Nutrient Cycling in Agroecosystems 60, 159–175.

Li, C. S., 2000. Modeling trace gas emissions from agricultural ecosystems. Nutrient Cycling in Agroecosystems 58, 259–276.

Li, C. S., Frolking, S., and Butterbach-Bahl, K., 2005a. Carbon sequestration in arable soils is likely to increase nitrous oxide emissions, offsetting reductions in climate radiative forcing. Climatic Change 72, 321–338.

Li, C. S., Frolking, S., and Frolking, T. A., 1992. A Model of Nitrous-oxide Evolution From Soil Driven by Rainfall Events .1. Model Structure and Sensitivity. Journal of Geophysical Research-atmospheres 97, 9759–9776.

Li, Y., Chen, D. L., Zhang, Y. M., Edis, R., and Ding, H., 2005b. Comparison of three modeling approaches for simulating denitrification and nitrous oxide emissions from loam-textured arable soils. Global Biogeochemical Cycles 19.

Lindquist, J. L., Arkebauer, T. J., Walters, D. T., Cassman, K. G., and Dobermann, A., 2005. Maize radiation use efficiency under optimal growth conditions. Agron. J. 97, 72–78.

Linn, D. M. and Doran, J. W., 1984. Effect of Water-Filled Pore Space on Carbon Dioxide and Nitrous Oxide Production in Tilled and Nontilled Soils. Soil Sci Soc Am J 48, 1267–1272.

Lokupitiya, E. and Paustian, K., 2006. Agricultural soil greenhouse gas emissions : A review of National Inventory Methods. Journal of Environmental Quality 35, 1413–1427.

Maag, M. and Vinther, F. P., 1996. Nitrous oxide emission by nitrification and denitrification in different soil types and at different soil moisture contents and temperatures. Applied Soil Ecology 4, 5–14.

Maag, M. and Vinther, F. P., 1999. Effect of temperature and water on gaseous emissions from soils treated with animal slurry. Soil Science Society of America Journal 63, 858–865.

Makowski, D., Hillier, J., Wallach, D., Andrieu, B., and Jeuffroy, M. H., 2006. Parameter estimation for crop models. In Wallach, D., Makowski, D., and Jones, J. W., editors, Working with dynamic crop models : evaluating, analyzing, parameterizing and using them chapter 4. Elsevier.

Makowski, D. and Jeuffroy, M. H., 2002a. Estimation des paramètres des modèles de culture. In Ecole-Chercheurs - Pour une bonne utilisation des modèles de culture chapter 4. INRA.

Makowski, D. and Jeuffroy, M. H., 2002b. Évaluation d'un modèle. In Ecole-Chercheurs - Pour une bonne utilisation des modèles de culture chapter 2. INRA.

Makowski, D., Wallach, D., and Tremblay, M., 2002. Using a Bayesian approach to parameter estimation ; comparison of the GLUE and MCMC methods. Agronomie 22, 191–203.

McSwiney, C. P. and Robertson, G. P., 2005. Nonlinear response of N2O flux to incremental fertilizer addition in a continuous maize (Zea mays L.) cropping system. Global Change Biology 11, 1712–1719.

Metropolis, N., Rosenbluth, A. W., Rosenbluth, M. N., Teller, A. H., and Teller, E., 1953. Equation of state calculations by fast computing machines. The Journal of Chemical Physics 21, 1087–1092.

Molina, J. A. E., Clapp, C. E., Schaffer, M. J., Chichester, F. W., and Larson, W., 1983. NCSOIL, a model of nitrogen and carbon transformations in doil : description, calibration and behavuoir. Soil Sci. Soc. Am. J. 45, 85–91.

Molina, J. A. E., Crocker, G. J., Grace, P. R., Klir, J., Korschens, M., Poulton, P. R., and Richter, D. D., 1997. Simulating trends in soil organic carbon in long-term experiments using the NCSOIL, and NCSWAP models. Geoderma 81, 91–107.

Monod, H., Naud, C., and Makowski, D., 2006. Uncertainty and sensitivity analysis for crop models. In Wallach, D., Makowski, D., and Jones, J. W., editors, Working with dynamic crop models : evaluating, analyzing, parameterizing and using them chapter 3. Elsevier.

Mosier, A. R., Duxbury, J. M., Freney, J. R., Heinemeyer, O., Minami, K., and Johnson, D. E., 1998. Mitigating agricultural emissions of methane. Climatic Change 40, 39–80.

Mosier, A. R., Halvorson, A. D., Peterson, G. A., Robertson, G. P., and Sherrod, L., 2005. Measurement of net global warming potential in three agroecosystems. Nutrient Cycling in Agroecosystems 72, 67–76.

Moureaux, C., Debacq, A., Bodson, B., Heinesch, B., and Aubinet, M., 2006. Annual net ecosystem carbon exchange by a sugar beet crop. Agr. Forest Meteorol. 139, 25–39.

Naud, C., Makowski, D., and Jeuffroy, M. H., 2007. Application of an interacting particle filter to improve nitrogen nutrition index predictions for winter wheat. Ecological Modelling 207, 251–263.

Nemecek, T., Heil, A., Huguenin, O., Erzinger, S., Blaser, S., Dux, D., and Zimmerman, A., 2003. Life Cycle Inventories of Production Systems. Final report Ecoinvent 2000, No 15. FAL Reckenholz, FAT Tanikon, Swiss Centre For Life Cycle Inventories, Dubendorf, CH.

Nicolardot, B. and Molina, J. A. E., 1994. C and N Fluxes Between Pools of Soil Organic-matter - Model Calibration With Long-term Field Experimental-data. Soil Biol. Biochem. 26, 245–251.

Nicolardot, B., Molina, J. A. E., and Allard, M. R., 1994. C and n fluxes between pools of soil organic-matter - model calibration with long-term incubation data. Soil Biol. Biochem. 26, 235–243.

Nisbet, R., Fisher, R., Nimmo, R., Bendall, D., Crill, P., Gallego-Sala, A., Hornibrook, E., López-Juez, E., Lowry, D., Nisbet, P., Shuckburgh, E., Sriskantharajah, S., Howe, C., and Nisbet, E., 2009. Emission of methane from plants. Proceedings of the Royal Society B : Biological Sciences 276, 1347–1354.

Oakley, J. E. and O'Hagan, A., 2007. Uncertainty in prior elicitations : a nonparametric approach. Biometrika 94, 427–441.

Ojima, D. S., Valentine, D. W., Mosier, A. R., Parton, W. J., and Schimel, D. S., 1993. Effect of Land-use Change on Methane Oxidation in Temperate Forest and Grassland Soils. Chemosphere 26, 675–685.

Papale, D., Reichstein, M., Aubinet, M., Canfora, E., Bernhofer, C., Kutsch, W., Longdoz, B., Rambal, S., Valentini, R., Vesala, T., and Yakir, D., 2006. Towards a standardized processing of net ecosystem exchange measured with eddy covariance technique : algorithms and uncertainty estimation. Biogeosciences 3, 571–583.

Pape, L., Ammann, C., Nyfeler-Brunner, A., Spirig, C., Hens, K., and Meixner, F. X., 2009. An automated dynamic chamber system for surface exchange measurement of non-reactive and reactive trace gases of grassland ecosystems. Biogeosciences 6, 405–429.

Parton, W. J., Holland, E. A., Del Grosso, S. J., Hartman, M. D., Martin, R. E., Mosier, A. R., Ojima, D. S., and Schimel, D. S., 2001. Generalized model for NOx and N2O emissions from soils. Journal of Geophysical Research-atmospheres 106, 17403–17419.

Parton, W. J., Mosier, A. R., Ojima, D. S., Valentine, D. W., Schimel, D. S., Weier, K., and Kulmala, A. E., 1996. Generalized model for N2 and N2O production from nitrification and denitrification. Global Biogeochemical Cycles 10, 401–412.

Pathak, H., Li, C., and Wassmann, R., 2005. Greenhouse gas emissions from Indian rice fields : calibration and upscaling using the DNDC model. Biogeosciences 2, 113–123.

Pattey, E., Edwards, G. C., Desjardins, R. L., Pennock, D. J., Smith, W., Grant, B., and MacPherson, J. I., 2007. Tools for quantifying N_2O emissions from agroecosystems. Agricultural and Forest Meteorology 142, 103–119.

Pihlatie, M., Syvasalo, E., Simojoki, A., Esala, M., and Regina, K., 2004. Contribution of nitrification and denitrification to N_2O production in peat, clay and loamy sand soils under different soil moisture conditions. Nutrient Cycling in Agroecosystems 70, 135–141.

Pilegaard, K., Hummelshoj, P., Jensen, N. O., and Chen, Z., 2001. Two years of continuous CO2 eddy-flux measurements over a danish beech forest. Agr. Forest Meteorol. 107, 29–41.

Plummer, M., Best, N., Cowles, K., and Vines, K., 2006. CODA : Convergence diagnosis and output analysis for MCMC. R News 6, 7–11.

Prieur, A., Bouvart, F., Gabrielle, B., and Lehuger, S., 2008. Well to wheels analysis of biofuels vs. conventional fossil fuels : a proposal for greenhouse gases and energy savings accounting in the French context. SAE Transactions Journal of Fuels and Lubricants In Press.

R Development Core Team, 2008. R : A Language and Environment for Statistical Computing. R Foundation for Statistical Computing Vienna, Austria. ISBN 3-900051-07-0.

Rabl, A., Benoist, A., Dron, D., Peuportier, B., Spadaro, J. V., and Zoughaib, A., 2007. How to account for CO_2 emissions from biomass in an LCA. Int. J. LCA. 12, 281–281.

Renault, P., Sierra, J., and Stengel, P., 1994. Oxygen-transport and anaerobiosis in aggregated soils - contribution to the study of denitrification. Agronomie 14, 395–409.

Rezzoug, W., Gabrielle, B., Suleiman, A., and Benabdeli, K., 2008. Application and evaluation of the DSSAT-wheat in the Tiaret region of Algeria. African Journal of Agricultural Research 3, 284–296.

Ricciuto, D. M., Butler, M. P., Davis, K. J., Cook, B. D., Bakwin, P. S., Andrews, A., and Teclaw, R. M., 2008. Causes of interannual variability in ecosystem-atmosphere CO_2 exchange in a northern Wisconsin forest using a Bayesian model calibration. Agricultural and Forest Meteorology 148, 309–327.

Robertson, G. P. and Grace, P. R., 2004. Greenhouse gas fluxes in tropical and temperate agriculture : The need for a full-cost accounting of global warming potentials. Environment, Development and Sustainability 6, 51–63.

Robertson, G. P., Paul, E. A., and Harwood, R. R., 2000. Greenhouse gases in intensive agriculture : Contributions of individual gases to the radiative forcing of the atmosphere. Science 289, 1922–1925.

Rochette, P. and Eriksen-Hamel, N. S., 2008. Chamber measurements of soil nitrous oxide flux : Are absolute values reliable ? Soil Science Society of America Journal 72, 331–342.

Rochette, P. and Janzen, H. H., 2005. Towards a revised coefficient for estimating N_2O emissions from legumes. Nutrient Cycling in Agroecosystems 73, 171–179.

Roelandt, C., Dendoncker, N., Rounsevell, M., Perrin, D., and Van Wesemael, B., 2007. Projecting future N_2O emissions from agricultural soils in Belgium. Global Change Biology 13, 18–27.

Roelandt, C., van Wesemael, B., and Rounsevell, M., 2005. Estimating annual N2O emissions from agricultural soils in temperate climates. Global Change Biology 11, 1701–1711.

Rojstaczer, S., Sterling, S. M., and Moore, N. J., 2001. Human appropriation of photosynthesis products. Science 294, 2549–2552.

Rolland, M. N., 2008. Modélisation biophysique des émissions de NO par les sols agricoles, spatialisation et impact sur la chimie troposphérique à l'échelle régionale. PhD thesis Université Pierre et Marie Curie Paris.

Rolland, M. N., Gabrielle, B., Laville, P., Serca, D., Cortinovis, J., Larmanou, E., Lehuger, S., and Cellier, P., 2008. Modeling of nitric oxide emissions from temperate agricultural soils. Nutrient Cycling in Agroecosystems 80, 75–93.

Sinclair, T. R. and Muchow, R. C., 1999. Radiation use efficiency. Adv. Agron. 65, 215–265.

Six, J., Ogle, S. M., Breidt, F. J., Conant, R. T., Mosier, A. R., and Paustian, K., 2004. The potential to mitigate global warming with no-tillage management is only realized when practised in the long term. Global Change Biology 10, 155–160.

Skopp, J., Jawson, M. D., and Doran, J. W., 1990. Steady-State Aerobic Microbial Activity as a Function of Soil Water Content. Soil Sci Soc Am J 54, 1619–1625.

Smith, J., Smith, P., and Addiscott, T., 1996. Quantitative methods to evaluate and compare soil organic matter (SOM) models. In Powlson, D., Smith, P., and Smith, J. E., editors, Evaluation of soil organic matter models using existing long-term datasets volume 38 of *1* pages 183–202. Springer-Verlag, Heidelberg.

Smith, K. A., 1997. The potential for feedback effects induced by global warming on emissions of nitrous oxide by soils. Global Change Biology 3, 327–338.

Smith, K. A., Thomson, P. E., Clayton, H., McTaggart, I. P., and Conen, F., 1998. Effects of temperature, water content and nitrogen fertilisation on emissions of nitrous oxide by soils. Atmospheric Environment 32, 3301–3309.

Smith, P., 2008. Land use change and soil organic carbon dynamics. Nutrient Cycling in Agroecosystems 81, 169–178.

Smith, P., Goulding, K. W., Smith, K. A., Powlson, D. S., Smith, J. U., Falloon, P., and Coleman, K., 2001. Enhancing the carbon sink in European agricultural soils : including trace gas fluxes in estimates of carbon mitigation potential. Nutrient Cycling in Agroecosystems 60, 237–252.

Smith, P., Martino, D., Cai, Z., Gwary, D., Janzen, H., Kumar, P., McCarl, B., Ogle, S., O'Mara, F., Rice, C., Scholes, B., Sirotenko, O., Howden, M., McAllister, T., Pan, G., Romanenkov, V., Schneider, U., Towprayoon, S., Wattenbach, M., and Smith, J., 2008a. Greenhouse gas mitigation in agriculture. Philosophical Transactions of the Royal Society B-biological Sciences 363, 789–813.

Smith, P., Martino, D., Cai, Z., Gwary, D., Janzen, H., Kumar, P., McCarl, B., Ogle, S., O'Mara, F., Rice, C., Scholes, B., and Sirotenko, O., 2007. Agriculture. In Climate Change 2007 : Mitigation. Contribution of Working Group III to the Fourth Assessment Report of the Intergovernmental Panel on Climate Change, Metz, B. and Davidson, O. R. and Bosch, P.

R. and Dave, R. and Meyer, L. A.[eds.]. Cambridge University Press, Cambridge, United Kingdom and New York, NY, USA.

Smith, P., Nabuurs, G., Janssens, I. A., Reis, S., Marland, G., Soussana, J. F., Christensen, T., Heath, L., Apps, M., Alexeyev, V., Fang, J. Y., Gattuso, J. P., Guerschman, J. P., Huang, Y., Jobbagy, E., Murdiyarso, D., Ni, J., Nobre, A., Peng, C. H., Walcroft, A., Wang, S. Q., Pan, Y., and Zhou, G. S., 2008b. Sectoral approaches to improve regional carbon budgets. Climatic Change 88, 209–249.

Soegaard, H., Jensen, N. O., Boegh, E., Hasager, C. B., Schelde, K., and Thomsen, A., 2003. Carbon dioxide exchange over agricultural landscape using eddy correlation and footprint modelling. Agr. Forest Meteorol. 114, 153–173.

Soussana, J. F., Fuhrer, J., Jones, M., and Van Amstel, A., 2007. The greenhouse gas balance of grasslands in Europe. Agriculture Ecosystems & Environment 121, 1–4.

Stanford, G., Dzienia, S., and Vander Pol, R. A., 1975. Effect of Temperature on Denitrification Rate in Soils. Soil Sci Soc Am J 39, 867–870.

Stehfest, E. and Bouwman, L., 2006. N2O and NO emission from agricultural fields and soils under natural vegetation : summarizing available measurement data and modeling of global annual emissions. Nutrient Cycling in Agroecosystems 74, 207–228.

Sutton, M. A., Nemitz, E., Erisman, J. W., Beier, C., Bahl, K. B., Cellier, P., de Vries, W., Cotrufo, F., Skiba, U., Di Marco, C., Jones, S., Laville, P., Soussana, J. F., Loubet, B., Twigg, M., Famulari, D., Whitehead, J., Gallagher, M. W., Neftel, A., Flechard, C. R., Herrmann, B., Calanca, P. L., Schjoerring, J. K., Daemmgen, U., Horvath, L., Tang, Y. S., Emmett, B. A., Tietema, A., Penuelas, J., Kesik, M., Brueggemann, N., Pilegaard, K., Vesala, T., Campbell, C. L., Olesen, J. E., Dragosits, U., Theobald, M. R., Levy, P., Mobbs, D. C., Milne, R., Viovy, N., Vuichard, N., Smith, J. U., Smith, P., Bergamaschi, P., Fowler, D., and Reis, S., 2007. Challenges in quantifying biosphere-atmosphere exchange of nitrogen species. Environmental Pollution 150, 125–139.

Svensson, M., Jansson, P. E., Gustafsson, D., Kleja, D. B., Langvall, O., and Lindroth, A., 2008. Bayesian calibration of a model describing carbon, water and heat fluxes for a Swedish boreal forest stand. Ecological Modelling 213, 331–344.

Thomassen, M. A., van Calker, K. J., Smits, M. C. J., Iepema, G. L., and de Boer, I. J. M., 2008. Life cycle assessment of conventional and organic milk production in the Netherlands. Agricultural Systems 96, 95–107.

Tonitto, C., David, M. B., Li, C. S., and Drinkwater, L. E., 2007. Application of the DNDC model to tile-drained Illinois agroecosystems : model comparison of conventional and diversified rotations. Nutrient Cycling in Agroecosystems 78, 65–81.

Trinsoutrot, I., Nicolardot, B., Justes, E., and Recous, S., 2000. Decomposition in the field of residues of oilseed rape grown at two levels of nitrogen fertilisation. Effects on the dynamics of soil mineral nitrogen between successive crops. Nutrient Cycling in Agroecosystems 56, 125–137.

Turner, D. P., Ritts, W. D., Law, B. E., Cohen, W. B., Yang, Z., Hudiburg, T., Campbell, J. L., and Duane, M., 2007. Scaling net ecosystem production and net biome production over a heterogeneous region in the western United States. Biogeosciences 4, 597–612.

Van Oijen, M., Rougier, J., and Smith, R., 2005. Bayesian calibration of process-based forest models : bridging the gap between models and data. Tree Physiology 25, 915–927.

Veenendaal, E. M., Kolle, O., Leffelaar, P. A., Schrier-Uijl, A. P., Van Huissteden, J., Van Walsem, J., Möller, F., and Berendse, F., 2007. CO_2 exchange and carbon balance in two grassland sites on eutrophic drained peat soils. Biogeosciences 4, 1027–1040.

Vergé, X. P. C., De Kimpe, C., and Desjardins, R. L., 2007. Agricultural production, greenhouse gas emissions and mitigation potential. Agricultural and Forest Meteorology 142, 255–269.

Verma, S. B., Dobermann, A., Cassman, K. G., Walters, D. T., Knops, J. M., Arkebauer, T. J., Suyker, A. E., Burba, G. G., Amos, B., Yang, H. S., Ginting, D., Hubbard, K. G., Gitelson, A. A., and Walter-Shea, E. A., 2005. Annual carbon dioxide exchange in irrigated and rainfed maize-based agroecosystems. Agr. Forest Meteorol. 131, 77–96.

Villalobos, F. J., Hall, A. J., Ritchie, J. T., and Orgaz, F., 1996. OILCROP-SUN : A development, growth, and yield model of the sunflower crop. Agron. J. 88, 403–415.

Wallach, D., 2006. Evaluating crop models. In Wallach, D., Makowski, D., and Jones, J. W., editors, Working with dynamic crop models : evaluating, analyzing, parameterizing and using them chapter 2. Elsevier.

Wang, J., Yu, Q., and Lee, X., 2007. Simulation of crop growth and energy and carbon dioxide fluxes at different time steps from hourly to daily. Hydrol. Process 21, 2474–2492.

Wang, Q. X., Masataka, W., and Zhu, O. Y., 2005. Simulation of water and carbon fluxes using BIOME-BGC model over crops in China. Agr. Forest Meteorol. 131, 209–224.

West, T. O. and Marland, G., 2002. Net carbon flux from agricultural ecosystems : methodology for full carbon cycle analyses. Environmental Pollution 116, 439–444.

Williams, M., Richardson, A. D., Reichstein, M., Stoy, P. C., Peylin, P., Verbeeck, H., Carvalhais, N., Jung, M., Hollinger, D. Y., Kattge, J., Leuning, R., Luo, Y., Tomelleri, E., Trudinger, C., and Wang, Y.-P., 2009. Improving land surface models with FLUXNET data. Biogeosciences Discussions 6, 2785–2835.

Wrage, N., Velthof, G. L., van Beusichem, M. L., and Oenema, O., 2001. Role of nitrifier denitrification in the production of nitrous oxide. Soil Biology & Biochemistry 33, 1723–1732.

Xiong, W., Matthews, R., Holman, I., Lin, E., and Xu, Y. L., 2007. Modelling China's potential maize production at regional scale under climate change. Climatic Change 85, 433–451.

Yao, Z., Zheng, X., Xie, B., Liu, C., Mei, B., Dong, H., Butterbach-Bahl, K., and Zhu, J., 2008. Comparison of manual and automated chambers for field measurements of N2O, CH4, CO2 fluxes from cultivated land. Atmospheric Environment In Press, Corrected Proof.

Zhang, Y., Li, C., Zhou, X., and Moore, B., 2002. A simulation model linking crop growth and soil biogeochemistry for sustainable agriculture. Ecological Modelling 151, 75–108.

Liste des tableaux

Table des figures

Annexe A

Modélisation des émissions de protoxyde d'azote d'origine agricole à l'échelle de la région Île-de-France

F. Chaumartin*, S. Lehuger, B. Gabrielle

*E-mail : fchaumartin@grignon.inra.fr ;
Institut National de la Recherche Agronomique ;
UMR 1091, INRA-AgroParisTech Environnement et Grandes Cultures
78850 Thiverval-Grignon, France
Fax : (+33) 1 30 81 55 63 ;
Tél. : (+33) 1 30 81 55 24

Les sols agricoles constituent une source importante de protoxyde d'azote (N_2O) dans l'atmosphère. En France, l'agriculture contribue à 75 % des émissions nationales, mais ces estimations sont entachées d'une grande d'incertitude. L'UMR INRA-AgroParisTech Environnement et Grandes Cultures doit produire des cartes (ou cadastres) d'émissions à haute résolution spatiale et temporelle, à l'aide de modèles d'agro-écosystème et de bases de données géo-référencées, dans le cadre du projet de recherche N-TWO-O.

La région d'étude est l'Île-de-France qui a une superficie de 12 072 km^2 et une surface agricole utile de 580 000 ha. Les simulations ont été effectuées pour une période de 14 mois grâce à l'extrapolation du modèle CERES-EGC de l'échelle parcellaire à l'échelle régionale.

Les premiers résultats ont permis de tester le modèle CERES-EGC en analysant différents scénarios de paramétrisation et de sources de données d'entrées (sols, météorologie). Ils montrent que les émissions régionales sont sensibles aux types de sols, aux données météorologiques spatialisées et aux choix des paramètres.

A.1 Introduction

Les sols agricoles constituent une source importante de protoxyde d'azote (N_2O) dans l'atmosphère. Ce composé azoté résultant des processus microbiologiques de nitrification-dénitrification dans les sols est un puissant gaz à effet de serre (GES) avec un pouvoir de réchauffement global équivalent à 300 fois celui du CO_2. En France, l'agriculture est responsable de 75 % des émissions totales de N_2O, mais avec une large fourchette d'incertitude. D'après l'inventaire des principaux GES en Île-de-France réalisé par Airparif (2005), les émissions de N_2O toutes sources confondues, pour la région en 2000 sont de 10 565 t N-N_2O an^{-1}, et l'agriculture contribue à 25 % des émissions, soit environ 2700 t N-N_2O an^{-1}. Ces émissions pourraient être quantifiées plus précisément par l'utilisation conjointe de modèles biophysiques fonctionnant à l'échelle de la parcelle agricole et de systèmes d'information géographiques.
Dans le cadre du projet de recherche N-TWO-O (décrit dans l'encadré ci-contre), l'UMR INRA AgroParisTech Environnement et Grandes Cultures doit produire des cartes (ou cadastres) d'émissions à haute résolution spatiale et temporelle pour les sources agricoles de N_2O en Île-de-France, à l'aide de modèles d'agro-écosystèmes et de bases de données géo-référencées.
Deux méthodologies sont envisageables pour le développement de tels cadastres :

- La première, de type «top-down», consiste à considérer la donnée statistique générale pour calculer les émissions nationales ou régionales et à utiliser des clés de répartition ou de désagrégation pour générer des données nécessaires au calcul à une échelle plus fine (département, canton ou maillage). Méthode globalement à faible coût en temps, et permettant de nombreux raccourcis méthodologiques et techniques ;
- La seconde, de type «bottom-up», se base sur une collecte de données du niveau le plus fin vers le niveau le plus agrégé en les rassemblant/redistribuant, privilégiant les sources de données détaillées aux clés de répartition. Approche plus coûteuse en temps et plus problématique car les données et la méthodologie doivent être adaptées l'une à l'autre pour former un modèle cohérent d'estimation des émissions.

L'objectif final de ce projet est de confronter des inventaires d'émissions de N_2O à des estimations obtenues par combinaison de modèles atmosphériques et de mesures intégratrices de N_2O pour la région. La zone d'étude couvre une surface de 12 072 km^2, et la période de simulation se déroule de novembre 2000 à décembre 2001, ce qui comprend les périodes de cultures et d'inter-cultures.

A.2 Matériel et méthodes

A.2.1 Méthodologie générale

La méthode utilisée dans notre cas est de type «bottom-up», telle que mise en place par Rolland (2008) pour les émissions d'oxyde nitrique (NO), et qui vise à conserver le niveau de précision des informations locales disponibles afin de construire un cadastre d'émission à haute résolution.
Les simulations effectuées avec le modèle CERES-EGC sont couplées aux méthodes de système

d'information géographique (SIG) pour produire des inventaires spatialisés d'émissions de N_2O, en fonction des données locales d'itinéraires techniques, de météo et de types de sol. CERES-EGC permet de calculer la dynamique temporelle des émissions de N_2O pour les principales cultures de la région. Pour réaliser ces calculs, une **base de données des entrées** a été constituée avec le SIG (Rolland, 2008). Celle-ci regroupe les itinéraires techniques des cultures, les types de sols et les variables météorologiques pour la région.
Les variables de sortie comme les émissions de N_2O, la température, l'humidité, la teneur en ammonium dans le sol et les rendements sont stockées dans la **base de données des sorties**. Cette base finale peut être lue sous le SIG, permettant ainsi de cartographier les émissions de GES, à différents pas de temps (journaliers, mensuels, annuels).

A.2.2 Description du modèle CERES-EGC

Le modèle de cultures CERES-EGC (Crop-Environment REsources Synthesis - Environnement et Grandes Cultures) permet d'évaluer la productivité et les impacts environnementaux des cultures. Il simule à un pas de temps journalier le développement et le rendement des cultures (Gabrielle et al., 1998b), ainsi que les sorties environnementales, comme le lessivage des nitrates et les flux de GES (N_2O, CO_2), de précurseurs d'ozone (NO) et d'ammoniac (NH_3 ; Gabrielle et al. (2006b)). Le modèle a été appliqué pour spatialiser les émissions de N_2O des sols agricoles de la Beauce, dont la surface agricole est de 59000 ha (Gabrielle et al., 2006a). Le modèle requiert comme données d'entrée les caractéristiques du sol cultivé, les pratiques culturales et les conditions météorologiques locales.

Données d'entrées
Les sols sont représentés par une superposition d'horizons élémentaires, caractérisés par le point de flétrissement, la capacité au champ, le point de saturation, le pH, le contenu en carbone organique, et la densité apparente. Il est nécessaire de définir des conditions initiales (concentrations en NH_4^+ et NO_3^-, humidité) pour chaque horizon de sol. Les itinéraires techniques sont définis par les opérations culturales suivantes : le semis d'une culture (date, variété, densité de graines), la fertilisation (date, type et quantité d'engrais), l'irrigation (date, quantité d'eau) et la gestion des résidus. Enfin, les variables météorologiques requises sont les valeurs journalières de température minimale et maximale de l'air à 2 m, le rayonnement global, les précipitations, l'évapo-transpiration potentielle et la vitesse du vent.

Le calcul et la spatialisation des émissions de N_2O
Pour ce travail, les émissions de N_2O sont simulées sur une période de 14 mois pour la région Île-de-France. Des **routines de spatialisation des données sols et météo** permettent au modèle de lire la base de données des entrées contenant les identifiants des unités de simulation qui affectent un type de sol et une météo à chaque unité.
Les émissions de N_2O sont calculées à partir des processus de nitrification et de dénitrification, fonctions de la température, de l'humidité, et du contenu en azote minéral dans le sol.

A.2.3 La base de données des entrées

A.2.3.1 Définition des unités de simulation

Les unités de simulation sont nécessaires pour estimer les émissions de N_2O avec CERES-EGC, chacune possédant un identifiant unique qui permet de distribuer la météo ainsi que l'itinéraire technique correspondant. Elles ont été obtenues en croisant 3 types de couches d'information : "sol $*$ occupation des sols $*$ cantons". La couche "cantons" permet de positionner les statistiques agricoles, c'est-à-dire l'assolement des cultures par canton. On distingue 16 types de sols sur la région Île-de-France, distribués dans les unités de simulation, pour former la carte des sols de l'Île-de-France (Fig. A.1).

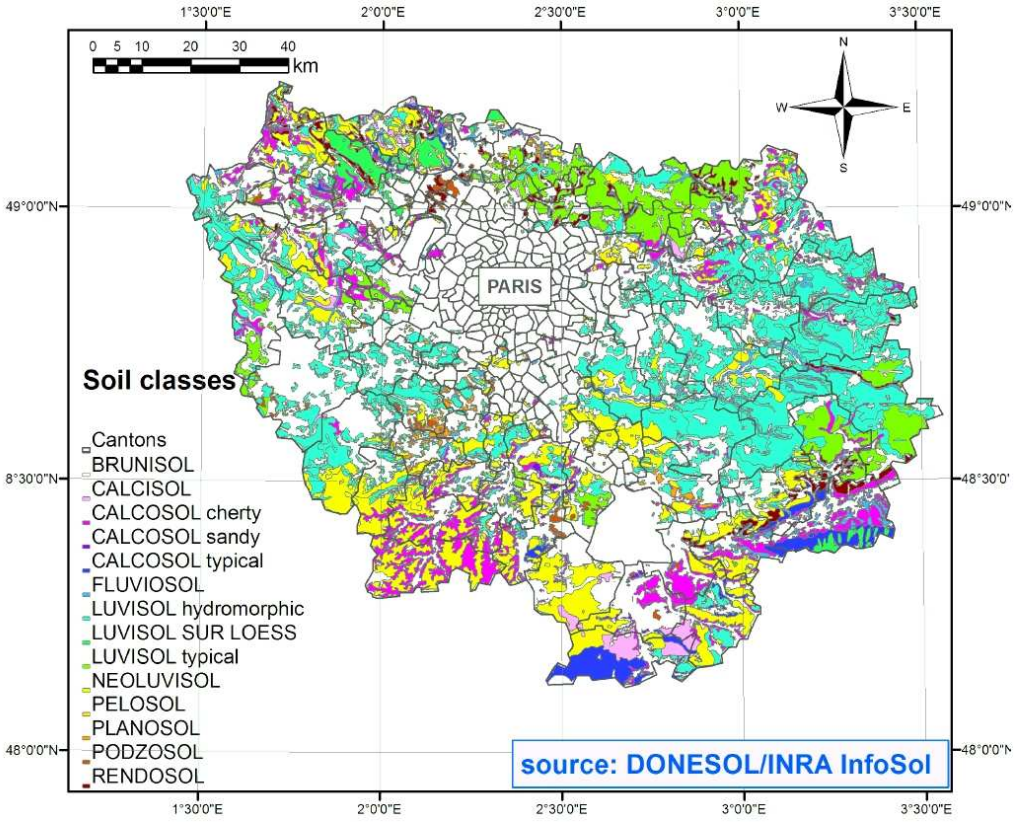

FIG. A.1 : *Carte des sols cultivés pour la région Île-de-France (Rolland, 2008).*

A.2.3.2 Les données météorologiques

Les données météorologiques proviennent des simulations avec le modèle méso-échelle MM5[1] (résolution de 5 km $*$ 5 km) pour la période 2000/2001 (par la suite sera utilisée une météo provenant du modèle WRF [2] pour la période 2006/2007). La météo est distribuée sur l'Île-de-France

[1] *Mesoscale Model - http ://www.mmm.ucar.edu/mm5/*

[2] *Weather Research and Forecasting model - http ://wrf-model.org/index.php*

en fonction d'identifiants, par interpolation sous le SIG de leur maillage d'origine sur le maillage régulier de la version francilienne de CHIMERE [3] (résolution de 6 km $*$ 6 km), qui est le modèle atmosphérique de chimie-transport qui sera utilisé pour simuler le devenir des émissions de N_2O. Grâce à la base de données des entrées ainsi constituée, qui regroupe, pour chacune des unités de simulation, le type de sol, les itinéraires techniques et la météorologie, il est possible de réaliser les simulations spatialisées.

A.2.4 Simulations et spatialisation des émissions

Les simulations régionales sont réalisées sur une période de 14 mois (du 01.11.2000 au 31.12.2001) pour les différentes cultures : maïs, orge, blé, betterave, colza, pois et jachère. Celles-ci permettent d'obtenir les flux de N_2O (journaliers g N-N_2O ha^{-1} j^{-1} ou totaux g N-N_2O ha^{-1}). Ensuite, connaissant la répartition surfacique des cultures pour chaque unité de spatialisation (pourcentage estimé à l'échelle cantonale (Rolland, 2008)), nous pouvons obtenir les flux de N_2O des sols cultivés de l'Île-de-France de la manière suivante :

$$F_{N2O,i} = \%S_{i,c}\ F_{N2O,i,c} \tag{A.1}$$

avec $F_{N2O,i}$ le flux de N_2O (journalier en g N-N_2O ha^{-1} j^{-1} ou total en g N-N_2O ha^{-1}) par unité de simulation i, $\%S_{i,c}$ la répartition des surfaces des cultures par unité de simulation et $F_{N2O,i,c}$ le flux de N_2O (journalier en g N-N_2O ha^{-1} j^{-1} ou total en g N-N_2O ha^{-1}) par unité de simulation pour une culture.
La dernière étape consiste à cartographier les émissions (ou d'autres sorties tels que les rendements) à l'aide du logiciel de SIG, ce qui permet d'obtenir la base de données des sorties. La méthode ainsi décrite peut être résumée par la Figure A.2.

A.2.5 Définition des scénarios pour l'analyse de sensibilité

Des tests ont été effectués sur les cultures de blé (culture d'hiver), de maïs (culture de printemps) et d'orge d'hiver, pour observer la sensibilité des émissions de N_2O à différents facteurs (types de sol, scénarios météo, jeux de paramètres).

Type de sol
L'influence du sol sur les émissions de N_2O a été testée pour quatre types de sol (Calcosol caillouteux, Luvisol hydromorphe, Neoluvisol et Fluvisol). Ces tests ont été réalisés pour une culture de blé, en simulant les émissions régionales successivement avec un unique type de sol.

Scénarios météo
L'influence de quatre scénarios météorologiques a été testée, pour analyser la sensibilité des émissions aux facteurs climatiques. Le nom et la définition des scénarios sont définis de la manière suivante :

[3] *CHIMERE chemistry transport model - http ://www.lmd.polytechnique.fr/chimere/*

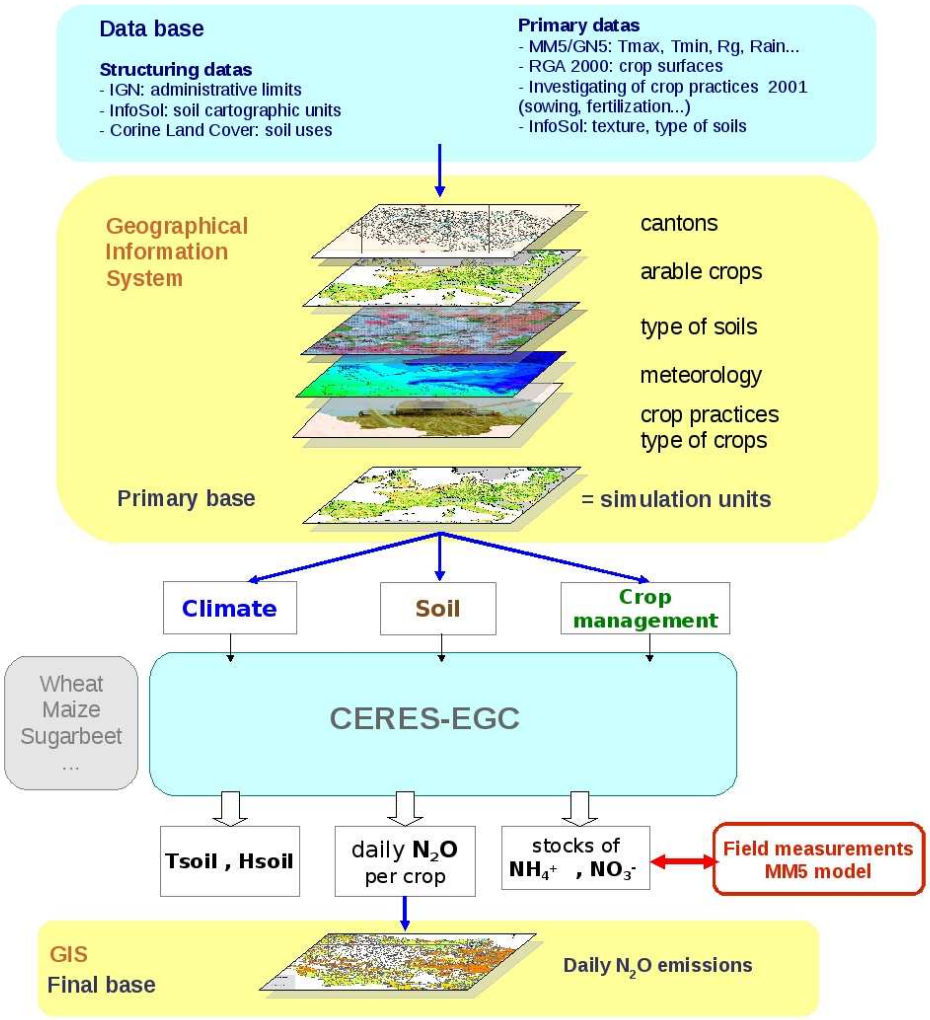

FIG. A.2 : *Méthodologie utilisée pour réaliser une carte régionale d'émissions de N_2O avec un pas de temps journalier (adapté de Rolland (2008).*

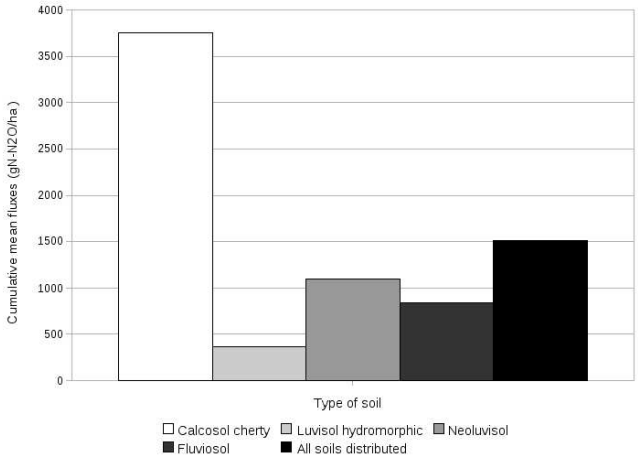

FIG. A.3 : *Effet du type de sol sur les émissions de N_2O pour la période de nov. 2000 à déc. 2001.*

- *Météo Grignon mesurée* : météo mesurée sur le parc météorologique de Grignon, assez bien représentative de la météo des Yvelines (en terme de précipitations minimales, maximales et cumulées, et étendue à toute la région) ;
- *Météo Grignon simulée* : météo du pixel MM5 contenant le site de Grignon, étendue à toute l'Île-de-France ;
- *Météo MM5 moyenne* : moyenne spatiale des pixels MM5 sur l'ensemble de l'Île-de-France, et appliquée à toute la région ;
- *Météo MM5* : météo distribuée spatialement, obtenue avec le modèle MM5.

Scénarios de paramétrisation

Deux jeux de paramètres du module N_2O de CERES-EGC ont été testés (Tab. A.1) :

- *paramètres initiaux* : valeurs des paramètres initiales du modèle ;
- *paramètres calibrés* : jeu de paramètres calibrés avec les données journalières obtenues sur le site expérimental de Grignon avec la méthode des chambres automatiques, sur une période d'un an.

Paramètres (description)	initiaux	calibrés
vpd (potential denitrification rate (kg N/ha/day))	7.000	0.34
ratio (ratio of N_2O to total denitrification flux (unitless))	0.250	0.36
TrWFPS (WFPS treshold for denitrification (%))	0.620	0.610
Km (half-saturation constant (denit) (mgN/kg soil))	22.000	24.690
TTr (temperature treshold (degrees C))	11.000	10.050
POWdenit (exponent of power function (unitless))	1.740	0.460

TAB. A.1 : *Récapitulatif des jeux de paramètres.*

A.3 Résultats et discussions

Effet des classes de sols

La Figure A.3 présente les émissions de N_2O pour quatre types de sols, et avec les sols spatialisés. Le type de sol a un effet important sur les émissions, en effet, celles-ci varient considérablement en fonction du type de sol (de 365 à 3 750 g N-N_2O ha^{-1}).

Effet des scénarios météo

Le Tableau A.2 présente l'effet des 4 scénarios météo, définis dans la partie A.2.5, sur les émissions de N_2O et sur les rendements, pour les cultures de blé et de maïs. L'effet de la météo se remarque particulièrement avec la comparaison des scénarios *Météo Grignon mesurée* et *Météo Grignon simulée*), et on constate :

- qu'appliquer la météo Grignon mesurée revient à minimiser les flux de N_2O par rapport à ceux obtenus avec la météo MM5 (resp. 1500 g N-N_2O ha^{-1} contre 1826 g N-N_2O ha^{-1} environ dans le cas du blé, et 2115 g N-N_2O ha^{-1} contre 3320 g N-N_2O ha^{-1} environ dans le cas du maïs) ;

- que les rendements sont plus élevés et cohérents avec les statistiques régionales pour la météo Grignon mesurée plutôt qu'avec la météo MM5 (pour le blé, 69 q/ha contre 30 q/ha resp., alors que la moyenne 2001 est de 76 q/ha pour la région Île-de-France[4]).

Pour simuler les émissions de N_2O il conviendra d'utiliser de préférence la météo spatialisée à condition que les données soient fiables. En effet, la précision des simulations MM5 peut être remise en question ; par exemple pour le pixel Grignon sur la période 2000/2001, on a observé que les précipitations simulées sont presque deux fois plus faibles que les précipitations mesurées (677 mm contre 1119 mm).

Les facteurs de conversion de l'engrais en N_2O calculés à partir de la *Météo Grignon mesurée* sont de 0.95 % pour le blé et de 1.5 % pour le maïs à l'échelle régionale.

Culture	Météo	Grignon mesurée	Grignon simulée	MM5 moyenne	MM5
Blé	Rendement moyen (q/ha)	69	25	34	32
Blé	Flux moyens (g N-N_2O ha^{-1})	1510	1827	1692	1841
Blé	Émissions totales (t N-N_2O)	341	400	368	409
Maïs	Rendement moyen (q/ha)	70	20	37	35
Maïs	Flux moyens (g N-N_2O ha^{-1})	2115	3321	3300	3190
Maïs	Émissions totales (t N-N_2O)	69	99	99	96

TAB. A.2 : *Comparaison de l'effet des 4 scénarios météo sur les émissions de N_2O et sur les rendements (blé et maïs) pour la période de nov. 2000 à déc. 2001.*

Effet de la paramétrisation

Nous avons analysé l'effet du choix des paramètres de CERES-EGC sur les émissions de N_2O. Les simulations ont été réalisées pour la région et pour la période de nov. 2000 à déc. 2001, pour trois cultures différentes (blé, maïs et orge) avec les deux jeux de paramètres : initiaux et calibrés. La météo MM5 spatialisée a été utilisée pour les simulations. Le tableau A.3 présente les rendements moyens et les émissions de N_2O. Les émissions obtenues avec les paramètres calibrés sont en moyenne 60 % inférieures aux émissions obtenues avec les paramètres initiaux. Dans les deux cas, les rendements faibles obtenus avec la météo MM5 suppose qu'une partie importante de l'azote apportée n'est pas absorbée par les plantes et est donc potentiellement disponible pour la dénitrification et la nitrification.

Cartes d'émissions

Les simulations ont permis de réaliser la spatialisation des émissions de N_2O pour la région Île-de-France. Les cartes A.4 et A.5 présentent l'évolution des émissions moyennes journalières de N_2O pour chaque mois de l'année 2001, pour toutes les cultures confondues. Ces cartes permettent d'identifier des "hot spots" au sud de l'Île-de-France principalement, et au nord pour les mois de mars et avril.

[4]Agreste, http ://agreste.agriculture.gouv.fr/

Paramètres	Type de culture	Rendement (q/ha)	Flux moyens (g N-N_2O ha^{-1})	Flux totaux (t N-N_2O)
initiaux	blé	32	1841	409
initiaux	maïs	35	3190	96
initiaux	orge	47	3364	182
calibrés	blé	32	841	199
calibrés	maïs	35	1291	42
calibrés	orge	47	1516	86

TAB. A.3 : *Comparaison des émissions de N_2O et des rendements moyens obtenus avec les deux jeux de paramètres initiaux et calibrés.*

A.4 Conclusion

Le modèle CERES-EGC couplé aux méthodes SIG permet de prédire les émissions de N_2O en fonction des facteurs d'entrées relatifs aux types de sol, aux conditions météorologiques locales et aux pratiques agronomiques. L'effet du type de sol et sa répartition géographique a une influence importante sur les émissions et sur leur localisation. Les conditions météo déterminent le rendement des cultures et les niveaux d'émissions, il convient donc d'avoir des données météo spatialisées représentatives de la réalité. Par exemple, si les précipitations sont sous-estimées, l'humidité du sol le sera également et la dénitrification sera peu active. Enfin, les paramètres de dénitrification doivent être correctement calibrés pour simuler au mieux les flux de N_2O.

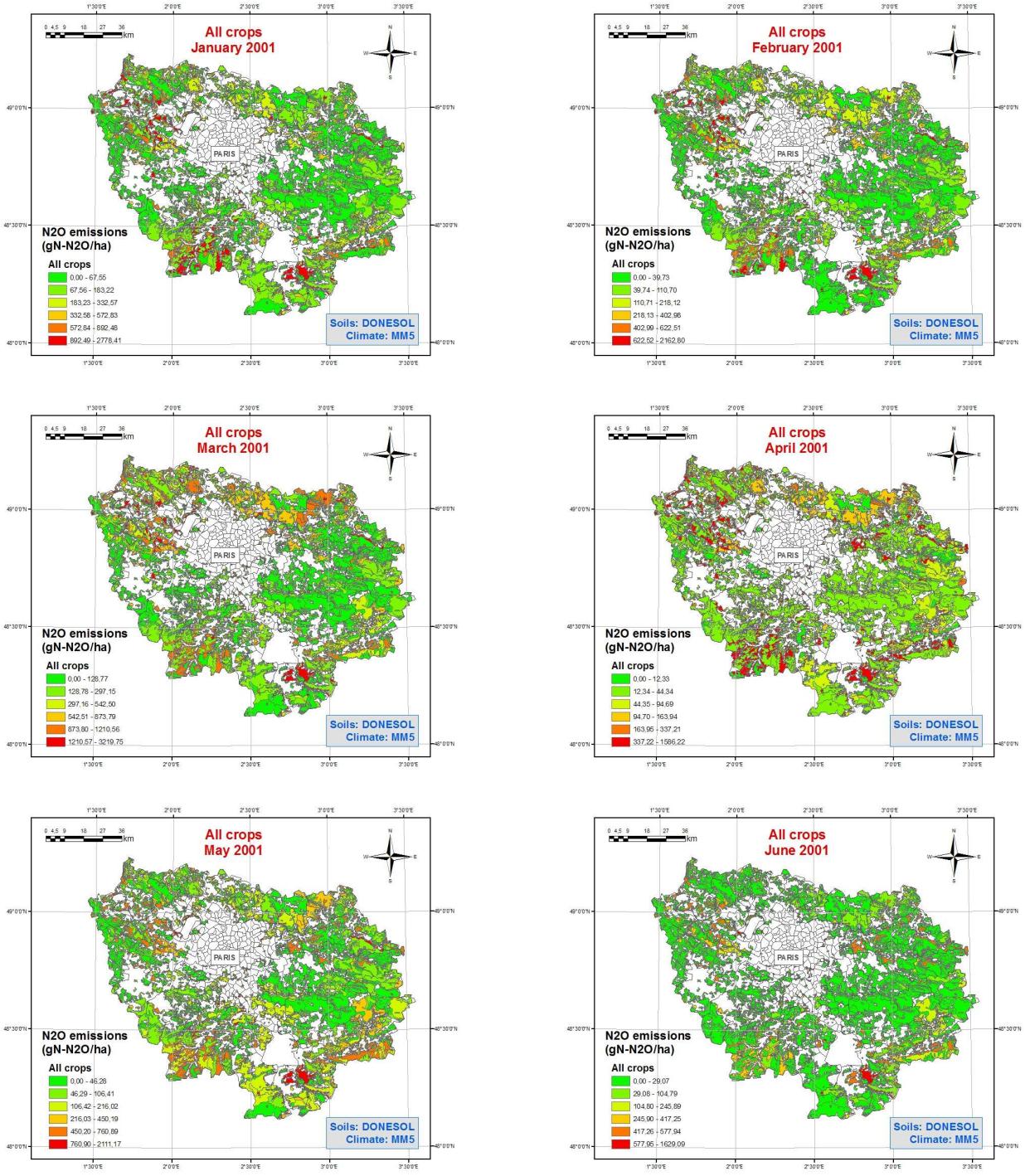

FIG. A.4 : *Émissions de N_2O moyennes mensuelles (g N-N_2O ha^{-1}) de janvier à juin 2001.*

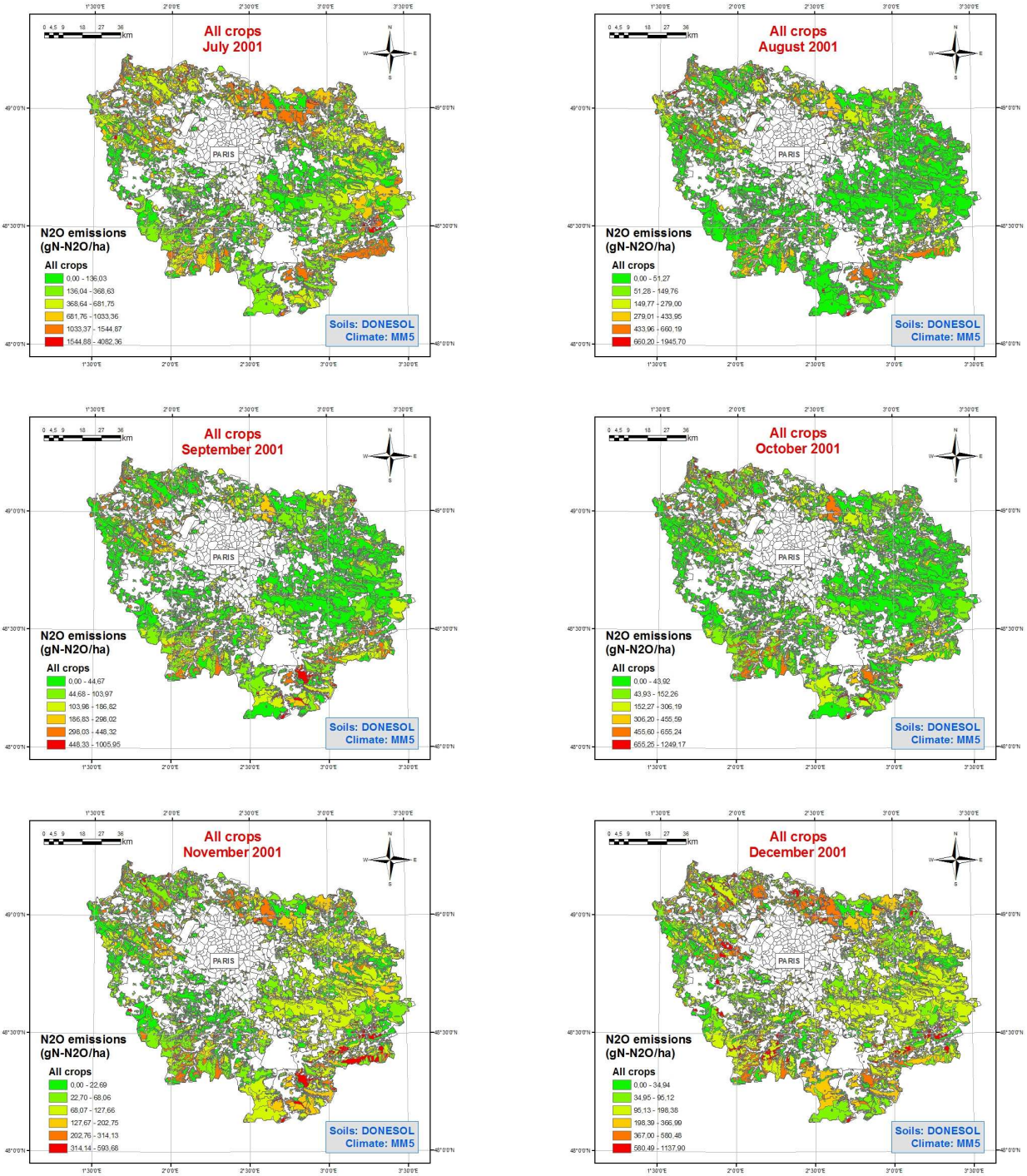

FIG. A.5 : *Émissions de N_2O moyennes mensuelles (g N-N_2O ha^{-1}) de juillet à décembre 2001.*

Annexe B

Analyse de sensibilité globale multivariée pour les modèles dynamiques

Cette annexe est un article traitant de l'analyse de sensibilité globale multivariée pour les modèles dynamiques. Ce travail a été réalisé par Matiyiendu Lamboni de l'Unité Mathématiques et Informatique Appliquées de Jouy-en-Josas en collaboration avec David Makowski (UMR Agronomie), Hervé Monod (UR MIAJ), Benoît Gabrielle (UMR EGC) et Simon Lehuger (UMR EGC). Il est en soumission pour la revue *Field Crop Research*. Les résultats de ce travail nous ont permis de sélectionner un sous-ensemble de paramètres du modèle CERES-EGC, qui, ensuite, a été estimé par calibration bayésienne.

Multivariate global sensitivity analysis for dynamic crop models

Matieyendou Lamboni[1*], David Makowski[2], Simon Lehuger[3],
Benoît Gabrielle[3] and Hervé Monod[1]

[1]INRA, Unité MIA (UR341), Domaine de Vilvert, F78352 Jouy-en-Josas Cedex, France
[2]INRA, UMR 211 INRA AgroParisTech, BP 01, F78850, Thiverval-Grignon, France
[3]INRA, AgroParisTech UMR1091 EGC, F78850, Thiverval-Grignon, France

Soumis à Field Crop Research

*Corresponding author : Matieyendou Lamboni.
Unité MIA, Domaine de Vilvert
F78352 Jouy-en-Josas Cedex,France
Tel (+33)(0)1 34 65 28 47
Fax (+33)(0)1 34 65 22 17
Email : matieyendou.lamboni@jouy.inra.fr

Abstract

Dynamic crop models are frequently used in ecology, agronomy and environmental sciences for simulating crop and environmental variables at a discrete time step. They often include a large number of parameters whose values are uncertain, and it is often impossible to estimate all these parameters accurately. A common practice consists in selecting a subset of parameters by global sensitivity analysis, estimating the selected parameters from data, and setting the others to some nominal values. For a discrete-time model, global sensitivity analyses can be applied sequentially at each simulation date. In the case of dynamic crop models, simulations are usually computed at a daily time step and the sequential implementation of global sensitivity analysis at each simulation date can result in several hundreds of sensitivity indices, with one index per simulation date. It is not easy to identify the most important parameters based on such a large number of values. The purpose of this paper was to study the interest of an alternative method called multivariate global sensitivity. Sequential global sensitivity analysis and multivariate sensitivity analysis were compared by using two dynamic models; a model simulating wheat biomass named WWDM and a model simulating N_2O gaseous emission in crop fields named CERES-EGC. N_2O measurements collected in several experimental plots were used to evaluate how parameter selection based on multivariate sensitivity analysis can improve the CERES-EGC predictions.

The results showed that sequential and multivariate sensitivity analyses provide modellers with different types of information for models which exhibit a high variability of sensitivity index values over time. Conversely, when the parameter influence is quite constant over time, the two methods give more similar results. The results also showed that the estimation of the parameters with the highest sensitivity indices led to a strong reduction of the prediction errors of the model CERES-EGC.

Keywords: crop model, mean squared error of prediction, N_2O emission, sensitivity analysis, parameter estimation.

1. Introduction

Dynamic crop models are frequently used in ecology, agronomy and environmental sciences for simulating crop and environmental variables of interest at a discrete time step. These models are useful for the management of endangered species (e.g Santangelo et al., 2007), for understanding intraspecific and interspecific competition (e.g Yakubu et al., 2002; Wu et al., 2007), for pest management (e.g Matsuoka and Seno, in press), for predicting plant growth (e.g Bechini *et al*, 2006; Boote *et al*., 1996; Passioura, 1996) or for greenhouse gas management (Gabrielle et al, 2006b). For instance, CERES-EGC is a discrete-time model that simulates the emission of nitrous oxide (N_2O), a potent greenhouse gas, into the atmosphere on a daily time step (Gabrielle et al, 2006a).

Discrete-time models can include many parameters whose values are uncertain. The uncertainty on the parameters is a major source of uncertainty on the model predictions. Consequently, the estimation of the uncertain parameters from experimental data is an important step and model performances depend for a large part on the accuracy of the parameter estimates (Butterbbach-Bach *et al*., 2004; Gabrielle *et al.*, 2006a; Lehuger *et al.*, in press; Makowski *et al*., 2006a; Wallach *et al.*, 2001). Model predictions based on inaccurate parameter values are unreliable and hardly meaningful.

In general, it is impossible to estimate all parameters of complex models simultaneously (Bechini *et al*, 2005). A common strategy consists in selecting a subset of parameters to be calibrated using sensitivity analysis, and fixing the others to some nominal values (Makowski *et al*., 2006a; Makowski *et al.*, 2006b; Monod *et al.*, 2006; Wallach *et al.*, 2001). Several local and global sensitivity analysis methods have been developed and applied to identify the parameters that require an accurate estimation (Cariboni *et al.*, 2007; Homma and Saltelli, 1996; Saltelli *et al.*, 2000b; Saltelli *et al.*, 2004; Saltelli *et al.*, 2006). Methods of global sensitivity analysis are useful and are easy to interpret. They allow modelers to perform factor prioritization, i.e to determine which subset of parameters accounts for most of the output uncertainty. Those factors with a small contribution can be set to some nominal value or to any value within their uncertainty range. The use of sensitivity analysis to select the parameters to estimate relies mainly on the intuitive idea that predictions are more accurate when the most influent parameters are accurately estimated. There have been few attempts to formalize this kind of relationship or even to check it empirically in realistic situations.

For a discrete-time model, global sensitivity analysis methods can be applied sequentially at each simulation date. In the case of dynamic crop models, simulations are usually computed at a daily time step and the sequential implementation of global sensitivity analysis at each simulation date can result in several hundreds of sensitivity indices, with one index per simulation date. It is not easy to identify the most important parameters based on such a large number of values (Campolongo *et al*, 2007). In addition, there is a high level of redundancy between neighbouring dates and interesting features of the dynamics may be missed out.

Campbell *et al.* (2006) proposed to use a different approach with dynamic models, called multivariate global sensitivity analysis. Their idea was to decompose the time series of model outputs upon a complete orthogonal basis and to compute sensitivity indices on each component of the decomposition. The orthogonal basis can be determined by principal component analysis from a set of model outputs computed using various combinations of parameter values. When the variability of the model outputs can be explained by a small number of principal components, this approach allow modelers to analyze the sensitivity of a large number of dynamic model outputs by computing a small number of sensitivity indices; one index value per parameter and per principal component instead of one index value per parameter and per simulation date. Although this approach looks promising, it has never been applied to dynamic crop models

The purpose of this paper was to study the interest of multivariate global sensitivity for dynamic crop models. Sequential global sensitivity analysis and multivariate sensitivity analysis were compared by using two dynamic models; a model simulating wheat biomass named WWDM (Makowski *et al.*, 2004; Monod *et al.*, 2006) and a model simulating N_2O gaseous emission in crop fields named CERES-EGC (Gabrielle *et al.*, 2006a, 2006b). N_2O measurements collected in several experimental plots were used to evaluate how parameter selection based on multivariate sensitivity analysis can improve the CERES-EGC predictions.

2. Material and methods

2.1. Models

2.1.1. *The Winter Wheat Dry Matter model*

The Winter Wheat Dry Matter model (WWDM) is a dynamic crop model running at a daily time step (Makowski *et al.*, 2004; Monod *et al.*, 2006). It has two state variables, the above-ground winter wheat dry matter $U(t)$, in g/m^2 and the leaf area index $LAI(t)$ with t the day number from sowing ($t=1$) to harvest ($t=223$). The state variable $U(t)$ is calculated on a daily basis in function of the cumulative degree-days $T(t)$ (over a basis of 0^oC) and of the daily photosynthetically active radiation $PAR(t)$. The model equations are defined by

$$U(t+1) = U(t) + E_b E_{imax} \left(1 - e^{-K.LAI(t)}\right) PAR(t) + \varepsilon(t) \quad (1)$$

and

$$LAI(t) = L_{max} \left(\frac{1}{1+e^{-A(T(t)-T_1)}} - e^{-B(T(t)-T_2)} \right) \quad (2)$$

where $\varepsilon(t)$ is a random term with zero expectation representing the model error. Only the deterministic part of the model was considered for this paper and so the error term was set to zero. The dry matter at sowing ($t=1$) was also set to zero : $U(1)=0$. In addition, the constraint $T_2 = \frac{1}{B}\log[1+\exp(A \quad T_1)]$ was applied, so that $LAI(1)=0$.

Seven uncertain parameters were considered for the sensitivity analysis. Uncertainty intervals in Table 1 were given by agronomists (Monod *et al.* 2006). Usually the climate should form one or several input factors for the sensitivity analysis. Here, preliminary investigations on 14 annual climate series showed little differences between years. For simplicity, results with a single series are presented. The model output considered in the sequel is the dynamic evolution of the dry matter $U(t)$ from sowing ($t=1$) until harvest ($t=223$). It is represented in Figure 1 for the nominal parameter values and for a sample of other possible parameter values drawn within the uncertainty ranges.

2.1.2. *The CERES-EGC model*

CERES-EGC was adapted from the CERES suite of soil-crop models, with a focus on the simulation of environmental outputs such as nitrate leaching or the emission of nitrogen oxides (Gabrielle *et al.*, 2006b). The CERES models are available for a large number of crop species that share the same soil components (Jones and Kiniry, 1986). CERES-EGC runs at a daily time step, and requires daily rain, mean air temperature and Penman potential evapo-transpiration as forcing variables.

The nitrous oxide emission module simulates the production of N_2O (kgN ha^{-1} day^{-1}) in soils through both the nitrification (Ni) and the denitrification (De) pathways (Hénault *et al.*,2005; Hénault and Germon, 2000). Nitrous oxide emissions resulting from the two processes are soil-specific proportions of total denitrification and nitrification pathways, and are calculated according to:

$$N_2O(t) = r\mathrm{De}(t) + c\mathrm{Ni}(t),\ t=1,2\ldots T$$

where r is the fraction of denitrified N and c is the fraction of nitrified N that both evolve as N_2O. For details on model equation see Lehuger et al. (in press). The N_2O sub-model of CERES-EGC involves a total set of 15 main parameters including the potential denitrification rate (PDR, kgN ha^{-1} day^{-1}), the maximum nitrification rate (MNR, kgN ha^{-1} day^{-1}), the fractions of nitrified (c) and denitrified (r) N. Parameter uncertainty intervals are listed in Table 2.

2. 2. Methods of sensitivity analysis for time series output

2.2.1. Structure of the simulated data

The output of a dynamic crop model with discrete time step can be written

$$y(t) = f(\mathbf{z}, t; \theta), \qquad (3)$$

where $y(t)$ is the scalar output on time t for $t = 1, 2, \ldots, T$, $\mathbf{z}$ is a vector of input variables and θ is a vector of parameters. Both input variables and parameters may be used as input factors for the sensitivity analysis. However, in the applications presented in this paper, $\mathbf{z}$ was fixed and so only the parameters in θ were used as input factors.

Simulations were performed according to complete or fractional factorial designs (Box and Draper, 1987; Ginot *et al.*, 2006). Each parameter was studied at three levels, the mean and the bounds of its uncertainty interval, making it possible to assess linear and quadratic effects. For the WWDM model, a complete 3^7 factorial design (seven parameters at three levels) was constructed, with $N = 3^7 = 2187$ simulations. For the CERES-EGC model; a fractional factorial design 3^{15-7} (fifteen parameters at three levels and $N = 3^8 = 6561$) was constructed with the FACTEX procedure of the SAS© 8.0/QC module (SAS Institute Inc., 2008) . It was of resolution 5, which means that all main effects and two-factor interactions could be estimated (Box and Draper, 1987; Kobilinsky, 1997).

Suppose that N simulation runs are performed according to a factorial design on the input factors. Then the output can be stored in a $N \quad T$ matrix:

$$\mathbf{Y} = \begin{matrix} y_1(1) & \ldots & y_1(t) & \ldots & y_1(T) \\ . & . & . & . & . \\ y_i(1) & \ldots & y_i(t) & \ldots & y_i(T) \\ . & . & . & . & . \\ y_N(1) & \ldots & y_N(t) & \ldots & y_N(T) \end{matrix} .$$

Each column $\mathbf{y}(t)$ in $\mathbf{Y}$ represents the simulated values of the output variable at a given time t, while each row of $\mathbf{Y}$ is an individual dynamic for a given set of input values. The rows of $\mathbf{Y}$ constitute a sample of output dynamics in $\mathbf{R}^T$ over the uncertainty domain of the input factors. In the sequel, we assume that $N \quad T$.

2.2.2. Method 1: sequential global sensitivity analyses

Sensitivity analysis of a time series output can first be performed separately on each output variable $y(t)$. Because orthogonal factorial designs were used for the simulations, classical analyses of variance (ANOVA) were performed. The complete variance decomposition is

$$\mathrm{Var}(y(t))=\mathrm{SS}_1(t)+\ldots+\mathrm{SS}_i(t)+\ldots+\mathrm{SS}_K(t)+\mathrm{SS}_{12}(t)+\ldots+\mathrm{SS}_{ij}(t)+\ldots+\mathrm{SS}_{K-1,K}(t)+\ldots+\mathrm{SS}_{1\ldots K}(t),$$

where SS_i is the main effect of parameter i, SS_{ij}, say, is the interaction between parameters i and j, and K is the total number of parameters. With a complete factorial design, the decomposition can be calculated with all factorial terms. With a fractional design of resolution 5, the decomposition must be limited to two-factor interactions because of confounding.

Sensitivity indices defined by

$$SI_W(t)=\mathrm{SS}_W(t)/\mathrm{Var}(y(t))$$

were derived from the ANOVA sums of squares at each time t and for each factorial term W in the model (see Monod *et al.*, 2006). The dynamic evolution of sensitivity indices was represented graphically as proposed by Saltelli *et al.*, 2000 (Figure 2). Computations were performed using the *R* statistical software (Venables and Ripley, 2003).

2.2.3. Method 2: PCA-based multivariate global sensitivity analysis

Sensitivity analyses can also be applied to a pre-defined function h of the model outputs $h(y(1),\ldots,y(T))$ with a biological interpretation. For example, $h=y(t_1)-y(t_2)$ may represent the difference in biomass between two key stages of plant growth. As many other features in the $y(t)$ dynamics are potentially interesting to look at, it is useful to identify automatically the linear combinations that contain most variability between the output dynamics. This identification step was performed here by Principal Components Analysis (PCA) of matrix $\mathbf{Y}$ (Krzanowski and Marriott, 1990; Anderson, 2003).

By definition, the total inertia is the sum of the $y(t)$ variances and the first principal component is the linear combination $h_1=l_{1,1}y(t_1)+\ldots+l_{1,T}y(t_T)$ of the columns of $\mathbf{Y}$ with the maximum proportion of inertia (or variance) subject to the constraint $\sum l_{1,t}^2=1$. Overall, there are T principal components in a decreasing order of importance as measured by the percentage of inertia. When an orthogonal factorial design is used, ANOVA-based sensitivity analysis can be applied to each principal component h_k according to the variance decomposition:

$$\mathrm{Var}(h_k)=\mathrm{SS}_{1,k}+\ldots+\mathrm{SS}_{i,k}+\ldots+\mathrm{SS}_{K,k}+\mathrm{SS}_{12,k}+\ldots+\mathrm{SS}_{ij,k}+\ldots+\mathrm{SS}_{K-1,K;k}+\ldots+\mathrm{SS}_{1\ldots K,k}.$$

Sensitivity indices $SI_{W,k}$ were derived from ANOVA sums of squares for each main effect or interaction W and each principal component k=1, …, T. The principal components were represented graphically by plotting the coefficients $l_{k,t}$ as a function of t. The sensitivity indices $SI_{W,k}$ were also be represented graphically by drawing a Pareto plot for each principal component k of interest (Figures 3, 4).

2.2.4. A synthetic multivariate sensitivity index

In addition to the PCA-based sensitivity indices, a synthetic sensitivity index GSI_W can be calculated to measure the contribution of each factorial term W to the total inertia between output dynamics. We propose to call it the *generalized sensitivity index* of factorial term W. GSI_W is equal to the weighted sum of the $SI_{W,k}$ indices over the principal components k, with weights

proportional to the inertia associated with the components *k* (Lamboni et al, 2008). Generalized sensitivity indices can be represented by Pareto plots (Figure 5).

In practice, only the first principal components carry useful information on the model output and higher-order interactions can be neglected. An approximation of GSI_W based on a subset of the principal components is called an *approximate generalized sensitivity index* and denoted by $\tilde{GSI}_w$ in the sequel. To quantify the approximation made when restricting the interpretation to a subset of principal components and a subset of factorial terms, the total proportion of inertia associated with these subsets is called the *approximation global quality* and denoted by GQ. If GQ is close to 1 then the approximation accounts for most of the inertia of $\mathbf{Y}$, whereas low GQ suggests that $\tilde{GSI}_w$ indices must be interpreted with much caution. In addition to the global quality criterion, *dynamic coefficients of determination* R_t^2 can be used to measure the quality of any approximation when coming back to the original time series output $y(t)$ (Lamboni *et al.*, 2008).

2.3. Mean Squared Error of Prediction (MSEP) of the CERES-EGC model

MSEP values were computed in order to see if model predictions were improved when sets of parameters with high sensitivity indices were estimated from experimental data.

2.3.1 Experimental data

MSEP were computed from data collected in an experimental trial carried out in Villamblaim (Central France), during the 1998-99 growing season. A winter wheat crop was grown with conventional management on a haplic Calcisol soil. The emissions of N_2O emissions were monitored at 18 different dates throughout the growing season using static chambers with eight replicates. At each sampling date, the chambers were closed with an airtight lid, and the head space was sampled 4 times over a period of 2 hours. The gas samples were stored in 3-mL Vacutainer tubes (Terumo Europe N.V., Leuven, Belgium), and analyzed in the laboratory by gas chromatography. See Gabrielle *et al.* (2006a) for a detailed description of the experimental methods. All the input variables required by CERES-EGC were measured in the experimental plot.

2.3.2. Statistical analysis

All possible sets of one, two or three parameters were defined from the 15 model parameters. A pooled value of the generalized sensitivity index defined above was calculated for each set by summing all the main effect and interaction terms of the parameters included in the set. Each set of one, two or three parameters was then estimated by using half of the 18 N_2O measurements. The other nine measurements were used to assess the errors of prediction of the fitted model. Data were permuted in order to estimate the MSEP by cross validation for each set of one, two or three parameters. Finally, the relationship between the generalized sensitivity index and the MSEP was investigated graphically.

In the estimation procedure, the non-selected parameters were fixed at their nominal values while the selected ones were estimated by least squares, subject to the constraint that all parameter values should remain in their uncertainty interval. We did not estimate more than three parameters because of the limited number of data.

3. Results

3.1. Sequential global sensitivity analyses

The results obtained by sequential sensitivity analysis of the WWDM model (Figure 2a) showed that the values of the sensitivity indices strongly vary over time. Before *t* = 50, the most important parameter is *A* followed by parameters *T1*, *Lmax*, and *B*. The strong influence of *A* at the beginning of the growing season is due to its influence on the increase of the leaf area index which occurs at

this stage. The influence of *A* decreases and becomes less influent than *T1*, E_b, and *Lma*x after *t* = 110. In the second half of the growth cycle, biomass growth becomes very sensitive to the parameter *Eb* due to the effect of this parameter on the conversion of the intercepted radiation into biomass. The influence of parameter *A* increases again after *t* = 150 and until harvest due to leaf senescence. Interactions between parameters are non-negligible during the whole growing period.
Unlike the WWDM model, the sensitivity indices computed for CERES-EGC are quite similar over time. The simulated values of N_2O emission are driven by the same three parameters during the whole period of simulation; *r*, PDR, Km (Figure 2b). For this model also, the interactions are important; the sensitivity index associated to interaction represents more than 40% of the total variability. This strong interaction is due to the fact that the parameter effects are not additive.

3.2. Multivariate sensitivity analysis

Results of the principal components and sensitivity principal indices are presented in Figure 3 for WWDM. For this model, the first three components explained 99% of the total inertia of the simulated dry matter dynamics. The inertia percentage associated with the first three components were equal to $\lambda_1 = 0.73$, $\lambda_2 = 0.23$ and $\lambda_3 = 0.03$ respectively. The first component was positively correlated with all outputs *y*(*t*). The largest correlations were obtained in the middle of the simulation period but the correlation values were quite similar over time. According to these correlation values, the first principal component corresponds to the global amount of dry matter produced during the growing season. The sensitivity indices computed for this component (Figure 3, bottom row) show that the global amount of dry matter was mainly sensitive to parameter E_b, but also to T1 and Lmax. The second principal component was positively correlated with dry matter during the first part of the growing season and negatively correlated with dry matter during the second half of the growing season. Thus, this principal component corresponds to the difference between early and late dry matter productions. It was mainly sensitive to parameter *A*. Finally, the third principal component accounted for a much smaller part of inertia, associated with the difference between the dry matter produced the middle of the growing season and the dry matter produced both very early and late. It was sensitive to T_1.
For CERES-EGC, the first three principal components explained more than 99% of the model output inertia. The first component corresponds to the mean of the simulated N_2O values. This component is sensitive to the parameters r, PDR, and Km (Figure 4). The second and third principal components correspond to the difference between the N_2O values simulated during the first and second halves of the simulation period, but the second component is positively correlated to the values simulated at a very early stage. The second component is strongly influenced by Seuil_wfps and puissance whereas the third component is strongly influenced by Seuil_wfps and r.

3.3. Generalized sensitivity indices

The Generalized sensitivity indices (GSI) are shown in Figure 5. These indices provide a unique ranking of the parameters. For WWDM, Figure 5a shows that E_b, and then *A* and T_1 had the strongest influence on the simulated dry matter values, all dates mixed together. Such ranking is quite convenient for selecting a set of parameters to be estimated from data. Thus, if one has to choose two parameters for calibration, it should be E_b and *A* according to Figure 5a. For CERES-EGC, Figure 5b shows that the parameters with the strongest effects were r, PDR and then Km over the entire simulation period. Parameters *min_wfps*, *opt_wfps* and *c* had negligible effects. Thus, if one had to estimate two parameters of the CERES_EGC model, it should be r and PDR according to the generalized sensitivity indices.

3.4. Parameter selection and estimation (CERES-EGC model)

Figure 6 shows the empirical relationship between MSEP and the generalized sensitivity index (GSI) values for the CERES-EGC model when one, two or three parameters were estimated from data. MSEP are presented in function of the pooled sensitivity index of each set of parameters. Overall, MSEP strongly decreases when GSI increases. This result shows that the MSEP was decreased, and so the prediction accuracy improved, when the parameters with the highest sensitivity indices were estimated. This is an argument in favor of GSI for selecting the parameters to estimate from data. According to Figure 6, the estimation of the sets of parameters with the highest sensitivity indices is a guarantee for a low MSEP. Figure 6 also shows that, in some cases, low MSEP were reached by estimating sets of parameters with low sensitivity indices but this was not systematic. The estimation of sets of parameters with low sensitivity indices is thus very risky.

4. Discussion and conclusion

The results presented above first show that, when performing sensitivity analysis on a dynamic model, it is essential to consider the output over the whole time series. The practical comparison between the sequential and multivariate sensitivity analysis showed that these methods are complementary.

In the sequential sensitivity analysis (Saltelli *.et al.*, 2000a; Pacala *et al.*, 1996), the sensitivity index is a function of time that measures when any given factor is more influent. Conducting separate sensitivity analyses on $\mathbf{y}(1),\ldots,\mathbf{y}(T)$ gives information on how the sensitivity of $y(t)$ evolves over time. However, it usually leads to a high level of redundancy because of the strong relationship between responses from one date to the next one. It may also miss important features of the $y(t)$ dynamics because many features cannot be efficiently detected through single-time measurements.

The second type of multivariate sensitivity analysis, proposed by Campbell et al (2006), decomposes the crude outputs into the non-correlated principal components and computes sensitivity indices on each PC. After interpreting the PCs, this analysis allows to understand more precisely the role of some parameters in the model. Sensitivity indices on each PC can give different ranking of model parameters and we showed that the overall effect of each parameter can be summarized by a global single sensitivity index.

These two methods are useful because they provide modellers with different types of information. The application of both methods is more interesting for models which exhibit much variability of sensitivity indices over time. Conversely, when the parameter influence is quite constant over time, the two methods give more similar results.

In addition to yielding information on model behaviour, sensitivity indices can be useful to select parameters before calibration. This is an intuitive and reasonable statement. However, there is no automatic relationship between sensitivity indices, which are based on simulated data purely, and prediction quality, which depends on experimental data. Discrepancies may arise because of modelling approximations, bad choice of the uncertainty intervals and nominal values, mesurement errors, or correlations between parameter estimates resulting from partial confounding in the data. To our knowledge, the relationship has rarely been verified using real data and a rigorous cross-validation approach. In this paper we proposed and applied such an approach in the particular case when predictions have to be made to complement observations that are too much dispersed in time. We found a relationship between MSEP and sensitivity indices; our results showed that the estimation of the parameters with the highest sensitivity indices led to a strong reduction of the prediction errors of the model CERES-EGC. However, the estimation of parameters with the highest sensitivity indices did not lead systematically to the very smallest MSEP and, conversely, small sensitivity indices did not lead systematically to a high MSEP. In our opinion, these results give weight to the use of sensible sensitivity analyses for selecting the parameters to estimate, especially since such a data-free approach to selection avoids selection bias.

The methods presented in this paper can be applied to any dynamic model predicting one or several output variables at a discrete time step. In the future, it will be interesting to apply and evaluate them on other modelling and prediction situations. Besides, they are quite flexible and extensions can be researched in several directions. For example, principal components could be made more flexible by considering functional principal components (Ramsey and Silverman, 1997) or Legendre polynomials (Campbell *et al.*, 2006), while well-designed Monte Carlo simulations could be a useful alternative to factorial designs in various situations.

Acknowledgements: We are grateful to colleagues of the Mexico (“Méthodes pour l'EXploration Informatique des modèles COmplexes”) network for useful discussion.

References

Anderson T.W., 2003. *An Introduction to Multivariate Statistical Analysis* (3rd ed., 721 pp.). Wiley, New York.

Bechini L., Bocchi S., Maggiore T., Confalonieri R., 2006. Parameterization of a crop growth and development simulation model at sub model component level. An example for winter wheat (Triticum aestivum L.). *Environmental modelling & software* **21**, 1042-1054.

Gabrielle, B., Laville, P., Hénault, C., Nicoullaud, B., Germon, J. C., 2006a. Simulation of nitrous oxide emissions from wheat-cropped soils using CERES. *Nutr. Cycl. Agroecosys*. **74**, 133–146.

Gabrielle, B., Laville, P., Duval O., Nicoullaud, B., Germon, J. C., Hénault, C., 2006b. Process-based modeling of notrous oxyde emissions from wheat –cropped soils at the sub-regional scale. *Global biogeochemical cycles* **20**, GB4018 X.1-x.13.

Boote K.J., Jones J.W., Pickering N.B., 1996. Potential uses and limitations of crop models. *Agronomy Journal* **88**, 704-716.

Box G.E.P., Draper N.R. (1987). *Empirical Model Building and Response Surfaces*. Wiley, New York.

Butterbach-Bahl, K., Kesik, M., Miehle, P., Papen, H., Li, C., 2004. Quantifying the regional source strength of N-trace gases across agricultural and forest ecosystems with process based models. Plant Soil. 260, 311–329.

Campbell K., McKay, M.D., Williams B.J., 2006. Sensitivity analysis when model outputs are functions. *Reliability Engineering and System Safety* **9**1, 1468-1472.

Campolongo F., Cariboni J., Saltelli A., 2007. An effective screening design for sensitivity analysis of large models. *Environmental modelling & software* **22**, 1509-1518.

Cariboni J., Galtelli D., Liska R., Saltelli A., 2007. The role of sensitivity analysis in ecological modelling. *Ecological Modelling* **203**, 167-182.

Ginot V., Gaba S., Beaudouin R., Aries F., Monod H., 2006. Combined use of local and ANOVA-based global sensitivity analyses for investigation of a stochastic dynamic model: Application to the case study of an individual –based model of a fish population. *Ecological Modelling* **193**, 479-491.

Hénault, C., Germon, J. C., 2000. NEMIS, a predictive model of denitrification on the field scale. Eur. J. Soil Sci. 51, 257–270.

Hénault, C., Bizouard, F., Laville, P., Gabrielle, B., Nicoullaud, B., Germon, J. C., Cellier, P., 2005. Predicting in situ soil N2O emission using NOE algorithm and soil database. Glob. Change Biol. 11, 115–127.

Homma T., Saltelli A., 1996. Importance measure in global sensitivity analysis of nonlinear models. *Reliability Engineering and System Safety* **52**, 1-17.

Jones, C. A., Kiniry, J. R., 1986. CERES-N Maize: a simulation model of maize growth and development. Texas A&M University Press, College Statio, Temple, TX.

Kobilinsky A., 1997. Les plans factoriels. In: Droesbeke J.-J., Fine J., Saporta G. (Eds.), Plans d'expériences: application à l'entreprise. Editions Technip, Paris, Ch.3, pp. 69-209.

Krzanowski W.J., Marriott F.H.C., 1990. *Multivariate Analysis. Part 1. Distribution, ordination, inference*. E. Arnold, London.

Lamboni, M. Makowski, D., Monod, H., 2008. Multivariate global sensitivity analysis for discrete-time models. Technical report 2008-3, 17pp, Unité MIA, INRA Jouy-en-Josas.

Lehuger S, Gabrielle B, VanOijen M., Makowski D., C.Germon J., Morvan T., Henault C., 2009. Bayesian calibration of the nitrous oxide emission module of an agro-ecosystem model. Agriculture, Ecosystem and Environment, in press.

Makowski, D., Jeuffroy M.-H., Guérif M., 2004. Bayesian methods for updating crop model predictions, applications for predicting biomass and grain protein content. *In : Bayesian Statistics and quality modelling in the agro-food production chain* (Van Boekel *et al.* eds), pp.57-68. Kluwer, Dordrecht.

Makowski, D., Hillier J., Wallach D., Andrieu B., Jeuffroy M.-H., 2006a. Parameter estimation for crop models. *In: Working with Dynamic Crop Models*. (Wallach D., Makowski D. and Jones J. eds), pp. 101-150. Elsevier, Amsterdam.

Makowski D., Naud C., Jeuffroy M.-H., Barbottin A., Monod H., 2006b. Global sensitivity analysis for calculating the contribution of genetic parameters to the variance of crop model predictions. *Reliability Engineering and System Safety* **91**, 1142-1147.

Matsuoka T., Seno H. Ecological balance in the native population dynamics may cause the paradox of pest control with harvesting. *Journal of Theoretical Biology*, in press.

Monod H., Naud C., Makowski D., 2006. Uncertainty and sensitivity analysis for crop models. *In: Working with Dynamic Crop Models* (Wallach D., Makowski D. and Jones J. eds), pp. 55-100. Elsevier, Amsterdam.

Pacala, S.W., Canham C. D., Saponara J., SilanderJr J.A.., Kobe R.K., Ribbens E., 1996. Forest models defined by field measurements: estimation, error analysis, and dynamics. *Ecological Monographs* 66:143.

Passioura J.R., 1996. Simulation models: science, snake oil, education or engineering. *Agronomy Journal* **88**, 690-694.

Ramsey I., Silverman B., 1997. *Functional Data Analysis* (311 pp). Springer, New York.

Saltelli A., Chan K., Scott E.M. (eds.), 2000a. *Sensitivity Analysis* (475 pp.). Wiley , New York.

Saltelli A., Ratto M., Tarantola A., Campolongo F., 2006. Sensitivity analysis practices: strategies for model based inference. *Reliability Engineering and System Safety* **91**,1109-1125.

Saltelli A., Tarantola A., Campolongo F., 2000b. Sensitivity analysis as an ingredient of modelling. *Statistical Science* **15**, 377-395.

Saltelli A., Tarantola A., Campolongo F., Ratto M., 2004. *Sensitivity Analysis in Practice*. Wiley, New York.

Santangelo G., Bramanti L., Iannelli M. 2007. Population dynamics and conservation biology of over-exploited Mediterranean red coral. Journal of Theoretical Biology 244, 416-423.

SAS Institute Inc., 2008. *SAS/QC User's Guide.* Cary, NC: SAS Institute Inc. http://v8doc.sas.com/sashtml/qc/chap14/index.htm

Venables W.N., Ripley B.D., 2003. *Modern Applied Statistics with S. Fourth Edition.* Springer, Berlin.

Wallach D., Goffinet B., Bergez J.E., Debaeke P., Leenhardt D., Aubertot J.N., 2001**.** Parameter estimation for crop models: a new approach and application to a corn model. *Agronomy Journal* **93**, 757-766.

Wu H-H., Lee H-J., Horng S-B., Berec L. 2007. Modeling population dynamics of two cockroach species: effects of the circadian clock, interspecific competition and pest control. *Journal of Theoretical Biology* **249**, 473-486.

Yakubu A-A., Castillo-Chavez C. 2002. Interplay between local dynamics and dispersal in discrete-time metapopulation models. *Journal of Theoretical Biology* **218**, 273-288.

Table 1. *Uncertainty intervals for the parameters of the winter wheat dry matter model.*

Parameter	Interpretation	Unit	Nominal value	Uncertainty interval
E_b	radiation use efficiency	g/m^2	1.85	0.9-2.8
E_{imax}	maximal ratio of intercepted to incident radiation	-	0.94	0.9-0.99
K	coefficient of extinction	-	0.7	0.6-0.8
L_{max}	maximal value of *LAI*	-	7.5	3-12
T_1	temperature threshold	°C	900	700-1100
A	coefficient of LAI increase	-	0.0065	0.0035-0.01
B	coefficient of LAI decrease	-	0.00205	0.0011-0.0025

Table 2. *Uncertainty intervals for the parameters of the CERES-EGC model.*

Parameter	Interpretation	Unit	Nominal value	Uncertainty interval
seuil_wfps	WFPS response threshold	-	0.62	0.4-0.8
Km	half saturation (denitrification)	mgN-NO3 kg^{-1}soil	22	5-120
Seuil_t	temperature threshold	-	11	10-15
q_dix_un		-	89	60-120
q_dix_deux		-	2.1	1-4.8
puissance		-	1.74	0-2
Opt_wfps		-	0.6	0.35-0.75
Min_wfps		-	0.1	0.05-0.15
Max_wfps		-	0.8	0.8-1
Km_amm	half saturation (nitrification)	mgN-NO3kg^{-1}soil	10	1-50
Q_dix_nit		-	2.1	1.9-13
PDR	potential denitrification rate	kg N ha^{-1} day^{-1}	7	0.1-20
MNR	maximun nitrification rate	kg N ha^{-1} day^{-11}	9	4-13
r	ratio of N_2O N_2O/denit	-	0.25	0.09-0.9
c	ration of N_2O/Nitri	-	0.018	0.0002-0.1

Table 3. *Sum of squares decomposition of the total inertia* $I(\mathbf{Y}_c)$ *based on principal component analysis and MANOVA.* A *and* B *denote the first two parameters,* $A.B$ *their interaction, and* W *a generic factorial term.*

Factorial term	Principal Component					Inertia
	PC_1	PC_2	PC_3	…	PC_T	
A	$SS_{A,1}$	$SS_{A,2}$	$SS_{A,3}$	…	$SS_{A,T}$	$SS_{A,\text{total}}$
B	$SS_{B,1}$	$SS_{B,2}$	$SS_{B,3}$	…	$SS_{B,T}$	$SS_{B,\text{total}}$
.	.	.	.	.	.	.
$A.B$	$SS_{AB,1}$	$SS_{AB,2}$	$SS_{AB,3}$	…	$SS_{AB,T}$	$SS_{AB,\text{total}}$
.	.	.	.	.	.	.
W	$SS_{W,1}$	$SS_{W,2}$	$SS_{W,3}$	…	$SS_{W,T}$	$SS_{W,\text{total}}$
.	.	.	.	.	.	.
Inertia	λ_1	λ_2	λ_3	…	λ_T	$I(\mathbf{Y}_c)$

Figure 1. *Daily simulated values of the winter wheat dry matter model in g/m^2 (a) and of the CERES-EGC N_2O emissions in gN ha^{-1}day^{-1} (b), for the nominal values of the parameters (thick lines) and for a sample of other possible values drawn within the uncertainty ranges.*

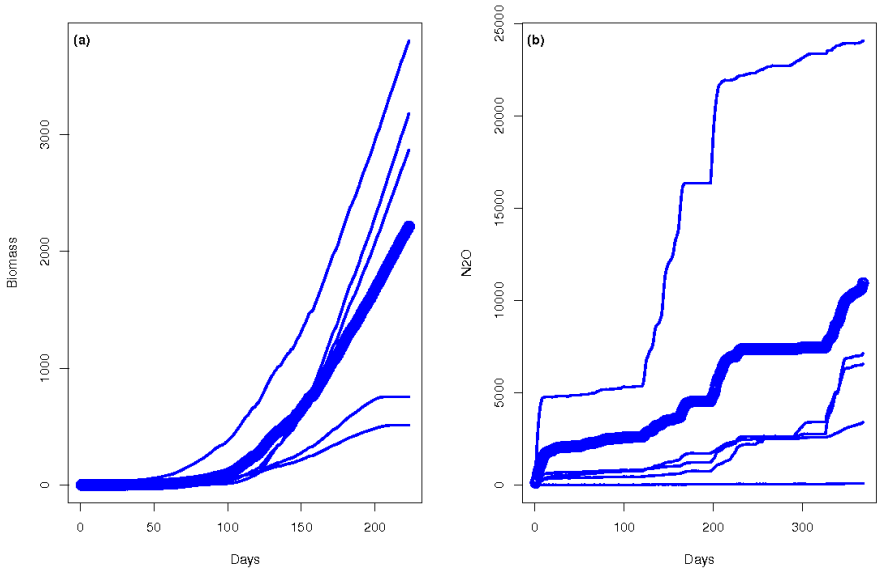

Figure 2. *Time-dependent pie charts of sensitivity indices for the WWDM model (a) and for the CERES-EGC model (b).*

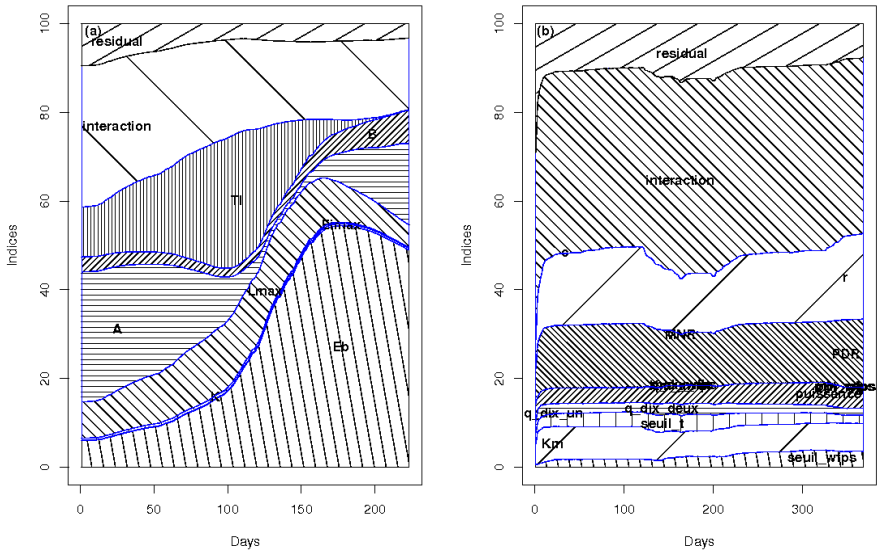

Figure 3. *PCA-based sensitivity analysis of the WWDM model. Columns: principal components 1 to 3. Top row: correlation coefficients (y-axis) between the principal component and y(t) (with t on the x-axis). Bottom row: first order sensitivity indices (dark bars) and total sensitivity indices (dark + pale bars).*

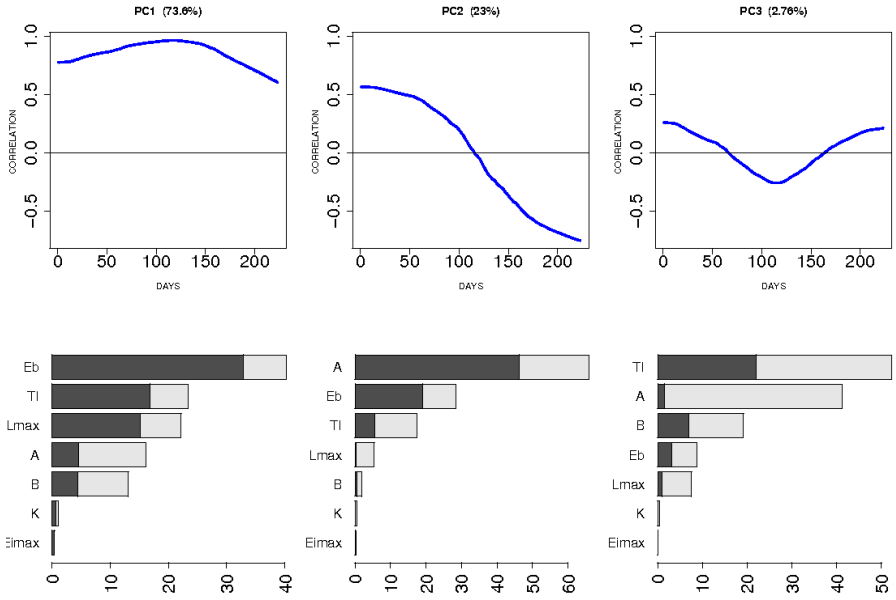

Figure 4. *PCA-based sensitivity analysis of the CERES-EGC model. Columns: principal components 1 to 3. Top row: correlation coefficients (y-axis) between the principal component and y(t) (with t on the x-axis). Bottom row: first order sensitivity indices (dark bars) and total sensitivity indices (dark + pale bars).*

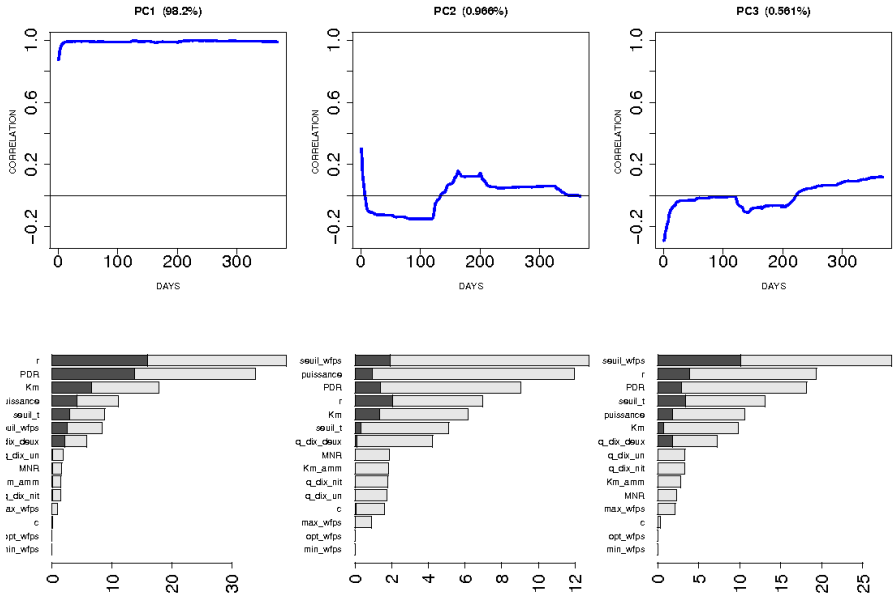

Figure 5. *Generalized Sensitivity Indices for the WWDM model (left) and for the CERES-EGC model (right). The main sensitivity indices are in dark bars and interaction ones are in pale bars. The total length of any bar represents the total sensitivity index.*

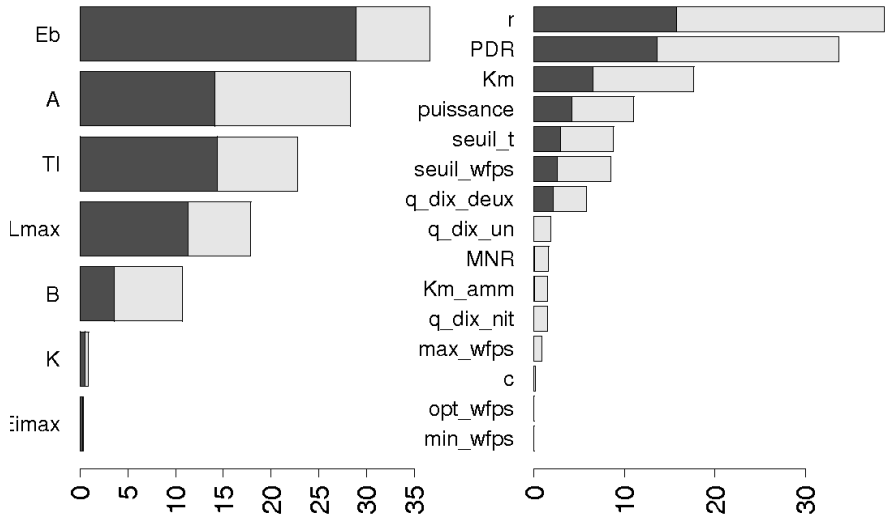

Figure 6. *Empirical relation between MSEP and generalized sensitivity index (GSI) by estimating only the most influent parameter (a) ; the two most influent parameters (b) and the three most influent parameters (c) of CERES-EGC model.*